University of Strathclyde

Strathclyde Institute of Pharmacy and Biomedical Sciences

Disrupting the Inhibitory Kappa B kinase (IKK) – Aurora A Axis in Cancer

By

Alastair Wilson

A Thesis submitted for the fulfilment of the requirements for the degree of Doctor of Philosophy

2013

This thesis is the result of the author's original research. It has been composed by the author and has not been previously submitted for examination which has led to the award of a degree.

ACKNOWLEDGEMENTS

Firstly, I would like to thank my supervisor, Dr Andrew Paul for all his help and patience with me over the years. I am very grateful for the opportunity he gave me to carry out this project and the support and unwavering encouragement he has provided especially through my frustrations with my work. His ability to parse my writing and help make sense of it has been nothing short of incredible and this thesis would have been considerably less coherent without his advice.

I would also like to thank Prof Robin Plevin for his ideas, which have helped steer me through some of the tougher parts of these last four years. I would also like to thank my collaborators Dr J. Beattie and Dr J. Branham for their expert guidance and willingness help me design and run the SPR experiments.

I would also like to sincerely thank everyone in Lab 401 for making the atmosphere in the lab always productive and highly entertaining even when science wasn't going our way. In particular I would like to thank Dr C. Gamble for helping me get started with this project and keeping me right, Dr. K McIntosh for answering any questions I had no manner how inane, Mark MacAskill for helping me get through the stats and scanning and finally Emma Torrance for giving me an outlet to vent my science rage, to bounce ideas off and to go to the pub when it all got a little too much. I must also thank the level 4 PhD office which has been the source of great amusement and bizarre conversation which was always a welcome respite.

I must also thank my parents and my sister, for their unwavering love and support which has been instrumental in getting me to this point in my life.

Last but not least, I would like to thank my fiancé Kirsty for her love and support throughout my PhD. Without her encouragement and her steadfast belief in me I would never have mustered the courage to actually start let alone finish my PhD. She has constantly put up with me throughout this process and has given me the strength to carry on even when I couldn't face it any more. This thesis is dedicated to her and our future together.

Table of Contents

LIST OF FIGURES

Chapter 1

Chapter 3

Chapter 4

Chapter 5

LIST OF TABLES

Abbreviations

ABIN	- A20-Binding Protein
ADP	- Adenosine Diphosphate
ALL	- Acute Lymphoblastic Leukaemia
AML	- Acute Myeloid Leukaemia
ANOVA	- Analysis of variance
APC/C	- Anaphase Promoting Complex/Cyclosome
APS	- Ammonium Persulfate
ATM	- Ataxia telangiectasia mutated
ATP	- Adenosine triphosphate
βTrCP	- β-transducin repeat-containing protein
Bcl2	- B-cell leukemia 2
Bcl-xL	- B-cell lymphoma-extra Large
BMS	- Bristol Myers Squibb
BSA	- Bovine Serum Albumin
CBP	- CREB Binding Protein
CDE	- Cell cycle-Dependent Element
CDK	- Cyclin Dependent Kinase
CHR	- Cell cycle gene homology region
CML	- Chronic Myeloid Leukaemia
CIA	- Collagen-Induced Arthritis
c-IAP	- c-Inhibitor of Apoptosis
CIKS	- Connection to IKK and SAPK

COPD	- Chronic Obstructive Pulmonary Disease
COX	- Cyclo-oxygenase
CPP	- Cell Permeable Peptide
DNA	- Deoxyribonucleic Acid
DS	- Disulfiram
DSS	- Dextran Sulfate Sodium
DTT	- Dithiothreitol
EAE	- Experimental allergic encephalomyelitis
ECL	- Enhanced Chemiluminescence
EGF	- Epidermal Growth Factor
EGFR	- Epidermal Growth Factor Receptor
ERα	- Oestrogen Receptor-α
ERK	- Extracellular signal-regulated kinases
ETS	- E-twenty six
FCS	- Foetal Calf Serum
FOXO3a	- Forkhead Box O3a
FSH	- Follicle Stimulating Hormone
GAB-P	- GA-Binding Protein
GFAP	- Glial fibrillary acidic protein
HCC	- Hepatocellular Carcinoma cells
HEK	- Human Embryonic Kidney
HEPES	- 4-(2-hydroxyethyl)-1-piperazineethanesulfonic acid
H/RS	- Hodgkin and Reed-Sternberg cells
HLH	- Helix-loop-Helix

HNSCC	- Head and Neck Squamous Cell Carcinoma
Hsps	- Heat-Shock Proteins
HTS	- High-Throughput Screening
IAP	- Inhibitor of Apoptosis
IBD	- Inflammatory Bowel Disease
IC_{50}	- Inhibitory Concentration (50%)
IgG	- Immunoglobulin G
IKIP	- IKK Interacting Protein
IKK	- Inhibitory κB Kinase
I□B	- Inhibitor of κB
IL-1	- Interleukin-1
IL -6	- Interleukin-6
INCENP	- Inner Centromere Protein
IRFs	- Interferon Regulatory Factors
JNK	- c-Jun N-terminal Kinase
KO	- Knockout
kDa	- Kilo-Dalton
LPS	- Lipopolysaccharide
LH	- Luteinizing hormone
LH-RH	- Luteinizing hormone-releasing hormone
MAPK	- Mitogen-activated protein kinases
MCAK	- Mitotic Centromere-Associated Kinesin
MDM2	- Murine double minute 2
MEFs	- Murine Embryonic Fibroblasts

MMP	- Matrix Metallo-Proteinase
NAK	- NF□B-Activating Kinase
NBD	- NEMO-Binding Domain
NDEL 1	- Nuclear distribution protein nudE-like 1
NEMO	- NFκB Essential Modulator
NIK	- NF□B Inducing Kinase
NF-□B	- Nuclear Factor kappa B
NLS	- Nuclear Localisation Sequence
NSAIDs	- Non-Steroidal Anti-Inflammatory Drugs
ORF	- Open Reading Frame
PAGE	- Polyacrylamide gel electrophoresis
PAK1	- Protein Activated Kinase 1
PBS	- Phosphate Buffered Saline
PCM	- Pericentriolar Material
PDGF	- Platelet Derived Growth Factor
PEI	- Polyethylenimine
PIN	- Prostatic Intraepithelial Neoplasia
PGE	- Prostaglandin E
PMA	- Phorbol Myritoyl Acetate
PMBC	- Peripheral Blood Mononuclear Cells
PPI	- Protein-Protein Interaction
PP1A	- Protein Phosphatase 1A
PRE	- Positive Regulatory Element
PSA	- Prostate Specific Antigen

RA	- Rheumatoid Arthritis
RAN	- RAs-related Nuclear protein
RANK	- Receptor Activator for Nuclear Factor κB
RANKL	- RANK ligand
RANTES	- Regulated upon Activation, Normal T cell Expressed and Secreted
RCC1	- Regulator of chromosome condensation 1
RHD	- Rel Homology Domain
RNA	- Ribonucleic Acid
ROS	- Reactive Oxygen Species
SAR	- Structure Activity Relationship
SAC -	- Spindle Assembly Checkpoint
SDS	- Sodium dodecyl sulphate
siRNA	- Small interfering RNA
SMC	- Structural Maintenance of Chromosomes
SMRT	- Silencing Mediator for Retinoic Acid and Thyroid Hormone Receptor
SOD	- Superoxide Dismutase
SSC	- Sodium Sodium Citrate
TACC3	- Transforming Acidic Coiled-coil-Containing protein 3
TAD	- Transcriptional Activation Domains
TAMS	- Tumour-Associated Macrophages
TAT	- Trans-Activator of Transcription
TNBS	- Trinitrobenzene sulphonic acid
TPX2	- Targeting protein for Xklp2
TGF-β	- Transforming Growth Factor-β

TRAFs	- TNF-Receptor-Associated Factors
TBK1	- TANK–Binding Kinase 1
TLR	- Toll Like Receptor
TNF-α	- Tumour Necrosis Factor- α
TRAMP	- Transgenic Adenocarcinoma of Mouse Prostate
UV	- Ultraviolet.
VEGF	- Vascular Endothelial Growth Factor
WT	- Wild Type

ABSTRACT

The IKK complex is an essential regulator of the NF-κB signalling pathway. It is comprised of three sub-units; catalytic subunits IKKα and IKKβ and the catalytically inactive scaffolding protein IKKγ/NF-κB Essential Modulator (NEMO). The complex can be assembled in multiple conformations as either hetero- or homo-dimers of IKKα/β with or without the scaffolding protein IKKγ. This regulates NF-κB signalling and related cellular inflammatory responses that are often constitutively active in many cancer cells. Beyond regulation of NF-kB signalling a number of other potential IKK substrates have been proposed including the mitotic kinase Aurora A, one of three serine/threonine kinases of the Aurora kinase family that mediate mitotic progression in cells. Aurora A kinase specifically has several roles in the cell cycle, regulating spindle formation/attachment, centrosome maturation and cytokinesis, and has been observed to be overexpressed in several cancers.

Several studies have linked IKK complex to Aurora A signalling, as either a substrate of IKKα (Prajapati et al, 2006) or as a target for IKKβ-mediated βTRCP-regulated degradation (Irelan et al, 2007) both linked to cell cycle progression independent of NF-κB signalling., Aurora A kinase has however also been linked to NF-κB signalling through the phosphorylation and degradation of IκBα in primary breast tumours in a subgroup of patients exhibiting Aurora A gene amplification (*Briassouli et al, 2007*).

Prostate cancer is a significant worldwide health issue and is the 2nd most prevalent cancer in males and 5th most prevalent cancer overall with over 900,000 new cases diagnosed in 2008 (*Ferlay et al, 2010*). The current therapies treating prostate cancer are far from ideal and have significant side effects. Both Aurora A and NF-κB-related kinases have been shown to be over-expressed or constitutively active in Prostate cancer and therefore the suggested novel interaction may serve as a potential mechanism for intervention in cancer. This study aimed to validate IKK-Aurora A interactions and potentially identify novel targets for the development of therapeutics in perostate cancer.

Using recombinant protein methodologies the direct interaction of IKKα and IKKβ with Aurora A were confirmed. Utilising peptide array technology, it has been possible to

further elucidate the nature of the interaction between Aurora A and IKKα/β. The interaction of Aurora A and IKKα/β was mapped to two key regions of the IKKs, the kinase domain and the NEMO binding domain. The NEMO-Binding Domain is a conserved hexapeptide sequence, L-D-W-S-W-L, across both IKKα and IKKβ mediating the interaction with the scaffolding protein IKKγ/NEMO. This highlighted a novel role of the NBD as a multi-protein docking site. Binding of these proteins was further confirmed endogenously in a cellular setting, by means of co-immunoprecipitation and also the kinetic profiles of these interactions were characterised using recombinant proteins and Surface Plasmon Resonance. Thereafter Cell Permeable Peptides (CPPs) based on the IKK NBD were utilised as pharmacological tools, to examine potential competitive perturbation of Aurora A-IKK interactions mediated by the NBD in prostate cancer cells. This identified in a cellular setting treatment with NBD CPPs resulted in the inhibition of Aurora A phosphorylation and induced Aurora A degradation, which correlated with cell cycle arrest. It was also suggested through molecular modeling that the IKK NBD peptides could bind to the Aurora A protein, potentially at sites engaged by TPX2, an activation accessory protein for Aurora A. This purported mechanism may account for the observed IKK NBD peptide-mediated de-phosphorylation and subsequent degradation of Aurora A.

Therefore, this study has identified the NEMO binding domain as a potential multi-protein binding site and has identified novel functionality of the IKK NBD cell permeable peptides. This may represent a novel target for the intervention of IKK-mediated regulation of the cell cycle and serve as the basis for the development of novel peptidomimetics and related small molecules for the treatment of Prostate cancer.

CHAPTER 1: INTRODUCTION

1.0 INTRODUCTION

1.1 Cancer

Cancer is one of the world's most significant health problems, affecting ~12.8 million people a year and accounting for around 13% of all deaths worldwide (based on studies by the WHO in 2008; *Ferlay et al, 2012*). Cancer is a term used to describe a wide variety of diseases, which can affect any region of the body, and is defined as a disease of uncontrolled abnormal cellular growth. The unregulated growth of human cells leads to tumour formation and in its malignant form can spread via the lymphatic system or the bloodstream to disparate regions of the body. This mechanism is referred to as metastasis and it is these metastases that are the leading cause of death from the disease, due to a spread of the tumour to essential tissues leading to a disruption of normal function and subsequently death (*Hanahan et al, 2000*).

The causes of cancer are hard to determine as there is such a wide range of tissue affected, over two hundred different cancers have been observed in humans, so there is often no way to ascertain one specific causative agent that leads to the development of cancer. Using large-scale epidemiological studies it has been possible to elucidate risk factors associated with certain cancers e.g. the strong statistical association between the smoking of tobacco and lung cancer incidence (*Sasco et al, 2004*). The external agents associated with the development of cancerous malignancies are known as carcinogens and can be split into three separate categories; physical carcinogens, chemical carcinogens and biological Carcinogens.

Physical carcinogens are defined as a physical agent, which can lead to the formation of cancer such as the exposure to ionising radiation or high levels of ultraviolet radiation. Long-term exposure to the sun without adequate protection has long been associated with the incidence of melanoma's (skin cancer) due to exposure to high levels of ultraviolet radiation. Many studies have highlighted the link between the levels of unprotected exposure to the sun and cancer with a recent study showing 95% of all malignant skin cancers occurring in sun exposed regions (*Andrade et al, 2012*).

Chemical carcinogens are any chemical agent, which can lead to carcinogenesis such as arsenic (water contaminant) or tobacco smoke components. Tobacco smoke contains up to 4000 chemicals many of which are carcinogenic, 93% of all incidence of lung

cancers have been associated with the inhalation of cigarette smoke (*Villneuve et al, 1994*; *Sasco et al, 2004*).

Finally, biological carcinogens are cancers caused by infection by viral/bacterial or parasitic infection. One such example of a cancer associated with a biological carcinogen is Kaposi's Sarcoma, a malignant form of skin cancer associated with cutaneous lesions. All incidents of this cancer are associated with infection by Kaposi's Sarcoma Herpes Virus (KSHV), otherwise known as Human Herpes Virus – 8 (HHV8) this is one of several cancers which have been shown to be caused through viral infection (*Shulz et al, 2000*).

These are all risk factors linked to exposure to an external source that leads to the increased chance of developing of this disease. However, there are also genetically linked internal risk factors also shown to be causative agents of cancer. There are genetic mutations that can increase the likelihood of developing cancer e.g. the hereditary mutations of the *BRCA1* gene increases both breast and ovarian cancer incidence and has been shown to be linked through generations of families (*Friedman et al, 1994*). Hormone imbalance can act as another internal risk factor as a number of hormones are responsible for the regulation of cell growth and development; so where these hormones are mis-regulated and levels are elevated this can lead to tumour development e.g. endometrial cancer is linked strongly to hormonal imbalance (*Tinelli et al, 2008*).

Fundamentally, all cancers are caused through genetic mutation, responsible for the loss of control of the mechanisms governing correct cellular proliferation. The development of these mutations can be somatic, such as link between *BRCA1* and breast cancer, but are more likely to be due to exposure to both external and internal risk factors over the lifetime of the patient leading to the development of the disease. Although reducing the exposure to the external risk factors can significantly decrease the probability of developing cancer, the risk factor with the strongest association to a rising cancer incidence is therefore age. The development of modern medicine has increased life expectancy of the population and with this increased life expectancy has come an increase in the prevalence of cancer. Considering the statistics published by the WHO at the conclusion of a worldwide study between 1976-2008 it was observed that in developed countries 78% of all new cancers were diagnosed in the over 55 population, this is reduced to 58% in developing nations (*Ferlay et al, 2012*). Most

cancers occur due to a cumulative exposure to one or several of the risk factors leading to an increase in genetic mutations and subsequent development of the disease, some cancers are directly associated with ageing. The most significant of these is cancer of the prostate.

1.2 Prostate cancer: Prevalence and incidence

Cancer of the prostate is an adenocarcinoma, a cancer of the epithelium in glandular tissues, in over 95% of all cases. Globally it is the most prevalent not-cutaneous cancer found in men (*Ferlay et al, 2010*) and is the sixth leading cause of death in men worldwide with 900,000 new cases diagnosed each year and an estimated 258,000 deaths occurring in 2008. The prevalence of prostate cancer is strongly linked to age, with the likelihood of developing the disease increasing exponentially as the patient ages. From a study of cancer incidence and age in the USA between 2001-2005 between the ages of 45-54 there is an increase in incidence from almost none under the age of 45 to 8.6%, with a total incidence recorded in the <65 population of 37%. The highest diagnosis rate in a single age range is that of 65-74 years with 36% of all cases and above this 27% of all incidences is recorded (*Crawford et al, 2009*). A study examining prostate cancer incidence in the autopsies of white males who had no prior intervention also showed an age-dependent increase in frequency with 35% of those aged 60-69 and 46% of 70-81 year olds were observed to have displayed cancer of the prostate (*Yin et al, 2008*). Although age is the most well established risk factor for the development of prostate cancers there has also been shown a link with both ethnicity and diet playing a role in the prevalence of prostate cancer amongst certain populations (*Crawford et al, 2009*). Studies investigating the links between diet alone and prevalence of prostate cancer have so far proven inconclusive. The most convincing of the studies highlighting a possible link between prostate cancer and diet has been that by *Cook et al*, *1999*. This study linked diet to a rising incidence of prostate cancer frequency amongst Asian immigrants and their descendants with an almost doubling of the incidence observed in Asian Americans born in the USA. The most obvious change in the environmental factors, which may have exerted an effect on this increase, is diet. The disparity between the ethnicities of those affected by prostate cancer becomes clear when the statistics are investigated. Studies carried out in the

USA show that African American men have a 1.6 times greater risk of developing cancer and almost double the probability of dying from the disease compared to white men (*Crawford et al, 2009*; *Howlander et al, 2012*). This trend was also observed on a global scale when worldwide incidence was investigated, as seen in the GLOBOCAN report by the International Agency for Research on Cancer (IARC). The report showed an incidence rate in Europe, North America and Australia at 66.8 per 100,000 while in Central Asia e.g. India/China the rate is less than 7.4 per 100,000. This is an almost 70 fold variance across the world (*American Cancer Society, 2011*). Some of this variance is attributable to the more widespread use of screening techniques in the countries with the highest prevalence. The differences observed in prostate cancers amongst different races are not well understood, with many factors attributable, such as diet or environmental factors, having been implicated. There is however some evidence for a genetic predisposition to the disease in men of African descent, for example a recent study into the deletion mutations of glutathione-S-transferase genes show a significant increase in the incidence of cancer when linked to smoking amongst African-American men (*Taioli et al, 2011*). The hereditary predisposition to prostate cancer through genetic links are well established (*Albright et al, 2012*). These strong familial links to increased risk of prostate cancer were established through analysis of Scandinavian monozygotic and dizygotic twins. These studies showed a strong hereditary genetic link to familial aggregation of cancer compared to the effect of shared environmental factors (*Lichtenstein et al, 2000*).

1.3 Current treatment modalities of cancer of the prostate

Although the rate of prostate cancer incidence has been rising steadily over the past 25 years, the rate of mortality associated with the disease has been steadily decreasing (*Howlander et al, 2012*). This has been attributed to the improvements and widespread implementation of screening techniques allowing for earlier detection greatly increasing the success of treatment and thereby reducing the mortality rates. There have however been some questions as to the efficacy of these screening methods as a result of two large-scale studies recently completed in Europe and USA that showed slightly different results. The European study showed a 20% decrease in mortality over a median of 9 years in those being screened. However the study conducted in the

United States of America showed no difference in the mortality rates. Although this study can be interpreted as a comparison of regular screening compared to high levels of screening as the control arm of the study received 'regular care' which included routine screening (*Etzioni et al, 2012*).

The screening for cancer of the prostate is carried out by two methods, either using a blood test to investigate the circulating levels of Prostate Specific Antigen (PSA) or manual assessment through digital rectal examination. A high circulating level of PSA has been indicated to associate strongly with a positive biopsy for prostate cancer (*Thompson et al, 2005*) and with advancements in the sensitivity of screening it has been possible to detect PSA at increasingly low levels. This leads to faster treatment of early stage cancers which has a positive effect on survival outlook, with an almost 100% five year survival rate post diagnosis seen in the USA and rates varying in Europe from 48% to 87% (*Ferlay et al, 2010*;*Howlander et al*, *2012*) when diagnosis occurred in the early stages of the disease. There are a wide range of treatment options once diagnosed; these are dependent on a wide variety of factors including age, stage and grade of the cancer (*Denmeade et al, 2004*). When considering the options for treatment it is important to determine if immediate treatment is in fact essential. prostate cancer has been shown to be a slow progressing localised form of cancer and doesn't rapidly develop into the more aggressive metastatic forms in the short term. The treatments for the disease on the other hand are highly invasive with common side effects including urinary incontinence and loss of erectile function, which can be severely detrimental to the patient's quality of life and are not necessary in the treatment in the early stages. The 'treatment' most employed at this stage is 'watchful waiting' which refers to a regimen of increased screening by digital rectal exams, biopsy or PSA level screening to monitor the progression of the cancer more accurately with the curative intent of identifying the disease before it advances to the more aggressive forms of the disease (*Sanda et al, 2009*). The increased monitoring of the disease allows for the tailoring of treatment to the individual. It allows for a more complete understanding of how the disease is progressing and how it is affecting the patient, which will be advantageous for improving both quality of life and long-term survival (*Denmeade et al, 2004*). Watchful waiting is more accurately referred to as deferred definitive therapy, as its function is to merely defer the time before more definitive treatments must be employed. There are three definitive therapies employed in the treatment of prostate cancer:

1. Radical prostatectomy
2. Radiotherapy
3. Brachytherapy

These methodologies are all applied to early and intermediate forms of the disease but for the more advanced metastatic forms androgen ablation therapy is also used in conjunction with one or more of these definitive therapies. The clinical model for those whom 'watchful waiting' is the recommended treatment was defined in 1993 by *Epstein et al* and has led to between a third to a half of all patients having no further treatments over 5 years (*Sanda et al, 2009*).

1.4 The current definitive treatments for cancer of the prostate

1.4.1 Treatment of Prostate cancer by Radical Prostatectomy

The progression of cancer of the prostate will eventually lead to the need for definitive therapies as described previously. The first of these is the surgical removal of the prostate otherwise known as radical prostatectomy. This is a highly invasive surgery requiring in-patient hospitalisation and a period of restricted activity post-operatively and is associated with negative perioperative events and several long-term side effects (*Johansson et al, 2011*). The perioperative effects include acute symptoms such as internal bleeding, infection and urinary retention, there are also severe and life threatening effects such as haemorrhage or rectal injury (*Sanda et al, 2008*). Prostatectomy is an invasive surgery in the gastrointestinal region and as such the risk of infection and sepsis are high both during the operation and post-surgery. The significant advancement in surgical techniques and correct vetting of candidates however has helped minimise these risks. Studies have shown there is also an increased risk of myocardial infarction amongst the older patients undergoing prostatectomy as observed in any serious surgery, coupling this with an overall reduction of morbidity and alternatives Radical Prostatectomy is unlikely to be recommended for this demographic (*Sanda et al, 2009*). There has been a move recently to more laparoscopic techniques to reduce the invasiveness of this surgery often using robotic assistance (*Patel et al, 2007*). This method reduces blood loss and is more cosmetically appealing; it however shows little improvement on the long-term side effects (*Tewari et al, 2012*). The most common side-effects which are associated with this treatment are erectile dysfunction and urinary incontinence; both affecting the patients' quality of life significantly and the methods used are constantly being improved to reduce these effects (*Sanda et al, 2008*).

1.4.2 Radiation Therapy in the treatment of prostate cancer

Commonly used as an alternative to radical prostatectomy is radiation therapy; a targeted dose of radiation from an external source can be used to kill the cancerous tissue; it is also commonly referred to as external beam radiation therapy. The use of

modern imaging techniques allows for accurate targeting of the radiation beam to only affect the cancerous cells and minimising the exposure of healthy tissue (*Sanda et al, 2009*). The use of targeted radiation has been shown to significantly improve survival rates over a 5-year period, one study showing an increase from 79% to 91% (*Zeitman et al, 2005*). As with all of the definitive therapies for prostate cancer there are significant risks and side effects associated and this is no different with radiation therapy. There have been toxic effects of radiation observed in both the short-term and long-term in patients undergoing this form of treatment, the more acute effects include an increased urinary frequency, difficulty in urination and increased urgency of urination as well as similar rectal effects also (*Sanda et al 2009*). Erectile dysfunction is observed in patients being treated by any of the definitive therapies although radiation therapy and brachytherapy of the three have the lowest prevalence in comparison to that observed for radical prostatectomy (*Mirza et al, 2011*). Radiation therapy is most commonly used in conjunction with androgen suppression therapy and when these therapies have been used in combination further increased survival rates, dependant on treatment length have been observed. However, a 2007 study showed there was an influence on time to fatal myocardial infarction by the use of short-term androgen suppressive therapies (*D'Amico et al, 2007*). A recent study comparing the mortalities related to either radical prostatectomy or radiation therapy indicated that patients treated using radical prostatectomy fare significantly better than their counterparts treated using only radiation therapy. These two studies combined with the advancement in surgery and reduction of surgical associated morbidities make the use of radiation therapy a less attractive option particularly for older patients (*Abdollah et al, 2012*).

1.4.3 Brachytherapy as a definitive treatment of prostate cancer

The final definitive therapy used in Brachytherapy, this is the implantation of radioactive isotope pellets (iodine 125, palladium 103) via a trans-peritoneal injection guided using advanced imaging techniques. These particular isotopes are used as they have relatively short half-lives and are of sufficiently low energy to affect only the tissues immediately surrounding the implantation site (*Denmeade et al, 2004*). This allows for high doses of radiation delivered to the affected regions directly and the ability to progressively scale up the amount of radiation to better control and treat the

disease (*Masson et al, 2012*). This technique is most commonly used in conjunction with external beam radiation, as with the implantation it is not possible to treat all the affected areas simultaneously. Brachytherapy can also be applied through the temporary implantation of a high dose emitting bead for a shorter time coupled with a high dose of external beam radiation. This method is referred to as high dose rate brachytherapy and is becoming increasingly popular (*Masson et al, 2012*). The use of external beam radiation as well as high dose rate brachytherapy also means that a higher dose of radiation can be given to the patient in a single treatment whilst remaining within the safe exposure guidelines for other organs. There has been reported a reduction in the acute rectal toxicity and reduced effect on urinary obstructions or incontinence and bowel/rectal function in patients treated with Brachytherapy compared to either radical prostatectomy or radiation therapy (*Sanda et al, 2008*). Currently the favoured form of this treatment is the high dose rate form as a 2009 review of efficacy showed an improvement in both progression-free survival and overall survival (*Pieters et al, 2009*) with a marked improvement in toxicity observed also.

There is a very significant side effect linked to the use of radiation, through either brachytherapy or rexternal beam radiation therapy, to treat prostate cancer and this is the persistence of localised cancer as observed in 12-16% of patients treated by External beam radiation therapy and 8% of brachytherapy patients (*Zelefsky et al, 2008*; *Stone et al, 2007*) This is a major disadvantage in the long term treatment of prostate cancer as it increases the probability of recurrence. Radical prostatectomy when used as the initial treatment can avoid this unfortunate side effect but has the most extreme effects on quality of life. For these reasons it can be difficult to determine the best course of treatment. These treatments are most commonly used in the early and intermediate stages of prostate cancer progression due to the localisation of the cancer predominantly to the prostate itself allowing for accurate targeting of the treatments to the affected area. The later stages of the disease however are considerably harder to treat, due to the highly metastatic nature of this form of cancer. The spread of metastases make it considerably harder to treat the disease via surgical or radiological means. In the latter stages of the disease in order to combat the problems associated with these treatments as described above, they are pursued increasingly in conjunction with androgen ablation therapy.

1.4.4 Androgen ablation therapy in prostate cancer treatment

Prostate cancer is an androgen dependent cancer with tumour cell proliferation relying on the production of testosterone in the gonads and adrenal glands in men (*Imamoto et al, 2008*). Therefore, the use of hormone therapy as a means to prevent the production of androgens and prevent tumour growth was introduced. Androgen ablation therapy has been used in the treatment of prostate cancer since the 1940's when Huggins and Hodges used bilateral orchiectomy to reduce the circulating testosterone levels in patients suffering from advanced forms of prostate cancer (*Huggins et al, 1941*). Surgical castration is a very effective method of reducing testosterone levels with effects seen in hours post-surgery, it is however an uncommon treatment due to the psychological implications for the patient (*Suzuki et al, 2008*). In the 1980's the use of luteinizing hormone-releasing hormone (LH-RH) agonists to reduce testosterone to the same levels as seen in castration patients were pioneered (*Suzuki et al, 2008*). The two most commonly used were Leuprolide and Goserelin, they act through the inhibition of luteinizing hormone (LH) and follicle-stimulating hormone (FSH) at the pituitary gland subsequently reducing circulating testosterone levels. Treatment with LH-RH agonists alone can lead to a 90% reduction of circulating testosterone and in combination with a non-steroidal anti-androgen, which prevents androgen uptake in prostatic tissue, this can be further reduced to close to 100% (*Gomella et al, 2010*). This treatment has some unique side-effects compared to the definitive therapies described previously, including short-term side-effects such as hot flashes, a loss of libido, gynecomastia and more severe long-term side effects such as osteoperosis and an increased risk of associated fatal myocardial infarction (*Zietman et al, 2005*;*Suzuki et al, 2008*). Progression of cancer of the prostate leads to the development of the castrate resistant form of the disease which results in the malignant cells no longer requiring hormones for growth. In both healthy and neoplastic prostate tissue the androgen receptor is an essential component of cellular proliferation, and has been linked to all stages of prostate carcinogenesis (*Koochekpour, 2010*). The androgen receptor is a nuclear transcription factor mediating the growth promotion actions of circulating androgens and as such is an obvious target for intervention in the treatment of cancer of the prostate. Treatment with anti-androgens remains effective for up to three years in the treatment of advanced prostate cancer, but as a direct result of the treatment however, the disease progresses into more aggressive and metastatic forms of the disease (*Gittes,*

1991). The molecular mechanisms resulting in this progression, to the hormone refractory form of the disease, are poorly understood but furthering our knowledge in this area is essential in aiding the development of new treatment modalities (*Koochekpour, 2010*). It has been observed in patients undergoing androgen blockade the androgen receptor is still activating and driving the expression of target genes independent of stimulation e.g. PSA. PSA is a target gene for the androgen receptor, and circulating levels return after time in patients treated in this manner. There have been many differing hypotheses as to how the androgen-receptor signalling regains function post-androgen ablation therapy, examples of which include somatic mutation inducing a gain of function and ligand-independent activation of the androgen receptor through cytokines or growth factors such as interleukin 6 (IL-6) or epidermal growth factor (EGF) respectively (*Feldman et al, 2001* and *Kim et al, 2004*). The side effects of this treatment in the long term have led to the use of androgen ablation therapy as primarily a treatment for the advance stages of the disease. It is used mostly in conjunction with other forms of definitive therapies therefore reducing the time the patient is being treated with hormones. Using hormone therapy in this manner also serves to increase the efficacy of the other treatments. The use of hormone therapy in combination with radiation has been suggested to be effective by several mechanisms; the hormone therapy will cause a shrinking of the prostate providing a smaller area to target with external beam radiation reducing toxicity to surrounding tissues, androgen ablation can also lead to radio-sensitisation of the cancerous cells and the reduction of the number of cancer cells to be treated (*Gomella et al 2010*). It is also used as part of the treatment schedule with radical prostatectomy to help suppress the regrowth of the cancer (*Denmeade et al, 2004*). Androgen ablation is also very useful for the treatment of the metastatic forms of the disease as it will be effective across all tissue as it is not a targeted therapy unlike prostatectomy or radiation therapy.

The treatment options implemented currently for prostate cancer as described all have their advantages and disadvantages, with no clear choice as to which would be the most suitable, it is therefore necessary for all options to be discussed with every individual patient as to which option will most suit them. The options for advanced metastatic hormone refractory prostate cancer however are limited and can have very severe side effects. There has been increasing interest in using chemotherapy as a novel mechanism for treatment of prostate cancer for patients suffering from this form of the disease. At present the first line of treatment is using docetaxol as established by

trials published in 2004 (*Tannock et al, 2004*). This drug belongs to the taxane family and acts as an anti-mitotic blocking microtubule depolymerisation. However, this treatment is not curative and as such novel therapeutics has been pursued. The most famous of which is Abiraterone a selective inhibitor of androgen biosynthesis, which has been shown to significantly prolong overall patient survival (*Fizazi et al, 2012*). However, this only translates to a few months survival and it is therefore essential for the cellular mechanisms governing oncogenesis and tumourigensis to be further investigated to provide insight into the molecular mechanisms that cause this disease. There have been significant advances over the last decade into the links between inflammatory signalling and its role in the development of cancer. This has led to the further research into a range of pathways and in particular the use of the NF-κB signalling pathway as a potential target in the development of novel therapeutics.

1.5 Nuclear Factor-kappa B (NF-κB) signalling pathway and the inhibitory Kappa B Kinases (IKK)

1.5.1 NF-κB sub-units

The NF-κB signalling pathway is a family of transcriptional regulatory factors regulating the inducible expression of a wide range of proteins essential to both innate and adaptive immunity, as a key mechanism of inflammatory signalling and cell survival pathways (*Solt et al., 2008*) and has been implicated in cell growth and division. NF-κB signalling is initiated in response to many different extracellular stimuli and is mediated through a series of intracellular adaptor proteins dictating the functional outcome of which aspect of the NF-κB pathway is activated. The NF-κB proteins are a family of 7 proteins (RelA (p65), RelB, c-Rel, NF-κB1 (p105/p50) and NF-κB2 (p100/p52)) (see Figure 1.1) that form dimeric complexes in mammalian cells (*Hayden et al, 2008*). These proteins exhibit high levels of homology (see Figure 1.1) forming various homo- and hetero-dimers through the Rel Homology Domain (RHD). Hydrophobic residues found at the C-terminal of this domain act as the dimerisation interface between proteins while the immunoglobulin like N-terminal regulates their DNA binding activity (*Hoffman et al, 2006*). The formation of these homo- and hetero-

dimers results in the NF-κB proteins existing in both transcriptionally active and inactive confirmations. These dimers are complexed to the Inhibitory Kappa B (IκB) family of proteins in the cytoplasm, this complexation of active NF-κB dimers renders them inactive until the IκB proteins are phosphorylated and ubiquitinated leading to their degradation by the 26S proteasome allowing NF-κB translocation to the nucleus to occur, promoting DNA binding which mediates the expression of NF-κB regulated transcription products (*Gilmore,* 2006) The NF-κB proteins all share the structurally homologous N-terminal sequence termed the RHD which mediates the homo-/hetero-dimerisation of the NF-κB subunits and also regulates the DNA binding mechanisms essential to this pathway (see Figure 1.1). The DNA binding regions are also known as κB sites and transcriptional activation domains (TAD) of the NF-κB proteins p65, c-Rel and RelB regulate transcription positively, p50 and p52 however lack this domain and therefore their hetero-dimerisation with other family members is essential to make them active components of the pathway. p50 and p52 although lacking a TAD domain can bind to the κB domains and prevent transcriptional activity down-regulating genes until an active component of the pathway displaces them (*Hoffman et al, 2006*). The RHD and TAD domains are subject also to post- translational modifications altering the transcriptional activity and DNA binding affinity adding a further layer of control to the regulation in the pathway. The activation of these transcription targets leads to an increase in the expression of proteins regulating cellular proliferation, components of the cell's apoptotic machinery (c-Inhibitor of Apoptosis [c-IAP] and TNF Receptor Associated Factors [TRAF] 1 and 2) and proteins that control cell cycle progression. The NF-κB pathway also possesses a self-regulatory capacity as the pathway activates the expression of molecules essential in both driving and inhibiting the pathway e.g. the pro-inflammatory cytokine TNFα and IκBα (*Yamamoto et al, 2004*). The IκB proteins act as the gatekeeper for the NF-κB nuclear translocation, mediated through degradation of the IκB by the 26S proteasome. This process is initiated through their initial phosphorylation catalysed by the Inhibitory Kappa B Kinase (IKK) complex driving the subsequent ubiquitination (*Solt et al, 2008*) and degradation of these proteins.

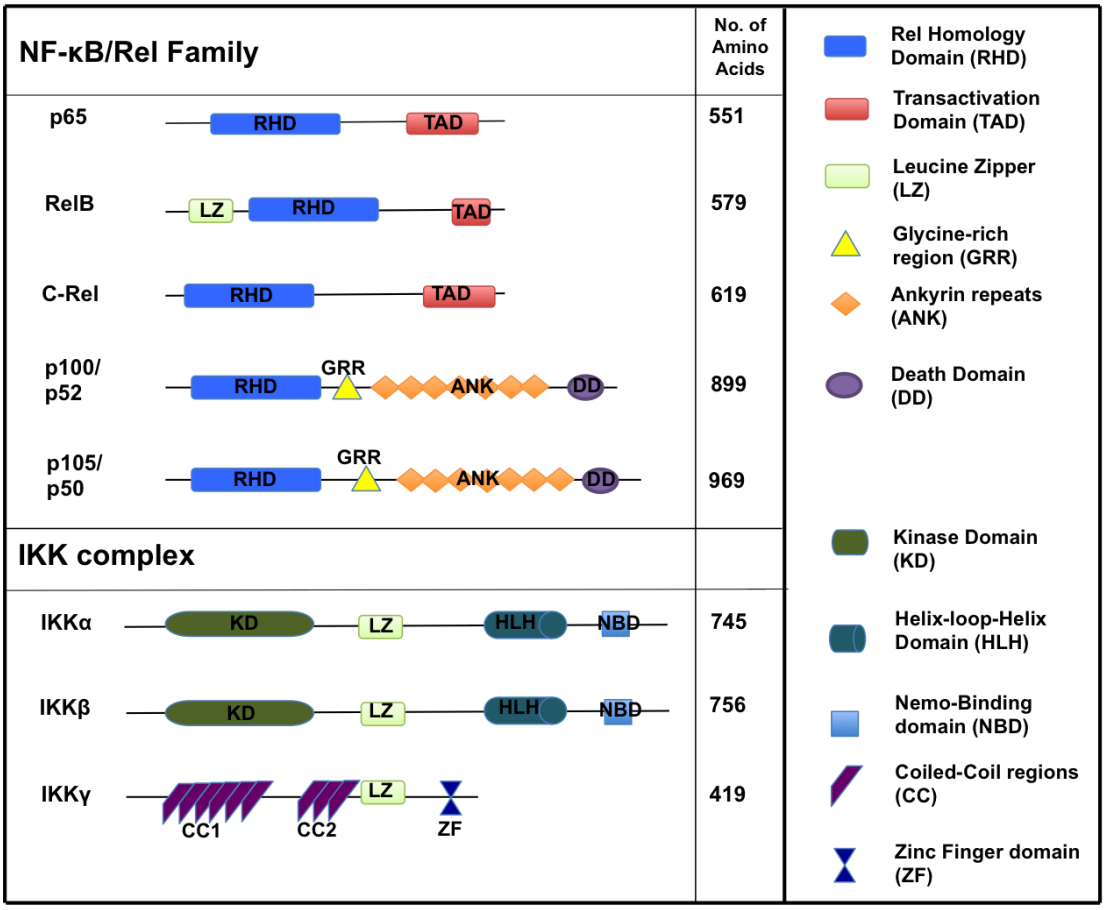

Figure 1.1. Schematic representation of NF-κB and IKK complex protein composition.

1.5.2 The Inhibitory Kappa B Kinases and the IKK complex

The IKK complex is comprised of three constituents; two catalytically active subunits IKKα and IKKβ and the catalytically inactive scaffold protein IKKγ or NF-kappa-B Essential Modulator (NEMO) (*Regnier et al, 1997; DiDonato et al, 1997; Zandi et al, 1998; Rothswarf et al, 1998*) . The catalytically active component IKKα and IKKβ share 52% sequence homology with the essential leucine zipper (LZ) motif sequence required for the binding and formation of the IKK homo- and heterodimers, the LZ motif is also essential for the kinase activity of both IKKα and IKKβ (*Mercurio et al, 1997*). IKKα and IKKβ both share a homologous C-terminal Helix-Loop-Helix (HLH) domains and the NEMO-binding domain scaffolding sequence at the extreme C-terminal, which allows for the scaffolding of NEMO and the formation of active IKKα/β/γ complex. This sequence is L-D-W-S-W-L (Leu-Asp-Trp-Ser-Trp-Leu) and is known as the NEMO-Binding Domain (NBD) and through this sequence the interaction of IKKα/IKKβ and NEMO is mediated (*Solt et al, 2009*).

The IKK complex can assemble in a combination of both homo- and hetero-dimers and the nature of the complex assembly defines by which mechanism the pathway acts. The canonical function (Figure 1.2) of the NF- κB pathway is predominantly mediated by the hetero-dimeric form of the IKK complex comprising of IKKα, IKKβ and the scaffolding protein IKKγ (NEMO) complex in a 1:1:2 ratio (*Yamamoto et al, 2001*). This complex regulates the phosphorylation of IκBα and IκBβ at Ser32 and Ser36 in IκBα and Ser19 and Ser23 in IκBβ after which they are ubiquitinated and subsequently degraded releasing the NF-κB proteins for nuclear translocation and so driving the up-regulation of gene expression through interactions with the promoter regions of NF-κB dependent genes. This is known as the canonical pathway. The IKKβ subunit plays an essential role in the canonical pathway and 'knockout' experiments in mice (*Hu et al, 1999; Tanaka et al, 1999*) show that regardless of the high sequence homology IKKα is not necessary for the activation of the canonical NF-κB pathway it can however replace the activity of IKKβ when it has been conditionally knocked out in mouse models (*Yamamoto et al, 2004*;*Solt et al, 2009*). These deletion models however are embryonically lethal highlighting the fundamental roles of the NF-κB pathway in cellular functions. In these models there were differing phenotypic outcomes to

deletion between kinases, IKKβ deficient embryos were observed to have severe extensive apoptosis in the liver leading to mortality also observed in NF-κB deficient models (*Li et al, 1999*). However in IKKα deficient embryos exhibit abnormal skeletal and craniofacial morphogenesis, which does not align with what is observed with NF-κB deficient models (*Sil et al, 2004*). These studies highlight the differences in transcriptional function these two subunits regulate.

IKKα although not an essential component of the canonical signalling pathway is essential for the activation of what is referred as the non-canonical pathway or alternative pathway. The non-canonical signalling pathway is regulated by IKKα homo-dimers, without the scaffolding protein NEMO, processing the NF-κB proteins RelB/p100 to RelB/p52 by the site specific ubiquitination of p100 allowing for nuclear translocation of RelB/p52, binding to promoter regions and up-regulation of NF-κB dependent genes (*Xiao et al, 2001*). The association of IKKα and NEMO is not essential for the non-canonical NF-κB pathway and in deletion of IKKβ was unable to rescue the canonical signalling. It is the association of NEMO and the NF-κB subunits undergoing processing which are used as the defining features that allow for the categorisation of these pathways into either the canonical or non-canonical forms (see Figure 1.2).

The IKK complex and NF-κB signalling is an area of intense research and the research done into this signalling cascade has made it increasingly apparent that the functions are not limited solely to NF-κB signalling. IKKα has been recently shown to associate and regulate with several new substrates e.g. de-repression of the silencing mediator for retinoic acid and thyroid hormone receptor (SMRT) (*Hoberg et al, 2005*) and phosphorylation of the Histone H3 in the nucleus (*Yamamoto et al, 2003*). Aurora A kinase has also recently been identified as a potential novel substrate of the IKK complex linking the NF-κB pathway to mitotic progression and the regulation of the cell cycle. In a 2006 study *Prajapati et al* showed that *in vitro* IKKα could be observed to regulate the phosphorylation of Aurora A kinase in the activation loop at the Threonine 288 residue, essential for the full activation of Aurora A suggesting a role for IKKα in M-phase of the cell cycle (*Prajapati et al, 2006*).

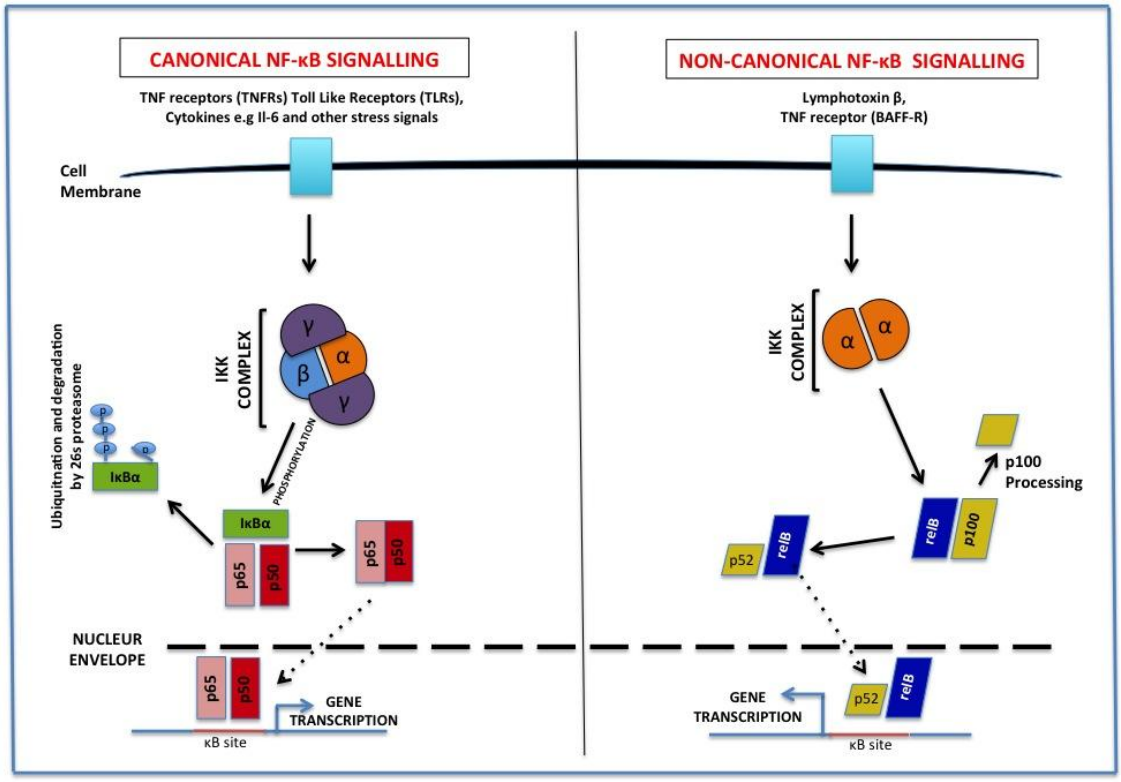

Figure 1.2. The Canonical and Non-Canonical NF-κB pathways.

1.6 Roles of the NF-κB signalling pathway in cancer

The involvement of the NF-κB signalling pathways in the formation and proliferation of tumour growth is an area of research under significant scrutiny. The hallmarks of cancer as defined by *Weinberg et al* (*Hanahan et al, 2011*) include limitless growth potential, independence from external growth stimuli, resistance to apoptotic signalling, sustained angiogenesis, tissue invasion and metastatic capabilities. The function of the NF-κB signalling pathways can be directly linked to several of these essential factors in tumour development. Increased activity of the NF-κB signalling pathway has also been observed in many of the most prevalent solid tumour cancer types e.g. lung (*Chen et al, 2011*), breast (*Shostak et al, 2011*), colon (*Sakamoto et al, 2010*) and prostate (*Jain et al, 2012*). It has also been observed in haematological malignancies such as multiple myeloma and leukemia *(Hideshima et al, 2009*). The observation of increased activity of this signalling cascade however only implies a relationship between the NF-κB signalling pathway and oncogenesis. However this increase in activity of NF-κB signalling has been linked directly to several essential features in the development of cancers through extensive research utilising both *in vitro* and *in vivo* methodologies and through these studies it has been demonstrated that the NF-κB signalling pathway can affect all of the hallmarks of cancer as defined in *Weinberg et al 2011.*

1.6.1 Malignant proliferation

Uncontrolled growth is an essential feature of carcinogenesis driving the formation of tumours, this is often regulated through the increased expression of growth factors, and e.g. platelet derived growth factor (PDGF) or transforming growth factor - alpha (TGFα). The over-expression and up-regulation of growth factor receptors can also lead to an increased in proliferative effects driving the growth of malignant cells (*Hanahan et al, 2011*). The NF-κB signalling pathway has also been shown to affect cellular proliferation as many of the target genes of the pathway play a significant role in proliferation. These target genes include cyclin D1, cyclin E and CDK2, which are essential components for the correct transition of the cell to progression through the cell cycle (*Pahl et al, 1999*). NF-κB target genes also include growth factors including

the cytokine IL-6 a growth factor for hepatocytes. Over-expression of IL-6 has been linked to Hepatocellular carcinoma through a MyD88/ IKKβ essential mechanism (*Naugler et al, 2007*); genetic studies in myeloid cells also show the decrease in IL-6 production upon IKKβ deletion prevents the proliferation of colitis associated colon cancers (*Becker et al, 2004*). In breast cancer models the link between NF-κB signalling and cellular proliferation is mediated through the interaction of IKKα and cyclin D1. Studies using inactive forms of IKKα were shown to prevent proliferation and significantly reduce tumour growth in the Neu/ErbB2 model as opposed to models in which tumours are activated through the Ha-Ras oncogene (Downward et al, 2003). Oestrogen receptor negative breast cancer cells often rely on the ErbB2/Her2 pathway to drive proliferation and this opens up the treatment with NF-κB inhibitors as a therapy in this form of disease with studies *in vitro* validating this as an effective treatment (*Cao et al, 2007* and *Singh et al, 2007*).

Mutation also plays an important role in the dysregulation of the proliferative signalling leading to the uncontrolled growth characteristics of cancer cells. The most commonly associated somatic mutation of cancer cells is of the RAS signalling pathway observed in 20-25% of all human tumours, its prevalence increasing further up to 90% in pancreatic cancers (*Downward et al, 2003*). NF-κB has also been shown to have several associated mutations acting to promote carcinogenesis. A study into roles of the NF-κB pathways in multiple myeloma highlights mutations of two proteins in particular, which play a significant role in the development of this disease. The first mutations are of NF-κB Inducing Kinase (NIK) through over-expression arising due to translocation or amplification of the genes LOCUS or mutations leading to the enhanced stability of NIK and as an upstream regulator of the non-canonical pathway promoting tumour cell survival. The second mutations of note were inactivating mutations in the form of homozygous deletion or the epigenetic silencing of TRAF3. The loss of TRAF3 function leads to the promotion of tumour cell survival through the NF-κB pathway although the mechanism that is yet to be fully elucidated (*Annunziata et al, 2007*) although it is suggested that it is mediated through stabilisation of NIK promoting non-canonical NF-κB signalling.

1.6.2 NF-κB and the evasion of apoptosis.

The NF-κB signalling pathway not only plays a role in the proliferation of cancerous cells but also in the evasion and prevention of apoptosis, the prevention of apoptosis has long been defined as a function of NF-κB and is perhaps the clearest mechanism by which NF-κB can promote tumourigenesis (*Karin et al, 2006*). The apoptotic pathways are a self-regulatory process by which immune and genetic mechanisms regulate and control correct cellular growth and prevent malignancies from developing. The primary function of many of the NF-κB target genes is the suppression of apoptotic signalling and includes Bcl-2, Inhibitors of Apoptosis (IAPs) and c-Flip. The link between NF-κB and apoptosis in cancer progression was observed in studies which noted an increased resistance in cancer cells to apoptosis, but when NF-κB signalling was disrupted there was an increase in sensitivity to apoptosis (*Rahman et al, 2007*). NF-κB can affect apoptosis at several different level of the signalling, with upstream components such as IKKβ phosphorylating and promoting the degradation of Forkhead Box O3a (FOXO3a), a pro-apoptotic transcription factor observed in several cancer cell types (*Hu et al, 2004*). The NF-κB mediated control of anti-apoptotic gene expression can also be implicated for example in a study investigating cell survival of Hodgkin and Reed-Sternberg cells (H/RS) in Hodgkins lymphoma. It was observed that when the NF-κB pathway was disrupted using the super-repressor form of IκBα a small characteristic group of genes were no longer expressed; the anti-apoptotic proteins Bfl-1/A1, c-IAP2, TRAF1, and B-cell lymphoma-extra-large (Bcl-xl), the cell cycle protein cyclin D2 and two cell surface receptors CD40 and CD86. Increased expression of these proteins all serve as markers of cancer in both primary and cultured forms of H/RS cells, the inhibition of NF-κB by this mechanism also induced significant levels of apoptosis in these cells although were able to be rescued through the expression of the pro-survival gene Bcl-xL (*Hinz et al, 2001*). The regulation of expression of CD40 and CD86 cell surface markers is an interesting feature of the NF-κB signalling in this cellular system as these are both TNF-activated receptors and are upstream regulators of the NF-κB pathway (*Rickert et al, 2011*) showing a self-regulatory mechanism controlling gene expression. This study serves to highlight the integral role of aberrant NF-κB signalling has within the proliferation and pro-survival signalling observed in Hodgkins lymphoma, with proliferative proteins (Cyclin D2), pro-survival protein (Bfl-1/A1, c-IAP2, TRAF1, Bcl-xL) expression and also the increased expression of NF-κB activating

cell surface receptors (CD40 and CD86) all working in concert to drive the progression of this cancer. It can be used as an example of the multi-faceted mechanisms by which NF-κB can regulate cancer progression.

Finally, a key mechanism of apoptotic signalling is the production of reactive oxygen species (ROS) through the c-Jun NH2 -terminal kinase (JNK) pathway. Studies carried out in IKKβ-deficient Hepatocellular Carcinoma cells (HCC) show that NF-κB will suppress persistent JNK mediated generation of ROS acting as a pro-survival mechanism in this form of cancer (*Bubici et al, 2006*). The subversion of apoptosis by NF-κB signalling shows another mechanism by which this pathway is intrinsically linked to the development and progression of cancers.

1.6.3 Metastasis and angiogenesis regulated via the NF-κB pathway

The NF-κB pathway has been shown to be involved in carcinogenesis and play a role in the early stages of cancer in the tissue. The role it plays in the disease however is not just limited to initial development and continuous growth of the tumour but also to the spread and further establishment of the disease in the body. The progression of cancer from its early stages to metastatic forms requires a shift in the signalling and molecular mechanisms driving the proliferation of the tumours. Although the exact pathways by which these changes occur are not fully understood there have been studies carried out to help elucidate this mechanism, one of the best examples of which specifically links NF-κB to the metastatic potential of prostate cancer. The over-expression and increased nuclear activation of the regulatory component of the non-canonical NF-κB pathway, IKKα, has been linked to the repression of Maspin, a metastatic suppressor protein. The expression of Maspin negatively associated with the levels of activated nuclear IKKα in late stage metastatic prostate cancer that is thought to be regulated through the expression of RANK ligand (RANKL) a previously defined IKK activator (*Bubici et al, 2006, Cao et al, 2001*). The Receptor Activator of NF-κB (RANK) is a member of the Tumour necrosis Factor (TNF) family of cytokines, expressed in numerous epithelial cell and mammary cells as well as in several cancerous malignancies. Infiltration of the advanced prostate tumours by T-Cells expressing RANKL, activator of the RANK receptor on the over-expressed in the malignant cells

and has also been suggested to be responsible for this mechanism of nuclear IKKα activation (*Maeda et al, 2005*). This link between the RANK receptor activation and IKKα mediated Maspin repression was also observed in breast cancer mice models and in the migration of melanomas to bone metastases in previous studies (*Luo et al, 2007*).

A critical step in the formation and continued growth of solid phase tumours is the formation new of blood vessels once the malignancy is too large for the native blood supply, this will act to provide the essential nutrients and oxygen while removing cellular waste products and carbon dioxide (*Hanahan et al, 2011*). Developing neovasculature in the tumour microenvironment is how cancer manages this. The formation of this new vasculature is often mediated through Tumour-Associated Macrophages (TAMs), which can act to both to create a immunosuppressive environment and to secrete a range of cytokines/chemokines and other factors aiding in the promotion of angiogenesis, metastasis and growth (*Hao et al, 2012*). The release of many of these cytokines including TNFα, IL-1, and IL-6 are all controlled through NF-κB signalling. The roles of IL-6 promoting cellular proliferation via IKKβ have been previously discussed, however this cytokine in conjunction with IL-1 and TNFα have all been shown to stimulate the activation of Vascular Endothelial Growth Factor (VEGF) a primary regulator of angiogenesis and itself a target of NF-κB mediated gene expression (*Su et al, 2004, Bancroft et al, 2002*). This was observed in prostate cancer cells after the blockade of NF-κB led a significant decrease in the expression of VEGF, IL-8 and MMP-9, a matrix metalloproteinase, all key for neoplastic angiogenesis (*Huang et al, 2001*). Furthermore a study in 2003 tied the expression of VEGF by macrophages in a NF-κB-dependent manner again linking the NF-κB pathway to the promotion of the tumour microenvironment created by TAMs (*Suh et al, 2004*, *Kiriakidis et al, 2003*).

There is a significant amount of literature linking the IKK complex and NF-κB signalling to a wide range of functions in cancer and for this reason they have been the focus of considerable efforts to develop novel therapeutics applicable to not only to cancer but a range of inflammatory-based diseases.

1.7 Development of IKK inhibitors

The IKKs are well defined essential regulators of the pro-inflammatory NF-κB signalling pathway which has been shown widely to play a role in many inflammatory diseases such as rheumatoid arthritis, Irritable bowel syndrome and asthma (*Grivennikov et al, 2010*), and also in the development of cancer through either the promotion of anti-apoptotic, proliferative responses as well as metastasis, inducing gene expression or NF-κB-independent roles in the regulation of the cell cycle. The NF-κB pathway as previously discussed has a broad spectrum of upstream activating mechanisms and resulting in highly varied downstream gene expression, closely regulated by the upstream signal. Despite the diverse functions of the signalling pathway all outcomes of the NF-κB pathway require at least one of the IKK family members to mediate the signalling (*Liu et al, 2012*). This has led to the IKKs being an attractive drug target hotly pursued in both academic and industrial research. There have been large scale and wide ranging implementation of High Throughput Screening (HTS) and 'hit-to-lead' development programmes designed to identify small-molecule inhibitors that target different structural features of the IKKs. This research has led to a wide range of small drug-like molecules being developed with two modes of action; adenosine tri-phosphate (ATP) competitive inhibitors acting on the kinase domain or allosteric binding compounds which act to reduce kinase activity. A major challenge has been the fact that the kinase domains of the IKKs are highly conserved across both kinases however a wide variety of compounds have been developed and pursued to target IKK function, the majority displaying selectivity for IKKβ. These compounds were initially tested *in vitro* against a range of cells and then carried forward into *in vivo* models of disease establishing potency. There have been promising effects pre-clinically however use of these inhibitors in the clinic are yet to be reported (*Gamble et al, 2012*). Table 1 shows a range of well-characterised IKK inhibitors from a variety of companies effective in blocking IKK-NF-κB signalling in pre-clinical animal models of disease; all compounds exhibit a high selectivity for IKKβ inhibition with supporting cellular and *in vivo* data.

Inhibitor molecule Chemical structure Chemical name	IC50s IKKα vs. IKKβ	Cell-based studies (Refs.) In *vivo* analysis (Refs.)
Bayer compound A 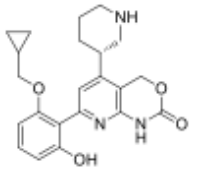 2-Amino-3-cyano-4-alkyl-6-hydroxyphenyl)pyridine	135nM vs. 2nM	B/T-lymphocytes, HEKs, PBM (Murata et al., 2003, 2004a, b). Pulmonary inflammation (Ziegelbauer et al., 2005).
PS-1145 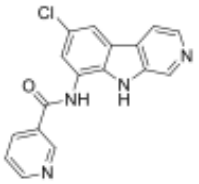 N-(6-chloro-9H-b-carbonlin-8-yl) nicotinamide b-carboline	>100 000 nM vs. 100 nM	HeLa cells (Castro et *al*., 2003). LPS-induced TNFα production (Castro et *al*., 2003).
ML120B 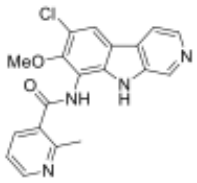 N-(6-chloro-7-methoxy-9H-b-carbonlin-8-yl)-2-methyl-nicotinamide b-carboline	>100000 nM vs. 45 nM	Synoviocytes, chondrocytes, mast cells (Wen et *al*., 2006). Inflammatory arthritis model (Schopf et *al*., 2006).
BMS-345541 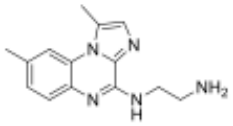 (4(2'-aminoethyl)amino-8-dimmethylimidazo(1,2*a*)quinoxaline)	4000nM vs. 300nM (N.D. vs. 10 – 60 nM)	HUVECs (MacMaster et *al*., 2003), THP-1 monocytes (Beaulieu et *al*,. 2007). Colitis model (MacMaster et *al*., 2003), LPS-induced TNFα production (Burke et *al*., 2003).
Wedelolactone 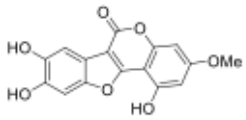 7-Methoxy-5,11,12-trihydroxy-coumestan	< 10 mM vs. < 10 mM	BALB/c fibroblasts, HeLa cells, murine splenocytes (Kobori et *al*., 2004). No information.

Table 1.1. An overview of IKK inhibitors and their structures.

1.7.1 ATP competitive inhibitors targeting the IKKs

"Compound A"

The first of the IKK targeted compounds in the table is the Bayer 'Compound A' developed by Bayer after a screen of their compound library supplied a 'hit' (*Murata et al, 2003*). Following, lead optimisation to improve the *in vitro* activity (*Murata et al, 2004*) the molecule termed 'Compound A' was shown to be a potent IKKβ selective inhibitor (*Murata et al, 2004*), showing IC_{50} values of 135 nM for IKKα and 2 nM against IKKβ (*Gamble et al, 2012*). Throughout the optimisation of this compound it was tested against a wide variety of cell types including Human embryonic kidney (HEK) cells, peripheral blood mononuclear cells (PBMC) and both B and T-lymphocytes (*Murata et al, 2003, Murata et al, 2004 and Murata et al, 2004*) and was followed with a study *in vivo* investigating the effect of 'Compound A' on pulmonary inflammation in a model of asthma. It was shown to be effective suggesting IKKβ inhibition was a viable target in the treatment of chronic pulmonary inflammation (*Ziegelbauer et al, 2005*).

PS1145 and ML-120B

The second and third compounds in Table 1.1, PS1145 and ML-120B, are both based around the same β-carboline scaffold and manufactured by Millennium Pharmaceuticals. These compounds were both shown to be highly selective towards IKKβ with a >100,000nM IC_{50} for IKKα and 45nM IC_{50} against IKKβ in the case of ML-120B and the less potent PS1145 had a similar IC_{50} values for IKKα being >100,000nM and IKKβ at 100nM (*Catley et al, 2006*). Both compounds have been shown to be effective in reducing inflammatory signalling in Human airway smooth muscle cells and have been suggested as a potential treatment for Asthma and Chronic Obstructive Pulmonary Disease (*Catley et al, 2006*). These compounds were also shown to be effective in synoviocytes, chondrocytes, mast cells to reduce inflammatory signalling as components of Rheumatoid Arthritis (*Wen et al, 2006*). Both compounds have also been used *in vivo* and shown to been effective in the treatment of multiple disease states, ML-120B specifically was observed to suppress antibody-induced Arthritis in both clinical and histopathological models (*Izmailova et al, 2007*) and through the

inhibition of IKKβ, ML-120B protected against bone marrow and cartilage destruction in rat models of Rheumatoid Arthritis (*Schopf et al, 2006*). PS1145 showed activity against lung inflammation in mouse models (*Newton et al, 2007, Chapoval et al, 2007*) and by reducing LPS-induced production of TNF in mice (*Yemelyanov et al, 2006*). These two compounds and 'Compound A' described above all have a similar mode of action in so far as they act as ATP competitive inhibitors.

1.7.2 Allosteric inhibitors and Natural product inhibitors of the IKKs

BMS 345541

Alternative mechanisms of action against and inhibition of IKK have been explored, an example of which is the Bristol Myers Squibb (BMS) compound BMS-345541. This has a much lower selectivity for IKKβ with only a 10-fold difference in IC_{50} values; 4000 nM IKKα vs. 300 nM IKKβ (*Catley et al, 2006*). In kinase assays *in vitro* it was shown to have non-mutually exclusive ability to bind to a peptide substrate and Adenosine Di-phosphate (ADP) in IKKβ while the inverse is true of IKKα. The mechanism of action has been proposed to be through allosteric binding to different regions on IKKα and IKKβ to leading to conformational changes of the active site specific to each subunit which affect the ability of ATP to bind and therefore the activity of the IKK complex (*Burke et al, 2003*). In cell-based studies it was shown to limit the function of IKKα and IKKβ in THP-1 cells (*Burke et al, 2003*) and HUVECS (*MacMaster et al 2003*). It has also been tested *in vivo* showing reduced TNF-α production in LPS-challenged mouse models (*Castro et al, 2003*) and as an effective treatment of dextran sulphate induced mouse colitis (*MacMaster et al, 2003*). BMS34551 like the compounds described above have all been developed through HTS strategies investigating synthetic small molecules however natural products are a well-established source of compounds to be developed into novel pharmacological agents.

Wedeloactone

Wedeloactone is an example of a natural product effective in targeting the IKKs, acting as an irreversible inhibitor of both IKKα and IKKβ with IC_{50} values for both enzymes <10mM; the efficacy was tested across a wide range of cell types including HeLa cells,

BALB/c fibroblasts and murine splenocytes (*Kobori et al, 2004*). Natural products have been heavily researched with respect to inhibition of NF-κB signalling (*Bremner et al, 2002; Luqman et al, 2010*) however have not been well studied in the context of IKK inhibition and the mechanisms by which they act the IKK complex remain to be fully elucidated.

The compounds described are a small selection of the constantly increasing libraries being developed, however the use of small molecule inhibitors directly targeting the kinase activity is not the only mechanism by which inhibition of the IKK complex is being approached.

1.7.3 Limitations of Small-molecule IKK inhibitors

These compounds all show activity against both IKKα and IKKβ, the high level of homology between these two subunits can be linked to this cross reactivity however these compounds almost uniformly show greater inhibition (Table 1.1) of IKKβ compared to IKKα. Although the reasons for this disparity are yet to be elucidated it suggests that subtle differences in the structures could be responsible. The difficulty in the development of these inhibitors lies in this cross reactivity and the effect of the pleiotropic outcomes of disrupting the IKK signalling. Although each activating stimulus of the NF-κB pathway converges on the IKK complex, they can all result in varying patterns of gene expression dependent on the upstream signals. This may be controlled through the different adapter proteins which mediate the upstream signals or through differential composition of the IKK complex into the various homo- and hetero-dimers possible (*Hayden et al, 2008*). In order to target the IKK complex as a mediator of the NF-κB signalling pathway it is therefore very important to fully understand these activating mechanism and also the effect of inhibition on the downstream effects on transcriptional regulation or other NF-κB-independent functions the IKKs have. The IKK complex has been linked independently of the NF-κB pathway to the cell-cycle (*Prajapati et al , 2006, Irelan et al, 2007*), proliferation, immune function and cell survival (*Chariot,* 2009) which all must be considered when developing novel therapeutics to minimise toxicities. The use of ATP competitive inhibition strategies is problematic in itself as the kinase domain is conserved across a wide range of enzymes which have many functions in the cell and can lead to significant

off-target effects (*Garber et al, 2006*), mutations of the kinase domain are also very common particularly in cancer and are mechanisms by which cancers can become resistant to treatment (*Karvela et al, 2012, Bonanno et al, 2011*). There has been therefore a focus on developing disruptors that do not specifically target either the kinase domain or act in an ATP- competitive manner e.g. the allosteric inhibitor BMS-345541. Research into kinase inhibition has led to an effort to find entirely novel targets from the kinase domain such as substrate competitive inhibitors (*Licht-Murava et al, 2011*) or the targeting of binding to activating proteins.

1.8 Protein-protein interactions as drug targets against the IKK complex

1.8.1 The Nemo-Binding Domain and disruptor peptides

An alternative target for the inhibition of the IKK complex that has come under some significant research is the disruption of the protein-protein interactions (PPIs) occurring between members of the IKK complex. The aim is to modulate the gene expression outcome specific to different IKK complex compositions that can significantly reduce IKK complex activity. The most successful of example of this approach is the development of the NEMO binding domain (NBD) peptide. This peptide mimics the binding site of NEMO with IKKα/β, this region contains a central conserved hexapeptide sequence L-D-W-S-W-L which occurs in a hydrophobic pocket of IKKα and IKKβ, predicted initially by the use of hydropathy plots (*May et al, 2000*) and was fully outlined through the analysis of the co-crystallisation of NEMO-binding domain peptide and a truncated form of NEMO (*Rushe et al, 2008*). Initial studies in the development of these peptides carried out by *May et al,* show that the NBD peptide can act as competitive disruptor of the interactions between NEMO and IKKα or IKKβ, disrupting the preformed IKK complexes through displacement of the IKKs from the hydrophobic pocket of NEMO (*May et al, 2002*). Interestingly, the concentrations required to disrupt the binding of IKKβ and NEMO were significantly higher than that required to disrupt IKKα/NEMO (*May et al, 2000*) which fits with the well characterised role of the IKKβ/NEMO interaction in the canonical pathway compared to the poorly understood

functions of the IKKα/NEMO interactions in non-canonical signalling. The NEMO-binding domain peptide was used in assays *in vitro* as either an 11 or 12 mer peptide derived from the primary amino acid sequence surrounding the core hexapeptide sequence effectively in the down regulated NF-κB target gene transcription (*May et al, 2004*). To investigate these peptides *in vitro,* and to allow for trafficking across cellular plasma membranes, they have been formulated with the addition of membrane transduction sequences derived from either *Drosophila* antennapedia protein (D-R-Q-I-K-I-W-F-Q-N-R-R-M-K-W-K-K) or from the HIV-1 Trans-Activator of Transcription (TAT) protein transduction domain (Y-G-R-K-K-R-R-Q-R-R-R) (*Console et al, 2003*). The NBD peptide inhibition of NF-κB signalling has been extensively investigated in both *in vitro* and *in vivo* settings, in these studies a WT NBD peptide is used alongside a dual Trp-Ala mutation of the NBD which serves as the control by reducing the binding ability of the peptides. Initially observed to block the TNF- and IL-1-mediated NF-κB activation in HeLa cells, NO production by macrophages and TNF-mediated adhesion molecule expression in vascular endothelial cells (*May et al, 2000*). These peptides were further investigated and successfully used to block osteoclast differentiation (*Jimi et al, 2004, Dai et al, 2004*) *in vitro* and to inhibit the activation of intestinal epithelial cells, B-cells, T-cells, macrophages, neutrophils and dendritic cells (*Orange et al, 2008*). The NBD peptides have also been shown to be effective in a wide range of cell types and disease models *in vitro* and more recently have been tested *in vivo* against a range of models including inflammatory arthritis where it successfully reduced osteoclast formation and therefore reduced bone erosion (*Dai et al, 2004*). Models of Rheumatoid arthritis were also used and the NBD peptide was effective in reducing the NF-κB gene expression and subsequently down-regulating inflammatory signals decreasing bone cartilage destruction and bone erosion as well as an overall reduction in osteoclast formation (*Jimi et al, 2004*). Other examples include mouse and rat models of pancreatitis (*Ethridge et al, 2002, Long et al, 2009*) where it was observed to reduce inflammation and the associated tissue damage. The NBD peptides act by reducing neutrophil infiltration and necrosis, down-regulating p65 expression and mononuclear cell invasion of the spinal cord in Experimental allergic encephalomyelitis (EAE) mouse models improving clinical symptoms and slowing disease progression (*Dasgupta et al,2004*) . The use of the NBD peptide across the range of *in vitro* and clinically relevant *in vivo* disease models to successfully block pro-inflammatory cytokine induced NF-κB activation while leaving the basal activation unaffected is a very attractive feature of using these peptides as it may contribute to a decrease in unwanted side effects such as

increased apoptosis (*Kucharczak et al, 2003*). The NEMO binding domain and associated disruptor peptides although well studied in the inflammatory disease setting both *in vitro* and *in vivo* have not been used in cancer models *in vivo* as of yet. This is an area in which they could be of significant use and is an exciting area to be investigated further.

The NBD peptides proved successful in affecting the regulation of NF-κB in disease models however limitations to this approach are apparent. Most notably due to the NBD being present in both IKKα/β therefore the NBD peptide can disrupt the interaction of IKKα and NEMO (*May et al, 2000*), although this relationship remains poorly understood and the effects IKKα/NEMO interaction disruption are still unknown. The NBD peptide itself will prove to be invaluable as a pharmacological tool in the elucidation of the functions of this domain and the PPIs it mediates both *in vitro* and *in vivo*.

1.8.2 Substrate specific NF-κB targets for Cell Permeable Peptides (CPP)

The success of the NBD cell permeable peptide in down-regulating the NF-κB pathway led to the development of peptides targeting the IKK-binding domain on NEMO, these peptides however were not able to disrupt the IKK complex and in fact increased signal induced NF-κB activity (*Marienfield et al, 2006*). Further mutant peptides in this study highlighted the requirement of NEMO oligomerisation for the correction formation of the IKK complex assembly (*Marienfield et al, 2006*). Peptides targeting regions essential for NEMO oligomerisation were also investigated and have been shown to inhibit NF-κB gene expression and induce apoptosis in cells (*Agou et al, 2004*). The CPP's focused on the disruption of NEMO/IKK interactions are the most characterised of the NF-κB targeting peptide disrupters however CPPs targeting other critical components of classical NF-κB signalling e.g. p65 and IκBα phosphorylation, have also been developed. Phosphorylation of p65 occurs at serine residues at positions 276, 529 and 536 respectively; these modification are essential for the normal transactivating activity of p65, and peptides were therefore developed to mimic these residues and their surrounding sequences (*Takada et al, 2004*). These peptides were tested in human head and neck squamous cell carcinomas and against KBM-5 chronic myeloid leukaemia cells, where they were effective in the inhibition of constitutive activation,

cell proliferation and pro-inflammatory signal induced NF-κB (*Takada et al, 2004, Aggarwal et al, 2004*) signalling. Similarly peptides were developed against the essential phosphorylation events of IκBα responsible for the ubiquitination and degradation of the protein promoting NF-κB nuclear translocation to occur. The critical residues in this instance are the serines located at positions 32 and 36, peptides have not been targeted specifically against these residues rather have been developed as full-length chimeras of IκBα with the critical residues substituted to alanine or through the truncation of the N-Terminus encompassing the S32 and S36. Due to it's effectiveness at reducing IL-1β and TNF-stimulated NF-κB activity independent of ERK, MAPK and c-Jun when tested in HeLa, A459 and Jurkat cells the construct/peptide became known as the TAT super repressor (*Kabouridis et al, 2002*). This peptide has been tested *in vivo* against carrageenan-induced pleurisy and was effective in reducing the infiltration of leukocytes at sites of inflammation (*Blackwell et al, 2004*).

The use of CPP mediated peptide transduction as a method for pharmacological intervention has been shown extensively to be an effective mechanism in the down-regulation of NF-κB signalling in response to an array of different stimulus in a variety of cell types both *in vitro* and *in vivo.* The use of these peptides as a direct therapy is unlikely due to the high cost of the manufacturing the peptides themselves, they will however be very useful in the research and development of novel small molecule inhibitors either based upon CPP structures that have been validated in cells or the CPPs being used to validate PPIs as a novel target for intervention. The CPP peptides however are not only useful for in the development of pharmaceuticals they will also be invaluable tools for researchers to better understand the signalling components which regulate the IKK/NF-κB pathway and lead to the many transcriptional outcomes of this pathway.

The NF-κB field is constantly evolving and with it our understanding of its role in the cell. This will serve to help in the development of more effective drugs targeting IKK-NF-κB in the treatment of a vast range of diseases. A major limitation in the development of IKK inhibitors has been the difficulties in solving the crystal structures of the IKK complex, recently however the structure of *Xenopus* IKKβ in complex with an inhibitor was solved to a resolution of 3.6A (*Xu et al, 2012*). This will provide valuable structural information that will help inform future development and refinement of the current strategies against IKKβ and hopefully with this the structures of human forms

of IKKα and NEMO are forthcoming helping improve the synthesis of more specific inhibitors.

1.8.3 NF-κB independent substrates of the IKK complex as novel drug targets

Currently the development of drugs targeting the IKK complex have been targeted specifically towards its roles as a regulator of NF-κB signalling either through ATP-competitive inhibition or the use of CPPs against NF-κB substrates. However there is increasing evidence that both IKKα and IKKβ play many roles in the cell independent of NF-κB signalling and the increasing diversity in IKK function opens up novel avenues to be pursued in the development of IKK inhibitors through substrate specific inhibition.

These NF-κB independent IKK substrates can make attractive drug targets. IKKβ substrates include tumour suppressor FOXO3a (*Hu et al, 2004*) and 14-3-3β (*Gringhuis et al, 2005*) which both can play a role in cell proliferation and tumourigenesis. IKKβ phosphorylation of the insulin-receptor substrate-1 (IRS-1) leads to the inhibition of insulin signalling which can contribute to the development of type-2 diabetes (*Nakamori et al, 2006*). There are also several links to the MAP kinase-signalling pathway through IKKβ substrates including the inhibitory adaptor protein DOK1 (*Lee et al, 2004*) and IKKβ induced proteolysis of p105 can release TPL2, inducing MAP kinase regulated cellular proliferation (*Beinke et al, 2006*). The novel substrates of IKKα include; the transcriptional co-repressor SMRT which can de-repress transcription of NF-κB via the release of histone deacetylase-3 (HDAC3) (*Hoberg et al, 2005*), CREB binding protein (CBP) through which IKKα can phosphorylate Histone H3 regulating chromatin remodelling and gene expression of NF-κB target genes (*Yamamoto et al, 2003*) and the interferon regulatory factor-7 (IRF7) which induces Interferon alpha expression (*Hoshino et al, 2006*). IKKα can also play a role in controlling cellular proliferation through the regulation of cyclin D1, an essential regulator of the G_1/S phase transition in mitosis. Cyclin D1 is substrate of IKKα and the phosphorylation at Thr 286 by IKKα leads to the degradation of cyclin D1 inducing cell cycle arrest at the G_1/S phase transition (*Kwak et al, 2006*). However phosphorylation by IKKα of substrates β-catenin and oestrogen receptor-α (ERα), and its co-activator SRC3, both induce the Cyclin D1 promoter causing increased expression thus promoting cellular proliferation which may play a role in breast cancer oncogenesis (*Park et al, 2005*).

IKKα has also been shown to phosphorylate and activate the mitotic kinase Aurora A driving the cell through mitosis (*Prajapati et al, 2006*).

The identification of these novel substrates and their roles in essential cellular processes such as proliferation make this a pertinent strategy for the development of novel therapeutics against the IKK complex.

1.9 The Aurora kinase Family

The Aurora Kinases are a family of three highly conserved serine/threonine kinases essential for the correct progression of the cell through mitosis. First identified in 1995 by *Glover et al* when screening for genes regulating spindle function in *Drosophila,* it was observed that mutations of the gene Aurora led to failure of the centrosome separation and bi-polar spindle formation. This led to the formation of Circular mono-polar spindles leading to pupal lethality and mitotic arrest (*Glover et al, 1995*). Previously however a homologous gene was identified in 1993 in *Saccromyces Cervesiae* named *IpL1* and confirmed to be essential for the progression of cells through the cell cycle (*Chan et al, 1993, Bischoff et al, 1998*). From the first discovery of this homologue in fungi and then its discovery in multi-cellular organisms in the following years, there were homologues observed in many mammalian cells reported by research groups worldwide under a wide variety of nomenclatures. The Human homologues were first identified in 1998 by *Bischoff et al* and named Aurora A, B and C (*Bischoff et al, 1998*). All the Aurora homologues were recognised as being derived from a common ancestor and any sequence divergence observed was due to natural evolutionary pressures driving mutations to occur during gene duplication (*Caravagal et al, 2006*). In humans there are three homologues of the Aurora kinase each with unique functions, however in the lower organisms such as *Xenopus* or *Caenorhabitis elegans* only two have been identified corresponding to the human Aurora A and B. In *S. Cervesiae* only one form has been observed showing the closest homology to human Aurora B. This provides the evidence for the evolution and divergence in function from a common ancestor amongst the Aurora Kinase family (*Bolanos-Garcia, 2005*). Amongst the members of the Aurora kinase family there is a high level of sequence homology

observed in all human members of the subfamily with >70% homology observed in the catalytic domains of Aurora A, B and C. All three of the kinases share the same basic structural homology; an N-terminal domain 39-132 residues long, a Catalytic domain of 251 residues and C-terminal domain 15-20 residues long (*Fu et al, 2007*) as shown in Figure 1.3.

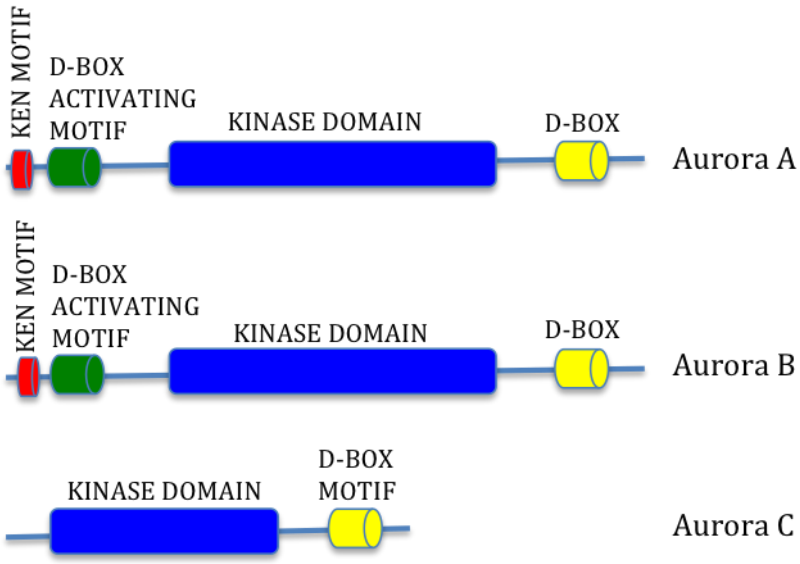

Figure 1.3 Schematic representations of all three members of the Aurora kinase Family.

The catalytic domains of all three Aurora kinases contain a structural feature known as the Activation loop. This is necessary for the correct function of these enzymes. In each member of the subfamily there is a key Threonine residue located within the activation loop, the phosphorylation of which is essential for the full activation of the Aurora kinase (*Bayliss et al, 2003*). This phosphorylation is regulated through the interaction with several distinct co-factors, all unique to Aurora A, B and C (*Karthiygeyan et al, 2010*). These act to regulate the specific activity of each Aurora kinase outwith the catalytic domain(s). The N-terminal domains however do not show the same levels of sequence homology and has been suggested to the function as an element of the protein structure that may regulate the PPIs specific to each member of the subfamily (*Carmena et al, 2003*). The N-terminal regions of Aurora A and B however do both contain the homologous sequence referred to as the A-box or D-activating Box, and in conjunction with the C-terminal D-Box has been shown to be required for the targeting of Aurora A for degradation by a E3 ubiquitin-ligase known as the Anaphase Promoting Complex/Cyclosome (APC/C). The APC/C and its specificity partner Cdh1 maintain the low levels of Aurora kinase A and B during early stages of the cell cycle and target it for destruction during mitotic exit (*Vader et al, 2008*). These structures arrange themselves around a hinge controlling the selectivity towards and positioning of the substrate. The N-terminal lobe has been shown to position the ATP-phosphate group through a αHelix and the C-terminal lobe harbours and positions the substrate for phosphorylation (*Yan et al, 2011*). The 26 amino acid ATP binding region is highly conserved between the three members of the subfamily, with only three differences observed all of which occur in Aurora A occurring at positions L215, T217 and R220 (Brown et al, 2004). The Aurora Kinases in spite of their sequence homologies have markedly different cellular spatio-temporal localisations and functions.

1.9.1 Aurora Kinase Localisation through the cell cycle

Aurora A kinase is ubiquitously expressed in the cell. The expression profile of this protein however changes throughout the cell cycle with expression levels remaining low until S-phase, and begin to increase again through G_2 and M phase eventually peaking during pro-metaphase. As mitosis is completed Aurora A is subsequently

degraded upon mitotic exit via the interaction with the APC/C. Aurora A is an essential regulatory mechanism for the control of mitotic entry, centrosome maturation/separation and bipolar spindle assembly (*Barr et al,* 2009). In prophase and metaphase Aurora A localises initially to the centrosomes and microtubules, then migrates during anaphase and telophase localising to the spindle mid-zone whilst also remaining at the centrosomes. Aurora B however is expressed later and becomes detectable only in prophase and maintains its expression until degradation at mitotic exit. Aurora B's specific functions include essential roles in chromosome condensation, sister chromatid condensation, correct chromosomal orientation, mitotic spindle assembly, checkpoint control and cytokinesis. Aurora B localises to the centromeres throughout pro-metaphase/metaphase and after the separation of the chromatids it relocates to the mid-zone of the cell where it remains until cytokinesis is complete. It then undergoes degradation via the APC/C pathway (*Caravagal et al, 2006, Fu et al, 2007, Vader et al, 2008*). The localisation of Aurora A and B are shown in Figure 1.4 with the functional roles they play at each stage of the cell cycle also outlined. Both Aurora A and B are ubiquitously expressed in all tissues across the body. Aurora C however has been shown to be predominantly expressed in the testes and plays a role in embryonic development and in meiosis (*Tang et al, 2006, Kimmins et al, 2007, Avo Santos et al, 2011*). The localisation and function of Aurora C is however poorly understood in comparison to Aurora A and B although it is worth noting that it was recently observed that in the absence of Aurora B, Aurora C can act to compensate and replace its mitotic functions (*Slattery et al, 2009*). In recent studies it was observed that the inclusion of a mutation of Glycine 198 to Asparagine in Aurora A it was possible to mimic the localisation and functionality of Aurora B although Aurora A and B are unable to compensate for the loss of each other (*Hans et al, 2009*). The Aurora kinases all show similar expression patterns in both their messenger RNA and protein levels, peaking during G_2/M phase of the cell cycle and their expression is closely linked during mitosis. However they maintain distinct localisation and function, as seen in Figure 1.4. These differences can be attributed to their relationships with the activating and regulatory proteins specific to each member of the Aurora kinase family and so maintain the distinct mitotic functions of these three kinases(*Karthigeyan et al, 2010*).

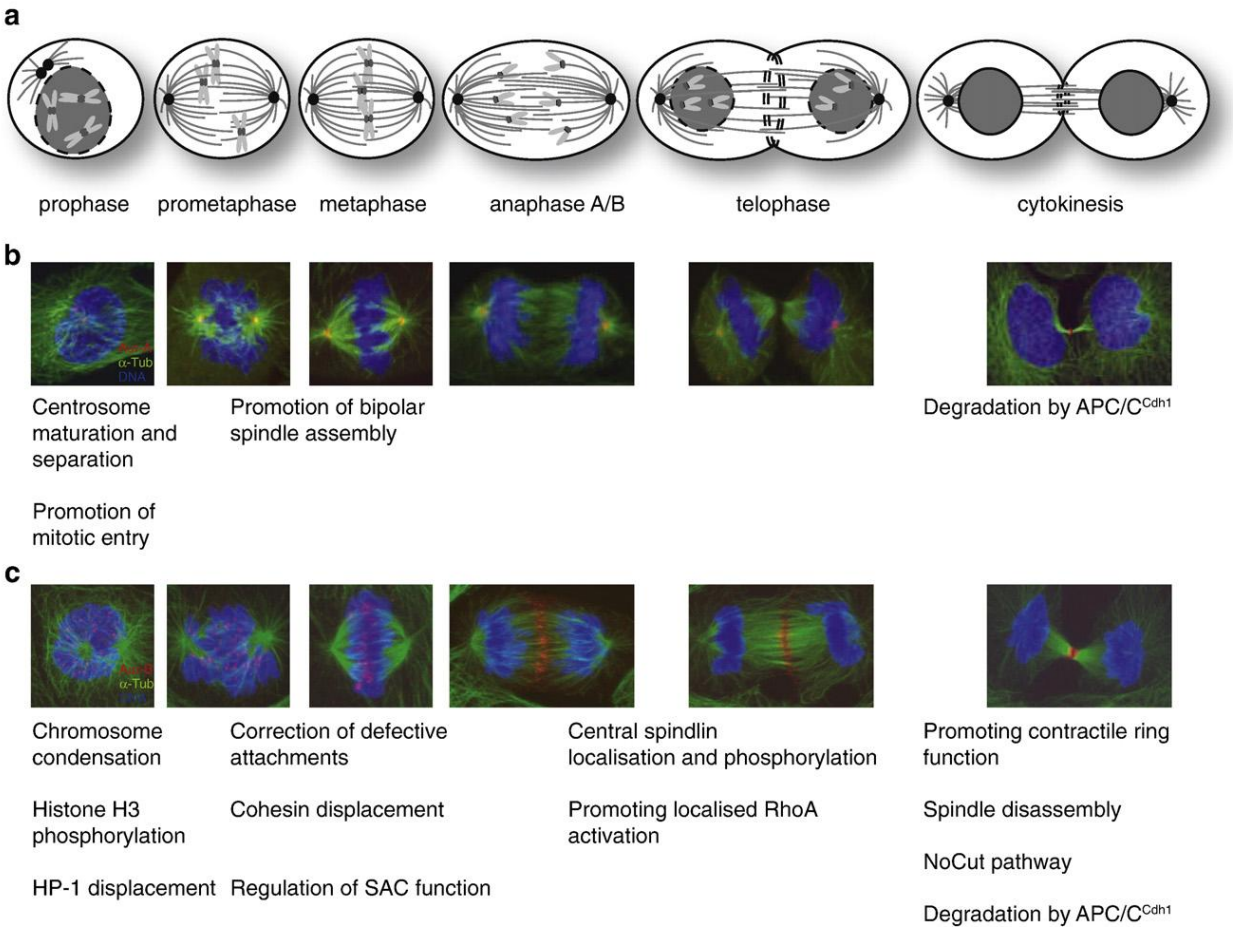

Figure 1.4. Localisation of Aurora A and Aurora B in Mitosis

a) Illustration of the mitotic stages in dividing cells. b) Aurora A (red) localisation throughout mitosis Aurora A can be seen to be localised to the centrosomes in early mitosis and moving to the kinetochores and chromatids promoting bi-polar spindle assembly. c) Aurora B (red) is seen mostly in mid-to late mitosis and localises strongly to the mid-zone of the cells where it acts in a regulatory role ensuring spindle attachment is correct and repairing faulty interactions. (Vader et al, 2008)

1.9.2 Roles of Aurora A kinase in the cell

There are several aspects controlling the regulation of expression and contribute to the activation of Aurora A kinase. The Aurora A gene is located on the chromosome locus 20q13 and mutations in this gene region are frequently observed in breast cancers (*Lengauer et al, 1998*) and prostate cancer (*Mosquera et al, 2013*). Aurora A has an open reading frame (ORF) of 1,209 base pairs which codes for the 403 amino acids comprising the Aurora A protein sequence. The transcription of the Aurora A gene is regulated by positive regulatory element 1 (PRE1) PRE1 is a 7 base pair sequence at position -85 and -79 and has the sequence CTTCCGG. This region controls the gene expression through the predominantly via the E4TF1 transcription factor, a member of the ETS family also containing the Aurora A regulatory factors Endothelial Growth Factor Receptor (EGFR) and GA-Binding Protein (GABP). E4TF1 is a hetero-dimeric complex of E4TF1-60 and E4TF1-53 with the ETS DNA binding region located in the N-terminal of E4TF1-60. The regulation of Aurora A kinase is tightly controlled with expression linked closely with cell cycle progression in particular expression of Aurora A only occurs during G_2/M phase. This is controlled at the transcriptional level by the CDE (cell cycle-dependent element)/CHR (cell cycle gene homology region) element which act as cell cycle specific repressor of transcription and are located downstream of the PRE1 region (*Tanaka et al, 2002*). Post-translational control of Aurora A kinase can be attributed to covalent modification of the kinase itself through interaction with co-factors specific to the functional outcomes and it is these modifications which are responsible for the functional control of Aurora A kinase. The phosphorylation of the threonine residue at position 288 (Thr288) of Aurora A is an important step in the full activation of this kinase and is controlled through (auto) phosphorylation mediated by several interacting proteins. The Thr288 residue is located in the activation loop near the ATP-binding region and it is the phosphorylation of this residue which regulates the kinase activity, the preceding threonine residue at position 287 can also rescue activity in the case of Thr288 mutation (*Zhao et al, 2008, Walter et al, 2000*). The underlying mechanism of auto/phosphorylation of Thr288 in Aurora A is poorly understood with several different activator proteins suggested to play a role. *Zhao et al* in 2005 showed that p21 Protein Activated Kinase 1 (Pak1) binds and can promote the phosphorylation of Aurora A kinase at Thr288 in *Xenopus* models (*Zhao et al, 2005*). This mechanism however has not been confirmed in human studies. The status and

activity of Aurora A is reliant on its interaction with several co-factors regulating function in relation to the progression of cell cycle. Aurora A regulates the entry of the cell into mitosis through the recruitment and subsequent activation of the CDK-1/cyclin B complex. Aurora A directly phosphorylates the phosphatase CDC25B at serine353 which in turn leads to the activation of CDK1/cyclin B, this interaction is mediated through the association of Aurora A with its co-factor Ajuba (*Hirota et al, 2003*). Aurora A also acts in conjunction with Polo-Like Kinase 1 (PLK1) to regulate CDK1/cyclin B activity. When PLK1 is in an active confirmation through interaction with its co-factor Bora, Aurora A has been shown to phosphorylate threonine 210 within the PLK1 kinase domain allowing the Bora-PLK1 complex to become activated fully phosphorylating and activating the phosphatase CDC25B (*Seki et al, 2008*), targeting the CDK1 inhibitory kinase Wee1 for degradation (*van Vugt et al, 2004*). The phosphorylation of PLK1 by Aurora A is regulated through the interaction with the co-factor Bora inducing a conformational change allowing Aurora A full access to the activation loop, this mechanism is self-regulatory with activated PLK1 targeting Bora for ubiquitination (*Seki et al, 2008*). It is through this mechanism that entry of the cell into mitosis is regulated via CDC25B and CDK1/Cyclin B recruitment. Aurora A is also an essential regulatory mechanism for the maturation of centrosomes and bipolar spindle assembly in early to late G_2 phase of the cycle (*Barr et al, 2009*). Aurora A regulates centrosome maturation through the recruitment of pericentriolar material (PCM) proteins. PCM proteins include; the Aurora A substrate serine/threonine kinase LATS2 an essential enzyme for the recruitment of γ-tubulin for microtubule nucleation (*Abe et al, 2006, Toji et al,* 2004). NDEL1 is another Aurora A substrate essential for the recruitment and phosphorylation of katanin p60 which promoting the microtubule remodelling. NDEL1 is also essential for the targeting of TACC3 to the centrosomes, which in turn is phosphorylated by Aurora A (*Mori et al, 2007*) driving the formation of a complex comprising of XMAP215/Msps promoting microtubule growth and organisation. The control of the microtubule nucleation to the centrosome is also regulated through Aurora A dependent phosphorylation of the C-terminal of centrosomin; mediating the targeting and anchoring of γ-tubulin to the centrosomes (*Terada et al, 2003*). These PCM proteins all work in concert to regulate centrosome maturation, microtubule remodelling and ultimately mitotic entry. These co-factors also play a critical role in controlling the sub-cellular localisation of Aurora A throughout the cell cycle, particularly in the localisation to the centromeres. The co-factor Ajuba has also been suggested to be an activating protein for Aurora A kinase

(*Hirota et al, 2003*) however more recent studies in *Drosophila* indicate that it is not actually controlling the activation rather acting in a scaffolding role to ensure the correct localisation of Aurora A at the centrosomes mediating microtubule attachment and centrosome separation/maturation (*Sabino et al, 2011*). PLK1 has also been shown to recruit Aurora A to the centromeres at the beginning of maturation (*Terada et al, 2003*). The exact mechanisms of how all these substrates and interacting proteins contribute to the successful progression and completion of mitosis has not been fully elucidated however it is apparent that centrosome maturation is a complex and tightly regulated system ensuring the process is highly accurate.

One of the characteristic defects observed in Aurora A deficient cells is abnormal mitotic spindles (*Glover et al, 1995*), which can be attributed to defects in centrosomal maturation and its role in the activation and localisation of acid coiled-coil protein TACC3. TACC3 is an exclusive substrate of Aurora A which is responsible for the localisation of TACC3 to the centromeres either through direct phosphorylation or through the Aurora A mediated activation of NDEL1. At the centrosomes TACC3 complexes with ch-TOG/XMAP215 (TOG), promoting microtubule stability through the stabilisation of the kinetochores by inter-microtubule bridging (*Booth et al, 2011*). The binding of TACC3/TOG complex to microtubules is essential for microtubule stability as it acts antagonistically to Mitotic Centromere-Associated Kinesin (MCAK), which mediates destabilisation, regulated by Aurora B, to ensure correct assembly of the microtubules at the centromeres occurs (*Barr et al, 2007*). Aurora A also maintains a secondary role in the bipolar spindle assembly in the absence of centrosomes through a RAN-GTP mediated pathway at the chromosomes. RAN is first converted to RAN-GTP by RCC-1 around the chromosomes, thus forming a gradient of active RAN-GTP related to the proximity of the mitotic chromosomes. The activated RAN-GTP can then interact with importin-β releasing microtubule assembly factors Numa, NUSAP, Rae1 and the Aurora A co-factor TPX2 (*Nachury et al, 2001*). Aurora A phosphorylates TPX2 which in turn drives the (auto)phosphorylation of Aurora A and therefore it's catalytic activity. TPX2 also mediates a conformational change in the Aurora A tertiary structure which has a protective role in preventing de-phosphorylation of Thr288 by Protein Phosphatase 1A (PP1A) (*Bibby et al, 2009*). Activated Aurora A can then recruit the essential proteins of the EXTAH complex which drive centrosome-independent microtubule assembly (*Barr et al, 2007*). The binding of Aurora A and TPX2 during this mechanism is an essential regulatory step in the function of Aurora A in mitosis, as this

interaction maintains the activation and stability of Aurora A through the cell cycle (*Bibby et al, 2009, Giubettini et al, 2011*).

More recently Aurora A has been implicated in several novel mitotic functions such as the correct fragmentation of the golgi machinery to ensure the correct segregation into the daughter cells (*Persico et al, 2010*) and novel mechanisms of activation via calcium dependent processes regulating ciliary disassembly (*Plotnikova et al, 2012*). These new studies show that Aurora A plays a far more diverse range of functional roles in cellular proliferation than previously established and is leading to novel areas of study which will provide a better understanding of the cell cycle and Aurora A's role within it.

1.9.3 Aurora A kinase co-factor TPX2

TPX2 is a co-factor of Aurora A, essential for the activation and function in mitosis. TPX2 activates Aurora A by binding of the Aurora A N-terminus with the C-terminus of TPX2. This promotes enhanced phosphorylation and activation through (auto) phosphorylation of Aurora A at Thr288 (*Eyers et al,2003*) inducing an 8Å change in the conformation; this conformational change exposes the ATP binding domain and fully activates the kinase by exposing the Thr288 residue promoting auto/phosphorylation. This conformational change also has a protective role by preventing de-phosphorylation and subsequent deactivation by Protein Phosphatase 1A (PP1A) (*Bayliss et al, 2003*). TPX2 is also responsible for the targeting of Aurora A to the microtubules and spindle poles (but not the centrosomes) within the cells, maintaining correct spindle length and the stabilisation of the microtubules in the late stages of mitosis (*Bird et al, 2008, Tsai et al, 2003*). The TPX2/Aurora A activated complex has also been associated with the interaction of p53 and Aurora A. Aurora A catalyses the phosphorylation of p53 at serine residues 215 and 315 within the DNA binding regions; the phosphorylation of these residues prevents the DNA binding and transactivation activities of p53, increases the binding of p53 to Mdm2 and subsequently increases ubiquitin targeted degradation of p53 (*Liu et al, 2004, Katayama et al, 2004*). Aurora A overexpression observed in several cancers may therefore down-regulate the p53 activity as an essential component required for cell cycle checkpoint activation and pro-apoptotic pathways (*Pascreau et al, 2008*). TPX2 has also recently shown to control the spatio-temporal organisation of the essential kinesin motor protein and Aurora A

substrate Eg5 in the cell cycle (*Gable et al, 2012, Carmena et al, 2009*). This cross functionality of the TPX2-Aurora A complex highlights its essential role in the progression from G_2 to M phase of the cell cycle and it too may represent a potential strategy in the development of Aurora A (kinase) inhibitors.

1.9.6 The Roles of Aurora kinases in Oncogenesis

Disruption of the tightly controlled expression of the Aurora kinases through gain/loss of function or over-expression altering the normal cellular function thus can be linked to increased cancer susceptibility. There has been a significant amount of research into the roles of Aurora A kinase in tumourigenesis and there still remains no clear conclusion as to its importance. The over-expression of Aurora A kinase has been shown to transform rodent cells *in vitro,* and these cells lead to tumour formation upon introduction into a nude mice (*Sen et al, 1997, Bischoff et al, 1998*). However, studies carried out using a transgenic mouse model over-expressing Aurora A kinase showed no formation of malignant tumours even after a long latency period, suggesting that Aurora A kinase alone cannot act as an oncogene (*Zhang et al, 2004*) but can act in concert with other oncogenic mutations such as those of the RAS pathway to potentiate tumourigenesis (*Tatsuka et al, 2004*). The function that Aurora B plays in tumourigenesis on the other hand is far less clear, the locus for Aurora B has been identified as at 17p13 but has not been observed to be amplified in tumours as of yet. However, studies indicate the over-expression of Aurora B in several cancer cell lines (*Katayama et al, 2004*) is linked to polyploidy and chromosomal instability similar to what has been observed with Aurora A over-expression. Although the polyploid cells over-expressing Aurora B can induce tumour formation in nude mice, this was shown to have been through Aurora B promoting Ras-mediated cellular transformation in these cells (*Kanda et al, 2005*). The over-expression of Aurora B in tumours therefore may not function as an oncogenic mechanism independently but rather the over expression is a feature of the highly proliferative nature of tumour cells.

Centrosome amplification and aneuploidy are also hallmarks of cancer, regulation of these features are controlled through Aurora kinases. Over-expression of Aurora A drives centrosome amplification and the subsequent tetraploidisation due to associated cytokinesis failure leading to the multi-nucleation of cells (*Meraldi et al, 2002*). The increased centrosome number leads to monopolar or multipolar spindle

formation, in healthy cells these abnormal spindle configurations lead to trigger mitotic arrest. In normally cycling cells the polyploid cells would arrest through at the post G_1 checkpoint mediated by the p53-Rb pathway and the cells would subsequently undergo apoptosis. p53 interacts with Aurora A in normal cells through a several mechanisms suppressing centrosome amplification and cellular transformation. Aurora A subverts this mechanism by phosphorylating p53 at two sites; serine 215 preventing DNA binding and thus inhibiting downstream p53 targets (*Liu et al, 2004*) and serine 315 which promotes MDM2 binding targeting p53 for ubiquitination and degradation (*Katayama et al, 2004*). The over-expression of Aurora A in tumour cells therefore disrupts this feedback loop checkpoint mechanism by reducing the cellular p53 concentration which in turn prevents the p53-Rb pathway triggering allowing polyploid cells to pass into mitosis and resulting in aneuploid cells, a characteristic feature of all cancers (*Rajagoplan et al, 2004*). Over-expression of Aurora A was not however enough to induce cellular transformation alone, mutations rendering p53 inactive or deleted were also required and in p53 knockout mice studies the over-expression of Aurora A was observed to induce the malignant transformation of cells (*Zhang et al, 2008*). As established in several studies, Aurora A cannot promote tumourigenesis alone however Aurora A over-expression in conjunction with p53 mutations or the HRAS mutations lead to the oncogenic effects of Aurora A over-expression. Dysregulation of the E3 ubiquitin-protein ligase CHFR is another mechanism that has been suggested to drive Aurora A mediated tumourigenesis. Aurora A ubiquitination is controlled through the interaction with mitotic checkpoint protein CHFR, in 20-50% of all primary tumours and cancer cell lines CHFR expression is lost leading to Aurora A over-expression, chromosomal instability and ultimately tumourigenesis (*Yu et al, 2005*).

The Aurora Kinases have not only been linked to tumourigenesis but also have been implicated in having several other oncogenic functions. Aurora A has been linked to enhanced invasiveness and genomic stability in breast carcinoma's with over-expression documented in 94% of all invasive duct breast adenocarcinomas (*Harrington et al, 2004*) and is also an early pathological event in the onset of ovarian tumours (*Karthiyegan et al, 2010*). Aurora B has also been directly associated with a poor prognosis in glioblastoma, ovarian and hepatocellular carcinomas (*Diaz et al, 2012*).

The Aurora kinases have been implicated by several studies as having an oncogenic role in prostate cancer development. Aurora A has recently been shown to regulates the androgen receptor of prostate cells, the over-expression of Aurora A in prostate cancer cell lines, observed in 98% of prostate cancer lesions (*Mckeelven Buschhorn et al, 2005*), through the phosphorylation and activation of the Androgen Receptor may drive Androgen-independent growth of the tumours (*Shu et al, 2010*). Aurora A over-expression is thought to be an early event in the carcinogenesis of prostate tissue as it is observed in 98% of cancer lesions and 96% of high-grade prostatic intraepithelial neoplasia (PIN) lesions, however Aurora A over-expression is also observed in 20% of the normal prostate tissue surrounding these lesions. This suggests that Aurora A over-expression may play a role in instigating genomic instability, which subsequently drives carcinogenesis in prostate cells (*Diaz et al, 2012*). Aurora A and B over-expression has been shown to be significantly linked to the Gleason score and therefore the severity of prostate cancer (*Kumano et al, 2010, Chieffi et al, 2006*). This link between the Aurora Kinases and the progression of prostate malignancies was shown by studies utilising RNAi (*Kumano et al, 2010*) or kinase specific inhibitors (*Chieffi et al, 2006*) on prostate tumours that suppressed tumour growth but had no effect of normal prostate tissue proliferation. These studies suggest the therapeutic potential of the Aurora kinases as a drug target for the treatment of prostate cancer.

1.9.4 The mitotic roles of Aurora B kinase

The second Aurora kinase is Aurora B, between Aurora A and B there is a high level of shared sequence homology with >70% similarity observed within the kinase domain. They do however maintain distinct functions within the cell (*Vader et al, 2008*). In early mitosis Aurora B is located in the nucleus and has been demonstrated to phosphorylate Histone H3 at both Ser10 and Ser28. The function of this is largely unknown in mammalian models. When mutations of these residues were carried out in other species, such as *Tetrahymena thermophilia* and *Saccromyces Pombe,* it was been observed to be essential for chromosome condensation (*Wei et al, 1998, Mellone et al, 2003*). However, in a previous study, the mutation of Aurora B showed no effect of H3 phosphorylation by Aurora B in *Saccromyces Cervesiae* (*Hsu et al, 2000*) so the role of

Aurora B in chromosome condensation is as of yet not fully defined although this function has been suggested to occur in mammalian cells also (*Fu et al, 2007*). Aurora B has also been linked to the Condensin 1 complex that is essential for chromosome cohesion and correct chromatid formation. It has been proposed that Aurora B phosphorylates the non-Structural Maintenance of Chromosomes (SMC)-subunits of this complex (*Fu et al, 2007, Giet et al, 2001*). The Cohesin complex binds sister chromatids in a ring like structure until the completion of metaphase-anaphase transition and are released via Aurora B mediated pathways. The "prophase pathway" controls the regulation of Cohesin through the Aurora B interaction with the centromeric Shugosin protein of SGO1 driving the localisation SGO1 to the centromeres promoting cohesin binding and association to the chromosome arms (*Dai et al, 2006*). Aurora B subsequently regulates the dissolution of the cohesin complex through the phosphorylation and degradation of securin via the Anaphase Promoting Complex/Cyclosome (APC/C). Following the degradation of securin the enzyme separase is located to the chromosomes through an interaction with Aurora B degrading cohesin and allowing the cells to move into anaphase (*Yuan et al, 2009*). Aurora B also plays a much greater role in the regulation of the chromatid separation not just in the regulation of chromosome condensation. Aurora B is involved in several mechanisms vital for chromatid separation, microtubule attachment, error correction and control of the spindle assembly checkpoint (SAC). Aurora B regulates the spindle orientation and attachments through two groups of complexes. Firstly the microtubule/kinetochore-capture factors Ncd 80/Hec1- and Dam1- complexes are used to regulate the dissociation of the microtubules through phosphorylation by Aurora B decreasing the affinity of microtubules to the kinetochores preventing attachment of misaligned spindles and allowing for correct associations to be formed (*Cheeseman et al, 2006*). Secondly, the correction and attachment of the microtubules by Aurora B through the deactivation of MCAK acts as a depolymerisation agent to destabilise the incorrect attachments at the kinetochores, causing the coupling to fail and causing the microtubule attachment process to repeat until the correct spindle arrangement is achieved. Aurora B phosphorylates MCAK, deactivating its spindle destabilisation activity; when not phosphorylated the MCAK will continuously destabilise microtubules therefore preventing attachment and progression to separation in a negative feedback process. Chromatid separation can only occur when the correct spindle bi-orientation occurs, that is to say that each of the sister chromatids are attached to microtubule from each pole respectively (*Andrews et al,*

2004). These mechanisms are all part of the larger process known as the spindle assembly checkpoint, consisting of a group of regulatory proteins including Mps1 and the Mad and Bub families (*Ditchfield et al, 2005*). This ensures that all chromatids are bi-orientated and attached before the progression from metaphase to anaphase can occur. Aurora B regulates the kinetochore attachments through the recruitment of attachment proteins as described previously. If no attachments or faulty attachments have occurred, Aurora B inhibits the APC/C, a regulatory factor necessary for the progression to anaphase. APC/C is a ligase that targets securin and Cyclin-B for destruction by the 26S proteasome. If there are any incorrect attachments i.e. monopolar attachment or mono/syntelic attachments it will act to de-stabilise kinetochore attachment thereby preventing the progression through the SAC (*Pinsky et al, 2005*). The APC/C acts in conjunction with two specificity co-factors CDC20 and cdh1 (*Visintin et al, 1997*) controlling the progression of mitosis, particularly the transition into anaphase from metaphase. The APC/C^{cdc20} complex is required for the Spindle Assembly Checkpoint and the role of the APC/C^{cdh1} complex in the degradation of Aurora A and B has already been discussed. The complex it forms with SAC proteins at the kinetochores inhibits APC/C^{cdc20}. This complex assembly is regulated by microtubule tension, which will allow for the discrimination between correctly and incorrectly assembled microtubules attachments. The role of Aurora B in destabilising microtubules has been described previously and indicates its vital role in the SAC. Once the SAC has been passed the progression to anaphase occurs the sister chromatids are pulled by actin motors to opposing poles of the cells and the cells then progress to telophase and then into cytokinesis. At this stage in the cell cycle Aurora B localises to the centre of the cells (mid-body/central spindle) and interacts with several substrates e.g. Vimentin (*Goto et al, 2003*), Desmin and GFAP (*Kawajiri et al, 2003*). All of these proteins are essential components of cytokinesis, however our understanding of the mechanisms controlling cytokinesis has yet to be fully determined and the involvement of Aurora B yet to be fully characterised (*Ozlu et al, 2010*).

Aurora B, like Aurora A, relies heavily on its association with co-factors to determine its localisation and activation. Analogous to the relationship between Aurora A and co-factor TPX2 promoting the activation of the kinase, Aurora B is activated via association with the cofactor INCENP (*Honda et al, 2003*). Aurora B phosphorylation is driven by the interaction with INCENP and is essential for activation of the kinase. The full activation of Aurora B is further driven by the phosphorylation of INCENP by Aurora B in a positive feedback loop that regulates the activity of Aurora B (*Bishop et al, 2002*).

INCENP activates Aurora B through the allosteric binding of INCENP to the T-loop of Aurora B promoting the (auto) phosphorylation of Thr232 partially activating the kinase. This interaction and partial activation in turn leads to the phosphorylation of the two Serine residues of the INCENP Threonine – Serine – Serine (TSS) motif located at the C-terminal IN box enabling a conformational change to occur in INCENP then fully activate the Aurora B kinase (*Bishop et al, 2002, Sessa et al, 2005*). This (auto) phosphorylation mechanism is essential in the correct activation of Aurora B kinase and its spatio-temporal functionality as demonstrated in studies mutating the Thr232 to Ala. In cell-based studies this mutation leads to the failure of cytokinesis and subsequently an observed increase in the number of multi-nucleated cells (*Yasui et al, 2004*) showing phosphorylation at this site was an essential step in the control of cytokinesis and in the completion of mitosis.

The degradation of Aurora A and B are closely regulated through the activity of APC/C^{cdh1} complex, however the temporal differences in expression have been observed this may be due to the differences in structure between the Aurora A and B kinases. The sequences required for recognition and degradation have been defined for the Aurora Kinase families: the KEN-box, D-box and A-box. These motifs are required for the regulation of the degradatory mechanisms however they are not all essential and between the members of the subfamily which motifs are required vary. Aurora A requires both the KEN and D boxes but not the A-box and alternatively Aurora B requires KEN and A boxes; and it is these differences that are likely to account for the variation in temporal degradation that is seen during mitosis (*Crane et al, 2004, Nguyen et al, 2005*).

1.9.5 Aurora Kinases and the development of Cancer

The Aurora kinase family as regulators of cell cycle progression and normal cellular proliferation have been frequently linked to tumourigenesis and the progression of cancer (Table 1.2). Unregulated cellular proliferation and aberrant progression through the cell cycle are two of the most significant hallmarks of cancer; therefore the Aurora kinases as essential mitotic kinases are strongly associated with tumourigenesis and the progression of cancer. Aurora A was in fact first isolated through a screen of the BTAK gene (Breast Tumour Amplified Kinase) located on the 20q13 region of the genome (*Sen et al, 1997*). The 20q13 gene is frequently observed to be amplified both

in cancer cell lines e.g. colon, prostate and ovarian, and is also in many primary tumours such as breast and colorectal cancers (*Bischoff et al, 1998*). The overexpression of the Aurora kinases has been identified in a wide range of cancers and is shown to have a wide variety of functions in the cell. Table 1.2 shows a summary of cancers that the Aurora Kinases have been linked to and their correlation to each type of the disease.

Cancer type	Specimen type	Findings
Aurora A		
Bladder	Cell lines	Overexpression
	In vivo	Amplification and overexpression
Breast	Cell lines	Amplification and overexpression
	In vivo	Overexpression in 94% and amplification in 12%
Colorectal	Cell lines	Amplification and overexpression
	In vivo	Amplification and overexpression in >50%
Cervical	Cell lines	Amplification and overexpression
Endometrial	In vivo	Amplification in 56%
Esophageal	In vivo	Overexpression in 68%
Gastric	Cell lines	Amplification in 29%; overexpression in 44%
	In vivo	Amplification in 5–13%; overexpression in 41–50%
Glioma	In vivo	Amplification in 26–31%; overexpression in 60%
Hepatocellular	In vivo	Amplification in 3%; overexpression in 61%
Head and neck	In vivo	Overexpression
Kidney	Cell lines	Amplification and overexpression
Laryngeal	In vivo	Overexpression in 68%
Leukemia	Cell lines	Overexpression
	In vivo	Overexpression
Melanoma	Cell lines	Amplification and overexpression
Non-Hodgkin's lymphoma	In vivo	Overexpression
Ovarian	Cell lines	Amplification in 10–15%; Overexpression in 67%
	In vivo	Overexpression in 50%
Pancreatic	Cell lines	Overexpression
	In vivo	Overexpression in 56–93%
Prostate	Cell lines	Amplification and overexpression
	In vivo	Overexpression in 98%
Aurora B		
Breast	Cell lines	Overexpression
Colorectal	Cell lines	Overexpression
	In vivo	Overexpression
Glioma	In vivo	Overexpression
Kidney	Cell lines	Overexpression
Leukemia	Cell lines	Overexpression
	In vivo	Overexpression
Lung	Cell lines	Overexpression
	In vivo	Overexpression
Prostate	In vivo	Overexpression
Thyroid	Cell lines	Overexpression
	In vivo	Overexpression

Table 1.2. Aurora A and Aurora B overexpression in Cancer types (Adapted from Mountzious et al, 2008).

1.9.7 A review of Aurora Kinase inhibitors and their history

The Aurora Kinases are an attractive anti-cancer drug target thanks to their essential mitotic role coupled with their frequently observed over-expression in malignant cells (*Zhou et al, 1998*), this aberrant expression can manifest by blocking tumour suppressor gene function (*Liu et al, 2004*) leading to tumourigenesis. These features of Aurora kinase signalling can lead to development of highly aggressive tumours which are potentially reversible through inhibition of these enzymes.

Aurora A kinase has also been shown to functionally interact with several other critical cancer related proteins such as NF-κB pathway components; IKKα/IKKβ (*Prajapati et al, 2006, Irelan et al, 2007*) and IκBα (*Hideshima et al, 2009, Sun et al, 2007*), the Aurora A mediated phosphorylation and subsequent inactivation of tumour suppressor proteins; BRCA1 (*Ouchi et al, 2004*) and p53 (*Liu et al, 2004*) and also the up-regulation of several proliferative and transformative oncogenic pathways through direct phosphorylation an example of which is the GSK activation by Aurora A upregulating β-catenin/TCF transcription complex down-stream targets of which include Cyclin D1 and c-myc (*Dar et al, 2009*). The multi-faceted roles of Aurora A kinase in cancer through the aforementioned pathways have made this a focus of research into the development of novel therapies. Targeting the Aurora kinases also has the additional feature of having an inbuilt selectivity for proliferating cells due to their increased expression in mitosis; this makes them ideal candidates for cancer therapies due to the highly proliferative nature of tumours (*Lapenna et al, 2009*). *In vitro* studies of an early Aurora kinase inhibitor highlighted feature as it was shown to preferentially affect the viability of only dividing cells (*Warner et al, 2006*).

1.9.7.1Development of ATP-Competitive inhibitors of the Aurora Kinases

The development of Aurora Kinase inhibitors have been driven through a variety of different methods encompassing both experimental methodologies such as fragment-based screening (*Warner et al, 2006*) and structure-based computational techniques such as virtual screening (*Fu et al, 2008*). This has led to the development of more than 30 Aurora Kinase inhibitors in various stages of clinical and preclinical studies. The first generation of Aurora kinase inhibitors developed were Hesperadin (Boehringer Ingleheim), VX-680 (Vertex) and the first ZM44743 (AstraZeneca). These three Aurora Kinase inhibitors all have similar actions as small molecule inhibitors of the Aurora Kinase ATP-binding site. Both Hesparadin and ZM44743 were initially discovered in drug screens looking for compounds that have kinase inhibitory properties (*Hauf et al, 2003, Ditchfield et al, 2003*) while VX-680 was tailored specifically to have binding affinity against the Aurora kinase specific ATP binding pocket (*Harrington et al, 2004*). These inhibitors were extensively used in the research of the Aurora Kinases and have been an invaluable tool in the understanding of Aurora Kinase functions in the cell cycle. ZM44753 and Hesparadin when tested alongside VX-680 *in vitro* predictably were far less potent inhibitors of Aurora kinase function. Enzymatic assays allowed for the specificity of these inhibitors to be fully investigated, and it became apparent that Hesparadin was an Aurora B specific inhibitor, while ZM44753 and VX-680 were more selective for Aurora A although still hitting Aurora B. The specificity of Hesparadin towards Aurora B was used extensively and led to the elucidation of many of the proliferative and mitotic roles Aurora B plays in cancer (*Hauf et al, 2003*). ZM44753 was also used extensively as a tool in both the validation of novel Aurora Kinase inhibitors and in the determination of normal Aurora A cellular functions (*Ditchfield et al, 2003*) Hesparadin and ZM44753 were primarily used as pharmacological tools rather than as potential drugs, however VX-680 was more comprehensively characterised in pre-clinical and early stage clinical trials as a potential therapeutic. *In vitro* and *in vivo* studies showed reduction of colony formation, tumour growth progression and increased apoptosis of Acute Myeloid Leukaemia (AML) cells of mouse and rat colon and pancreas xenograft models (*Lin et al, 2008*) replicated in ovarian cancer models (*Lin et al, 2008*). The IC_{50} values for the inhibition of proliferation determined across a range of tumour cell lines were from 15nM to 130nM (*Kollareddy et al, 2012*). It was also observed to induce apoptosis through the failure mitotic spindle

checkpoints causing an accumulation of aneuploid cells (*Harrington et al, 2004*) *in vivo*. The pre-clinical data suggested VX-680 as an effective treatment and it was therefore carried forward as the first Aurora kinase inhibitor into clinical trials with varied results. The initial study in patients with solid tumours showed that it had good tolerability and the does limiting side effect was asymptomatic neutropenia. Further trails were initiated but were promptly abandoned after one patient developed corrected QT interval prolongation leading to heart failure (*Boss et al, 2009*). However, an interesting off-target effect was noted in one of the trails targeting Chronic Myeloid Leukaemia (CML) and Philadelphia-positive acute lymphoblastic leukaemia (ALL) and was shown to be effective in the treatment of the T351I and V299L BCR-ABL mutants which are resistant to imantinib (*Katayama et al, 2010*). This led to a re-evaluation of the compound as an Aurora Kinase inhibitor and it showed an inhibition profile against WT BCR-ABL tyrosine kinase and the T351I BCR-ABL mutants with IC_{50} values of 10nM and 30nM respectively (*Katayama et al, 2010*). Recently it has been used in clinical trails and has shown successful inhibition of mutant BCR-ABL and positive haematological outcomes (*Boss et al, 2010*). This has led to the reassessment of many clinical compounds against drug resistant forms of disease perhaps leading to novel uses for previously abandoned compounds.

1.9.7.2 Specific inhibitors of the Aurora Kinases

VX-680 is one of the first generation of Aurora A inhibitors and is an excellent example of a pan-Aurora inhibitor with an inhibition profile that mimics that of Aurora A and B loss of function (*Katayama et al, 2010*). There are many examples of pan-Aurora inhibitors currently in development e.g. PHA-739358, AMG-900 and CYC116, all at various stages of clinical trials. There are questions however as to the efficacy of targeting both Aurora A and Aurora B due to the varied roles they may play in disease states and potentially contradictory roles possible. The development of kinase specific inhibitors therefore has been a significant area of research. Two examples of which are the Aurora A specific inhibitor MLN8237 and the Aurora B specific inhibitor AZD1152.

1.9.7.3 Aurora A specific inhibitors MLN8237/MLN8054

MLN8237/MLN8054, developed by Millennium pharmaceuticals are highly specific Aurora A selective compounds, MLN8237 has an IC_{50} of 1nM and is 200 fold more sensitive for Aurora A over Aurora B. It was designed through the refinement of the earlier compound, MLN8054. MLN8054 was extensively characterised in colorectal, prostate, NSCLC, breast, and ovarian cancer cell lines showing effective inhibition of growth and was further investigated *in vivo* in tumour xenograft models of these cancers, inducing cell death and senescence (*Cheetham et al, 2007*). When taken into the clinic the trials for this compound indicated a lack of target inhibition and were deemed unsuccessful. The structure of this compound however was used as a scaffold for further refinement through Structure Activity Relationship (SAR) optimisation leading to the synthesis of the more potent MLN8237. This compound has been more successfully used in Phase 1 clinical trials against a range of solid tumours showing disease stabilisation and in one case preliminary anti-tumour activity in metastatic ovarian cancer (*Boss et al, 2009*). The success of this compound in its Phase 1 trial has supported the planning of Phase II trials and patients are being recruited with a range of both solid and blood tumours. It must also be acknowledged the role these compounds have played in the discovery of Aurora A specific cellular function particularly in defining the spindle assembly checkpoint regulation by Aurora A. This was defined in studies due to the multinuclear phenotype observed after treatment of cells with this compound and microtubule perturbing agents (*Wysong et al, 2009*).

1.9.7.4 Aurora B specific inhibitor AZD1152

The AstraZeneca developed compound AZD1152 is a highly selective compound towards Aurora B. It was observed to exhibit Ki values of 0.37nM against Aurora B and 1329nM against Aurora A and when screened against a panel of 50 kinases show a highly specific activity toward Aurora B (*Yang et al, 2007*). It has been extensively tested *in vitro* and *in vivo* against a large range of leukaemia cell lines successfully inhibiting proliferation in all cell types with IC_{50} values ranging between 3nM to 40nM. *In vivo* it was shown to effectively inhibit 55-100% of growth in mouse xenograft models of colon cancer and other haematological malignancies in a dose-dependent manner. It was most effective in HL-60 Human promyelocytic leukaemia cells with

complete regression of the tumours being observed (*Wilkinson et al, 2007*). Histological staining of these tumours was used to confirm increased caspase-3 levels, an apoptotic marker, in the tumours supporting the findings *in vitro.* The results of these studies suggest that Aurora B inhibition leads to an increased cellular DNA content due to cytokinesis failure and the subsequent aneuploidy causes the cells to undergo apoptosis (*Yang et al, 2007*). As with other Aurora kinase inhibitors AZD1152 was taken into the clinic in a Phase I clinical trail targeting a range of solid and haematological tumours. It was shown to be effective in the stabilisation of disease progression in 5 of the 13 patients, the pharmokinetics of the drug were shown to be highly favourable with rapid conversion of the drug to an active state with good safety and tolerability profiles in all patients. A more specific trail was then set up focusing on newly diagnosed and relapsed AML patients, results of the study show a 25% positive response rate was observed with no major side effects reported (*Lowenberg et al, 2011*). The success of these trails have allowed for the progression of this inhibitor into larger phase II B-Cell lymphoma trails taking it one step closer to being a novel effective therapy against this disease.

1.9.7.5 The limitations of Aurora kinase inhibitors

The Aurora kinase inhibitor field is vast with many drugs proving effective in both *in vitro* and *in vivo* settings many of which are in the early stages of clinical trails. The examples provided are a just a few of the best characterised compounds in terms of clinical efficacy and their uses as a pharmacological tool in elucidation of Aurora kinase signalling in general. These novel drugs however have some limitations common to the development of all kinase domain targeting inhibitors, notably the off-target effects observed due to the high kinase domain homology shared amongst all kinases and the development of drug resistance. The Aurora B specific inhibitor AZD1152 was recently shown to become ineffective due to resistance developed after chronic treatment in both colon cancer cell lines and pancreatic cell lines (*Guo et al, 2009*). The main focus of all Aurora kinase inhibitor development is targeted toward the kinase domain regardless of the high levels of homology across the kinome; however the development of allosteric inhibitors or substrate-competitive inhibitors may ultimately be more suitable targets for inhibition.

The validity of Aurora kinases as drug targets however is under scrutiny also as their oncogenic properties remain far from fully understood and there is no clear understanding of the effects of inhibition in a singular cancer cell type. Most of the studies both *in vitro*, *in vivo* and in the clinic have all focused on a wide range of malignancies to testing for any possible effect, rather than against a single model fully elucidating the mechanism of action. The roles of the Aurora kinases in regulation of proliferating tumour cells however is clear with a wide range of cell types and primary tumours showing an over-expression of both Aurora A and B (*Gautschi et al, 2008*). This has led to debate in the field as to which is the most effect target to be pursued between these two kinases and with no consensus come to as of yet. This had led to the most promising feature of Aurora kinase inhibitor development driving research into both Aurora A/B and the use of pan-inhibitors that are constantly helping to further our understanding of these kinases and well as the nature of tumourigenesis and proliferation.

1.10 Aurora A kinase and the IKK complex

There is extensive published literature that links the NF-κB signalling and the IKK complex to a wide variety of oncogenic and tumourigenic properties. The relationship between the IKK complex and the cell cycle however has been established more recently. There have been two studies and several suggestions in the literature of the IKK complex playing a role in the regulation of the mitotic kinase Aurora A. *Prajapati et al* published the first in 2006, reporting that IKKα regulates the M phase of the cell cycle through the phosphorylation of T288 in the activation loop of Aurora A kinase, increasing the kinase activity of the enzyme (*Prajapati et al, 2006*). It was also observed that when treated with IKKα siRNA a cell cycle arrest in the cell in the G_2/M phase occurred. It was determined that this occurred through the decreased levels of active Aurora A kinase in the cell rather than any effect of transcriptional regulation of Aurora A. The potential interaction of Aurora A and IKKα was also investigated and using a sucrose gradient to fractionate the cellular components it was possible to immunoprecipitate Aurora A using an anti-IKKα polyclonal antibody from the centrosomal fraction, this fraction also contained PLK1 but no IKKβ. The nature of the

interaction of IKKα and Aurora A was not fully elucidated but suggested the formation of a unique Aurora A/IKKα complex at the centrosome (*Prajapati et al, 2006*).

The second study followed this a year later and investigating the role of IKKβ in the bipolar spindle assembly. *Irelan et al* showed that upon the deletion of IKKβ, using siRNA run down, cells showed multipolar spindle assembly and a failure to undergo normal mitotic progression. Using recombinant protein it was shown to be possible to co-immunoprecipitate Aurora A kinase with the cellular forms of the IKK complex. The mechanisms by which IKKβ acts upon Aurora A were investigated through the transfection of mutant forms of IKKβ and the E3 ligase β-TRCP which has previously shown to associate with IKKβ phosphorylated substrates targeted for proteasomal degradation. The study showed the interaction of Aurora A kinase and β-TRCP to be dependent on IKKβ, which implies that IKKβ-regulated Aurora A phosphorylation is controlling the mitotic expression of Aurora Kinase and through this mechanism may regulate the mitotic spindle assembly (*Irelan et al, 2007*).

These two studies establish the relationship between IKKα, IKKβ and Aurora A suggesting the formation of a 700-800kDa complex (*Prajapati et al, 2006, Irelan et al, 2007*) however what this complex is actually comprised of is not fully understood.

The effect of disruption of this interaction on the cell cycle has been investigated through the use of siRNA knockdown of both IKKα and IKKβ and has led to somewhat contradictory results that may be due to cell type specific mechanisms. *Prajapati et al* used siRNA to knock down protein expression of IKKα resulting in a G_2/M accumulation in HeLa cells which supports their findings of Aurora A being activated through this mechanism. Both this study and that of *Irelan et al* showed results of siRNA run down of IKKβ generated findings that were somewhat contradictory. One showed no effect on the cell cycle progression (*Prajapati et al, 2006*) when observed through the cell cycle and the other showed an accumulation of the cells in the G_2/M phase (*Irelan et al, 2007*). This is not a cell type specific event as the studies were both in HeLa cells. These are not the only studies however that have observed this phenomenon. A study using a conditional IKKβ knock-out system in mice show that upon deletion of IKKβ in melanoma cells there was a cell cycle arrest at the G_2/M phase of the cell cycle. Immunoblotting of these cells also show the Aurora A expression in these cell was reduced upon the ablation of IKKβ (*Yang et al, 2010*), which again is a contradictory discovery to previously published data (*Irelan et al, 2007*). The last of the

studies used lentiviral transfection of shRNA against IKKα to investigate the biological significance of IKKα inhibition in Multiple Myeloma cells. Upon the transfection of IKKα shRNA a significant growth inhibition was observed and when investigated the expression of Aurora A was decreased following the depletion of IKKα (*Hideshima et al, 2009*). This finding supports the previous studies that suggest IKKα as a regulatory component essential for the activation and correct expression of Aurora A through the cell cycle.

Consequently, the relationship between the IKK complex and Aurora A is a poorly understood area of research with seemingly conflicting data in the literature however there is strong evidence that there is a relationship between these kinases and that the IKK complex can play a significant role in the function of Aurora A kinase. This interaction is a very attractive drug target as it combines two well-defined and heavily researched drug targets areas.

As shown in the literature described previously, Aurora A is a recently defined novel substrate of the IKK complex which is an essential component of the NF-κB signalling pathway. Interestingly, Aurora A kinase has been also shown to affect NF-κB signalling through several IKK independent mechanisms. It was initially observed that the inhibition of Aurora A through pharmacological intervention led to the subsequent down-regulation of NF-κB signalling leading to the decreased expression of NF-κB transcriptional targets Bcl-XL and Bcl-2; anti-apoptotic genes thought to play a role in the development of chemoresistance in cancer cells (*Sun et al, 2007*). This study was followed by the observation in breast carcinoma that Aurora A can regulate the NF-κB pathway through both the phosphorylation of IκBα leading to its degradation and through p65 nuclear translocation subsequently activating the transcription of downstream NF-κB targets (*Briassoulli et al, 2007*). Aurora A kinase has also been seen to be over-expressed in a many different cancers and the over-expression has been suggested to drive pro-survival signalling through the NF-κB pathway and could be a mechanism by which Aurora A and NF-κB converge to drive tumourigenesis and circumvent chemotherapeutic interventions (*Briassoulli et al, 2007*). This theory can be directly addressed when observing the effect of the reduction of the E3 ligase checkpoint with fork head-associated and ring finger (CHFR), a component of the regulatory mechanism controlling the ubiquitination and degradation of Aurora A in the cell cycle. In T-cells infected with Human T-cell leukaemia virus type 1 (HTLV-1; HTLV-1 is the etiologic agent for adult T-cell leukaemia (ATL) and normal ATL cells

Aurora A overexpression is observed. In both these cell types decreased CHFR mRNA levels are also observed due to abnormal methylation in the promoter region which leads to a reduction in transcription. This reduction in CHFR expression is responsible for the over-expression of Aurora A which in turn leads to an increase in NF-κB activity which is directly linked to the expression of anti-apoptic proteins such as survivin and also an increase in IKKβ phosphorylation driving the NF-κB signalling (*Tomita et al, 2009*) and leading to increased proliferation. The activation of NF-κB signalling by phosphorylation of IκBα by Aurora A (*Briassoulli et al, 2007*) has been suggested to be a mechanism by which Aurora A promotes oncogenic survival. The down-regulation of IκBα by Aurora A is controlled through Akt activation which stimulates the IκBα degradation and the nuclear translocation of NF-κB which up-regulates the pro-survival gene product Bcl-XL (*Yao et al, 2009*). The relationship between the over-expression of Aurora A and the NF-κB signalling pathway demonstrably drives pro-survival signalling in cancer cells having been linked to breast (*Briassoulli et al, 2007*), lymphoma (*Tomita et al, 2009*), tongue (*Yao et al, 2009*) and ovarian (*Chefetz et al, 2011*) cancers survival by this mechanism of action. It is for this reason that the relationship between Aurora A and NF-κB signalling pathway either via Aurora A driving IκBα degradation or through IKK-mediated interactions with Aurora A has been put forward as a potential area to be exploited for novel therapeutics.

1.11 Aims of the Study

The Aurora Kinases and the IKK complex are both significant areas of research in the development of novel therapeutics targeted at the treatment of many cancers. However much of this research is focussed on the development of ATP-competitive inhibitors, which have been shown to have significant limitations. One method for circumventing these limitations is through the use of substrate competitive or allosteric inhibitors. Recent studies have identified several novel substrates for the IKKs and among them Aurora A is suggested to be one. Aurora A has a central role in mitotic progression and therefore represents an important chemotherapeutic target. Aurora A and the NF-κB pathway have both been identified as being overexpressed and constitutively active in many primary tumours and numerous cancer cell lines, including, those derived from tumours of the prostate or related metastases.. The potential link between the IKKs and Aurora A represents an attractive point of convergence of two key therapeutic strategies in the development of novel drugs against prostate cancer as has been discussed above.

In this thesis, the experimental work, detailed across three chapters, aims to;

1. Characterise the novel IKKα/β interactions with Aurora A through the use of scanning peptide arrays, to map potential interacting regions between the two proteins, and through the use of alanine scanning and truncation arrays identify critical residues and any minimal binding sequence.

2. Recapitulate and confirm the relative importance of an identified sites/regions of interaction as identified by the peptide array in a cellular transfection system utilising the xogenous expression of mutant and/or truncated IKK plasmids.

3. Use biophysical methodologies to further characterise any interaction of IKKα and IKKβ with Aurora A and to identify kinetic profiles for binding events which may be exploited in the design of peptide based inhibitors, and

4. Develop competitive peptide-based inhibitors of IKK-Aurora A interaction(s) based on identified binding sites and to assess the impact of said peptides on; a) Aurora A-IKK binding, b) Aurora A and/or IKK status including potential

modulation of expression/phosphorylation, and c) related signalling events and functional outcomes, in particular mitotic and cell cycle progression.

Collectively, these studies therefore aim to identify the possibility of targeting any IKK-Aurora A interactions in prostate cancer cells and provide the basis towards the development of peptide-related disruptor molecules for intervention in prostate cancer.

CHAPTER 2:

MATERIALS AND METHODS

2.0 MATERIALS

2.1 General reagents

All materials used were of highest commercial purity available and were supplied by Sigma-Aldrich Co Ltd. (Poole, Dorset, U.K.) unless otherwise stated.

Pre-stained SDS-PAGE molecular weight markers: **Biorad Laboratories (Hertfordshire, U.K.)**

Bovine serum albumin: **Gibco BRL (Paisley, UK)**

DTT: **Boehringer Mannheim Ltd (East Sussex, UK)**

Ethanol: **Bamford Laboratories**

Hydrochloric acid: **Fisher Scientific (Leicestershire, UK)**

Methanol: **Bamford Laboratories**

Nitrocellulose membrane (Protran): **Schleicher & Schuell (Surrey, UK)**

Recombinant TNF-uel**Insight Biotechnology Ltd (Wembley, UK)**

3MM paper: **Whatman (Kent, U.K.)**

Lipofectamine RNAiMax: **Invitrogen Ltd (Paisley, UK)**

Polyethylenimine (PEI): **Polysciences (Warrington, UK)**

Rotiphorese® Gel (37.5:1) Acrylamide:**Carl Rothe GmbH + CO.KG (Karlruhe, Germany)**

2.1.2 Reagents for cell culture and transfection

Corning B.V. (Netherlands)

Cell Culture plastic ware

Invitrogen GIBCO BRL. (Paisley, U.K.)

Antibiotics (Penicillin streptomycin), Foetal calf serum (FCS), Geneticin (G148), Medium 199 with Earls salts (M199), Versene (0.2% EDTA/PBS), L-glutamine, HAT supplement, Dulbecco's Modified Eagles Medium (DMEM), RPMI 1640, Minimal Essential Medium (x10), Non essential amino acids, Penicillin/Streptomycin, Sodium Bicarbinate.

Sarsredt AG & Co LTD (Leicester, UK)

Serological pipette 5ml

Serological pipette 10ml

Serlogical pipette 25ml

2.1.3 Antibodies

Santa Cruz Biotechnology Inc (CA, USA)

Rabbit Polyclonal IgG anti – IKK α/β (H-470)

Rabbit Polyclonal IgG anti – IKK γ (FL419)

Rabbit Monoclonal anti – IκBα (C-21)

Mouse Polyclonal IgG anti- actin (C-22)

Rabbit Polyclonal IgG anti- NF-κB p65 (C-20)

Cell signalling Technology Inc. (MA, USA)

Rabbit Polyclonal IgG anti - Aurora A (1G4)

Rabbit Polyclonal IgG anti – P- Aurora A [Thr 288] (C39D8)

Rabbit monoclonal IgG anti-Phospho-Aurora A (Thr288)/Aurora B (Thr232)/Aurora C (Thr198) (D13A11)

Rabbit Polyclonal IgG anti – cdc2

Rabbit Polyclonal IgG anti – Phospho-cdc2 (Tyr15)

Rabbit Polyclonal IgG anti – p-p65(Ser^{536})

Rabbit monoclonal IgG anti-GAPDH (14C10)

Abcam Inc. (MA, USA)

Rabbit Polyclonal IgG anti - TPX2

Mouse Polyclonal IgG anti - Aurora A (35C1)

Rabbit Monoclonal IgG anti-IKKβ (Y466)

Invitrogen Ltd., Paisley, UK

Mouse monoclonal IgG Anti-Xpress (R91025)

Stratech Scientific Limited, Oaks Drive, Newmarket, Suffolk, CB8 7SY

Horseradish peroxidase (HRP)-conjugated sheep anti-mouse IgG,

HRP-conjugated donkey anti-rabbit IgG

2.1.4 Reagents for Site Directed Mutagenesis

BD Bioscience (Oxford, UK)

Advantage Ultrapure dNTP mix

Eurofins MWG Operon (Ebersberg, Germany)

All custom designed primers were synthesised and purified by Eurofins MWG Operon, Ebersberg, Germany.

Agilent Technologies (Chesire, UK)

PfuUltra High-Fidelity DNA Polymerase

Invitrogen Ltd (Paisley, UK)

One Shot® Top10 Chemically competent cells

Qiagen Ltd (West Sussex, UK)

Plasmid Plus *Maxi/Mini* Kit

Parental IKK plasmids were a kind gift from Dr. M. May, University of Pennsylvania

Aurora A plasmids were a kind gift from Prof. S. Dimitrov, Institut Albert Bonniot, Grenoble, France

2.1.5 NEMO-Binding Domain Peptides

All NEMO binding domain peptides were obtained from **Genscript USA Inc., New Jersey, USA** at >95% purity.

2.1.7 Radiochemicals

PerkinElmer life sciences, Cambridge, UK

$\gamma[^{32}P]$-ATP (3000 Ci/mmol^{-1})

2.1.8 Recombinant Proteins

Invitrogen ltd., Paisley, UK

His-Tag IKKα

His-Tag IKKβ

Millipore, Dundee, UK

GST-IKKβ

GST-IKKα

His-Aurora A

2.1.9 BiaCore Reagents

All reagents purchased from GE Healthcare,

2.2 METHODS

2.2.1 Cell Culture

All cell culture carried out under aseptic conditions in a Class II cell culture hood unless otherwise stated.

2.2.1.1 Cell lines

Human Caucasian prostate adenocarcinoma, PC3, Catalogue No. 90112714 were obtained from European Collection of Cell Cultures (ECACC), United Kingdom.

Human Embryonic Kidney cells, HEK293, Catalogue No. 85120602 were obtained from European Collection of Cell Cultures (ECACC), United Kingdom.

2.2.1.2 PC3 Cell Culture

The PC3 cells were maintained in RPMI 1640 supplemented with 10% (v/v) Foetal Calf serum, L-glutamate (27mg/ml) and penicillin/streptomycin (250 units/ml;100µg/ml) in a humidified atmosphere at 37^0C and 5% CO_2. Cells were grown as a monolayer in vented 75ml flasks in 10ml RPMI 1640 and incubated until subculture.

2.2.1.3 Subculture of PC3 Cells

PC3 cells were grown as monolayer and upon reaching 70-85% confluent media was aspirated and cells washed twice with 1.5ml sterile 5% (w/v) trypsin solution or Versene solution. The Trypsin/Versene was then aspirated and the flasks were gently tapped to ensure the cells were fully detached. 10ml RPMI 1640 was added to the flask re-suspending recovered cells for passage. A proportion of the cell suspension was then added to new plastic ware and fresh media to seed a fresh monolayer as required.

2.2.1.4 HEK293 cell culture

Human embryonic kidney (HEK) 293 cells were maintained in modified eagles media (MEM) supplemented with; penicillin (250units/ml), streptomycin (100µg/ml), L-glutamine (27mg/ml) and 10% (v/v) Foetal calf serum (FCS). Cells were maintained in a humidified atmosphere of 5% CO_2 at 37^0C in 75cm^3 vented flasks with 10ml media until subculture.

2.2.1.5 Subculture of HEK293 cells

Once cells were 80-90% confluent the media was aspirated and 1.5 mls of 1 x sodium sodium citrate (SSC) (8.78g of NaCl and 4.41g of sodium acetate dissolved in 1 litre of water then pH adjusted to 7.0 with a few drops of sterile NaOH) used to wash the monolayer then aspirated. A further 1.5ml 1 x SSC was added and the monolayer washed thoroughly and left to rest for 30s-2min, aspirated and 1 x SSC replaced with 10ml HEK293 media to resuspend cells and were seeded into new plastic ware as required.

2.2.1.6 Cell synchronisation and preparation of whole cell extracts

Double Thymidine Treatment

To synchronise the cells at the G_1/S phase transition Double Thymidine block treatment was used to synchronise the cells. PC3 cells were subcultured and plated into single 2ml plates and were grown until 40% confluent. The media was then changed to fresh RPMI1640 and each plate was treated with a 2mM Thymidine 5'-triphosphate diluted in sterile PBS.Cultures were returned to the incubator for a further 16-18 hours. Cells were then washed three times with sterile PBS (1ml) and the media replaced to release the cells from the initial block and returned to the incubator for 8-10 hours. Cells were removed from the incubator and washed again with sterile PBS (1ml) three times to ensure all the media was removed. A second treatment of 2mM Thymidine 5'-triphosphate was pursued to initiate the second block of 16-18 hours. Cells were then washed three times with sterile cold PBS (1ml) and returned to full media releasing the cells from the second block. At the time point outlined in the experimental design the cells were washed twice with ice cold PBS (1ml) and lysed using DTTSB (Sample Buffer 1x [trizema base 63mM, $Na_4P_2O_7$ 2mM, EDTA 5mM, Glycerol 10% (v/v), SDS 2% (w/v), Bromophenol Blue 0.007% (w/v)], 50mM DTT) Cells were then scraped and chromosomal DNA sheared by the repeated uptake and ejection with a syringe needle. The lysates were then transferred to

Eppendorf tubes (1ml) and boiled for 4-5mins allowing the proteins to become fully denatured, lysates are then allowed to cool and stored at -20°C until use.

Nocodazole Treatment

Cells were subcultured into 12 or 6 well plates and grown until 70-80% confluent in full media. Cells were treated with 50ng/ml Nocodazole for 16-20 hours and then washed with full media and media replaced releasing the cells from Nocodazole mediated arrest in early pro-metaphase.

2.2.2 Western Blotting

2.2.2.1 Sample Preparation

Cells treated as appropriate were upon termination of experiments were washed twice with ice-cold PBS and lysed using DTTSB (Sample Buffer 1x [trizema base 63mM, $Na_4P_2O_7$ 2mM, EDTA 5mM, Glycerol 10% (v/v), SDS 2% (w/v), Bromophenol Blue 0.007% (w/v)], 50mM DTT) at an appropriate volume. Cells were then scraped to fully recover the cells from the monolayer and chromosomal DNA sheared by the repeated uptake and ejection with a syringe needle. The lysates were subsequently transferred to Eppendorf tubes (1ml), placed in a boiling water bath at 100°C for 4-5mins to fully denature the proteins. Prepared cell lysates were then allowed to cool and subsequently stored at -20°C until use.

2.2.2.2 SDS-Polyacrylamide Gel Electrophoresis (SDS-PAGE)

Resolving gels comprising of N-methylenebis-acrylamide (30:0.8), 0.375M Tris pH 8.8, 0.1% (w/v) SDS and 0.05% (w/v) ammonium persulfate (APS) were initially prepared. The acrylimide gel polymerisation occurs at room temperature upon the addition of N,N,N,N,N-tetramethylethylenediamine (TEMED) 0.05%(v/v). The resolving gels were prepared at suitable acrylimide concentrations relative to the size of the protein being investigated (11% (w/v), 10% (w/v), 9% (w/v), 7.5%(w/v) of acrylimide). The gel solution was poured between two glass plates with 0.05ml spacing (Bio-rad), leaving a space 1-1.5cm to the top that is overlaid with 0.1% SDS solution. Dependant on ambient temperature the gel will take between 30-60 minutes to fully polymerise which can be visualised as a solid line underneath the 0.1% SDS solution. The 0.1% SDS solution was then discarded and the stacking gel is added directly to the top of the resolving gel. The stacking gel contains 10% (v/v) acrylimide: N, -methylenebis-acrylamide

(30:0.8) in 125mM Tris, pH6.8 0.1% (w/v) SDS, 0.05% (w/v) ammonium persulfate and 0.05% (v/v) TEMED. A comb (10 or 15 well) was inserted to the stacking gel immediately after the addition to the resolving gel to provide wells for protein loading. The polymerisation occurs more rapidly for the stacking gel, 5-15 minutes. The comb was then removed and the gels are assembled into a Bio-Rad Protean II™ electrophoresis tank and filled with Running buffer (25mM Tris, 129mM glycine, 0.1% (w/v) SDS). An aliquot of pre-stained SDS-PAGE molecular weight marker containing known molecular weights is loaded into a well. Aliquots of prepared cell lysates loaded into wells using a syringe washed with ethanol in an order outlined in the experimental design and run concurrently with the marker for identification of the protein of interest by molecular weight. The samples were electrophoresed at a constant voltage of 130V until the bromophenol dye in the sample buffer had run off the end of the gel.

2.2.2.3 Electrophoretic Transfer of Proteins to a Nitrocellulose Membrane

Once completed the separated proteins were transferred from the gel to a Nitrocellulose membrane by electrophoretic blotting following a protocol devised by Towbin et al., 1979. The gel was placed, and pressed firmly onto a nitrocellulose sheet, sandwiched between sheets of 3MM paper and two sponge pads in a transfer cassette. The cassette was then be placed in a Bio-Rad Mini Trans-Blot ™ tank with the nitrocellulose orientated towards the anode and fully immersed with a blotting buffer (25M Tris, 19mM glycine, 20% (v/v) methanol) a constant current of 240mA was then applied for 1 hour 45 minutes. The tank is cooled by the addition of an ice reservoir. The negative charge conferred to the proteins due to the presence of SDS in the resolving gel will transfer to the proteins to the nitrocellulose membrane for the analysis by Antisera detection of protein.

2.2.2.4 Detection of the Protein utilising Antisera

Once the transfer has occurred the proteins will be affixed to the nitrocellulose membrane, the membrane was incubated with a 3% Bovine Serum Albumin (BSA) (w/v) in NATT buffer (pH7.4) solution (150mM NaCl, 20mM Tris, pH7.4, 0.2%(v/v) Tween-20) blocking buffer and agitated constantly on a shaking platform for 2 hours. The blocking buffer was then discarded and replaced with a 0.2% (w/v) BSA NATT pH7.4 solution in which antisera specific to the protein of interest (primary antibody) was added at an appropriate concentration. This was left

on a platform shaker overnight at 50rpm min^{-1} and then washed every 15 minutes with NATT pH 7.4 solution for 1.5 hours. The secondary antibody, an IgG antibody raised against the primary antibody species and conjugated to horseradish peroxidase, was added in 0.2% BSA in NATT pH 7.4 and left at room temperature in the platform shaker for 2 hours. The membrane was then washed every 15 minutes for 1.5 hours with NATT pH 7.4 and was then developed using enhanced chemiluminescene (ECL) reagents. The final wash was then discarded and to the membrane 3ml of both ECL solution 1 and ECL solution 2 was added and washed over the membrane for 3-5 minutes. The membrane was then loaded to an exposure cassette and covered with cling film. In a dark room Kodak X-OMAT LS film was exposed to the membranes for an antibody sensitivity dependent length of time, film was developed in a Kodak M35-M-X-OMAT processor.

2.2.3 Peptide Array Protocols

The peptide libraries were created using automatic SPOT synthesis on a continuous cellulose support using Fmoc (fluoren-9- ylmethoxycarbonyl) chemistry with the AutoSpot-RobotASS222 (Intavis Bioanalytical Instruments AG).

2.2.3.1 Glass Slide Array Protocol

The peptide arrays used contained had pre-defined peptide sequences printed on a membrane that is affixed to a microscope slide. The peptide sequences were printed in duplicate on each array slide and the controls for these arrays were run in parallel on different slides, as these arrays were not reusable. Arrays were initially blocked in TBST containing 5% BSA for 4 hours at room temperature on an orbital shaker. The slides were then rinsed in TBST and the recombinant protein diluted in 0.5% BSA/TBST at a concentration of 1 or 2μM and incubated with the slide at 4°C overnight. The slides were then washed three times in TBST for ten minutes per wash, after which the primary antibody was added in 1% BSA/TBST and incubated for 4 hours at room temperature. The slides were then washed twice with TBST for five minutes and the secondary antibody was then added for 1 hour at room temperature. Slides were then washed with TBST three times for ten minutes and developed using Enhanced Chemiluminescene reagents (ECL) in the same manner as western blotting.

2.2.4 Immunoprecipitation

1.5-2µg of an Antibody, specific to the protein intended to be isolated from the whole cells extract, was precoupled to 15-30µl of Protein G sepharose beads (Sigma, UK) in Solubilisation buffer (20mM Tris-HCl pH7.6, 1mM EDTA, 0.5mM EGTA, 10% [v/v] Glycerol, 0.1% [w/v] Brij 35, 150mM NaCl, 20mM NaF, 20mM β-GLucerophosphate, 0.5mM Na_3VO_4, 1mM PMSF, 10µg ml^{-1} Leupeptin, 10µg ml^{-1} Aprotinin, 10µg ml^{-1} Pepstatin A) at 4^0C for 1 hour on a platform shaker. Samples were prepared for Immunoprecipitation by adding solubilisation to either whole cells. The pre-coupled protein G beads were subsequently centrifuged at 14000rpm for 1min and solubilisation buffer was aspirated off with uncoupled antibody. The Solubilised extracts were then added to the beads and placed on a mixing wheel for 2-4hours. The samples were then removed and centrifuged at 14000rpm for 1min and the supernatants removed and kept. Beads were then washed with solubilisation buffer and centrifuged at 14000rpm for 1 minute then the solubilisation buffer is removed, this was carried out 2-4 times. The beads and supernatants were then treated with 2x and 4x sample buffer respectively and boiled for five minutes. Samples can then be frozen until analysis by western blot.

2.2.5 Polyethylnimine (PEI) Transfection

HEK293 cells were seeded at a 1:10 dilution into 6 well plates after subculture as described previously in section 2.2.1.5 Cells then allowed to grow until 80-90% confluent in the 6/12 well plates until transient transfection using Polyethylenimine (PEI, Polysciences Inc., Warrington, UK). It was found that to achieve maximal gene expression and low cytotoxicity with suitable levels of transfection a ratio of 2µg of DNA/11.4µl of PEI was optimal. The stock solution of PEI was prepared at 1mg/ml in deionised water then heated until dissolved and then filtered and stored at -80^0C. For each transfection 1-2µg of the plasmid DNA was added to 11.4µl PEI and 200µl of complete growth media in an eppendorf. This solution was mixed by a pipette and then left to incubate at room temperature for 10minutes. In this time the media in the wells was aspirated and replace with 1.8ml fresh media and after ten minutes the contents of the eppendorfs then added to the appropriate well. The plates were then incubated overnight at 37^0C in a humidified atmosphere at 5% CO_2. The cells were then harvested and Immunoprecipitated as described in section 2.2.4 .

2.2.6 Surface Plasmon Resonance (SPR)

SPR interactions studies were carried out using a BiaCore 3000 (BiaCore AB, Uppsala, Sweden BiaCore AB, Uppsala, Sweden) machine at Leeds University or using a BiaCore T100 (BiaCore AB, Uppsala, Sweden BiaCore AB, Uppsala, Sweden) at the University of Edinburgh Biophysical Characterisation Facility. Thanks to Dr. J Beattie and Dr J Branham for their guidance.

2.2.6.1 Immobilisation

Recombinant His-Aurora A protein was immobilised on the active Flow cell of a CM5 sensor chip. Final surface concentration of Aurora A varied between experiments and can be calculated due to 1000RU being equal 1pg/mm^2. The CM5 chip has a carboxymethylated dextran matrix that was activated by the flow over of a 1:1 mixture of NHS:EDC (N-hydroxysuccinimide:1-ethyl-3(3-dimethylaminopropyl)-carbodiimide hydrochloride). Once the surface was activated recombinant Aurora A was diluted with a 10mM Sodium acetate buffer (pH 5.5) and flowed over the surface at a constant rate of 5µl/min at 25^{0}C in a SPR running buffer (20 mM HEPES, 150 mM NaCl, 0.005% v/v surfactant P20, and 2 mM DTT at pH 7.4). The sensor chip was deactivated after protein immobilisation using a 1M ethanolamine solution (pH 8.5).

For the intial Protein-Protein interaction experiments on the reference surface BSA protein was immobilised as a reference surface to show any non-specific interactions. BSA is immobilised to a density of 3-4000 response units (RU); 3-4 pg/mm^2 of protein on the surface. BSA (1 mg/ml stock) was diluted to a final concentration of 5µg/ml with pH 4.5 sodium acetate buffer and then immobilised on the surface using the protocol described for the immobilisation of Aurora A.

After the proteins are immobilised and the chip is deactivated, the system is left at 25^{0}C with the running buffer flowing over at a low flow rate overnight to equilibrate the system.

2.2.6.2 SPR of IKK Complex Proteins

2.2.6.2.1Protein-Protein interaction study

The proteins that were to be analysed for an interaction were the catalytic members of the IKK complex family, IKKα/β. They were prepared at a range of concentrations; 0.125 µM-1µM in SPR

running buffer. The BiaCore machine was programmed to cycle through the concentrations, randomly injecting each concentration at a flow rate of 30µl/min for 180s with a 900s disassociation period prior to the regeneration step. The regeneration step is the injection of 2 x 30s pulses of regeneration buffer (2 mM EDTA and 1 M NaCl), followed by a 120s stabilisation. Each protein concentration range was analysed in series overnight. The interaction data can be followed in real time on a sensogram. These experiments were carried out on an Aurora A surface of 3000-3500RU.

2.2.6.2.2 Single Cycle Kinetics

Prior to the running of the single cycle kinetic runs of IKKα/β on the Aurora A surface proteins were buffer exchanged into the running buffer for these experiments (10mM HEPES, 150mM NaCl, 0.05% P20, 0.5mM DTT, 0.5mM EDTA) and prepared at a range of concentrations either 90nM, 30nM,10nM, 3.3nM, 1.1nM or 300nM, 100nM, 33.3nM, 11.1nM, 3.7nM. The BiaCore t100 was programmed to inject the range of concentrations sequentially from lowest concentration to highest concentration with no disassociation phase until after the final injection. The protein injections were at a 100µl/min for 60s and 90s between injections, final disassociation phase was for 1500s. The on rates would be calculated across all the concentrations but only the final off rate would be used.

Biaevaulation software (BiaCore AB, Uppsala, Sweden BiaCore AB, Uppsala, Sweden) is used to Analyse the data obtained from these studies.

2.2.7 Flow Asissted Cell Sorting (FACS) Analysis

Cells treated specific to the relevant assay, then trypsinised and resuspended in media and transferred to a 1.5ml eppendorf tube. Cells the centrifuged at 3000rpm for 10 mins and media aspirated off leaving the cell pellet. Cell pellet in resuspended in 150µl of PBS pH7.4 and 100% ice-cold ethanol added dropwise, vortexing between drops to fix the cells. Samples are stored overnight at -20^{0}C (samples can last up to a week). Samples are prepared for FACS analysis by adding 1ml of fresh cold PBS pH7.4 and vortexing samples then centrifuging the cells at 300rpm for 10 minutes removing supernatant and resuspending cell pellet in 250µl of cold PBS pH7.4. 5µl of RNAase (≥70units/ml) added to each sample and incubated in the dark at 37^{0}C and 5% CO_2 for 1 hour. FACS are tubes prepared during the incubation and after this is complete samples are transferred and 10ul Propidium Iodide (1mg/ml) is added to each sample and

vortexed. Samples are run on FACScanto cytometer and 10,000 events measured for each sample and data was analysed with FACSDiva software.

2.2.8 Transfection of siRNA

siRNA purchased from Thermo Scientific (Leicestershire, UK), Target sequences: IKKα (GCGUGAAACUGGAAUAAAU), IKKβ (GAGCUGUACAGGAGACUAA), Non-targeting (Cat. No. D-001810-01-05). siRNA resuspended in Rnase/Dnase free water and maintained at stock concentrations of 20μM.

Cells were subcultured into 12 or 6 well plates until 50% confluent. Two separate eppendorfs were prepared, 100nM siRNA added to tube 1 made up to 100μl with Optimem in the second tube 5μl Lipofectamine RNAiMAX was diluted into 100μl Optimem. Tube 1 is subsequently added to tube 2 and mixed gently by hand. Tubes were left for 15-20 minutes to allow complex formation. Full media was then aspirated off cultured cells and monolayer is washed with sterile PBS to remove and antibiotics, media is then replaced with optimum (800μl for 12 well, 1800μl for well) after 15-20 minute incubation of siRNA and lipofectamine transfection mixture was added to the appropriate wells dropwise. Plates were incubated overnight at 37°C at 5% CO_2, transfection mixture was aspirated off and monolayers washed with fresh media and full media replaced. Cells were then subsequently replaced in the incubators for 48hrs when maximal run down has been observed.

2.2.9 Surface Enhanced Raman Scattering (SERS) Analysis of NBD Peptide/Aurora A Binding

2.2.9.1 Labelling of Aurora A with MG ITC

Aurora A (Millipore, Billerica MA, USA) first underwent a buffer exchange procedure. 66.6 μl Aurora A (0.3 mg/ml) and 40 μl 0.1 M sodium bicarbonate buffer pH 9.2 were added to a 30K

MWCO centrifugal filter (Amicon Ultra – 0.5 ml, Millipore, Billerica MA, USA) and centrifuged at 13.4k rpm for 5 min. 90 µl 0.1 M sodium bicarbonate buffer pH 9.2 was added and the centrifugation step repeated. The addition of buffer and centrifugation step was repeated for a third time before the centrifugal filter unit was inverted and placed in a fresh eppendorf and centrifuged at 1.0 k rpm for 5 min resulting in 45 µl 0.44 mg/ml Aurora A in 0.1 M sodium bicarbonate buffer pH 9.2 (assuming 100% recovery of protein). The freshly buffer exchanged Aurora A was then conjugated to MG ITC. 6 mM MG ITC solution in anhydrous dimethyl sulfoxide (DMSO) (33 µl) was prepared and added in 10 µl aliquots to a vortexing solution of Aurora A (45 µl, 0.44 mg/ml, 0.1 M sodium bicarbonate buffer pH 9.2). After all of the MG ITC had been added, the resulting solution was protected from light and agitated for 2 h at r.t. After 2 h, the solution was added to a 30K MWCO centrifugal filter and centrifuged for 5 min at 13.4k rpm, 100 µl PBS was added and the solution was centrifuged for 5 min at 13.4 k rpm. This step was repeated before the centrifugal filter unit was inverted and placed in a fresh eppendorf and centrifuged at 1.0 k rpm for 5 min resulting in 35 µl 0.57 mg/ml Aurora A MG (12 µM – assuming 100% recovery of conjugate) in PBS. This solution was stored at 4˚C until use.

2.2.9.2 Functionalisation of Array Substrates with Wild Type and Mutant peptides

The wild type (WT) and mutant peptides were custom ordered from Genscript (Piscataway NJ, USA). The bimetallic nanohole array surfaces were prepared by Dr Debby Correia-Ledo at Université de Montréal. The nanohole arrays had a 1 nm chromium adhesion layer, a 62.5 nm silver underlayer and a 62.5 nm gold top layer. A 16-MHA SAM was formed on the surface of the arrays by incubating three nanohole substrates in a 5 mM solution of 16-MHA in DMF for 65 hours. The samples were then thoroughly washed with ethanol and dried under nitrogen before being placed into a microarray chamber. Activation of the carboxylic acid group to a NHS-activated ester was achieved by addition of 100 µl (per well) of a mixed aqueous solution of 400 mM EDC and 100 mM sulfo-NHS. This solution was agitated for 1 h at r.t. After activation, each well was washed twice with 100 µl PBS pH 4.5. 100 µl (per well) 2.5 mM solution of wild type peptide dissolved in PBS was added to the positive wells or 100 µl (per well) 2.5 mM solution of mutant peptide dissolved in PBS was added to the control wells. The samples were agitated for 3 h before being washed 3 times with PBS. 100 µl 1 M ethanolamine.HCl pH 8.5 was added to each well and incubated for 1 h with agitation. The wells were then washed three times with PBS prior to incubation with Aurora A MG.

2.2.9.3 Interaction of Aurora A MG with the peptide-functionalised surfaces

100 µl of MG labelled Aurora A was added to each well and incubated with agitation for 30 min. After the incubation period, the wells were then thoroughly washed with PBST and the samples were removed from the microarray chamber and washed again with ddH2O before being dried under nitrogen prior to analysis.

2.2.9.4 Analysis

Analysis was performed using a Renishaw Ramascope equipped with a Renishaw HeNe laser of 633 nm excitation All samples were analysed at 633 nm excitation using a 50x objective (Leica, NPlan, NA = 0.75), 10 % laser power and 10 s integration time. 8 replicate scans were collected from each substrate over the sample area.

2.2.10 Rigid Body Docking (ZDOCK)

Docking NBD of IKK1 and IKK2 in TPX2 binding site of Aurora A. IKK1 NBD taken from chain A of 3BRT, IKK2 NBD taken from chain A of 3BRV, Aurora A is PDB code 3HA6. The Dock Proteins (ZDOCK) protocol in DS is used to attempt docking of the protein pairs. Residues more than 7 Å away from the TPX2 fragment (chain B) of 3HA6 will be used as "Receptor Blocked Residues" for the docking (grouped as "Group" in 3HA6). "Ligand Blocked Residues" were defined in 3BRT (alpha) as SEELVAEAHNLCTLLENAIQDTVREQGNS and in 3BRV (beta) as SEELVAEAHNLCTLLENAIQDTVREQDQS, and in the Filter Poses parameter, "Ligand Binding Site Residues" were taken as MMNLDWSWLT (bolded) in 3BRT and FTALDWSWLQ (bolded) in 3BRV with a "Distance Cutoff" of 5 Å in both cases. All other parameters were left as default.

Repeated both the docking studies using an angular step-size of 6 degrees.

The docking was performed using the ZDOCK protocol in Accelrys Discovery Studio 3.1. All images prepared using Accelrys Discovery Studio 3.1.

2.2.11 Basic Molecular Techniques

2.2.11.1 Site directed Mutagenesis

Custom designed primers were synthesised by Eurofins MWG Operon and used in Site directed mutagenesis according to the manufacturers protocol outlined in QuikChange® II site directed mutagenesis kit (Stratagene, Ca, USA).

2.2.11.2 Bacterial culture

All plasmids were grown in broth cultures containing LB media (10g L^{-1} NaCl, 10g L^{-1} Bactotryptone, 5g L^{-1} Bacto yeast extract pH 7.0). Solid media was prepared by the addition of 1.5% (w/v) agar to LB media. All media was sterilised before use, by autoclaving and, upon cooling to below 60^{o}C, ampicillin was added (100µg ml^{-1}).

2.2.11.3 Isolation of plasmid DNA

For small-scale isolation of plasmid DNA, 5ml LB was inoculated with the appropriate plasmid DNA and grown overnight at 37^{o}C. DNA was isolated from the cultures following the manufactures protocol (Sigma MINIPREP Kit). For large-scale preparation of plasmid DNA, 100ml LB was inoculated with appropriate plasmid and grown at 37^{o}C overnight. DNA was isolated using an Endofree® Plasmid Maxi Kit, according to the manufacturer's instructions (Qiagen, UK).

2.2.11.4 Spectroscopic Quantification of DNA concentration

The concentration and purity of nucleic acid was quantified by a GeneQuant by spectroscopic measurement of the absorbance of UV radiation at wavelengths of 260nm and 280nm.

2.2.12 In vitro Kinase Assays

2.2.12.1 Aurora A and IKK in vitro activity assay

Recombinant His-Aurora A, His-IKKα and His-IKKβ in ng amounts were combined as appropriate in the absence or presence of 1μg GST-IκBN in a total volume of 25μl of kinase buffer 25mM Hepes, pH 7.6, 25mM $MgCl_2$, 2mM DTT, 5mM β-glycerophosphate, 0.1 mM orthovanadate). Reaction were then initiated by the addition of 5μl of 6x kinase mix generating final conditions of 50μM ATP/3.0μCi ^{32}P-ATP. This kinase mix was incubated at 30°C for 30 minutes and the reactions terminated by the addition of 10μl of4 x Laemmli SDS sample buffer. Samples were then resolved by SDS-PAGE on 10% (v/v) acrylamide gels, fixed in 20% (v/v) methanol, 10% (v/v) acetic acid for 30 minutes and rinsed in distilled water. The gels were then placed between two porous cellophane sheets in a drying frame and dried for approximately 60 minutes at 80°C by a Hoeffer Eazy-BreezeTM gel dryer. The extent of [^{32}P] incorporation into each protein was assessed by autoradiography. Kodak X-OMAT LS X-ray film was exposed to the dried gels for 16-24 hours at –20°C in a spring loaded metal cassette and developed by a KODAK M35-M X-OMAT processor.

2.2.12.2 Fixing and drying gels

Gels containing proteins and labelled with [^{32}P] were fixed in 20% (v/v) methanol, 10% (v/v) acetic acid for 30 minutes and rinsed in distilled water. The gel was then placed between two porous cellophane sheets in a drying frame and dried for approximately 60 minutes at 80°C by a Hoeffer Eazy-BreezeTM gel dryer. The radiolabelled protein was detected by autoradiography. Kodak X-OMAT LS X-ray film was exposed to the dried gels for 16 hours at –20°C in a spring loaded metal cassette and developed by a KODAK M35-M X-OMAT processor.

2.2.13 Scanning Densitometry

All western blots were analysed by scanning densitometry using Bio-RAD GS-800 calibrated Densitometer. All blots quantified with Quantity One 1-D analysis software (Bio-RAD, Herfordshire, UK). All immunblots normalised to loading controls prior to statistical analysis.

2.2.14 Data Analysis

All data shown expressed as mean ± S.E.M and were representative of at least three independent experiments unless otherwise stated. The statistical significane of differences between means was determined by either one-tailed Student's Unpaired t-test or a two-tailed one-way analysis of variance (ANOVA) with Dunnett's post test to 95% confidence levels ($P<0.05$).

CHAPTER 3:

CHARACTERISATION OF THE IKK AND AURORA A INTERACTIONS USING PEPTIDE ARRAYS

3.0 Characterisation of the IKK and Aurora A interactions using Peptide Arrays

3.1. Introduction

The interaction of Aurora A kinase and the IKK complex is poorly understood with limited experimental evidence in the published literature. *Prajapati et al*, in a study carried out in 2006 were able to co-immunoprecipitate Aurora A from the centrosomal fraction of the cells through the use of an IKKα specific polyclonal antibody. However, no IKKβ was present in this fraction and the conclusion was that an Aurora A/IKKα specific complex was formed at the centrosome and IKKβ and Aurora A did not interact (*Prajapati et al, 2006*). The following year a study was published by *Irelan et al* that showed interaction of Aurora A with all three members of the IKK complex through immunoprecipitation of endogenous IKK proteins incubated with recombinant Aurora A (*Irelan et al, 2007*). These studies therefore both suggested that an interaction(s) occurrs between the IKK proteins and Aurora A however no evidence has been presented to characterise and identify the protein domains/structures responsible for any interaction(s). One strategy towards confirming interactions of partner proteins *in vitro* and identify key protein domains/structures is that of peptide array technology.

Peptide arrays are a recombinant methodology for investigating protein-protein binding and characterising the essential components of these interactions. Peptide arrays are libraries of peptides affixed to a nitrocellulose membrane, which can be overlaid with recombinant proteins to map interacting regions of your proteins of interest. The concept of spotting synthesised peptides on a membrane sheet was initially proposed at the 21st European Peptide Symposium in Barcelona in 1990 *(Frank et al, 1990).* At this meeting it was shown that it was possible to affix peptides to a membrane in small quantities that could be arranged on the membrane as a series of spots. This observation opened up the possibility for the large scale screening of libraries of peptides against target proteins with wide ranging implications for drug design.

The basis of this procedure came from observations made when carrying out peptide and oligonucleotide synthesis (*Frank et al, 1983, Frank et al, 1998*) on individually labelled cellulose membranes that chemical reactions can proceed to completion when enough reagent is absorbed by the support material. From this it was extrapolated that peptide synthesis could be carried out on the support membranes. Using low volatility solvent it was possible to absorb reagents quickly in small spots on the membrane surface and this could then act as an open reactor for chemical reactions to take place, which was then used to affix short amino acid sequences in distinct regions simultaneously to a membrane (*Frank, 2002*). Each region would form a spot when attached to the membrane and dependent on the absorptive capacity of the membrane, volume dispensed and the support/solvent surface tension properties the size of each spot could be determined to create customisable arrays of peptides *(Frank, 2002).*

The control of spot size can then be used to determine the density of spots on each array. The materials most commonly used for the membrane support in this process are cellulose prepared from cotton linters, as this material is suitably compatible with Fmoc-peptide synthesis chemistry (*Frank et al, 1988).* Fmoc peptide synthesis chemistry is basic solid-phase chemistry producing high quality reproducible peptides on the membrane surface. The spotting of arrays can be carried out by hand but are usually carried out using an automated system to ensure the accuracy and consistency of the array that will be more uniform. An example of the commercially available systems is the AutoSpot-Robot ASS222 developed by Intavis Bioanalytical Instruments (*Hipler et al, 2007*).

The arrays have a multitude of uses for bioassays or screening of peptide libraries *(Frank et al, 2002).* One such use is for the analysis of protein–protein interactions by mapping of linear binding sites. The arrays can be easily printed breaking down the primary amino acid sequence of the protein into 6 to 25 amino acid sequences with 1 to 5 overlapping amino acid residues between each sequence (*Kazim et al, 1980*) and overlaying with full length recombinant protein of the other interacting partner. The use of peptide arrays in the characterisation of protein-protein binding interactions has become an increasingly important tool in biology and biochemistry with over 400 original and peer reviewed articles using this methodology (*Volkmer et al, 2012*).

Using binding domains identified by this method, sites of interaction can be further investigated through the use of alanine-scanning arrays and truncation analysis of the

binding regions to allow for critical binding residues to be identified which can then be further investigated using mutational approaches in a cellular system.

Therefore experimental examination of potential IKK-Aurora A interactions were constructed with the use of peptide array technology and parallel cell-based assays aimed at;

(i) Confirming direct protein-protein interaction(s)

(ii) Map regions/domains important for the interaction of IKK/Aurora A

(iii) Utilising alanine scanning arrays to identify any key residues in identified regions of binding

(iv) Utilising N-terminal and C-terminal truncation approaches either alone or in combination to investigate the potential for the existence of any minimal binding motif ,

(v) cell based work : endogenous IPs and exogenous transfections

All towards the aim of informing the development of disruptor peptides and potentially design of peptidomimetic compounds.

3.2 Investigating Aurora A binding with the IKK kinases using peptide Arrays

The binding of Aurora A and the IKK kinases were initially examined using peptide arrays displaying the full amino acid sequence of IKKα/β/γ. The arrays were printed using the following protein amino acid sequences/Accession Numbers; IKKα: AAC51662, IKKβ: AAD08997 and IKKγ: Q9Y6K9. The primary amino acid sequence of each protein was broken down into overlapping 25 amino acid peptides, with a 5 amino acid shift along the primary sequence between each peptide. The peptide array was printed in duplicate side by side on a nitrocellulose support affixed to a glass slide. The array was then incubated with a 1μM solution of recombinant His-tagged Aurora A, probed with Aurora A specific antisera, a HRP-coupled secondary antibody and developed using chemiluminescence to assess the interactions of Aurora A with each of the IKK kinases. This identified key regions involved in these interactions. As a control an array that was probed with the Aurora A antisera in the absence of any incubation with His-tagged Aurora A to check for any cross reactivity with the immobilised peptides

3.2.1 Aurora A binding to Full length IKKα Peptide array

The results of the overlay of recombinant Aurora A on the IKKα scanning peptide array are shown in Figure 4.1 i). From this array it was observed that recombinant Aurora A interacted with the IKKα derived peptides at two main regions of interest. Firstly, 10 spots on the 2nd row numbered 34 to 43 indicated binding of recombinant Aurora A to the IKKα array; these spots corresponded to the primary amino acid residues 171-221 of IKKα array are shown in Figure 4.1 i). From this array it was observain of IKKα encompasses residues 15-301 (*Perkins, 2006*) of the primary amino acid sequence. The identification of binding in this region suggests that Aurora A may act either as a substrate for IKKα or potentially a regulator of IKKα kinase activation/activity. The second region of binding was identified as the final spot (145) corresponding to residues 720-745 of IKKα. This peptide contained the NEMO binding domain (NBD) the essential scaffolding motif for the assembly of the hetero-dimeric form of the IKK

complex. The NBD is a hexapeptide sequence, L-D-W-S-W-L, which binds the regulatory sub-unit IKKγ (*May et al, 2002*).

This array also showed other regions of binding however the two outlined above encompassing elements of the kinase domain and NBD showed the strongest levels of binding and therefore were of the most interest.

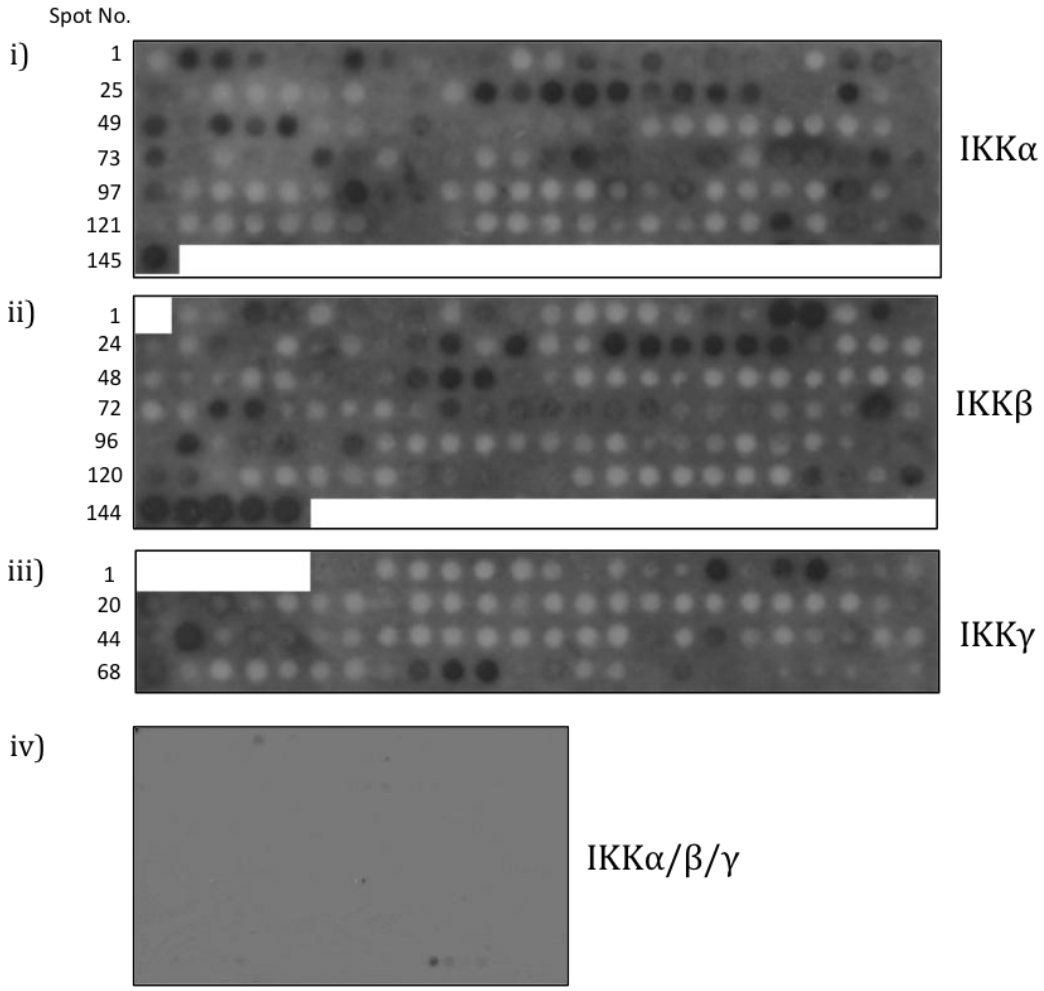

Figure 3.1 Binding of Aurora A kinase to IKK full length arrays

Immobilised peptide 'spots' were printed which corresponded to overlapping 25 mer peptides, each shifted 5 amino acids across the entire relevant IKK isomer amino acid sequence. The binding was assessed by overlaying with 1μM recombinant His-tagged Aurora A. The array was probed with an anti-Aurora A rabbit monoclonal antibody, then an HRP-conjugated anti-rabbit secondary antibody and binding visualised using ECL reagents. A control array was carried out with the primary antibody incubation on an array that had not been incubated with Aurora A to determine any non-specific binding to the arrays, i) The overlay of His-Aurora A (1μM) on the IKKα array, ii) The overlay of His-Aurora A (1μM) on the IKKβ array, iii) The overlay of His-Aurora A (1μM) on the IKKγ array iv) IKK arrays with no Aurora A protein overlay Antibodies were diluted at 1:3000 in TBST 0.3% BSA. Spots are numbered from right to left and correspond to the primary amino acid as follows: Spot 1 = amino acids 1-25, Spot 2 = amino acids 6-30 etc. Array printed in duplicate and binding was consistent on both arrays.

3.2.2 Aurora A binding to Full length IKKβ Peptide array

In Figure 3.1 ii) the interaction of Aurora A with IKKβ-derived sequences was confirmed by the IKKβ scanning array, several regions of interaction were identified. The regions of binding observed on this array follow a similar pattern to those observed on the IKKα array. The kinase domain of IKKβ corresponds to residues 15-300 (*Perkins, 2006*) and from the array several binding regions were identified to occur within this binding region. The most prominent binding that occured within this domain occurs at spots numbered 18-19 (amino-acids 86-121) in the first row and spots 38-43 (amino acids 186-235). Both these regions fall within the kinase domain of IKKβ, suggesting Aurora A as a potential substrate or alternatively as a possible modulator of IKKβ kinase activation/activity. As observed on the IKKα array in Figure 3.1 i) the spots containing the NBD of IKKβ also showed the strongest binding on this array. These spots are found at numbers 144-148 corresponding to the amino acids 711-751 of IKKβ. Each of the 5 spots of binding all contained elements of the NBD hexapeptide. Noteworthy is that the IKKβ protein is 14 amino acids longer than IKKα, which explained why the NBD sequence was present in more spots on this array when compared to the IKKα array, thus suggesting that the NBD, common to both IKKα and IKKβ, may represent a means of interaction with Aurora A.

The similarities between these two regions of Aurora A binding based on sequences present within both the IKKα and IKKβ sub-units made these spots the most interesting when considering a strategy to pursue further analysis of these interactions.

3.2.3 Aurora A binding to Full length IKKγ Peptide array

The binding of Aurora A to the scanning peptide array displaying 25-mer sequences derived from the regulatory sub-unit IKKγ is shown in Figure 3.1 iii); Recombinant His-Aurora A was shown to interact with several sequences/spots derived from IKKγ although fewer spots of binding were observed than with either IKKα or IKKβ. There were three main regions identified as binding sites on IKKγ; spots 13-16 (amino acids 61-100), spot 46 (amino acids 226-250) and spots 76-78 (amino acids 371-410). The first region of binding at amino acids 61-100 falls within the coiled-coiled region 1 of

IKKγ and encompasses an activation site that is recognised to be phosphorylated by ATM at serine 68 (*Wu et al, 2006*). The second and most pronounced region of binding observed in this array was at residues 226-250 which is found in an undefined region of the IKKγ sequence with no reported interactions occurring at these amino acids. The final binding site at amino acids 371-410 corresponds to the zinc-finger domain of IKKγ that contains ubquitin binding sites regulating IKKγ activity (*Tang et al, 2003*).

The interaction of Aurora A with sequences derived from IKKd in this array was at residues 226-250 which is found in anin and may therefore represent the mapping of novel interactions between this mitotic kinase and the scaffolding subunit of the IKK complex.

As described previously, as a control an array that was probed with the Aurora A antisera in the absence of any incubation with His-tagged Aurora A to check for any cross reactivity with the immobilised peptides was also pursued as shown in Figure 4.1 iv). This array showed no regions of binding that corresponded to the protein bound arrays and therefore the binding observed was deemed to be due to *bona fide* protein-peptide interactions.

3.2.4 Summary of Aurora A interactions with the full length IKK Peptide Arrays

From the overlay of recombinant His-Aurora A on the IKK full-length arrays, it was observed that there were multiple interactions between Aurora A and all three members of the IKK complex. The array showed that the regions of binding of Aurora A on both IKKα and IKKβ arrays were very similar with two prominent regions identified in both of these kinases. The first was in the kinase domains which suggested that either Aurora A may be a substrate for both IKKα and IKKβ or alternatively that Aurora A may potentially influence IKK activation and/or activity. The high levels of correlation between the observed binding regions for both IKKα and IKKβ could however be due to the high level of sequence homology in this domain. When the amino acid sequences common to both the observed binding regions on both the IKKα and IKKβ arrays were aligned it was identified that there exists a 74% match in identity and 82% match in amino acid charge, as seen in Figure 3.2. This suggests that the

similarities in the binding observed in these regions may be due to homology and Aurora A may only be a substrate for one of the IKK's and the shared binding in this region could be due to sequence homology. The kinase domains of IKKα and IKKβ are heavily researched drug targets and therefore these regions of binding were not considered to be further pursued by mutational and truncation array analysis.

```
             Identity      Positives
             26/35(74%)        29/35(82%)
IKKalpha  186  QYLAPELFENKPYTATVDYWSFGTMVFECIAGYRP  220
               QYLAPEL E + YT TVDYWSFGT+ FECI G+RP
IKKbeta   187  QYLAPELLEQQKYTVTVDYWSFGTLAFECITGFRP  221
```

Figure 3.2. Alignment of Kinase Domain residues bound by Aurora A, common to both IKK's.

BLAST sequence alignment of the amino acids in the kinase domain of both IKKα and IKKβ observed to be bound by Aurora A on the peptide arrays.

The second and most prominent regions of Aurora A binding observed on both the IKKα and IKKβ arrays occurred in the final spot of the IKKα array and the final 5 spots of the IKKβ array which represent the amino acids 720-745 and 716-756 of IKK beta respectively, all containing the majority, if not all, of the hexapeptide core sequence of the NBD. Figure 3.3 shows the alignment of the amino acid sequences represented by these spots.

From Figure 3.3 it can be seen that there is considerably less homology between these two regions of IKK and IKK, which in part is due to the post-NBD C-terminal extension of IKKβ. However, between these two sequences it was observed that the homologous sequence was that of the NEMO binding domain hexapeptide, L-D-W-S-W-L. This was an interesting observation as this is a well-recognised motif for the interaction of IKKα and IKKβ with the scaffolding protein IKKγ (*May et al, 2002*) and has been suggested to have a regulatory role in NF-κB signalling through phosphorylation of the central serine by PLK1 and has been suggested to potentially act as a multi-protein scaffolding site (*Higashimoto et al, 2008*).

Amino acid		
	IKKα	
726	S-T-I-I-H-E-A-N-E-E-Q-G-N-S-M-M-N-L-D-W-S-W-L-T-E	745
	IKKβ	
716	C-T-L-L-E-N-A-I-Q-D-T-V-R-E-Q-D-Q-S-F-T-A-L-D-W-S	740
721	N-A-I-Q-D-T-V-R-E-Q-D-Q-S-F-T-A-L-D-W-S-W-L-Q-T-E	745
726	T-V-R-E-Q-D-Q-S-F-T-A-L-D-W-S-W-L-Q-T-E-E-E-E-H-S	750
731	D-Q-S-F-T-A-L-D-W-S-W-L-Q-T-E-E-E-E-H-S-C-L-E-Q-A	755
732	Q-S-F-T-A-L-D-W-S-W-L-Q-T-E-E-E-E-H-S-C-L-E-Q-A-S	756

Figure 3.3. Sequence alignment of the final spot of the IKKα array and final five spots of the IKKβ array.

Primary amino acids sequences for the observed binding on the IKKα and IKKβ arrays. Homologous residues highlighted in red.

These spots were the strongest regions of Aurora A binding observed on the arrays alongside the other identified region of binding in the kinase domains of IKKlly act as a mult the strength of observed binding and the possibility of Aurora A representing an additional protein that could potentially interacts with the IKKs through the NBD as an emerging multi-protein docking site made the NBD containing spots more attractive sequences to characterise further using alanine-scanning and truncation arrays.

3.3 Investigating IKK binding with Aurora kinases using peptide Arrays

To further understand the nature of the interactions between the IKK proteins and Aurora A an Aurora A/B/C full-length scanning peptide array was printed using the amino acid sequences obtained from the NCBI database. The Accession numbers used for each kinase were as follows; Aurora A (NP_940839), Aurora B (NP_004208) and Aurora C (NP_001015878). The array was printed with the same format as for the full length IKK array, with 25 amino acid peptides in an overlapping arrangement with a 5 amino acid shift. Two arrays were overlaid with recombinant His-tagged IKKα and IKKβ individually at a 1μM final concentration and probed with IKKα and IKKβ specific antisera. A no-protein control array was carried out for each antibody to account for any non-specific antibody binding to the arrays. IKKγ was not used for these

experiments, as we were unable to obtain sufficient quantities of this enzyme at high enough purity to ensure a reliable response from the arrays. The control arrays probed with both IKKα and IKKβ antisera showed no non-specific interaction of antisera with the peptide arrays (data not shown).

3.3.1 IKKα interactions with the full length Aurora array

When the Aurora A/B/C array were overlaid with either GST- or His-IKK The control arrays probed with both I any of the three Aurora kinases (data not shown). These arrays were blank for both the control and protein overlay experiments.

3.3.2 IKKβ interactions with the full length Aurora A array

The Aurora array was also overlaid with His-IKKβ protein and interactions were observed with all three Aurora kinases as illustrated in Figure 3.4. The results from this array supported those displayed in Figure 3.1 ii) for Aurora binding of IKK-derived sequences. The overlay of His-IKKβ on the Aurora array in this instance acted as further confirmation of an interaction occurring between IKKβ and Aurora A-derived peptide sequences. It also suggested that IKKβ may interact with both the Aurora B and Aurora C as the other two members of this kinase family. The binding of His-IKKβ to the Aurora A array is shown in Figure 3.4 i) and can be mapped specifically to one main region of binding, occurring at spots 36-42 corresponding to the amino acids 176-230. A single spot was also identified at site numbered 53, the amino acids that are represented by this spot are 266-290. Spots number 65 (amino acids 321-350) and 71-72 (amino acids 351-380) also showed some interaction although to a lesser extent than observed with the previously described spots. All these binding regions fall within the defined kinase domain of Aurora A encompassing amino acids 132-383 (*Fu et al, 2007*). Interestingly, the interactions mapped to amino acids 176-230 and 266-290 that also correlate with the TPX2 binding sites (*Bayliss et al, 2003*).

This array confirmed the interaction of IKKβ and Aurora A-derived peptides and highlighted a possible binding site analogous to that of TPX2, an activating co-factor for Aurora A.

3.2.3 IKKβ interactions with the full length Aurora B array

Figure 3.4 ii) shows the interaction of His-IKKβ with the sequences/spots of the Aurora B array. The interaction of His-IKKβ with the array occured in one main binding site at spots 27-31, amino acids 126-170 of Aurora B. This binding site again falls within the kinase domain of Aurora B which is defined as 76-327 (*Fu et al, 2007*). The Aurora kinases show high levels of sequence identity within this region and this could therefore be a factor in defining the observed interactions.

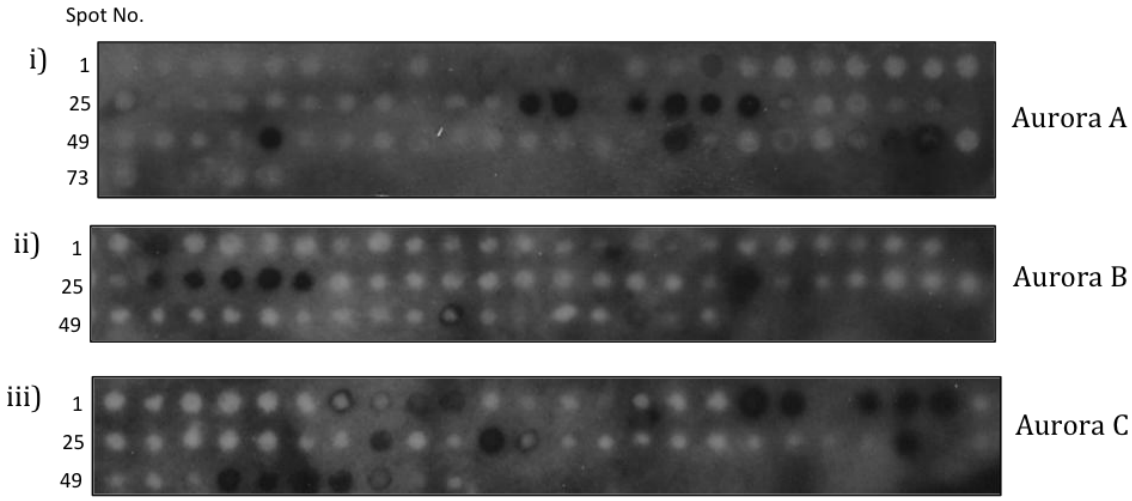

Figure 3.4 Binding of His-IKKβ kinase to the Aurora kinase full length scanning peptide arrays

Immobilised peptide 'spots' were printed which corresponded to overlapping 25 mer peptides, each shifted 5 amino acids across the entire amino acid sequence relevant to each Aurora protein. The array was overlayed with 1μM recombinant His-tagged IKKβ and the binding assessed. The array was probed with an anti-IKKβ rabbit monoclonal antibody, an anti-rabbit HRP-coupled secondary antibody and binding visualised using ECL reagents. A control array was carried out with the primary antibody incubation on an array that had not been incubated with His-IKKβ to determine to identify any non-specific binding to the arrays, i) The overlay of His-IKKβ (1μM) on the Aurora A array, ii) The overlay of His-IKKβ (1μM) on the Aurora B array, iii) The overlay of His-IKKβ (1μM) on the Aurora C array iv) Aurora array with no protein overlay. Antibodies were diluted at 1:3000 in TBST 0.3% BSA. Spots are numbered from right to left and correspond to the primary amino acid as follows: Spot 1 = amino acids 1-25, Spot 2 = amino acids 6-30 etc. Array printed in duplicate and data present was consistent on both arrays.

3.2.4 IKKβ interactions with the full length Aurora C array

His-IKKβ binding to the Aurora C array is shown in Figure 3.4 iii). There were several sites of His-IKKβ binding to Aurora C-derived peptides identified. The clearest sites of binding occured at spots 18-23 and 52-55 which corresponded to amino acids 86-135 and 256-295 respectively. There was also a site of binding observed at spot 35 (amino acids 171-195). These sequences also all correlated with the kinase domain of this protein, which is classified as residues 39-290. The interacting region at spots 52-55 also contained the D-box of Aurora C which is a motif used for the regulation of Aurora C degradation.

3.2.5 Summary of IKKf binding occured at spots 18-23 and 52-55 which correspond

The overlay of the Aurora array with His-IKKβ confirmed the interaction between IKKβ and peptide sequences of the Aurora A whilst also indicating potential novel interactions with the two other members of the Aurora kinase family. His-IKKβ showed binding with all three of the Aurora kinases displayed as scanning peptide arrays and this was observed to occur within the kinase domain of each enzyme. This domain shows >70% sequence homology between the three Aurora kinases (*Fu et al,* 2007). When the three Aurora kinases were compared by sequence alignment, as shown in Figure 3.5 the high level of homology was observed. The black lines under each sequence indicate the binding regions identified by the peptide arrays, when the identified interacting regions are compared it can be seen that the regions in which IKKβ is shown to interact with all three of the Aurora kinases are highly homologous. Due to the nature of the peptide arrays being printed as short amino acids sequences derived from the primary amino acid sequence of the proteins the interactions identified at these regions could be due to homology and therefore requires further examination and validation in a cellular setting.

The interactions of IKKβ with Aurora A-derived sequences, as shown in Figure 3.4 also identified an additional binding site not observed in the other two Aurora kinases, at amino acids 321-380. This region precedes the D-box of Aurora A present at amino acid 371-374- that is a requirement for the regulation of degradation by the APC/C complex

and controls the temporal regulation of Aurora A levels (*Crane et al, 2004*). The interactions of IKKThis region precedes the D-box of Aurora A present at amino acid 371-374- that is a reqll with the TPX2 binding sites of Aurora A, identified by *Bayliss et al*. to be apparent between amino acid residues 127-280.

Figure 3.5 Alignment of the kinase domains of the Aurora kinases by amino acid sequence.

Sequence alignment of Aurora Kinase family by COBALT software. Amino acid homology shown in red, binding sites identified by peptide arrays shown by black underlining.

3.4 Mapping of the Aurora A interactions with IKK using Alanine-scanning and truncation arrays

Following the full–length scanning arrays further arrays were developed to help further characterise the interactions of Aurora A with IKKα and IKKβ. From the initial full-length IKKα and IKKβ arrays overlaid with Aurora A (Figure 3.1) the strongest regions of binding identified were those containing the NBD and due to it's well characterised role in scaffolding the IKK complex (*May et al, 2002*) and it's potential to function as a multi-protein binding site (*Higashimoto et al, 2008*) this region was taken forward for further study through alanine-scanning and truncation arrays. These approaches take the identified interacting peptide sequences from the full-length

arrays and either sequentially mutate each amino acid to alanine, or truncate each amino acid one at a time from both directions (N-terminal; C-terminal) individually and then together on separate arrays. The aims of this approach is to identify the critical residues which mediate the binding between Aurora A and IKKα and IKKβ in these regions, and to determine if there are any unique to one Aurora kinase which could be exploited when considering specific design of disrupting peptides.

3.4.1 Interaction of Aurora A with the IKKα Alanine-scanning array

The binding region identified in the final spot of the IKKα full-length array corresponded to the amino acids residues 721-745 of IKKα (Figure 3.1 i)). This sequence was then printed as an alanine-scanning array where every amino acid of the primary sequence was sequentially mutated to an alanine residue. The array was overlaid with 1μM recombinant His-Aurora A and immunoblotted with Aurora A specific anti-sera, no-protein controls were also carried out in parallel and showed no cross-reactivity of the antibody with the array (data not shown). Each array is carried out in duplicate and each replicate is shown side by side. Figure 3.6 shows the result of the Aurora A overlay on this array. The initial spot on this array represented the 'parent' sequence to confirm that binding between Aurora A and this peptide sequence/spot. In both replicates the binding was again observed and further confirmed results reported in Figure 3.1. The alanine-scanning began in the subsequent spots, and any modulation of binding observed in both replicates was assumed to be an actual change in the interaction of Aurora A with the IKKα-derived peptide sequences at this spot. The first observed modulation of binding occured when the glutamic acid residue at number 729 was mutated, with little or no changes observed until methionine 736. The NBD hexapeptide sequence follows this mutation at amino acids 738-743 and it can be seen from the array that each of the tryptophans at 740 and 742 within the NBD were required for the interaction of Aurora A. This was further supported by the loss of Aurora A binding upon mutation of both of these residues to alanine in the final spot of this array. The mutation of luecine 743, tyrosine 744 and glutamic acid 745 all also ablated the interaction of Aurora A with the IKKα-derived sequences/spot at this site.

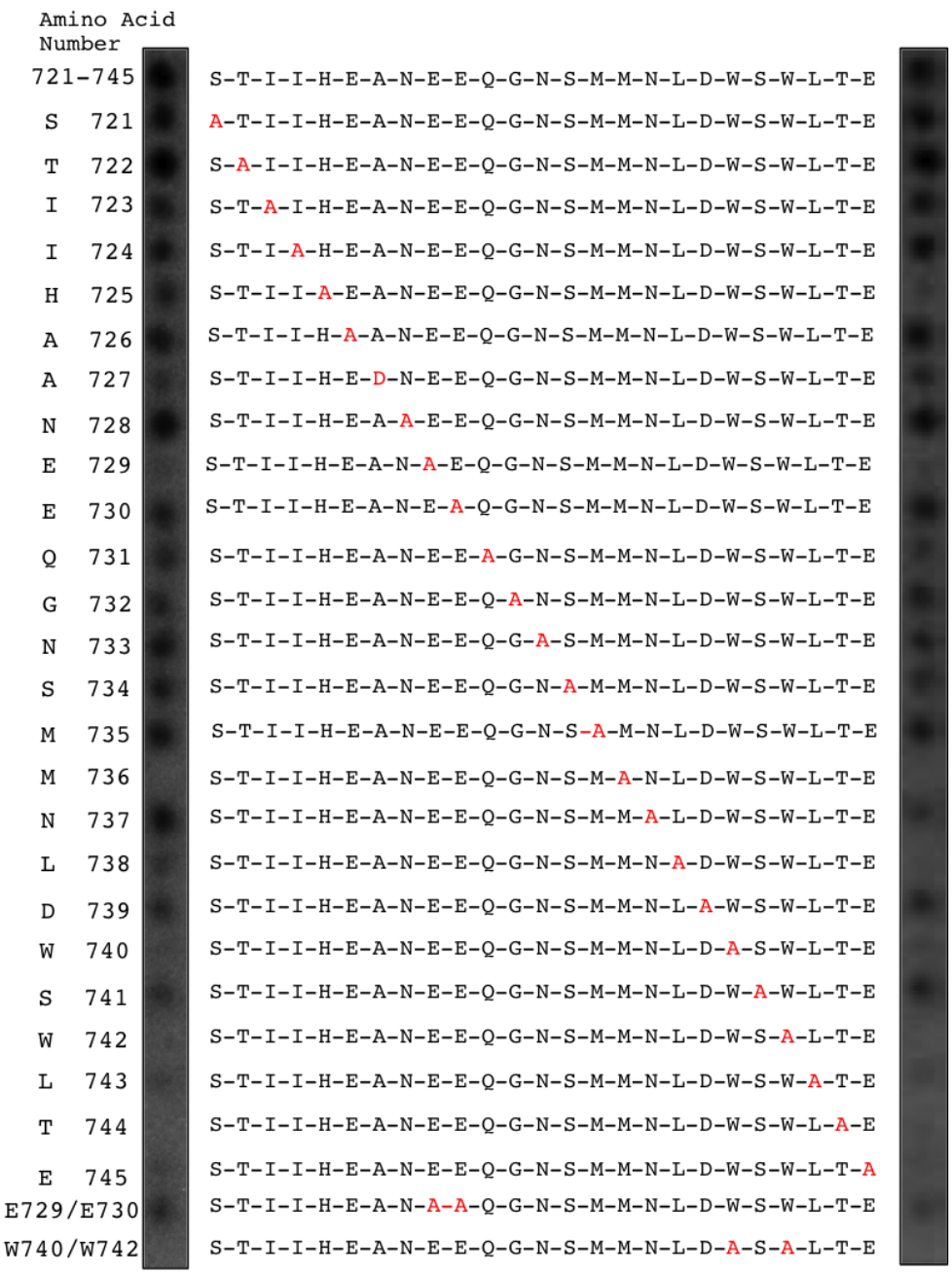

Figure 3.6 IKKα 721-745 alanine-scanning peptide array overlaid with His-Aurora A.

The IKKα 721-745 alanine scanning peptide array was printed based upon the 25 amino peptide sequence obtained from the "parent" spot observed on the full length IKKα scanning peptide array, shown as the top spot. Each amino acid was sequentially substituted by alanine. Any repeated amino acids in the sequence were substituted with Alanine in every permutation possible. The array was incubated with 1μM His-Aurora A and immunoblotted with Aurora A specific antisera at a 1:3000 dilution. Mutated residues are highlighted in red. The final two spots show the double tryptophan mutation within the NBD and double glutamic acid mutations.

3.4.2 Interaction of Aurora A with the IKKα truncation arrays

The parent sequence of IKKα was then used for truncation analysis to further inform on critical residues and suggest minimal sequences required for this interaction to occur. The overlay of Aurora A on the arrays was carried out as with previous experiments and any non-replicated loss or gain of binding was ignored. Figure 3.7 shows the result of the truncation analysis. Figure 3.7 i) is the N-C terminal truncations and from this it can be seen that no effect on binding was observed until the truncation of glutamic acid 730 which ablates binding until glycine 732 is also truncated whereby the interaction returns until the truncation of serine 734 which again leads to total loss of the interaction. Binding was subsequently restored after the truncation of methionine 737. The binding then remained until the loss of the NBD aspartic acid 739 after which the binding was not restored. The loss and return of binding observed in this array suggested that the binding of Aurora A with these IKKα-derived sequences/region requires multiple sites/amino acids, however they cannot all be essential as binding could be re-established with shorter sequences. This array also indicated that the NBD must remain intact to maintain binding by Aurora A kinase. Figure 3.7 ii) shows the C-N terminal sequential truncations from which it can be seen that the truncation of tryptophan 742 was enough to completely ablate binding with the rest of the sequence. This suggested that although the short sequences containing this residue in the N-C truncations (Figure 3.7 i) were not enough to maintain binding, loss of this amino acid was enough to prevent binding with any of the other potential regions of this binding site. The loss of glutamic acid 745 also seemed to reduce the levels of binding however did not completely ablate the interaction. The simultaneous truncation from the N and C terminals shown in Figure 3.7 iii) shows the loss of glutamic acid 745 and serine 721 in the first spot dramatically reduced the levels of binding however it is not until the truncation of both tryptophan 742 and isoleucine 723 that the binding was lost completely. Taken in conjunction with the data of in Figure 3.7 i) and ii) where no effect was seen with the truncation of isoleucine 723, this further supports the essential role of tryptophan 742 as a critical residue within the IKKα NBD for the interaction of Aurora A with IKKα.

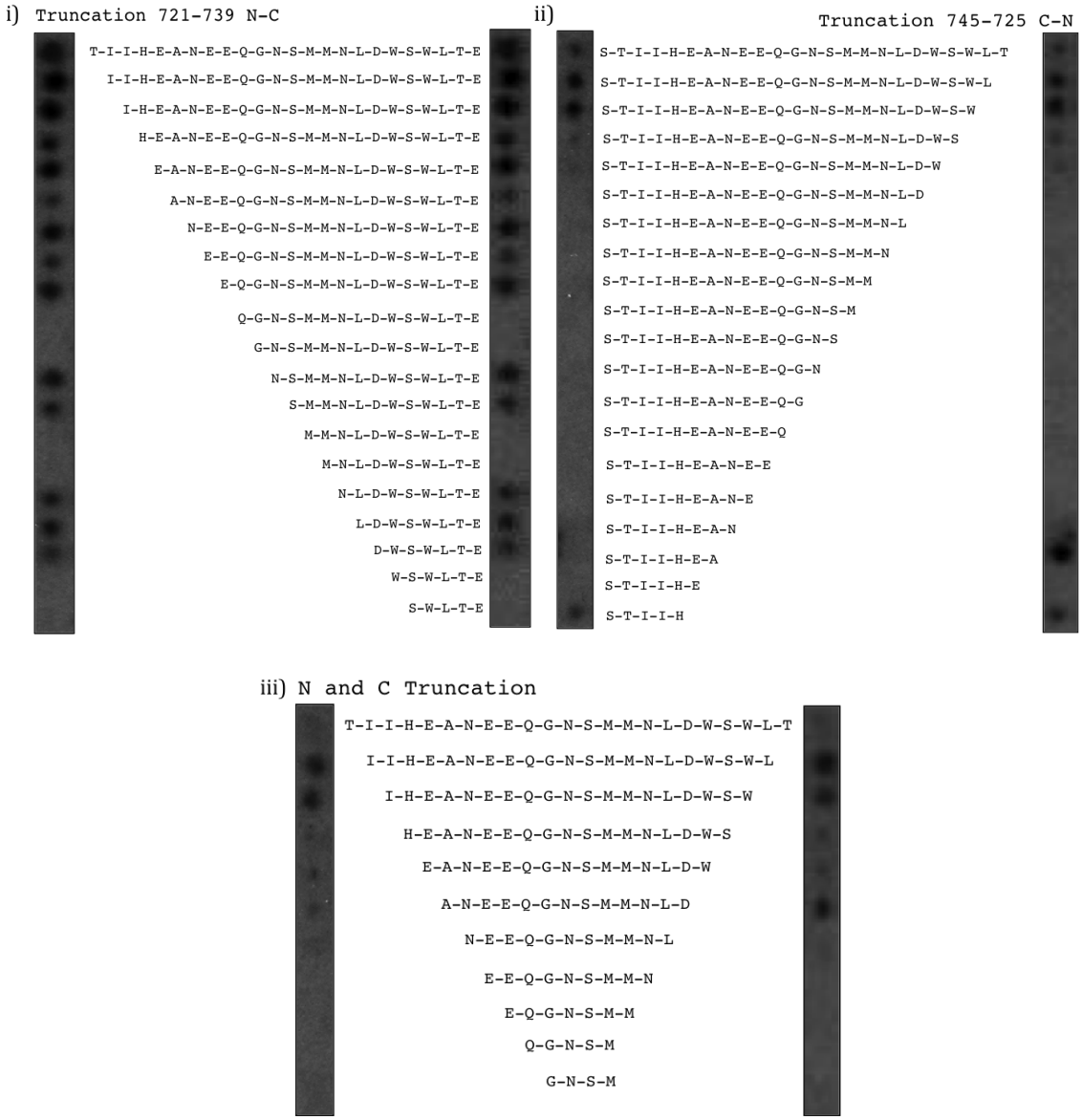

Figure 3.7 IKKα 721-745 truncation arrays overlaid with His-Aurora A

The IKK21-745 truncation arrays overlaid with His-Aurora AA kinase. Figure 3.7 ii) shows the C-N terminal sequential truncations froerved on the full length IKKα scanning peptide array and shown as the top spot in Figure 3.6. Each amino acid was sequentially truncated from either the N terminus or the C terminus or both until a 5 amino acid sequence remained. The array was incubated with 1μM His-Aurora A and immunoblotted with Aurora A specific antisera at a 1:3000 dilution.

3.4.3 Summary of Aurora A binding with IKKα alanine-scanning and truncation arrays

The further analysis of Aurora A interactions with IKKα-derived sequences/spots using alanine-scanning and truncation arrays have highlighted the essential role of the NBD in the interactions of Aurora A with IKKα. Figure 3.6 showed that upon the mutation of tryptophan 740 and 742, critical residues for the binding of IKKγ (*May et al, 2002*), the interaction with Aurora A was also abrogated (Figure 3.6). The truncation arrays also supported the observation that the NBD played an essential role in the binding of Aurora A, as seen when the truncation of NBD residues led to total loss of binding The data presented in Figure 3.7 ii) supported the critical role of tryptophan 742 in this interaction, as truncation of this residue was enough to prevent binding with the shorter sequences. Although the N-C truncation array indicated that the interaction may require multiple binding sites simultaneously the loss of some parts of this binding motif were enough to modulate binding as seen by the pattern of loss and return of binding apparent in Figure 3.7 i). Figure 3.7 ii) shows that without tryptophan 742 no binding occured and as such even if the interaction required multiple binding sites, loss of this residue was enough to prevent further interaction of Aurora A with the IKKα peptides at this site. These arrays indicate collectively the role of the NBD in mediating the binding of Aurora A with IKKα at this site.

3.5 Mapping the IKKβ interactions with Aurora A using alanine-scanning and truncation arrays

The C-terminal regions of IKKi that displayed binding by Aurora A, as identified by the full-length IKKβ array (Figure 3.1 ii), comprised the final five spots of the full-length scanning array encompassing residues716-756 from the primary amino acids sequence of IKKβ. This 40 amino acid region was too big to spot as a single sequence on an array, and due to the 5 amino acid overlap of the 25 amino acids spots from the full-length array only the first (716-740), second (721-745) and final (731-756) spots were chosen to represent this binding site. These spots together fully encompassed all the

residues that were identified from IKKβ as potential elements mediating Aurora A-IKKβ binding. Each of these spots was analysed using alanine-scanning and truncation arrays, which were prepared as previously described. The primary antibody control array with no protein overlay showed no non-specific binding (data not shown).

3.5.1 Interaction of Aurora A with amino acids 716-740 of IKKβ interaction site

3.5.1.1 Alanine-scanning Array of amino acids 716-740 of IKKβ overlaid with Aurora A

The overlay of Aurora A on the alanine scanning array of IKKβ Spot 1 is shown in Figure 3.8. This first chosen peptide spot of IKKβ lacked the sequence C terminal of the NBD hexapeptide from tryptophan 739. This however appeared not to have any effect on the interaction between Aurora A and IKKβ at this site. Consistent binding was observed across all the spots of this array apart from the initial 7 spots, which showed differential binding between the two duplicates but showed no total loss of binding across either duplicate. The mutation of tryptophan 739 also showed some loss of binding but was not seen in both of the replicates and therefore was discounted.

3.5.1.2 Truncation Arrays of amino acids 716-740 of IKKβ overlaid with Aurora A

The truncation analysis of IKKβ 716-72 was carried out to determine any minimal binding sequence. Figure 3.9 i) and ii) show the truncations from the N-C terminus and C-N terminus respectively. These truncations of the 'parent' spot appeared to have no reproducible effect on the interaction observed between Aurora A and IKKβ 716-740. However, upon the truncations of the first N-terminal leucine 718 and C-terminal aspartic acid 739 the binding was lost (Figure 3.9 iii)) though subsequently was re-established after the truncation of leucine 718 and leucine 737 in the next spot. It was noticeable that the loss of the C-terminal aspartic acid 739 within the NBD of this IKKβ-derived sequence paralleled the effects of truncation of the aspartic acid (D739) within

the IKKα NBD; the loss of which also ablated binding of Aurora A with IKKα 721-745(see Figure 3.5).

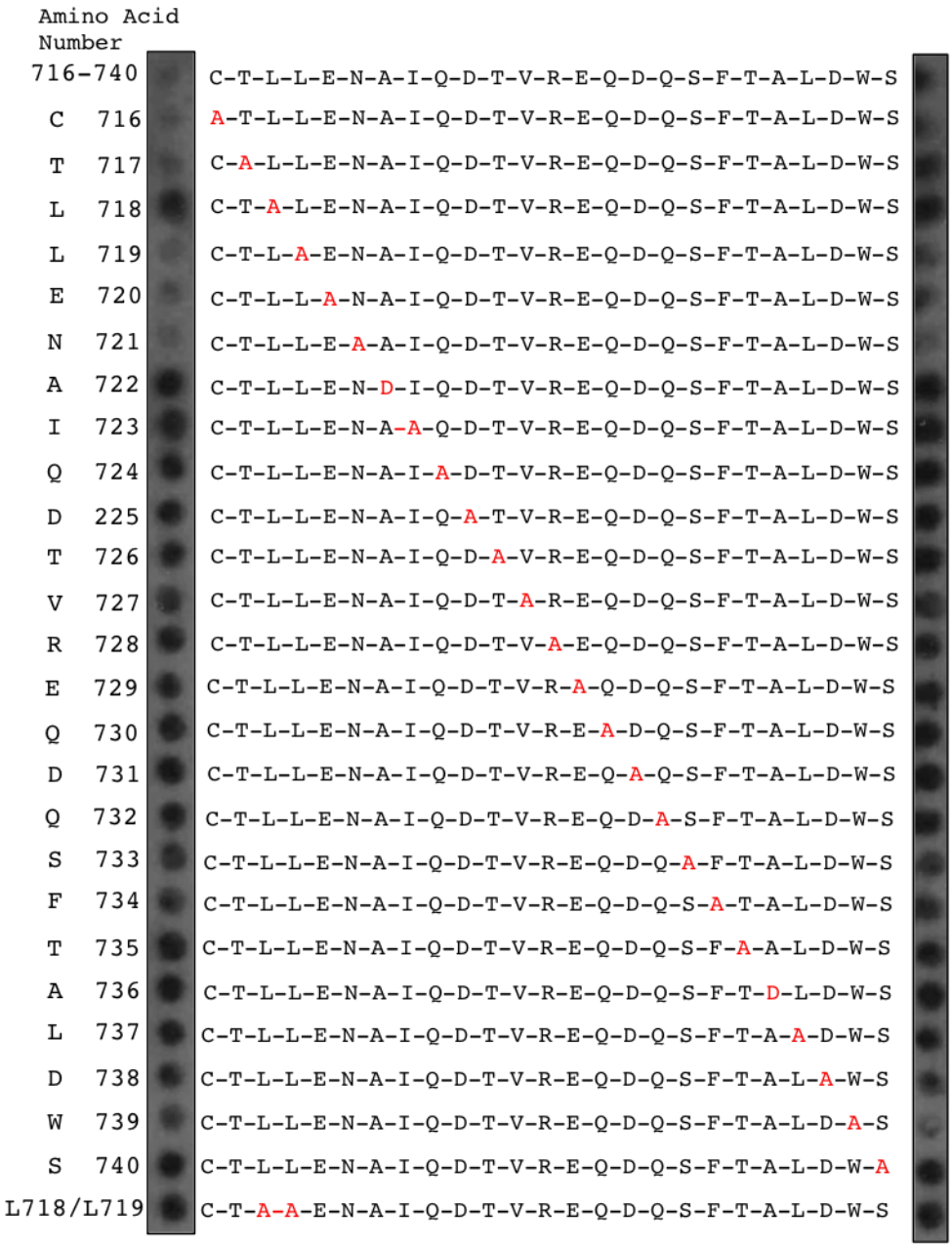

Figure 3.8 IKKβ 716-740 alanine-scanning array overlaid with His-Aurora A.

The alanine scanning IKKβ 716-740 peptide arrays were printed based upon the 25 amino peptide sequence obtained from the "parent" spot observed on the full length IKKβ scanning peptide array and shown as the top spot. Each amino acid was sequentially substituted by alanine. Any repeated amino acids in the sequence were substituted with Alanine in every permutation possible .The mutated residues are shown in red. The array was incubated with 1μM His-Aurora A and immunoblotted with Aurora A specific antisera at a 1:3000 dilution. The final spot shows the L718A/L719A mutations.

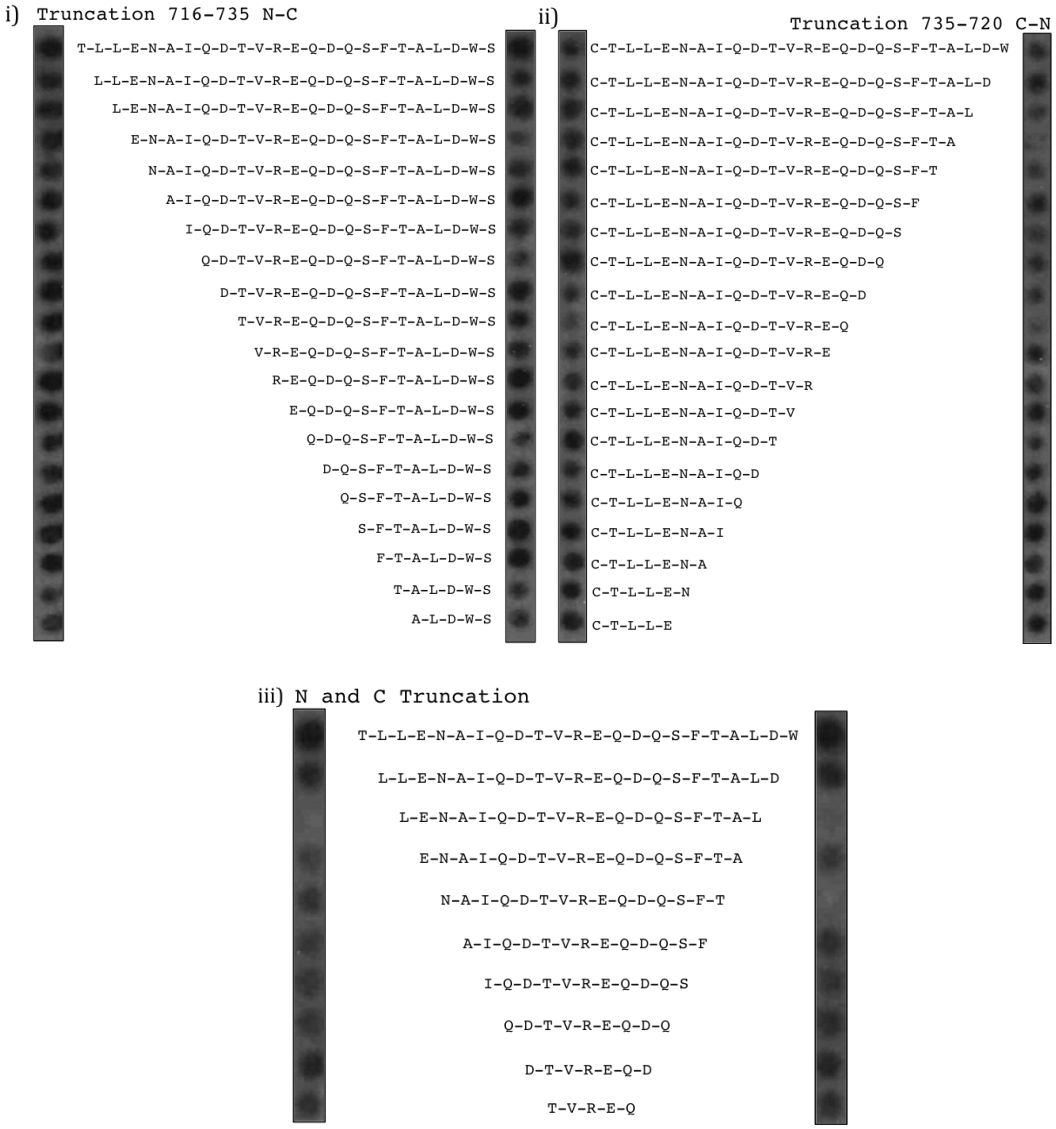

Figure 3.9 IKKβ 716-740 truncation arrays overlaid with His-Aurora A.

The IKK16-740 truncation arrays overlaid with His-Aurora A.ed based upon the 25 amino peptide sequence obtained from the "parent" spot observed on the full IKKβ scanning peptide array and shown as the top spot. Each amino acid was sequentially truncated from either the N-terminus or the C-terminus or both until a 5 amino acid sequence remained. The mutated residues are shown in red. The array was incubated with 1μM His-Aurora A and immunoblotted with Aurora A specific antisera at a 1:3000 dilution.

3.5.2 Interaction of Aurora A with amino acids 721-745 of IKK.

3.5.2.1 Alanine-scanning Array of amino acids 721-745 of IKKβ overlaid with Aurora A

Figure 3.10 represents the Aurora A binding of alanine-scanning arrays developed from the second of the 5 spots of binding within the C-terminal region of the IKKβ primary amino acid sequence. It was apparent from this data that there was no modulation of Aurora A binding/ interaction except in the final spot, where biding was completey lost following the dual mutation of both tryptophan 739 and 741 of the NBD. This suggested that at least one of these tryptophan residues must be present for this interaction to occur.

3.5.2.2 Truncation Arrays of amino acids 721-745 of IKKβ overlaid with Aurora A

The truncation arrays of IKKβ 721-745 can be seen in Figure 3.11. Overlay of His-Aurora A on the N-C terminal truncation array (Figure 3.11 i)) showed no modulation of binding with any of these truncations. This may have be due to the fact that the minimal truncated sequence present on this array still contained tryptophan 739 of the NBD. Therefore with all preceding mutations also containing this potentially critical residue for Aurora A-IKKβ interaction no further modulation was observed. The C-N truncation array in Figure 3.11 ii) however showed that the binding was lost after the truncation of both tryptophan 739 and 741 alongside aspartic acid 733 which interestingly in Figure 3.6 was seen to also ablate the interaction of His-Aurora A with IKKα 721-745. Binding returned after the truncation of leucine 730 but was lost again after alanine 729. The interaction returned after the truncation of aspartic acid 731 and was lost again after the mutation of glutamine 730 in the same spot, there was some weak binding seen in the following spots although less than was seen anywhere else on the array. The dual truncations (Figure 3.11 iii) showed that upon truncation of tryptophan 739 and aspartic acid 725 there was almost total loss of the interaction, which was restored after the truncation of serine 740 and threonine 726 but lost once again after the truncation of tryptophan 739 and valine 727. Some binding was

observed however it was poorly replicated by the parallel array and was subsequently discounted. The loss and re-establishment of His-Aurora A-IKKβ binding in both the C-N (Figure 3.11 ii)) and dual truncations (Figure 3.11 iii)) again suggested that there are multiple regions which mediate the interaction of Aurora A with IKKβ-derived sequences at this site. The NBD however was again shown to be critical for this interaction.

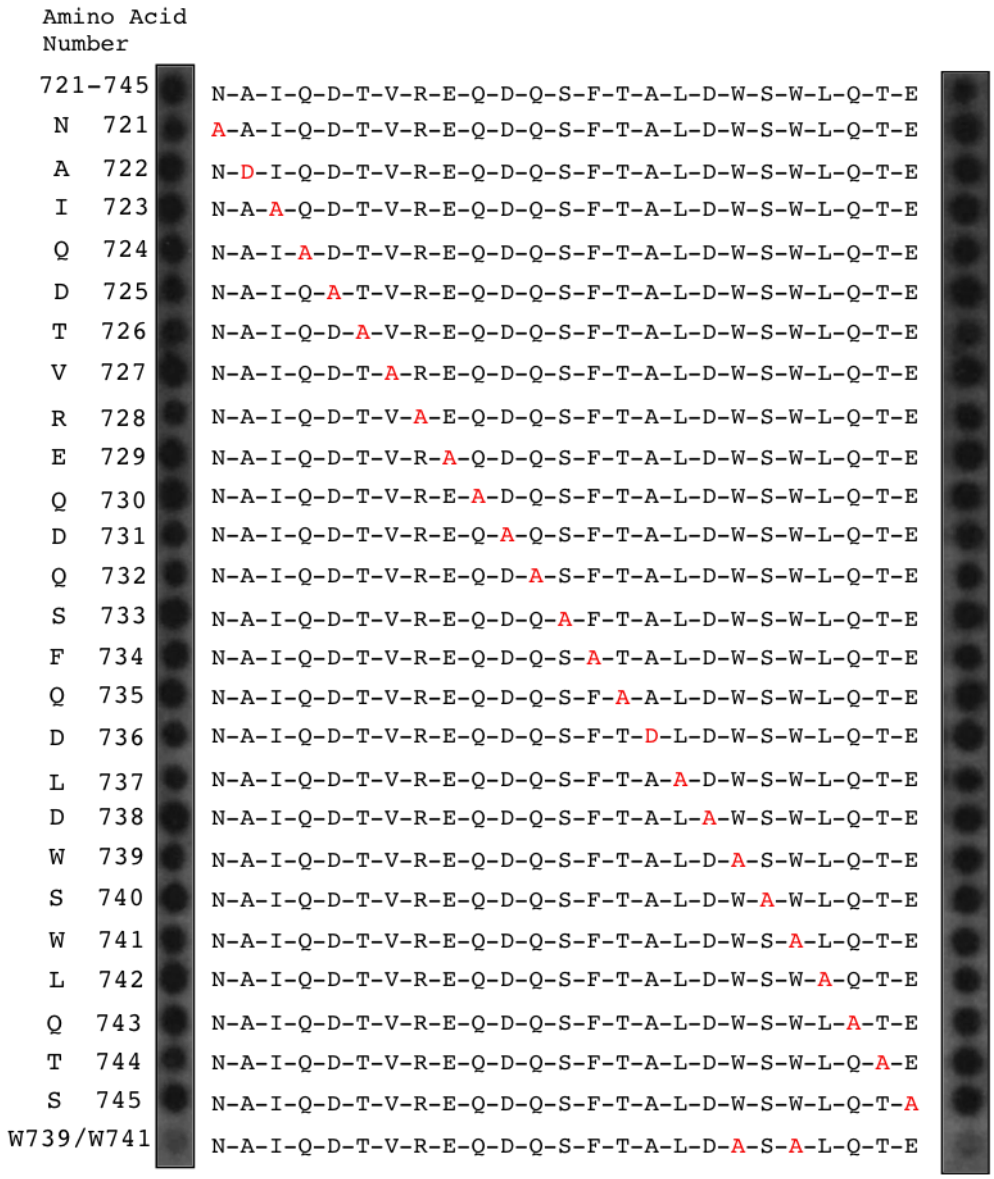

Figure 3.10 IKKβ 721-745 alanine-scanning array overlaid with His-Aurora A.

The alanine scanning IKKβ 721-745 peptide array was printed based upon the 25 amino peptide sequence obtained from the "parent" spot observed on the full length IKKβ peptide array and shown as the top spot. Each amino acid was sequentially substituted by alanine. Any repeated amino acids in the sequence were substituted with alanine in every permutation possible. The mutated residues are shown in red. The array was incubated with 1μM His-Aurora A and immunoblotted with Aurora A specific antisera at a 1:3000 dilution. The final two spots show the double NBD tryptophan mutation.

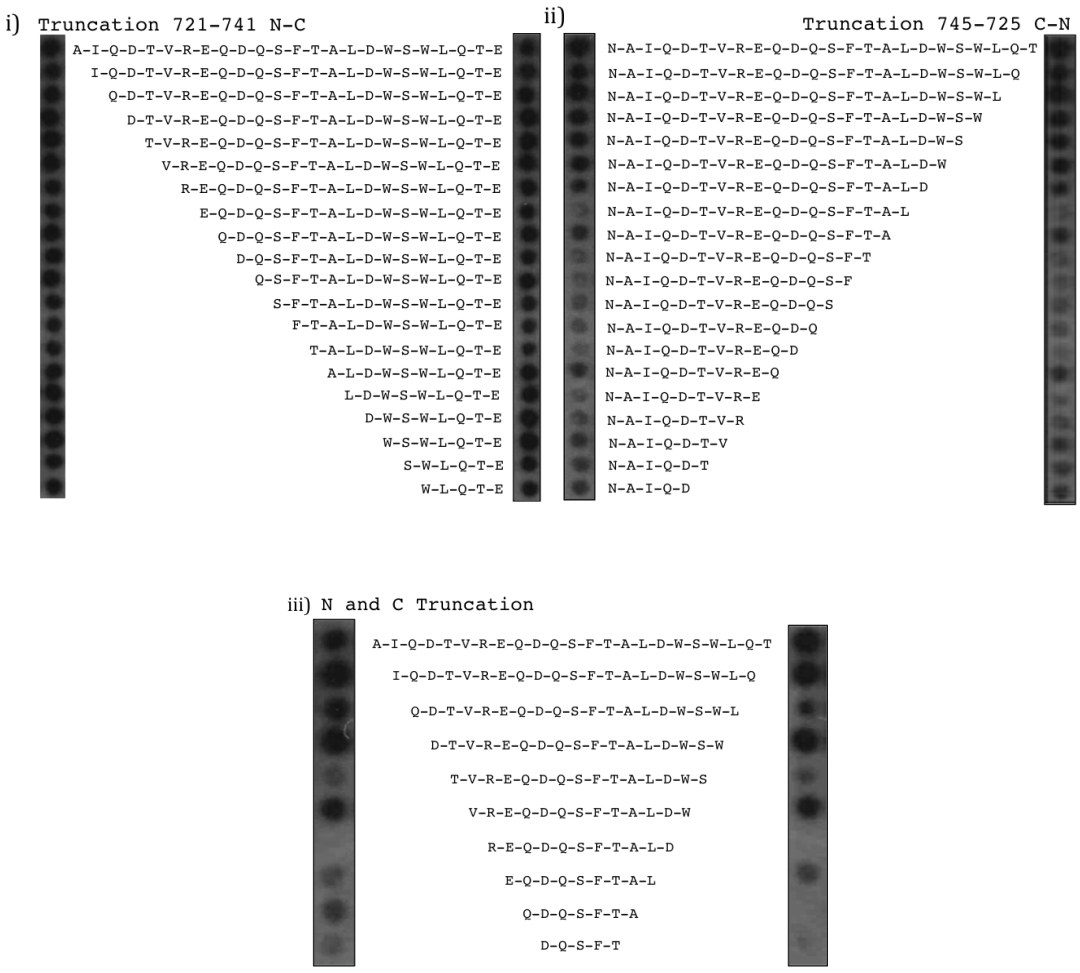

Figure 3.11 IKKβ 721-745 truncation arrays overlaid with His-Aurora A.

The IKKβ 721-745 truncation peptide arrays were printed based upon the 25 amino peptide sequence obtained from the "parent" spot observed on the full-length IKKβ peptide array and shown as the top spot. Each amino acid was sequentially truncated from either the N-terminus or the C-terminus or both until a 5 amino acid sequence remained. The mutated residues are shown in red. The array was incubated with 1μM His-Aurora A and immunoblotted with Aurora A specific antisera at a 1:3000 dilution.

3.5.3 Interaction of Aurora A with amino acids 731-756 of IKKa

3.5.3.1 Alanine-scanning Array of amino acids 731-756 of IKKβ overlaid with Aurora A

A final alanine-scanning array based on the last of the 5 spots of Aurora A binding to the C-terminal IKKβ sequences was developed for further overlay experiments with His-Aurora A, as shown in Figure 3.12. This array was printed with the IKKβ sequences that contained the IKKβ NBD as well as the 15 amino acid C-terminal extension specific to IKKβ not present in IKKα. Overlay and binding of His-Aurora A on this array was not affected until mutation of glutamic acid 753 at the extreme C-terminus of this sequence. Mutation of this residue led to the total loss of interaction. This was the sole single alanine mutation to cause any loss of binding however IKKβ 731-756 sequence contained a run of 4 glutamic acids at amino acids 745-747. Individually when these amino acids were mutated no loss of binding was observed but when 2 or more of these residues in any combination were mutated this led to the interaction being ablated. This suggested that the total charge of the 4 glutamic acid was contributing to the interaction of His-Aurora A with IKKβ and when this was reduced by the loss of any of these residues the interaction no longer occurred.

3.5.3.2 Truncation Arrays of amino acids 731-756 of IKKβ overlaid with Aurora A

The sequential truncation arrays of the amino acids 731-756 of IKKh Aurora Aually when these amino ed the role of glutamic acids 745-748 in the interaction with Aurora A. In Figure 3.13 i) no total loss of binding occured with any of the N-C terminal truncations shown on this array, which could be explained by the fact that as glutamic acid 753 remained in all of the peptides on this array. Mutation of glutamic acid 753 in the alanine-scanning array was the only single amino acid mutation that led to the loss of binding and this suggested that this residue may play a role in the interactions of Aurora A with IKKβ. The C-N terminal truncations as seen in Figure 3.13 ii) further supported the role of the NBD as an element regulating IKKβ and Aurora A binding at this site. This array showed no loss of interaction until the truncation of NBD

tryptophan 739 after which both of the critical NBD tryptophans were truncated and therefore the binding was lost. The interaction returned however after the truncation of NBD aspartic acid 738 and after the truncation of the final NBD residue leucine 737 the binding was lost totally. The final spot of this array was the sequence D-Q-S-F-T corresponding to amino acids 731-735, which in this settings howed binding however in Figure 3.11 iii) this was the final sequence also, but showed no interaction. This was therefore discounted as a potential minimal sequence for the interaction of Aurora A with this C-terminal region of IKKβ..

The dual truncation array in Figure 3.13 iii) shows no total loss of binding upon any of these truncations, however there was some reduction after truncation of tryptophan 741; tryptophan 739 was however still present and was sufficient to maintain binding of Aurora A with the IKKβ-derived peptide sequences.

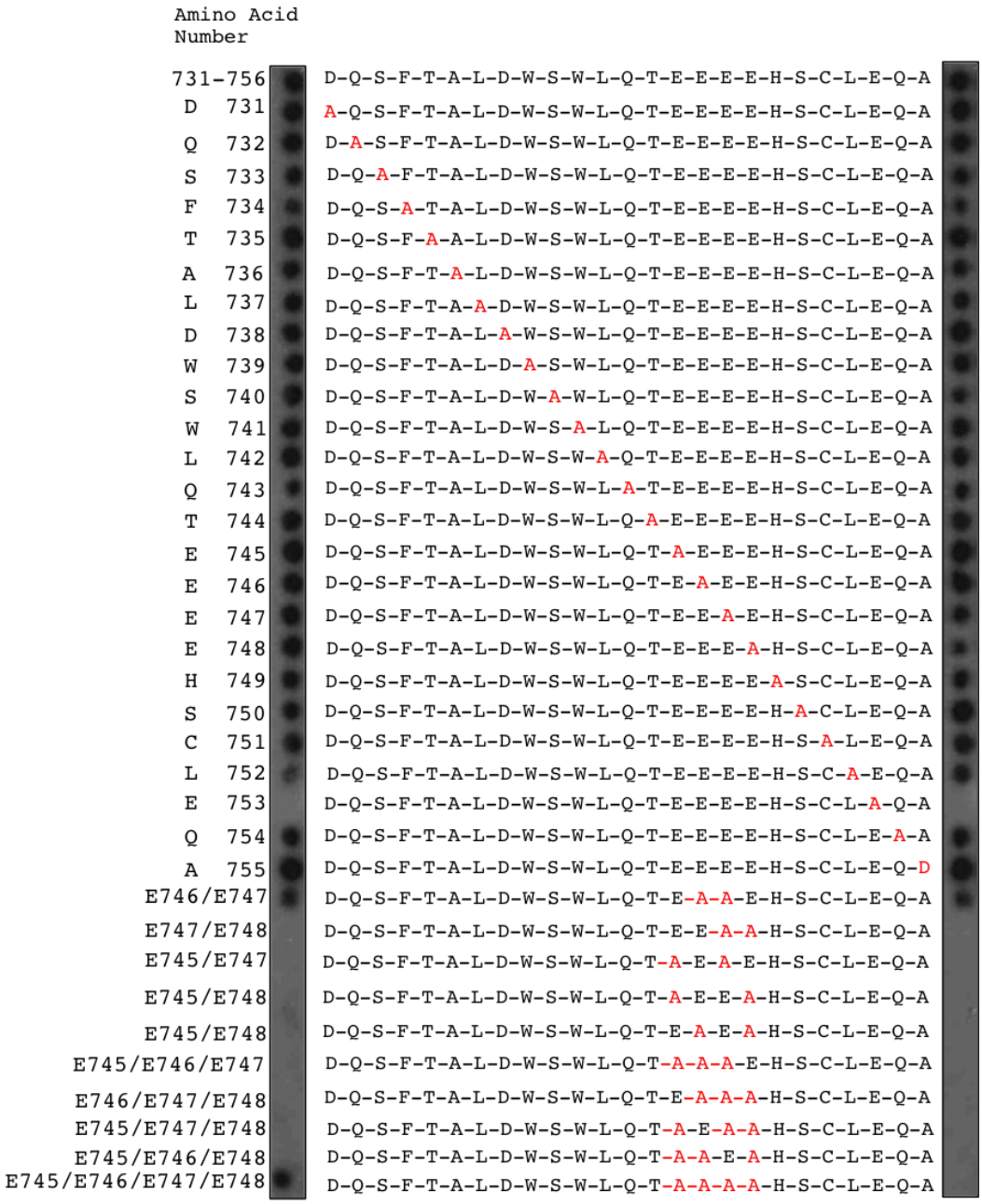

Figure 3.12 IKKβ 731-756 alanine-scanning array overlaid with His-Aurora A.

The alanine scan IKKβ 721-745 peptide arrays were printed based upon the 25 amino peptide sequence obtained from the "parent" spot observed on the full length IKKβ peptide array and shown as the top spot. Each amino acid was sequentially substituted by alanine. Any repeated amino acids in the sequence were substituted with alanine in every permutation possible. The mutated residues are shown in red. The array was incubated with 1μM His-AurA and immunoblotted with Aurora A specific antisera at a 1:3000 dilution.. Mutation of glutamic acids 745-748 were carried out in every permutation and shown at the end of the array.

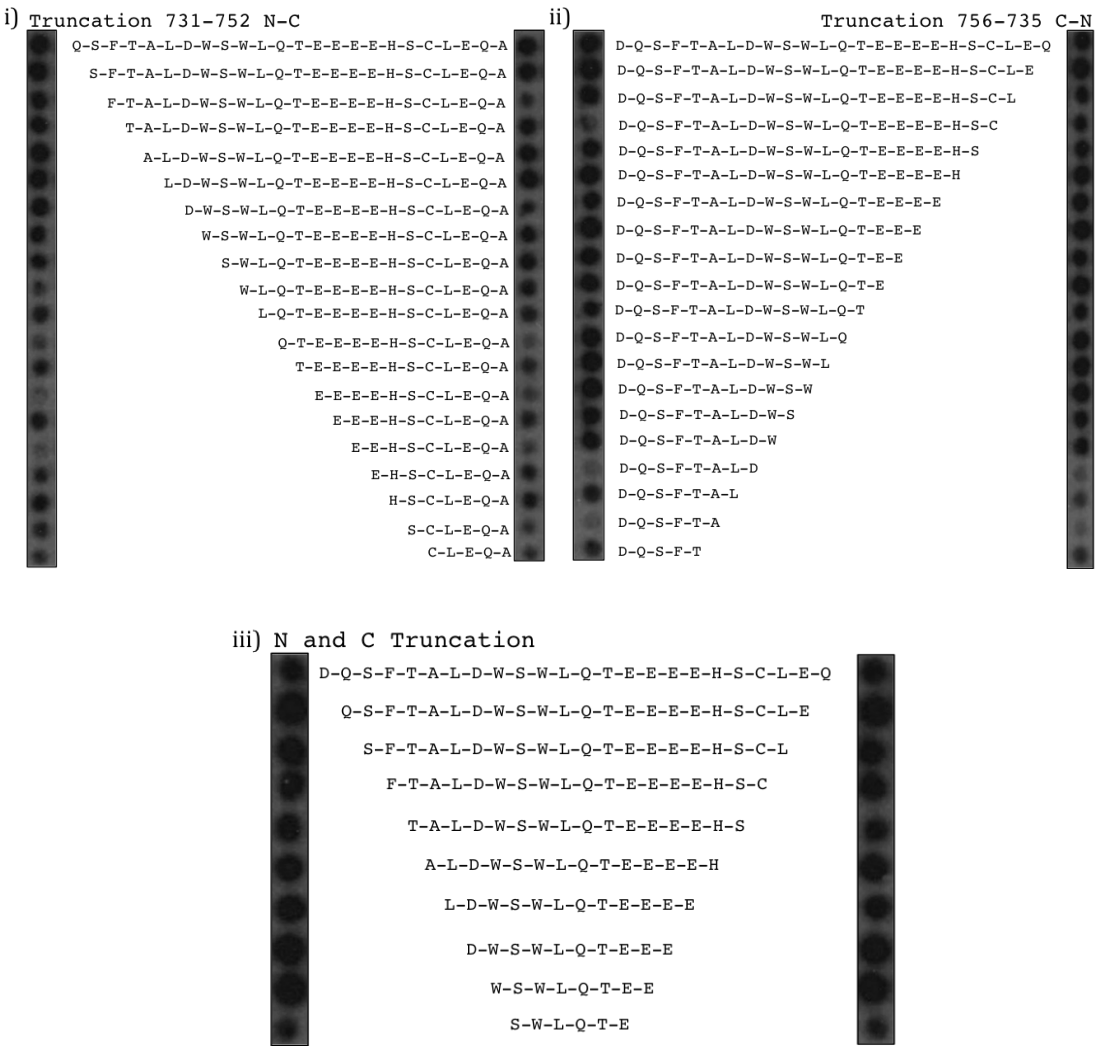

Figure 3.13 IKKβ 731-756 truncation arrays overlaid with His-Aurora A.

The IKK31-756 truncation arrays overlaid with His-Aurora A.ased upon the 25 ano peptide sequence obtained from the "parent" spot observed on the full length IKKβ peptide array and shown as the top spot. Each amino acid was sequentially truncated from either the N-terminus or the C-terminus or both until a 5 amino acid sequence remained. The array was incubated with 1μM His-Aurora A and immunoblotted with Aurora A specific antisera at a 1:3000 dilution.

3.6 Summary of Aurora A binding with IKKβ alanine-scanning and truncation arrays

The C-terminal site identified within IKKβ for Aurora A binding comprised amino acids 716-756, although this is a larger site as identified within IKKα which was comprised of 721-745. This was due partially to the C-terminal extension of IKKβ post-NBD. As this sequence was comprised of more that 25 amino acid residues it was not possible to use a single sequence for the alanine-scanning or truncation arrays and as shown in Figures 3.8 to 3.13 three separate sequences were individually analysed in this manner to attempt to clarify which elements within IKKβ were essential for Aurora A interaction. From these arrays however it was clear that interaction relied upon multiple regions which all contributed to the binding by Aurora A and due to this it was very difficult to assess firstly which residues were critical for binding and secondly establish any minimal sequence for this interaction. However, it was apparent that in all the sequences a critical role was played by the NBD tryptophans 739/741. It was shown in Figure 3.8, 3.9 iii), 3.10, 3.11 iii) and 3.13 ii) that upon the loss of both of these residues in all of the arrays was enough to totally ablate any interactions with Aurora A. These observations identified the only common feature to all three of the sequences analysed. This suggested that the NBD hexapeptide sequence L-D-W-S-W-L, homologous to that of IKKα, and in particular tryptophans 739/741, were key to the interaction of Aurora A with the C-terminal region of IKKβ.

This hexapeptide sequence is common to and identical between both of the catalytic subunits of the IKKs (*May et al, 2000*) and therefore this binding could be due to homology between subunits, however as seen in the alanine scanning and truncation arrays both IKKα and IKKβ do not have high levels of identity surrounding the NBD. It was shown in both IKKα/β that these surrounding regions made a significant contribution to the binding by Aurora A. The NBD may therefore act as the critical element to this protein-protein interaction and the surrounding residues may play more regulatory role in modulating the binding of Aurora A with the IKKs.

3.7 Interaction of Aurora A with the NEMO binding domain

The regulation of the Aurora A and IKK interactions at this site was reliant on the presence of the NBD as demonstrated previously. Therefore to determine the key residues of the NBD essential for Aurora A binding, the sequence N-L-D-W-S-W-L-T which contains the essential NBD hexapeptide was printed and the interactions investigated by truncation analysis. Due to the short length of this sequence the truncation from both the C-terminal and N-terminal individually and together was not required as there would be overlap between the sequences presented, the array was therefore prepared with permutations of this the 'parent' sequence to represent all permutations. The array was overlaid with His-Aurora A as previously described and the blank control array showed no binding (data not shown). Figure 3.14 shows the result of the Aurora A overlay on this array. This array showed that there were several residues within the NBD that contribute to the binding of His-Aurora A with this sequence. The first of which was aspartic acid 738, truncation of this residue in the N to C-terminal truncations was enough to ablate binding even with the continued presence of the two NBD tryptophans 739/741 that were previously observed to be critical to the interaction. However, this array also showed that upon truncation of tryptophan 741 in the C to N-terminal truncation was also enough to lead to loss of binding. This suggested that both aspartic acid 738 and tryptophan 741 are the critical elements for the interaction at this site and therefore the optimal binding sequence for Aurora A would be D-W-S-W-L.

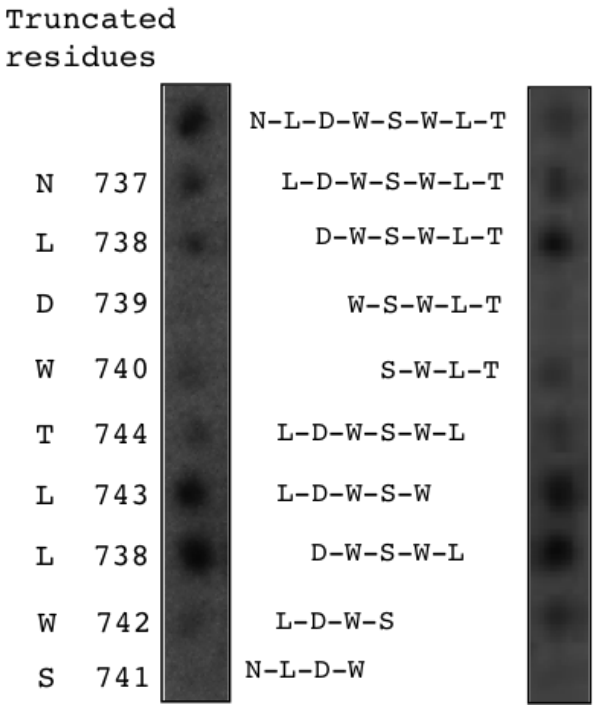

Figure 3.14 IKKα 737-744 NBD truncation array overlaid with His-Aurora A.

The IKK37-744 NBD truncation array overlaid with His-Aurora A.was enough to ablate binding even with the continued presence of the two NBD tryptophans 739/741 that were previously observed to be critical to the interaction. Hnce possible. The array was incubated with 1μM His-Aurora A and immunoblotted with Aurora A specific antisera at a 1:3000 dilution.

3.8 Discussion of Aurora A-IKK binding as assessed by peptide arrays

The interactions of Aurora A with components of the IKK complex (and vice-versa) were investigated extensively through the use of peptide arrays. Initially regions of Aurora A binding were identified through the use of the full-length IKK peptide arrays, which identified two main regions of binding (Figure 3.1); the first occurred within the kinase domain and the second at the extreme C-terminii which contained the NBD of the IKKs (*May et al, 2000*). Following this the full length Aurora kinases were printed as peptide arrays and overlaid with recombinant IKKα and IKKβ. The overlay of IKKα however was unsuccessful with no binding observed with any of the Aurora kinases. Initially this was believed to be due to the IKKα protein used having a Glutathione-S-Transferase (GST) tag; the GST tag is a 220 amino acids long (26kDa) sequence which is commonly used to help purify proteins as well as make the protein amenable for the analysis of protein-protein interactions by tag-specific pull-downs (*Vikis et al, 2004*). The large size of the GST tag was thought to have masked any binding of GST-IKKα to Aurora A, therefore the interaction was subsequently investigated with a His-tagged form of IKKα. Again no binding was observed. The fact that the Aurora A protein bound to the IKKα array suggests that an interaction does occur so the lack of binding of IKKα to the Aurora arrays was unexpected. This however may be a reflection of the limitations of this technique; peptide arrays are a methodology to investigate protein-protein interactions in a discontinuous manner i.e. short peptides of the full-length sequence representing interaction sites. This means that any interactions relying on specific secondary structure or protein folding are not possible to be observed. Also binding kinetics of interactions must be considered as protein interactions that are very quick, such as those mediating post-translational modifications, may not remain on the arrays long enough or are not strong enough to enable detectable protein remaining bound to the peptide arrays. This limitation is one of the reasons why the data obtained by peptide arrays must be supported by the use of complimentary techniques (*Katz et al, 2011*). The potential role of IKKα in the phosphorylation of Aurora A at threonine 288 as shown in the study by *Prajapati et al* may suggest that this interaction is transient which can be further investigated by the use of more quantative techniques for measuring protein-protein binding kinetics such as Surface Plasmon Resonance (*Prajapati et al, 2006*).

IKKβ on the other hand was seen to bind to all three members of the Aurora kinase family (Figure 3.2) although some of the regions identified across the Aurora kinases may be due to sequence homology as previously discussed. The binding sites identified on Aurora A however were observed to encompass the same regions that TPX-2, the Aurora A co-factor, has been shown to interact with (*Bayliss et al, 2003*). TPX2 binding is essential for Aurora A localisation to the spindle microtubules, induces a conformational change promoting auto-phosphorylation of Aurora A which also protects the protein from de-phosphorylation by Protein Phosphatase 1 (PP1) (*Bibby et al, 2009*). Disruption of TPX2 binding by IKKβ may be a potential mechanism that could prevent this conformational change subsequently driving the degradation of Aurora A by the APC/C. The role of IKKβ in regulating the β-TRCP mediated Aurora A degradation has been suggested by *Irelan et al*, (*Irelan et al,* 2007) however this potential mechanism of activation/deactivation requires to be characterised fully in a cellular setting.

The strongest binding of Aurora A to both of the IKK catalytic subunits was apparent at the extreme C-terminii and due to the role of this region in NEMO binding (*May et al, 2002*) and also its reported function as a multi-protein docking site (*Higashimoto et al, 2008*) this region was further analysed by alanine scanning and truncation arrays. From this it was determined that this site on both IKKα and IKKβ can mediate binding by Aurora A and there are multiple residues within this region that contribute to the interaction. The essential region to the interaction in both IKKα and IKKβ was identified to be the NBD hexapeptide sequence L-D-W-S-W-L, with the central tryptophans being critical for this interaction as previously described in (see Section 3.X Figure 3. XX). These results further support the idea of the NBD as a multi-protein binding site with the central hexapeptide sequence as the critical feature for not just NEMO binding but also for other additional alternative IKK interacting proteins.

This observation must be further investigated using alternative techniques as peptide arrays are an artificial system by which to analyse protein-protein interactions that only considers small sections of the full protein at any given time and therefore cannot accurately replicate the true nature of these interactions (*Katz et al, 2011*). These results were therefore further pursued in a cellular system.

3.9 Investigating the IKK/Aurora A interaction in a cellular system

The peptide arrays allowed for the mapping of binding sites of protein-protein interactions, however there are limitations to this methodology. Therefore the potential for Aurora A-IKK interactions were investigated further in a cellular system. The standard methodology for investigating protein-protein interactions in a cellular system is through the use of (co-)immunoprecipitation. Immunoprecipitation is the separation of a known protein from a crude mixture of proteins in solution i.e. solubilised cell lysates through the use of specific antibody. If the protein of interest is bound to other proteins as part of a larger complex these proteins can in theory be extracted from the mixture alongside the protein(s) of interest. The complexes isolated from the mixture can then be analysed by immunoblotting to determine the components of this complex, this is known as co-immunoprecipitation. The aim of this technique is to solubilise intact protein complexes prior to incubation with the antibody. The cell lysates are therefore prepared using a lysis buffer, which will maintain the complexes structural integrity and allow for the enrichment of these complexes to analyse the component parts. The lysis buffer uses non-ionic detergents (e.g. Triton X-100, NP40) to permeabilise the cell membrane while keeping the non-covalent protein-protein interactions intact. A combination of protease inhibitors is also used to prevent protein degradation (e.g. Pepstatin, Leupeptin, Aprotinin) within the cells. Once the cells are lysed two methods are typically used for immunoprecipitation of protein complexes. The first is the direct capture method in which the antibody is pre-coupled to an agarose/sepharose support bead through either protein A or protein G, bacterially expressed surface proteins that express multiple Ig binding sites. Once coupled to the beads are incubated with the solubilised cellular lysates and will isolate the protein of interest from the mixture. The second method used is referred to as indirect capture is when the antibody is incubated with the crude lysate for 12 hours or more to allow for the binding of the antibody to the protein of interest and this mixture is subsequently incubated with the protein A/G beads which in turn will bind any protein-antibody complexes assembled and separate your protein of interest from the mixture, this is referred to as ‘pulling down’ of the protein.

The composition of the isolated complexes can then be investigated by immunoblotting. For SDS-PAGE these complexes are eluted from the beads with loading buffer. This is a harsh eluent and will also elute antibody fragments and non-covalently bound antibody that will be visible on immunoblots.

Using either direct or indirect methods it is possible to isolate larger complexes assembled with the protein of interest and can therefore be used to investigate interaction between proteins. In order to further investigate the interaction of both IKKα and IKKβ co-immunoprecipitation of the complex with Aurora A was pursued using a direct capture methodology.

3.9.1 Co-Immunoprecipitation of the catalytic sub-units of the IKK complex with Aurora A

Co-immunoprecipitation of endogenous IKKα and IKKβ with Aurora A specific antibodies was pursued initially. 1µg of Aurora A rabbit polyclonal antibody was coupled to Protein G-agarose beads and mixed with a solubilised cell lysate of PC3 cells at 4˚C for 2 hours. As a control, beads alone were incubated with a parallel solubilised cell lysate in the absence of primary anti-Aurora A antibody to identify any non-specific binding of proteins agarose beads/ support matrix. It was possible to co-immunoprecipitate both IKKα and IKKβ (see Figure 3.15), it was not possible however to visualise the immunoprecipitation of endogenous Aurora A by the Aurora A specific antibody in these experiments as the molecular weight of Aurora A (48kDa) is the same as that of the heavy chain of the antibody fragments and therefore was obscured by the immunoglobulin Heavy Chain. The beads alone showed very little non-specific binding of the IKK proteins and therefore this interaction is likely mediated through the interaction of the IKK proteins with Aurora A. The level of binding observed was very low however and close to the limits of detection. This may have been due to the fact that this immunoprecipitation was pursued with an asynchronous population of cells with variable Aurora A expression. As Aurora A expression is tightly regulated and is at its maximal level during mitosis further experiments were carried out using PC3 cells treated with Nocodazole to arrest the cells during pro-metaphase. This experimental strategy towards elevating cellular Aurora A expression had however no effect on the levels of either IKKα or IKKβ co-immunoprecipitated with Aurora A (data not

shown).The use of beads alone incubated with solubilised cell lysate in the absence of antibody demonstrated that the IKK proteins did not interact non-specifically with the protein G-sepharose beads/support matrix, as illustrated in Figure 3.15 i) and ii). This suggested the co-immunoprecipitation of these proteins was through interaction with recovered cellular Aurora A and not due to non-specific binding to the beads. The inability to visualise Aurora A distinct from the Immunoglobulin Heavy Chain polypeptide also made it impossible to demonstrate the co-immunoprecipitation of Aurora A with the IKKs using IKK specific antibodies.

To circumvent these problems and allow also the manipulation of the IKK proteins to incorporate mutations of the residues identified as key regulators of Aurora A binding in the peptide arrays an alternative methodology was developed. This methodology was based upon the use of transient transfection of cells with plasmid expression constructs encoding affinity-tagged proteins (e.g. Haemaglutinin (HA)). These affinity tags would enable firstly specific immunoprecipitation of exogenous over-expressed proteins in a tag-specific manner distinct from endogenous counterparts and secondly allow cross-detection of any co-expressed affinity-tagged proteins using anti-tag antibodies thereby allowing assessment of any potential protein-protein interactions in a cellular setting.

Figure 3.15 Co-immunoprecipitation of IKKα and IKKβ with Aurora A from PC3 solubilised cell lysates.

1µg rabbit monoclonal anti-Aurora A antibody was pre-coupled to protein G-sepharose beads and incubated with solubilised cell lysates of PC3 cells for 2 hours. Recovered proteins present in immonoprecipitate pellets versus unbound proteins present in the supernatants were assessed by Western blotting as descried in the Methods section.i) anti-IKKα mouse monoclonal antibody at 1:3500 dilution was used to detect co-immunoprecipitation of IKKα ii) IKKβ rabbit monoclonal antibody at 1:3000 dilution was used to detect co-immunoprecipitation of IKKβ. Beads alone were incubated with the solubilised cell lysates to act as a negative control for non-specific interactions of the IKK proteins with the matrix. Pre-stained markers were run in parallel to prepared samples to indicate molecular weights of detected proteins. Data shown is representative of three independent experiments.

3.9.2 Co-Immunoprecipitation of components of the IKK complex with Aurora A in a co-transfection system.

To further analyse the Aurora A-IKK interactions, a cellular transfection system was developed using exongenous DNA expression constructs. Plasmid constructs encoding affinity-tagged cDNAs of hAurora A and hIKKα/β/γ were kindly supplied by Prof. S. Dimitrov (Institut Albert Bonniot, Grenoble, France) and by Dr. M. May (University of Pennsylvannia, PA, USA) respectively. These constructs were used in a transient transfection system in Human Embryonic Kidney 293 (HEK293) cells, as this is a commonly used system highly amenable to transfection. The plasmid constructs for the IKK complex additionally expressed an Xpress tag (D-L-Y-D-D-D-D-K) at the N-terminus of each of the full-length IKK proteins and the Aurora A constructs additionally expressed an N-terminal HA tag (Y-P-Y-D-V-P-D-Y-A). This allowed for co-expression and co-immunoprecipitation through the use of antibodies specific to the tags. The use of tag specific antibodies to isolate tagged proteins also allowed for the detection of any potential larger protein complex assembled by the over-expressed proteins by virtue of cross-blotting for the alternative tags. The co-transfection of these constructs was optimised so a near equal level of expression of all subunitss of the IKK complex and simultaneously the co-transfected Aurora A protein was observed in whole cell lysates by Western blotting. Co-immunoprecipitation was carried out as previously described using 1μg of anti-HA antibody to recover HA-Aurora A and then cross-blotted for Xpress to show any co-immunoprecipitation of the IKK proteins (see Figure 3.14). Following co-transfection of HEK cells with each of the Xpress-IKKs and HA Aurora A all three members of the IKK complex were recoverable following immunoprecipitation of HA-Aurora A using anti-HA antibodies (Figure 3.16 i). In parallel, whole cell lysates were immunoblotted to determine the level of expression of each Xpress-IKK subunit and HA-Aurora A in the cell lysate. Empty plasmid vectors, HA and His C, were simultaneously expressed and immunoprecipitated as controls to determine if the vector was leading to any expression detectable in the lysates or by immunoprecipitation. It was apparent from this experiment that IKKα, IKKβ and IKKγ were all able to interact and could be 'pulled-down' in association with Aurora A. The expression and immunoprecipitation of HA-Aurora A was also assessed by immunblotting of the same samples with anti-HA antibody as shown in Figure 3.16 ii). The expression of HA-Aurora A was consistent between lysates showing that it was

possible to co-express the Xpress-IKK proteins alongside HA-Aurora A. However, due to cross reactivity of the detecting antibodies with the heavy chain of the immunoglobulin used for immunoprecipitation present in the pellets of these samples it was impossible to determine the effectiveness of HA-Aurora A pull down.

To confirm that the co-immunoprecipitation of the IKK proteins was occurring through an interaction with Aurora A and not through the non-specific interaction of the expressed proteins with the beads a no-antibody-beads alone immunoprecipitation was carried out with the individually expressed constructs. The results of these experiments are shown in Figure 3.17 and showed that the exogenous IKK proteins and Aurora A all bound to the beads non-specifically. This made it impossible to interpret any suggested co-immunoprecipitation of the IKK proteins with Aurora A and vice-versa This was an unexpected result as it had been found in the immunoprecipitation of endogenous IKKs (Figure 3.15) pursued previously that there were no observed non-specific interactions of any of the IKK subunits with beads in the absence of antibody. Therefore, in the transient transfection system the observed non-specific binding of the beads by the exogenously expressed Xpress-IKKs may potentially have been due simply to increased expression of the proteins in the cells, leading to detectable levels of non-specific interactions. The structural nature of the over-expressed proteins may also have contributed to the observed non-specific interactions, as the sepharose support matrix is hydrophobic like the IKK proteins that contain large hydrophobic regions at their surfaces to facilitate protein-protein interactions. . Several further experimental conditions were then assessed in an attempt to reduce the levels of non-specific binding. This included shorter incubations of the prepared solubilised whole cell lysates with the Protein G-sepharose beads ranging from from 15 minutes to 2 hours. These approaches had no effect on the levels of binding of the over-expressed Xpress-IKKs to the beads alone. More stringent washing of the beads after incubation was also pursued but again showed no effect (data not shown).

The binding of all expressed proteins to the Protein G-sepharose beads in the absence of anti-tag antibodies, as shown in Figure 3.17, meant that it was impossible to assess binding of the IKK proteins with Aurora A using this antibody support structure.

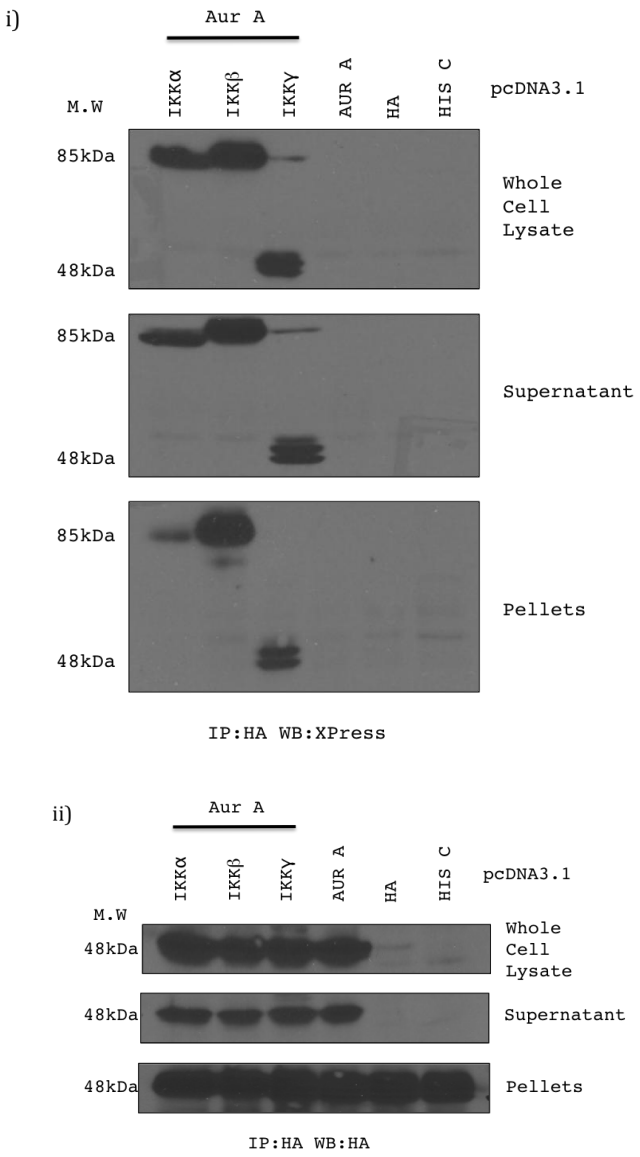

Figure 3.16 Co-Immunoprecipitation of transfected IKKα/β/γ proteins in association with HA-Aurora A recovered from HEK293 whole cell lysates

HEK293 were transiently transfected with 1µg pcDNA3.1 of expression constructs as indicated. 1µg rabbit monoclonal anti-HA antibody was pre-coupled to protein G- sepharose beads and incubated with solubilised whole cell lysates prepared from transfected HEK293 cells for 2hrs. Proportions of whole cell lysates were each immunoblotted to assess expression of all constructs. i) anti-Xpress mouse monoclonal antibody at 1:12,000 dilution used to detect co-immunoprecipitation of IKKα/β/γ ii) anti-HA rabbit monoclonal antibody at 1:12,000 dilution used o detect immunoprecipitation of HA-Aurora A. Pre-stained protein markers were included in all immunoblots to indicate molecular weights of detected proteins. Data show is representative of three independent experiments.

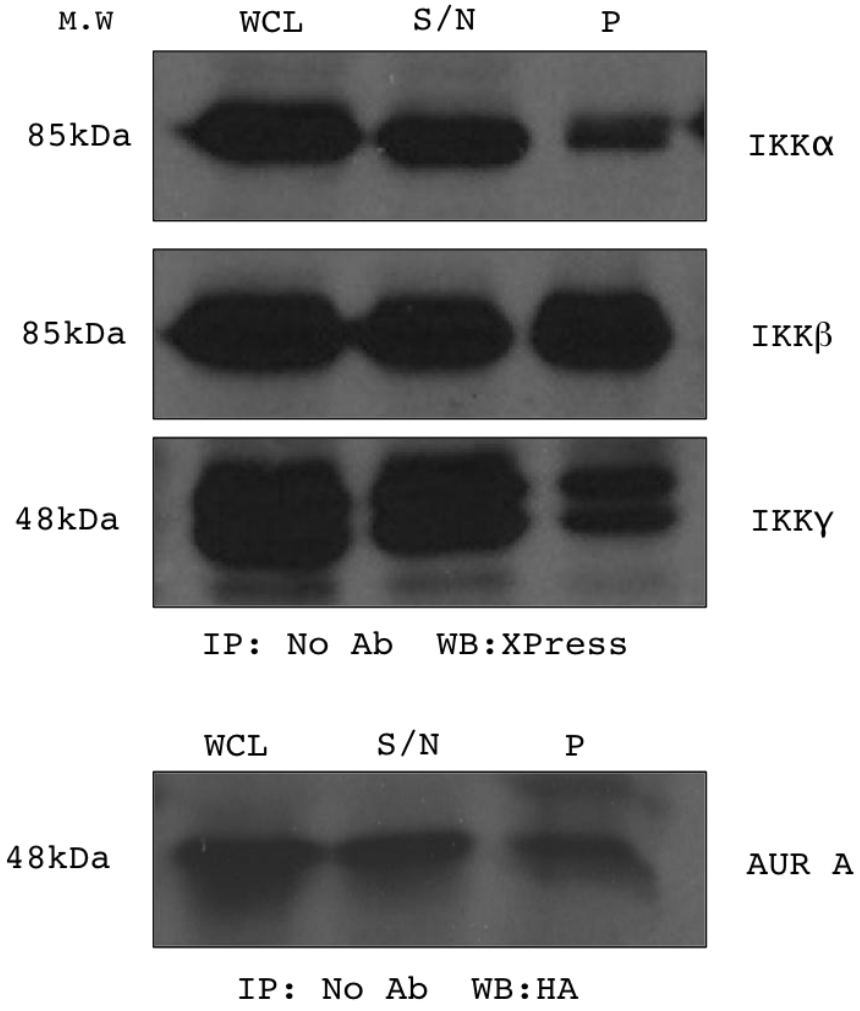

Figure 3.17 Precipitation of transiently expressed Xpress-IKKs and HA-Aurora A by Protein G sepharose beads in the absence of anti-tag antibodies.

HEK293 cells were transiently transfected with 1μg pcDNA3.1 of expression constructs as indicated. Protein G-sepharose beads were incubated with whole cell lysates of transfected HEK293 cells for 2 hours and following this 'pellets' (P) and 'supernatants' (S/N) prepared . A proportion of whole cell lysates (WCL) were kept and immunoblotted to assess expression of constructs in the cells. anti-Xpress mouse monoclonal antibody at 1:12,000 dilution used to detect immunoprecipitation of Xpress-IKK and anti-HA rabbit monoclonal antibody at 1:12,000 dilution used to detect immunoprecipitation of HA-AurA. Pre-stained protein marker included in all immunoblots to indicate molecular weights of stained proteins. Data shown is representation of three independent experiments.

3.10 Design and expression of IKK mutants

The peptide array analysis of Aurora A and IKKs interactions as reported in Sections 3.2-3.5 showed that a key site of interaction of Aurora A with IKKα and IKKβ occurs within the NBD common to both IKKα/β. This region has been well defined in the literature (*May et al, 2000, Rushe et al, 2008 and Strnad et al, 2006*) as a key regulator of IKKγ binding to both IKKα and IKKβ, however it was recently shown to also interact with PLK1 and has been proposed to function as a multi-protein docking site (*Higashimoto et al, 2008*). In order to support the findings of the peptide arrays the expression constructs for wild-type (WT) IKKα and WT IKKβ, kindly supplied by Dr. M. May, were used as templates to prepare mutants of the NBDbased on the residues identified in the alanine-scanning and truncation arrays to be essential for Aurora A binding. The residues identified for Aurora A binding have also been described to be critical for NEMO interactions with IKKα and IKKβ, most notably the central tryptophan residues of the NBD hexapeptide sequence; L-D-W-S-W-L (*May et al, 2002; Rushe et al, 2008*) The strategy for the design of the mutations was to use the results obtained from the peptide arrays combined with what has been defined in the literature as the essential residues for NEMO binding to determine if the interactions occur at the same site and whether there is any conserved or divergent hierarchy associated with individual amino acid residues.

Site-directed mutatgenesis (SDM) was used to synthesise the mutant expression constructs, Table 3.1 shows the range of mutants and the primer sequences used to create the said NBD mutants of IKKβ. All mutants were successfully made and incorporation of the mutation was confirmed by sequencing of the mutated plasmid DNA. To ensure no additional mutations were incorporated into the parent DNA plasmid the sequencing was carried out across the entire DNA insert. The mutations shown in Table 3.1 were all incorporated successfully into new expression constructs. In addition, the use of the primers for each of the IKKβ W739/741A and F734A mutants sequentially on the same construct a plasmid expression construct of the IKKβ triple W739A/W741A/F743A mutant was prepared. This triple mutation was carried out as these three residues were identified in the the peptide arrays studies as being essential for Aurora A binding but also by the independent co-crystallisation studies of *Rushe et al* as being the critical amino acids for IKK NBD-NEMO binding.

These mutants were subsequently optimised for expression in the HEK293 system by transient transfection and were able to be expressed to an equivalent level in the cells as shown in Figure 3.18. The mutant IKKβ expression constructs were also examined in a cellular co-transfection system and co-immunoprecipitation experiments pursued however non-specific interactions of these constructs were observed to interact non-specifically with the protein G-sepharose beads in the absence of anti-Xpress/anti-HA antibodies as seen with the WT IKKα constructs (Figure 3.17) (data not shown).

The creation of IKKα mutant constructs were also pursued but at time of writing were still being carried out.

WT IKKβ	IKKβ WT: 733 756 S F T A L D W S W L Q T E E E E H S C L E Q A S & AGTTTCACGGCCCTAGACTGGAGCTGGTTACAGACGGAAGAAGAAGAGCACAGCTGCCTGGAGCAGGCCTCATGA
IKKβ Post NBD Trunc.	IKKβ Post NBD truncation MUTANT: SFTALDWSWL&TEEEEHSCLEQAS Primers: SDMF: 5'- GCCCTAGACTGGAGCTGGTTATAGACGGAAGAAGAAGAGCAC -3' SDMR: 5'- CGGGATCTGACCTCGACCAATATCTGCCTTCTTCTTCTCGTG -3'
IKKβ Pre NBD Trunc.	IKKβ Pre NBD truncation MUTANT: SFT&LDWSWLQTEEEEHSCLEQAS Primers: SDMF: 5'- GACCAGAGTTTCACGTAACTAGACTGGAGCTGG - 3' SDMR: 5'- CTGGTCTCAAAGTGCATTGATCTGACCTCGACC - 3'
IKKβ W742A	IKKβ W739/741 MUTANT: SFTALDASALQTEEEEHSCLEQAS Primers: SDMF:5'GAGTTTCACGGCCCTAGACGCGAGCGCGTTACAGACGGAAGAAGAA 3' SDMR:5'TTCTTCTTCCGTCTGTAACGCGCTCGCGTCTAGGGCCGTGAAACTC 3'
IKKβ F734A	IKKβ F734A MUTANT: SATALDWSWLQTEEEEHSCLEQAS Primers: SDMF: 5' - GGAACAAGACCAGAGTGCCACGGCCCTAGACTGG - 3' SDMR: 5' - CCAGTCTAGGGCCGTGGCACTCTGGTCTTGTTCC - 3'
IKKβ S741A	IKKβ S740A MUTANT: SFTALDWAWLQTEEEEHSCLEQAS Primers: SDMF: 5' - CGGCCCTAGACTGGGCCTGGTTACAGACGG - 3' SDMR: 5' - CCGTCTGTAACCAGGCCCAGTCTAGGGCCG - 3'
IKKβ S741E	IKKβ S740E MUTANT: SFTALDWEWLQTEEEEHSCLEQAS Primers: SDMF: 5' - GTTTCACGGCCCTAGACTGGGAATGGTTACAGACGGAAGAAGA- 3' SDMR: 5' - TCTTCTTCCGTCTGTAACCATTCCCAGTCTAGGGCCGTGAAAC- 3'

Table 3.1 Table of primers used to make IKKβ mutants

Primers designed for SDM enabling the incorporation of several mutations into the NBD of IKKβ. Codons changed are highlighted in red, altered amino acids are highlighted in blue and stop codons are represented by an ampersand and highlighted in blue.

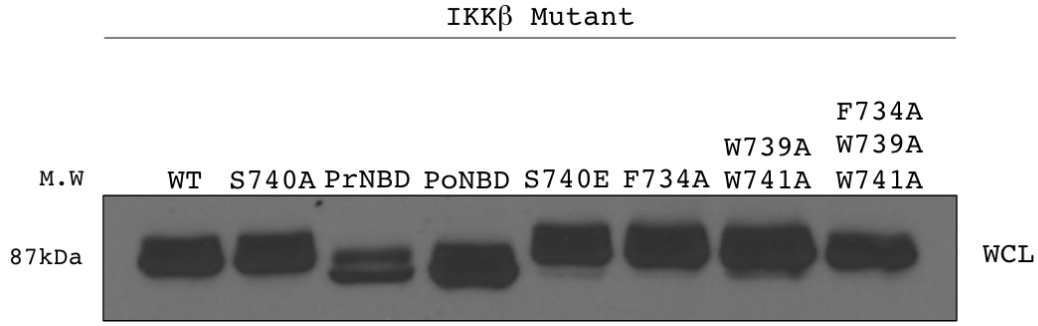

Figure 3.18 Expression of mutant Xpress-IKKβ in HEK293 cells.

HEK293 cells were transiently transfected with 1µg pcDNA3.1 expression constructs. 48hours post transfection whole cell lysates were prepared and immunoblotted with anti-Xpress mouse monoclonal antibody. Pre-stained protein marker were included in all immunoblots to indicate molecular weights of visualised proteins. Data shown is representative of three independent experiments.

3.11 Conclusions

The use of peptide arrays to study Aurora A-IKK interactions has demonstrated that Aurora A binds potentially to both IKKα and IKKβ via interactions mediated by theNBD. The critical residues for this interaction were shown to fall within the NBD hexapeptide sequence L-D-W-S-W-L (*May et al, 2000*, *Rushe et al, 2008*). From the peptide arrays it was also evident that all residues of the NBD wereinvolved in the binding of Aurora A, the central tryptophans being essential to the interaction, with the more C-terminal residue as the most critical. The surrounding sequences were also identified to play a role in mediating the interactions of the IKK proteins with Aurora A, interestingly the C-terminal sequence post-NBD in IKKβ seemed to have an important role inthe binding of Aurora A. This region has not generally been considered in the literature when assessing the function of the IKKβ NBD (*Rushe et al 2008, May et al 2000*) binding with NEMO and therefore maybe plays a specific role in mediating interactions with Aurora A.

The interaction of IKKα and IKKβ with Aurora A was also suggested to occur in an endogenous co-immunoprecipitation, which has not been observed nor reported in the literature previously. However when further investigated through the use of tagged protein expression constructs it was observed that the over-expressed forms of the protein bound non-specifically to the Protein G-sepharose beads which were used as the antibody support matrix. This unfortunately negated any attempts to interpret any suggested interactions between the over-expressed forms of the IKKs and Aurora A proteins. In order to circumvent these problems it will be necessary to investigate alternative support matrices for any further antibody-based immunoprecipitation strategies or utilise alternative *in vitro* methods to further investigate these protein-protein interactions.

CHAPTER 4:

CHARACTERISING AURORA A/IKK INTERACTIONS USING SURFACE PLASMON RESONANCE

4.1 Introduction

It is well recognised that the IKK complex assembles through protein-protein interactions of catalytic subunits as homo- and hetero-dimers toward the generation of a fully functional signalosome. The IKK complex can assemble in several different confirmations constituting IKKα and/or IKKβ alone or with the non-catalytic scaffolding protein IKKγ/NEMO. The hetero-dimeric form of the complex is observed to be the most active in classical NF-κB signalling (*Huynh et al, 2000, May et al 2002*) however the multiple confirmations of the IKK complex allows for the divergence in function of IKKα and IKKβ as they contribute to two divergent pathways; the canonical and non-canonical NF-kB signalling pathways as described in Chapter 1. However, it is more recently that more diverse functions of the IKKs have been identified.

The IKKs have been shown to play a far more diverse role in cellular signalling than initially realised with the recent identification of many NF-κB independent functions. In recent years, there has been a wide range of novel binding partners regulators and substrates all identified. IKKα, has been shown to play a role in the transcription of cyclin D1, through the activation and stabilisation of β-catenin (*Lamberti et al, 2001*), and through the direct phosphorylation of threonine 286 can induce degradation of cyclin D1 (*Kwak et al, 2005*). This directly implicates IKKα in the regulation of the cell cycle. A considerable number of novel substrates/regulators/interactors have also been identified for IKKβ also, such as FOXO3a, a tumor suppressor that can drive apoptosis or mediate a cell cycle arrest (*Hu et al, 2004*).

In the context of this study the identification of Aurora A as a substrate for both IKKα and IKKβ has given a potentially significant role for the IKKs in the correct mitotic progression of the cells (*Prajapati et al, 2006, Irelan et al, 2007*). In both the studies that have linked the IKKs to Aurora A it has been shown that disruption of this interaction leads to failure of the cells to fully progress through mitosis and leads to an arrest in the cell cycle, therefore identifying this potential interaction an attractive drug target for the treatment of a range of disease states.

Through the use of peptide arrays it has been possible to map the Aurora A-IKK interactions, identifying several key regions of binding of the IKKs with Aurora A and vice versa. Furthermore, the endogenous interactions of these proteins were confirmed by immunoprecipitation in a cellular system. The interactions were pursued further using an exogenous transfection system, however there were significant technical

issues with this methodology and therefore as a further strategy to further understand the IKK-Aurora A interactions, to examine their binding events and to build on the findings of Chapter 3. a biophysical approach was undertaken using full-length, purified recombinant proteins and Surface Plasmon Resonance (SPR)

This component of experimental work focussed on and aimed to ;

1. Prepare and establish a Aurora A surface/chip for use in SPR assays,
2. Examine the potential interactions of IKKα and IKKβ as analytes with an established Aurora A surface/chip, and
3. Use Surface Plasmon Resonance to inform on the kinetics of and identify potentially binding affinities for the IKK-Aurora A interactions.

4.2 Introduction to Surface Plasmon Resonance (SPR)

Surface Plasmon Resonance is a surface electromagnetic wave that propagates in parallel to a metal/dielectric surface interface. At the metal/dielectric boundary surface plasmon waves (SPW) are formed through the interaction of light and the surface chargers on the metal (usually Gold or Silver). The SPW is a transverse wave that propagates along this surface and forms an evanescent field at the metal/dielectric interface decaying into both the dielectic medium and the metal surface, however travels further in the dielectric medium due to the damping effect of the metal surface (*Homola et al, 1999*). This decaying evanescent field makes the surface plasmon wave highly sensitive to changes in refractive index at the metal surface. In the 1960's it was demonstrated that the surface plasmon waves could be excited through the principles of total internal reflection (*Otto et al, 1968, Kretschmann et al, 1968*).

Total internal reflection is the principle that states that when light travels between optically dense material such as air and a material of lesser optical density such as water, if the incident light hits the boundary between materials at an angle greater than the critical angle the light becomes totally internally reflected with a reflected angle equal to that of the incident light.

Otto and Kretschmann observed when a metal surface was placed at the interface between the different optical densities the incident light excites electrons at the metal surface forming a SPW (*Homola et al, 1999, Otto et al, 1968 and Kretschman et al, 1968*). The propagation of a SPW at the metal surface causes the loss of energy from the incident light, which alters the intensity of the reflected light. Resonance occurs when the energy of the incident photons of the light is equal to the energy of the SPW and it is at the angles where Surface Plasmon Resonance occurs the intensity of reflected light is reduced. It was first suggested that SPR could be used in biosensor applications in 1983 by *Liedberg et al* as a label free method to monitor interactions occurring between biomolecules. As the angle at which SPR occurs causes a decrease in intensity of the reflected light and the relationship between the angle of incident light causing SPR is associated with the nature of the metal surface it is possible to measure any changes in real-time that are occurring at the metal surface by determining the angle at which SPR occurs as outlined in Figure 4.1. BioSensors were developed by using the Kretschman set up to create a metal/dielectric medium interface at which fluidic systems could be used to deliver buffer and analytes to the sensor surface in highly controlled manner. The penetration of the evanescent wave into the dielectric medium occurs on a gold surface between 162-400nm depending on the wavelength of light used to propagate the SPW. This means that any changes to the surface within this range will induce changes in the amount of energy required for SPR therefore biomolecules can be immobilised on the surface (this is termed the ligand) by a range of chemical processes and the interacting partner (known as the analyte) can be flowed over the immobilised ligand and binding can be assessed in real time by following the changes in SPR angle (Figure 4.1).

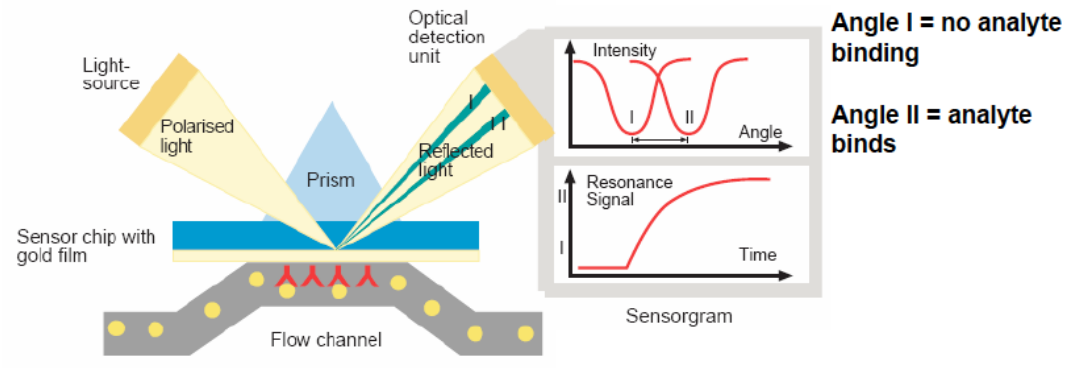

Figure 4.1 Principle of SPR detection in a BiaCore System

Basic principles of SPR using a microfluidics system to measure the binding of analyte to a bound surface ligand.

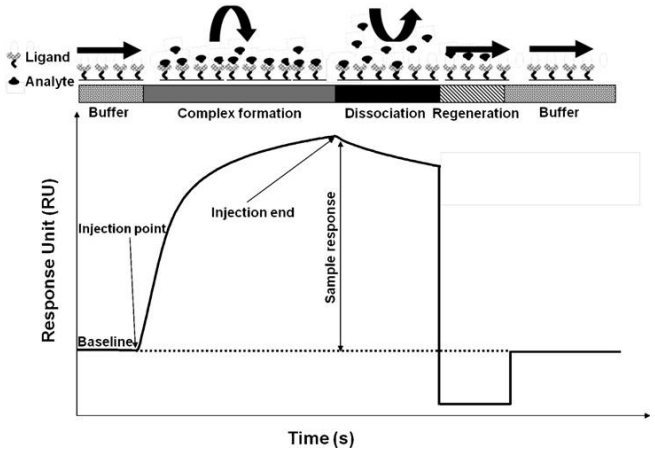

Figure 4.2 Sensorgram output of BiaCore SPR system (adapted from *Gopinath, 2010*)

The changes in SPR angle are shown as a sensorgram (Figure 4.2), the interactions are measured in Response Units (RU) as the SPR angle and the amount of surface bound biomolecules are directly proportional; 1RU is equivalent to 0.0001^{o} change in SPR angle or $1pg/mm^2$ biomolecule on the sensor surface. This real-time nature of this technique allows for the in-depth characterisation of the interactions occurring at the sensor surface. It is possible to determine rate constants for both on-rates and off-rates specific to an interaction as well as affinity data giving an indication of how strong or weak any interaction between the two molecules may be.

The BiaCore systems from GE healthcare utilise an automated microfluidic system with the sensor surfaces on a removable chip. The sensor surface is affixed with a series of micro-channels at to deliver buffer and analyte at a constant flow-rate controlled by the system and adaptable to specific assay requirements. The use of microfluidic channels

also allows for multiple ligand binding to be analysed and used simultaneously with the same analyte. Figure 4.3 shows the arrangement of Flow cells on the sensor surface as used in BiaCore chips.

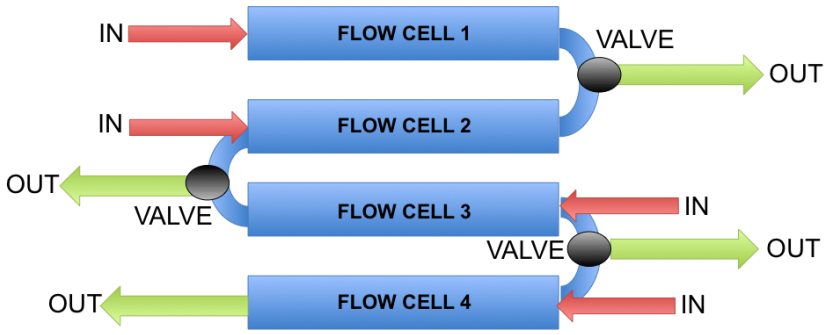

Figure 4.3 Schematic representation of Microfluidic system on BiaCore chips

The system of valves allows the flow cells to be analysed individually or in series so that reference surfaces can be used as an internal control for the binding.

The most commonly used chip for protein-protein interactions is the CM5 chip and was used in this chapter for all experiments. The CM5 chip surface is made of a 50nM layer of gold coupled with a 100nM layer of methyl-dextran, which is used to covalently bind the ligand via a range of surface chemistries such as amine, thiol, aldehyde or maleamide coupling depending on the ligand requirement.

The use of SPR based systems as a method for probing biomolecular interactions has become steadily more prevalent with 1514 published papers in 2009 containing biosensor data obtained from commercial SPR systems (*Rich et al, 2011*) and has been extensively validated through large scale comparative studies of the same interaction by several independent research teams resulting in consistent reporting of rate constants (*Rich et al, 2009*).

4.3 Preparation of Protein Surface

The interaction of the IKK complex and Aurora A kinase was therefore further investigated through the use of Surface Plasmon Resonance as a biosensing methodology using recombinant forms of these proteins. All proteins were His-tagged,

as the larger GST tag at 22kDa was perceived as a potential means of generating non-specific binding and therefore could potentially disguise or perturb the IKK/Aurora A interactions. Aurora A kinase was chosen as the ligand and immobilised on the chip surface when investigating these interactions as it was thought to facilitate the assay development by requiring a single surface to be used. Additionally, the basic pI of Aurora A of 9.45 results in the protein being positively charged under the assay conditions and would lead to non-specific binding to the un-modified negatively charged dextran surface if Aurora A was used as the analyte. The IKKα and IKKβ proteins have lower pI values between 5.7 and 6.5 respectively and under the assay conditions would be negatively charged thereby minimising non-specific interactions with the dextran surface.

Aurora A kinase was immobilised using an amine coupling reaction on a dextran surface of a BiaCore chip; the surface was activated by the injection of a 1:1 mixture of NHS:EDC. The EDC was used as a coupling agent and facilitated the formation of an NHS ester at the carboxylic acid of the dextran. It was anticipated that the primary amine groups of lysine side chains of Aurora A kinase would attack the NHS ester leading to the formation of amide bind between Aurora A kinase and the dextran surface. The subsequent injection of ethanolamine deactivated any unreacted ester bonds on the dextran surface, blocking any non-specific binding and it as appreciated that a surface prepared in this manner would likely have a heterogenous arrangement due multiple possible amino acids interactions with the dextran surface.

The lengths of protein injections were varied to tailor the surface ligand density as required for each experiment. In all experiments an active surface was prepared alongside a reference surface with no ligand coupled, which was then be used to monitor any non-specific interactions occurring due to the dextran surface.

The sensorgram in Figure 4.4 demonstrates the immobilisation of Aurora A forming a low density surface of 72RU. 1000 RU is equivalent to 1ng/mm^2 of bound surface protein (*Sternberg et al, 1991*) therefore this surface had 0.07ng/mm^2 of protein immobilised. The sensorgram shows the change in surface binding at the chip surface as a function of time. Any change in solution flowing over the surface will cause a refractive index shift which is also measured by the instrument and can lead to bulk changes in the sensorgram and these bulk refractive index changes are accounted for through the use of a reference surface during binding experiments. The amount of

protein immobilised is calculated by measuring the increase in baseline after the ethanolamine deactivation step and comparing it to the baseline level after NHS:EDC activation.

Figure 4.4 is representative of all immobilisation methods described in this chapter.

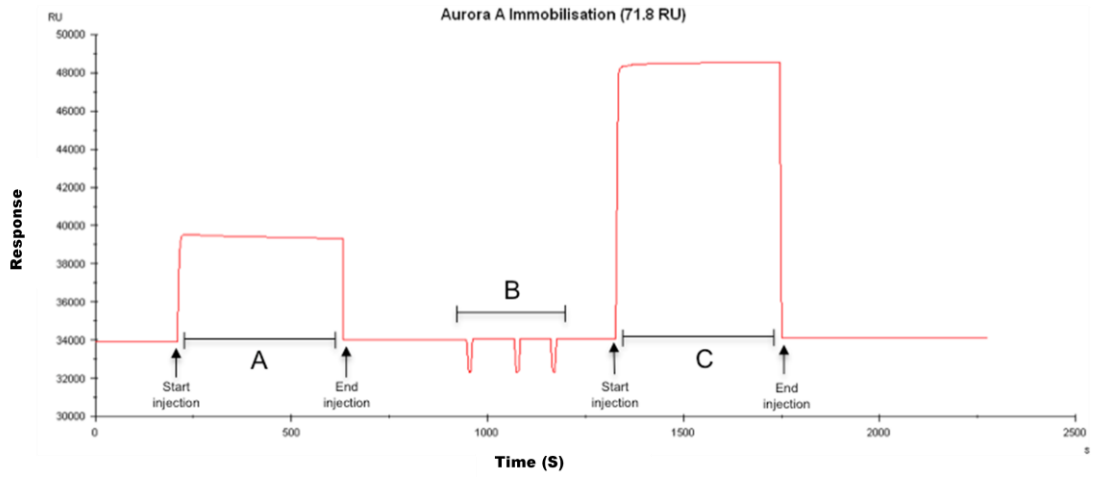

Figure 4.4 Immobilisation of Aurora A on Dextran Surface of CM5 chip

Immobilisation of Aurora A kinase (100nM solution) in pH6.0 Sodium acetate buffer on active flow cell of CM5 chip. (A) Dextran surface was activated with a 1:1 mixture NHS:EDC for 420 seconds at 5µl/min, (B) sequential 10 second injections of protein in pH 6.0 sodium acetate buffer at 10µl/min were added until desired surface density was achieved(C) Surface deactivated by 420s injection ethanolamine at 5µl/min. Final level of Immobilisation determined by the difference between end of injection A and injection C.

4. 4 Investigating the Interaction of the IKK complex proteins and Aurora A kinase by Surface Plasmon resonance

Initially an experiment was conducted as a proof of concept to analyse the interaction of Aurora A kinase with either IKKα or IKKβ. A high-density surface of Aurora A of 6-6500RU was prepared in flow cell (Fc) 2 of a CM5 as described previously and BSA was coupled to the reference surface in Fc1 at an equivalent level. The BSA was used on the reference surface to account for any potential non-specific interactions. The analytes were prepared as a decreasing range of concentrations between 1μM-62.5nM in duplicate in the running buffer and for each analyte the concentrations were randomly injected over Fc1-Fc2 for 180 seconds at a flow rate of 30μl/min with a 15 minute disassociation phase followed by a regeneration injection of 2mM EDTA and 1mM NaCl. The data is presented as a sensorgram as Fc1 subtracted from Fc2 to account for the non-specific interactions of the analyte. The experiments investigating the interactions of IKKα and IKKβ were carried out under identical conditions on the same surfaces at 25^0C using a BiaCore 300.

Figure 4.5 shows the reference subtracted sensorgrams for IKKα and IKKβ binding with Aurora A. The sensorgrams show the duplicate runs of both IKKα/β across all concentration previously described with the Aurora A surface. The injections of analyte can be observed by the large spikes on the sensorgram (175s and 350s). The rising response upon injection of analyte on the sensorgram (IKKα Figure 4.5 i), and IKKβ Figure 4.5 ii)) indicates that the analyte (IKKα/β) and the ligand (Aurora A) are interacting and the level of binding is measured in with an arbitrary measurement known as Response Units (RU). The gradient of the sensorgram can be measured to inform on the kinetics of the binding events between the IKKs and Aurora A. The analyte injection is subsequently stopped and the interaction is allowed to disassociate which is shown by the decreasing the profile of the sensorgram upon the injection ending.

The interaction of IKKα and Aurora A was observed to occur in a concentration dependent manner with the highest concentration IKKα demonstrating a binding response of 240 Response Units (RU) (Figure 4.5 (i)). From the sensorgram it can be seen that the binding kinetics showed a fast on-rate and a slow dissociation rate across all the concentrations of protein examined. The binding of IKKβ to Aurora A was also

observed to occur in a concentration dependent manner, the highest concentration giving a response of 150RU (Figure 4.5 ii)). This response was less than observed with IKKα and displayed a differing kinetic profiles suggesting that the interactions of IKKα/β with Aurora A were occurring by different modes of action.

The analyte concentrations were prepared in duplicate and each concentration was injected in a random order and when the replicate cocncentrations are observed on the sensorgram the response should be identical for each injection. However, this was not observed in this experimental data. There is poor duplication of results at the higher concentrations and there was considerable degradation of the active surface, which can be seen by an increase in signal 'noise' in the disassociation phases of each run. The degradation of the surfaces can lead to a loss of activity in the surface that may explain the poor replication of the duplicate runs. An accumulation of the analyte on the surface is visible due to the increasing baseline during the disassociation phase rather than returning to a steady baseline consistent between runs, which, again, may explain the poor replication of binding between the protein runs. The accumulation on the active surface suggests the regeneration conditions were not adequately removing any excess analyte bound to the surface.

This experiment however confirmed there were interactions between both IKKα and IKKβ with the Aurora A surface occurring and there appeared to be a marked difference between the kinetics of these two interactions which was then then taken forward for further investigation

i)

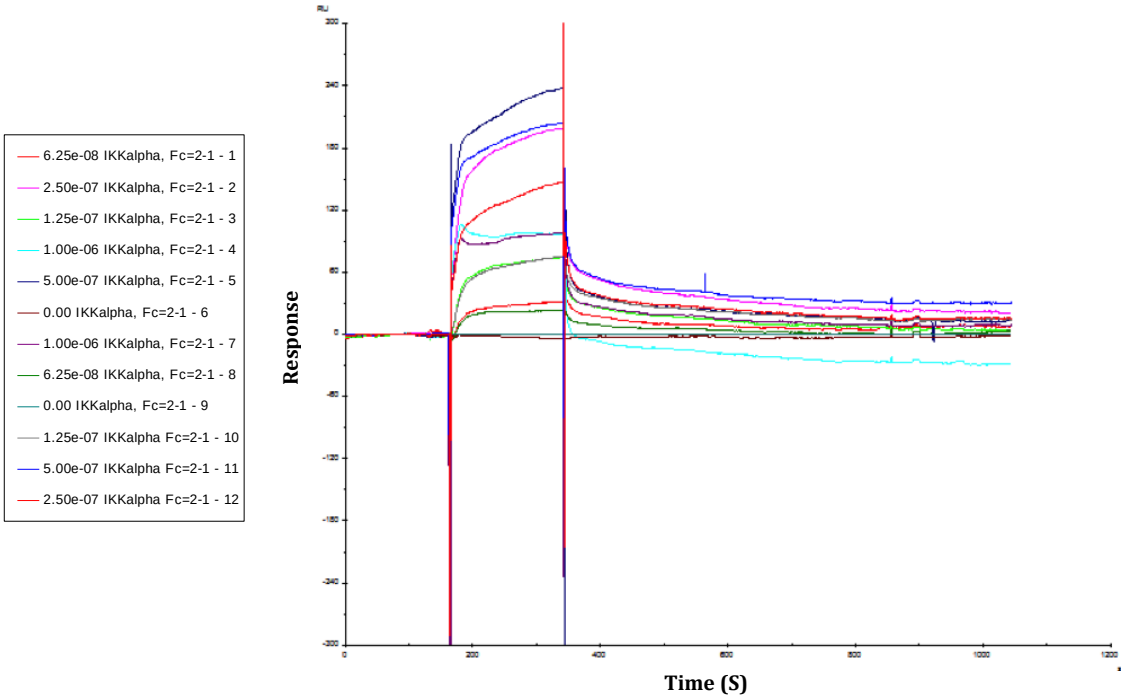

ii)

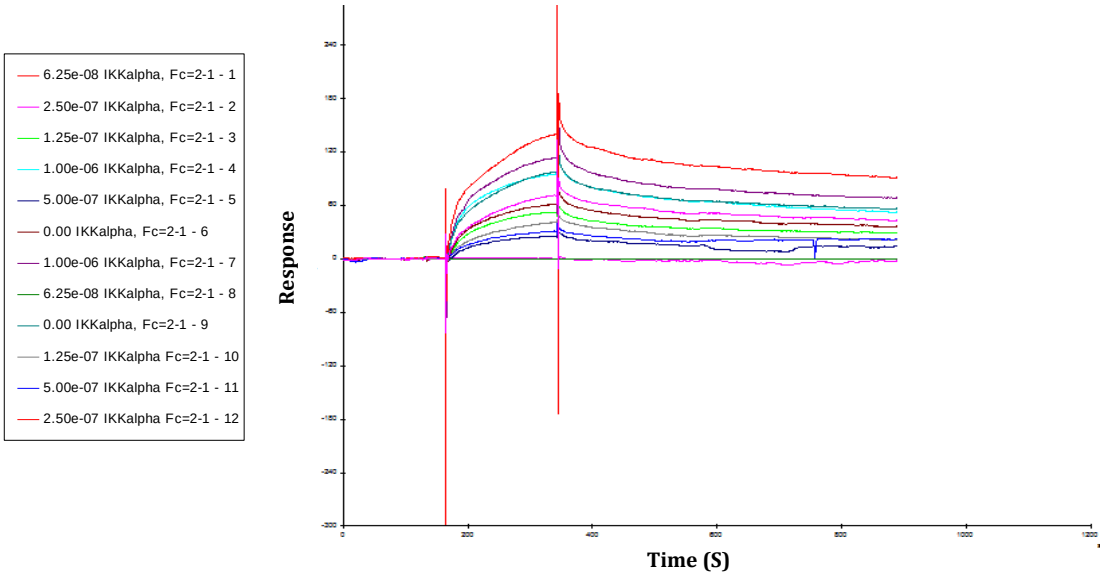

Figure 4.5 Interaction of IKKα and IKKβ with Aurora A kinase analysed by Surface Plasmon Resonance

IKKα and IKKβ analyte concentration range (1μM-0.0625μM) was flowed over a high density Aurora A (3500RU) coupled sensor surface at a constant rate (30μl/min) i) His-IKKα protein binding to Aurora A kinase ii) His-IKKβ protein binding to Aurora A kinase. The data has been parallel subtracted between Fc2-Fc1 to account for non-specific binding. These data are representative of 2 independent experiments.

4.5 Kinetic analysis of the IKK/Aurora A interaction

4.5.1 Experimental Design

Initial experiments carried out on the high density Aurora A surface indicated both IKKα and IKKβ bound and interacted with Aurora A. The conditions for this assay were however unsuitable for more accurate analysis of the kinetics of this interaction. It was therefore necessary to further optimise the experimental conditions to establish suitable regeneration conditions and an optimal concentration range to give the best data to further characterise this interaction. The subsequent experiments were carried out using a BiaCore T100 instrument. The preparation of protein surfaces was carried out as previously described at lower densities to minimise the accumulation of analyte on the ligand surface. All experiments were carried out at a constant temperature of 25^0C.

New surfaces were prepared with Aurora A as the active surface diluted in pH6.0 sodium acetate buffer and a blank immobilisation with no protein used as the reference surface. Optimisation experiments were carried out to investigate suitable concentration ranges and regeneration steps on an Aurora A surface of 1300RU (data not shown) immobilised on Fc2 of a fresh CM5 chip with blank immobilisation of Fc1 as a reference. A range of regeneration conditions was investigated including 0.5-3M NaCl, 50% (v/v) Ethylene Glycol solution and 0.1-0.5% (w/v) SDS solution. The high salt and ethylene glycol solutions had no effect on the bound analyte, the SDS successfully removed the analyte but dramatically reduced the activity of the protein surface leading to a lack of reproducibility between protein binding injections and therefore was not suitable for surface regeneration. With these outcomes no viable regeneration conditions that would maintain surface activity and remove any remaining analyte were identified. This therefore made any kind of kinetic analysis impossible when conditions were configured using a randomised concentration injection assay protocol, as used previously. However, it was possible to use a single cycle methodology to investigate kinetic dynamics of protein-protein interactions.

BiaCore SPR systems can determine the equilibrium-binding constant (K_D) of protein-protein interactions by analysing the kinetics of the on-rate (k_a) and off-rates (k_d) of the interaction. The K_D is calculated by using the following equation:

$K_D = k_a / k_d$

When k_a and k_d are considered to be:

$$A + L \underset{k_d}{\overset{k_a}{\rightleftharpoons}} AL$$

This is the simplest binding model for biomolecular interactions and is analogous to the Langmuir isotherm for the adsorption of a gas to a metal surface (*Langmuir et al, 1916*).

The k_a and the k_d values are determined by fitting the experimental data to the simplest binding model. Generally the k_a and the k_d are calculated individually for each concentration, giving a K_D value at each concentration which should be consistent for all concentrations and any variance between the values is considered to be standard error. However in the case for proteins that show very tight binding and would require very long disassociation phases between protein injections, single cycle kinetics are used. In single cycle kinetics the protein concentrations are sequentially injected at increasing concentrations with short disassociation phases (90s) until the final concentration after which there is a long disassociation phase of 15 minutes or more. The k_a values are calculated across all the binding events but the k_d value is only calculated for the final disassociation phase. This method allows for strong interactions with high affinity to be investigated and the K_D values to be calculated.

To optimise this approach single cycle kinetics runs were set up using the 1300RU protein surface using several concentration ranges from 1µM-62.5nM to 10nM-0.625nM (data not shown) and a flow rate consistent with previous experiments. From this it was ascertained that at the higher concentrations of analyte and immobilised ligand the re-binding effect was occurring. The re-binding effect occurs when higher order analytes i.e. analytes which form dimers or larger complexes disassociate then dimerise with a still bound monomer on the surface therefore giving an artificially slow k_d value and giving a K_D value suggesting an interaction tighter than it may actually be.

In order to minimise the re-binding effect it was necessary to use an even lower density surface. The on-rates for both IKKα and IKKβ remained very fast and therefore to more accurately determine the k_a value the analyte flow rate was increased to 100µl/min, the maximum possible for the machine, which can help to give a more accurate measurement of k_a and also contribute to minimising the re-binding effect. Due to the nature of the IKK proteins and their ability to form higher order homo- and hetero- each protein was investigated on individual Aurora A surfaces at approximately equivalent immobilisation levels to prevent any re-binding between the IKKs caused by any residual analyte remaining on the ligand surface between runs.

Two Aurora A surfaces were prepared alongside the blank immobilisations on Fc2-4 and Fc1-3 respectively. Aurora A was immobilised to 72RU on Fc2 as shown in Figure 4.6 and 68.5RU on Fc4. Initially the analyte concentration range used was 300nM, 100nM, 33.3nM, 11.1nM and 3.7nM for both IKKα and IKKβ.

In initial experiments examining IKKα as an analyte the sensorgram showed the real-time binding events occurring on the reference surface and active surfaces between IKKα and Aurora A (Figure 4.6 i) and ii)). The sensorgram showed the increasing levels of IKKα bound to the active surface compared to the reference surface indicating IKKα interacted with Aurora A in a concentration dependent manner. To further analyse this data the reference surface was subtracted from the active surface to give a single sensorgram showing the binding of IKKα and Aurora A accounting for any non-specific or mass-transport effects. Prior to each protein run a blank run was crried out, this was identical to the protein run but the analyte concentration series was replaced with buffer injections (Figure 4.6 ii.)). This accounted for any bulk refractive index changes that occurred dude to variations between running buffer and the sample buffers. The blank run and the referece surface were the internal controls for each binding event and were sbracted from the sensorgram at the active surface to give the adjusted sensorgram as seen in Figure 4.6 iii). The adjusted sensorgram (Figure 6. iii)) was then utilised in the analysis of binding kinetics wih respect to IKKα.

Furthermore, Figure 6 collectively is representative of each SPR kinetic run and all SPR data presented from this point on will be as ‘Blank adjusted’ sensorgrams.

i)

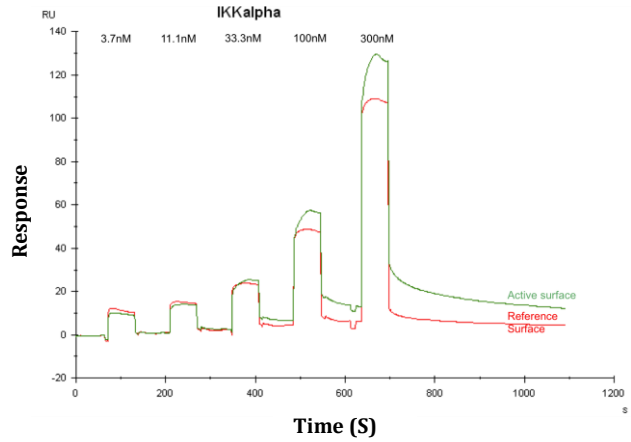

ii)

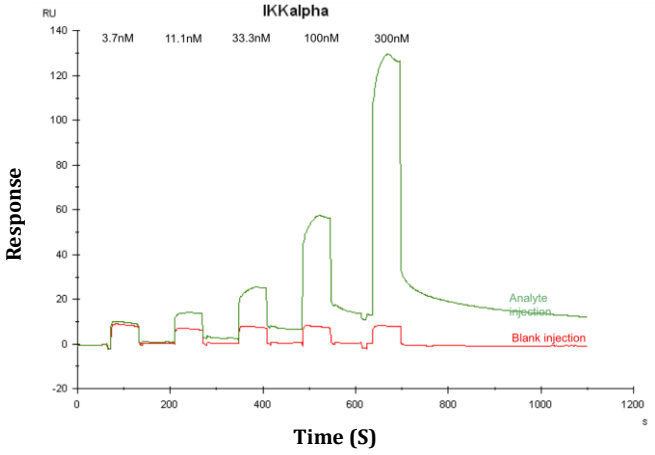

iii)

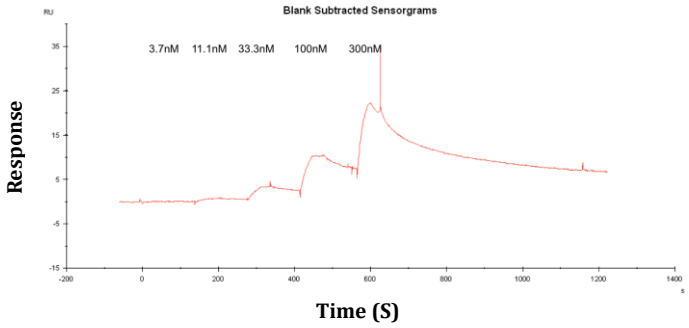

Figure 4.6 Single cycle runs of IKKα binding to low density Aurora A surface.

IKKα analyte concentrations were prepared from 300nM-3.7nM and sequentially injected over the low density (72RU) Aurora A active surface for 60s with a 90s disassociation between injections and a 15 minute disassociation phase after the final injection. i) sensorgram showing interaction of IKKα and Aurora A on reference surface (red) and active surface (green) ii) blank (red) and analyte (green) injections on active surface iii) adjusted sensorgram showing the reference surface subtracted from active surface. This data is from 1 independent experiment.

4.5.2 Kinetics of IKKα binding to Aurora A surface

4.5.2.1 SPR runs using High Concentrations of IKKα as analyte

Kinetic analysis of the 300nM-3.7nM analyte concentration range was carried out with the data depicted in Figure 4.6 iii); the data was modelled as a 1:1 interaction using the Langmuir binding model and the fit is shown in Figure 4.7.

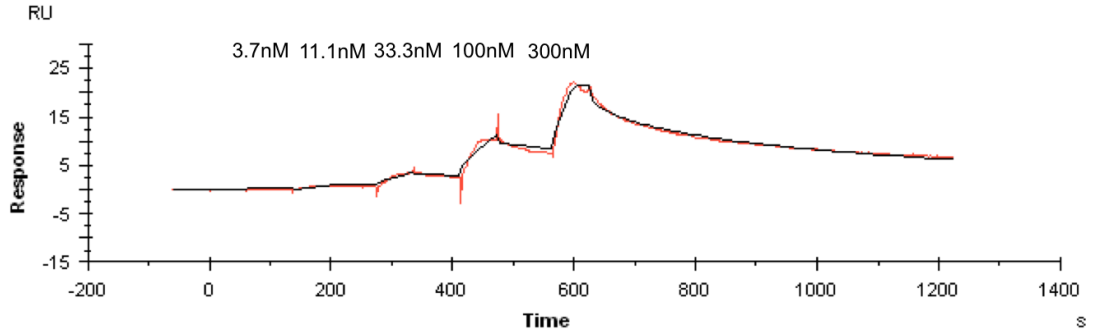

Figure 4.7 Kinetic analysis of IKKα and Aurora A binding at high concentrations

Blank adjusted sensorgram fitted with a 1:1 binding model (black) by BiaEval software (Uppsala, Sweden). These data are representative of 1 independent experiment..

Although both the on-rate and off rates appeared to be modelled well using a 1:1 fit, no accurate K_D could be calculated. It was not possible from this range of concentrations to determine the on-rate as it was beyond the capabilities of the instrument. The measured on rate was very fast for the interaction of IKKα and Aurora A and showed an interesting binding profile. In Figure4.6 iii) it was apparent that the on-rate for IKKα rose very quickly, then reached a peak and subsequently began to disassociate before the completion of the injection, this was observed most prominently at the 300nM concentration. This was and remains a highly unusual profile for protein-protein

interaction and made it difficult to analyse. This phenomenon was highly reproducible and may be due to the binding kinetics of this interaction.

It was also apparent that this may have been due to the IKKα protein having a very fast and transient interaction with Aurora A and therefore bound very quickly to the available Aurora A and thereafter began to disassociate. This suggested the peak achieved represented the saturation of the surface and instead of reaching equilibrium the proteins began to disassociate. Another alternative possibility suggested by the data was that the IKKα protein reached equilibrium, could then form homo-dimers at the surface and when the dimers began to degrade the observed unusual binding profile occurred. This phenomenon was most clearly observed at the highest concentration of the series therefore a lower concentration series was prepared and run in triplicate with long equilibration steps between runs to minimise this effect.

4.5.2.2 SPR runs using low Concentrations of IKKα as analyte

Given the outcomes of Section 4.5.2.1 further kinetic studies were then pursued using lower analyte concentrations of IKKα in an attempt to generate Kd values for IKKα binding/interaction with Aurora A. These were developed over a concentration range of 90nM, 30nM, 10nM, 3.3nM and 1.1nM. The runs were set up as previously described with a 60s analyte injection at a constant flow rate of 100 µl/s and a 90s disassociation phase between the lower concentrations and a 15 minute disassociation phase after the final analyte injection and a long equilibration phase between cycles to allow for surface bound analyte to disassociate and the baseline to be re-established. Each analyte run was preceded by a blank run of buffer injections to be used for blank subtraction. The results of these single cycle kinetic runs carried out in triplicate are depicted in Figure 4.8

The three runs all showed very high levels of reproducibility with approximately 4RU difference in maximum binding levels. This can be explained by the differences in R_{max}. The R_{max} is the binding capacity of the surface and can be calculated theoretically by the equation:

R_{max} = (Analyte MW/Ligand MW) x Immobilised Ligand x Stoichiometry

For this surface the theoretical R_{max} was calculated to be 130RU, assuming that the surface is 100% active and all immobilised ligand is correctly orientated for binding. However, when the R_{max} is calculated experimentally it is usually lower than this value as it is unlikely that the surface will be 100% active. The R_{max} values calculated for the single cycle kinetics indicated the availability of an active surface of between 8.1-11.6RU. This could be due to the immobilised ligand being inactive or due to the heterogenous nature of amine coupling some of the ligand may be orientated in such a way that the binding sites were masked. Although the experimental R_{max} values were small it was still possible to determine kinetic data from this run. The kinetics of the interaction were all determined relative to the individual R_{max} values accounting for variability in the surface activity.

The data was then fitted globally with a Langmiur 1:1 binding fit. The kinetics of the interaction shows a k_a value of 1.64 $x10^{10}$ Ms^{-1}. This was a very quick on-rate for the interaction and very close to the limit of detection by the instrument. The fit for the on-rate however was quite poor for the second and third independent runs that coincided with the increasing R_{max} of the runs. This was due potentially to inefficient regeneration of the surface between runs leading to an accumulation of analyte at the ligand surface. It is well established that IKKα forms homo-dimers (*Chen et al, 1996, Woronicz et al, 1997*) and therefore any accumulation of said dimers at the surface could potentially mask any interactions with Aurora A and therefore a feature of the on-rate could be not only analyte-ligand interactions but analyte-analyte interactions. This was also observed in the higher concentration kinetic runs.

The disassociation phase fitted very well to this binding model generating a k_d value of 85.99 s^{-1}. The off-rate for this interaction was fast and fitted very well with this model, across all three of the repeat cycles.

Using the calculated k_a and k_d values the binding constant was determined for this interaction and was shown to be 5.25 nM which indicates a very tight interaction occured between IKKα and Aurora A.

i)

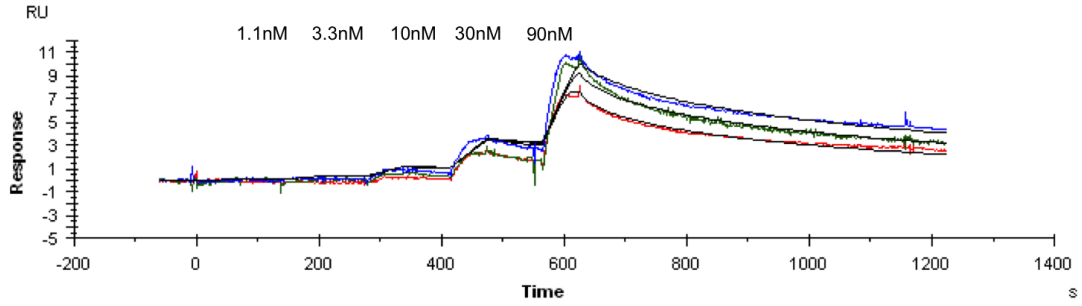

ii)

	k_a (1/Ms)	k_d (1/s)	K_D (M)	R_{max} (RU)
	1.64×10^{10}	85.99	5.25×10^{-9}	
Cycle 1				8.1
Cycle 2				9.9
Cycle 3				11.6

Figure 4.8 Kinetic analysis of IKKα and Aurora A binding at lower analyte concentrations of IKKα

i) Single cycle kinetics run on 72RU Aurora A surface in triplicate, first run (red line) second run (blue line) final run (green line) with 1:1 binding fit overlaid (black line) individually calculated using R_{max} specific to each run. Kinetic runs carried out on 72RU Aurora A surface in series with a blank immobilised reference surface. ii) Table showing kinetic analysis of 1:1 binding model. Sensorgram is reference surface and blank subtracted. Data presented in panel A is from from three independent experiments carried out using the same surface.

4.5.3 Kinetics of IKKβ binding to Aurora A surface

4.5.3.1 SPR runs using High Concentrations of IKKβ as analyte

To investigate the binding of IKKβ and Aurora A, a new Aurora A immobilised surface was prepared. A single Aurora A surface could not be used to assess both IKKα and IKKβ binding as these proteins are known to dimerise (*Chen et al, 1996, Woronicz et al, 1997*), therefore any accumulated analyte on the surface could potentially interact with the analyte that is being flowed over which would be detected alongside the analyte-ligand interactions and give rise to inaccurate kinetic data.

The new Aurora A surface was prepared as previously described alongside a new blank immobilised reference surface of Fc4 and Fc3. The same level of Aurora A immobilisation as was achieved on Fc2 was attempted, to allow the data for IKKα and IKKβ to be as comparable as possible. 68.5RU of Aurora A was immobilised for the kinetic analysis of the IKKβ and Aurora A interaction. This surface had a theoretical R_{max} of 123RU, which is at a comparable level to that used for the IKKα kinetic analysis.

The BiaCore T100 system allowed for the kinetic runs to be carried out in parallel on different surface due to the microfluidic chip system that was employed. The higher concentration series (300nM, 100nM, 33.3nM, 11.1nM, 3.3nM) therefore was developed for the IKKβ/Aurora A interaction at the same time as for the IKKα/Aurora A interaction. Figure 4.9 i) illustrates the blank adjusted sensorgram for the IKK β/Aurora A interaction. It can be seen from this sensorgram that the level of binding observed between IKKβ/Aurora A was lower than that with IKKα and that the binding kinetics differed considerably between the two proteins.

The fit for this kinetic run modelled better than that of IKKα and within the parameters that the machine could measure reliably. Figure 4.9 ii) shows the fit calculated to a 1:1 Langmuir binding model and in iii) the calculated rate constants are shown. The calculated k_a value for this interaction was 1.25 $x10^5$ Ms^{-1} and the k_d value was 8.435 $x10^{-3}$ s^{-1} generating a K_d value of 67.3nM. The experimental R_{max} value was slightly lower for this run also at 7.161 RU.

At the higher concentrations of IKKβ displayed a similar profile of binding as observed for IKKα; the sensorgram showed the binding reached a peak and then began to

decrease although to a lesser degree than was observed in the IKK□/Aurora A interactions at the same concentrations. Although it was possible to calculate some kinetic values for this run, it was once again deemed more appropriate to use lower concentrations for the triplicate runs to match the IKKα/Aurora A interactions toward the calculation of quantitative binding constants.

i)

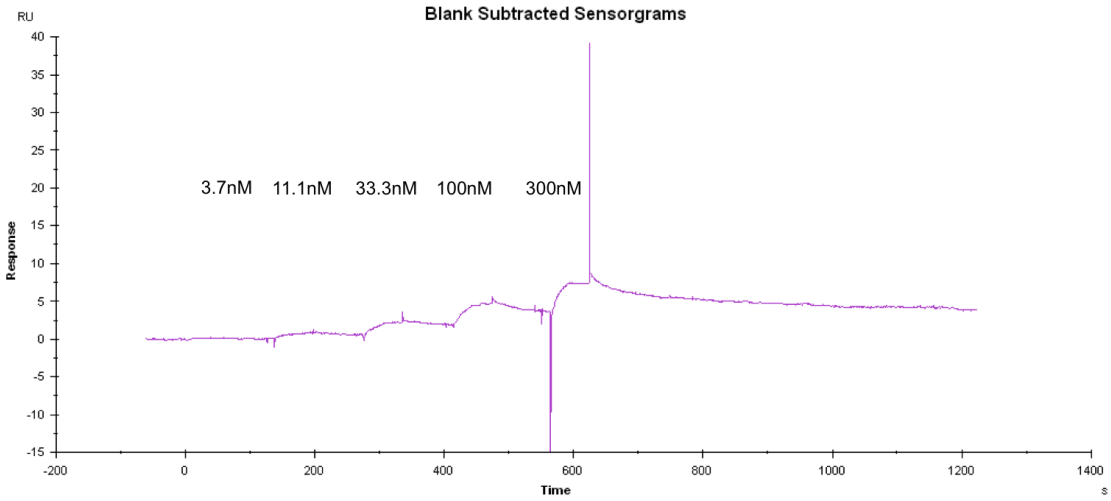

ii)

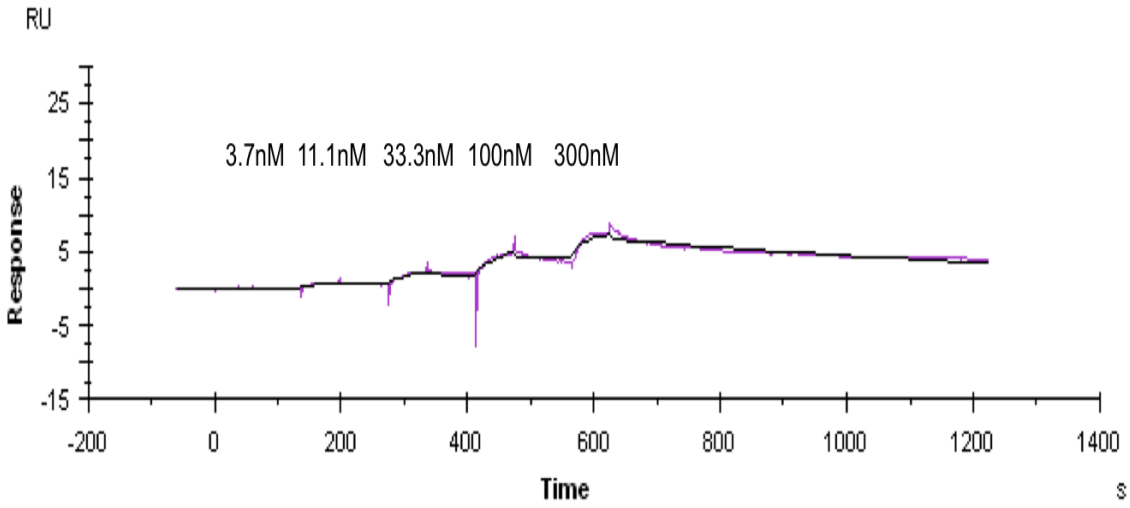

iii)

	k_a (1/Ms)	k_d (1/s)	K_D (M)	R_{max} (RU)
IKK β	1.25 x10^5	0.008435	6.73 x 10^{-8}	7.161

Figure 4.9 Kinetic analysis of IKKβ and Aurora A binding at higher analyte concentrations of IKKβ.

i)IKKβ analyte concentrations were prepared from 300nM-3.7nM and sequentially injected over the low density (72RU) Aurora A active surface for 60s with a 90s disassociation between injections and a 15 minute disassociation phase after the final injection. ii) Blank adjusted sensorgram fitted with a 1:1 binding model (black) by BiaEval software (Uppsala, Sweden) iii) Rate constants as calculated by BiaEval software. Data represents 1 independent experiment.

4.5.3.2 SPR runs using low Concentrations of IKKβ as analyte

Further protocols were pursued to examine IKKβ binding with the Aurora A surface using lower concentration of analyte IKKβ concentrations were prepared at 90nM, 30nM, 10nM, 3.3nM and 1.nM and were flowed over the 68.5RU Aurora A surface at a constant flow rate of 100µl/s for 60s with 90s disassociation phases until the final concentration where a 15 minute disassociation was carried out. Between cycles a long equilibration phase was used to allow for any surface bound analyte to disassociate and for the active surface to return to baseline.

The results of these runs are shown in Figure 4.10. The sensorgram of the triplicate analyte runs across the concentration range of IKKβ were well replicated with the second and third runs almost identical whilst the first showed a greater total level of binding. This may reflect the recorded experimental R_{max} values. In the first run the active surface was calculated to be 7.3RU, this then reduced to 4.9RU and 4.7RU for the second and third runs respectively. This drop in activity of the surface may explain the observed differences in total level of binding; it also showed that in runs 2 and 3, when the R_{max} values were very close, the sensorgrams showed excellent replication of binding suggesting that the available active surface was responsible for these differences. Each fit was calculated to individual R_{max} values as defined previously so differences in total binding were not considered when calculating the k_a and k_d values.

The k_a value determined from the kinetic analysis for the IKKβ/Aurora A interaction at the lower concentrations was 3.32 $x10^5$ Ms^{-1} which correlates well with 1.25 $x10^5$ Ms^{-1} , the k_a as calculated at the higher concentration range giving values in the same order of magnitude. The on-rate for this interaction was well fitted by this model in all replicates suggesting that the on-rate for this reaction is in this order of magnitude.

The k_d values obtained from the triplicate single cycle runs was 9.14 $x10^{-4}$ s^{-1} which is close to that calculated following the development of IKKβ analytes at the higher concentration, namely 8.435 $x10^{-3}$ s^{-1}. Although these values were not consistent this was likely due to the poor fitting of the off-rate. This off rate is very slow indicating a very tight interaction as has been suggested by the initial interaction experiments shown in Figure 4.4.

The fact that the off-rate was poorly fitted identified that it wouldn't be possible to accurately calculate the K_D in a manner similar to that pursued previously. The calculated K_D however can give an indication of what range this value would be; it was calculated to be 2.25nM in this experiment. The previously calculated K_D value from the higher concentration range on the same surface was 67.3nM. These values taken together suggest that the interaction of IKKβ and Aurora A has K_D value of below 100nM.

An alternative methodology for the calculation of the K_D is to use a steady state affinity model, this can be calculated when the interaction reaches equilibrium during the analyte injection. It was possible to determine a K_D value from the lower concentration range using this method and this fit is shown in Figure 4.11 i). The K_D value calculated by this method was 52.4nM which is close to that obtained by a 1:1 Langmuir binding model and these values taken together showed that the K_D value obtained for this interaction is in low nano-molar range.

i)

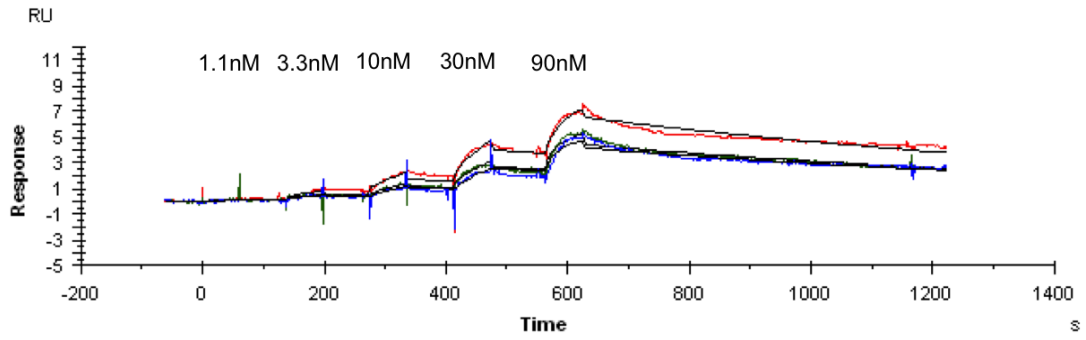

ii)

	k_a (1/Ms)	k_d (1/s)	K_D (M)	R_{max} (RU)
	3.32×10^5	9.14×10^{-4}	2.25×10^{-9}	
Cycle 1				7.3
Cycle 2				4.9
Cycle 3				4.7

Figure 4.10 Kinetic analysis of IKKβ and Aurora A binding at lower analyte concentrations of IKKβ

i) Single cycle kinetics run on 68.5RU Aurora A surface in triplicate, first run (red line) second run (blue line) final run (green line) with 1:1 binding fit overlaid (black line) individually calculated using R_{max} specific to each run. Kinetic runs carried out on 68.5RU Aurora A surface in series with a blank immobilised reference surface. Sensorgram is reference surface and blank subtracted ii) calculated rate constants from 1:1 langmuir binding fit. Data presented in panel A is from triplicate runs from three independent experiments

i)

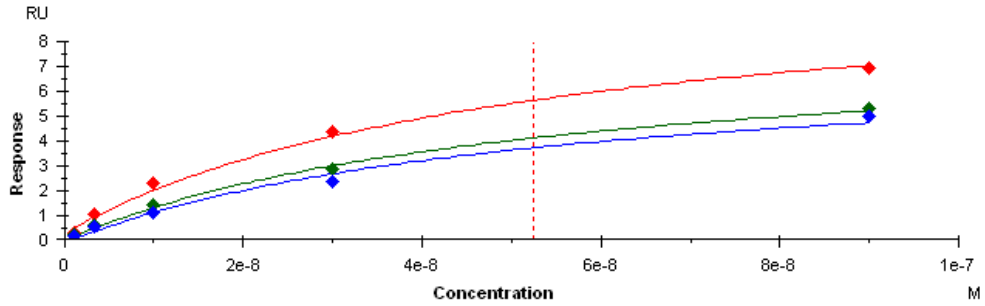

ii)

	KD (M)	Rmax(RU)
	5.24E-08	
Curve 1		10.68
Curve 2		8.25
Curve 3		7.67

Figure 4.11 Use of a steady state affinity model for the calculation of the K_D value for IKKβ binding to the Aurora A surface

i) Steady state affinity model of IKKβ and Aurora A interaction at 90-1.1nM concentration range for triplicate runs K_D as calculated from the graph is show as the red dotted line. ii) Calculated K_D values by BiaEval software.

4.5 Discussion

The interactions of IKKα and IKKβ were successfully analysed using SPR to give approximate K_D values, which informs on the strength of these interactions. One of the key advantages of using SPR in the investigation of protein-protein interactions is the ability to also determine the kinetics of interactions, which can give more information on the nature of the affinity of interactions being studied.

The complex nature of protein-protein interactions must be taken into account when considering the data obtained from SPR. Although the majority of interactions will fit to a 1:1 binding model, it is possible that any interaction(s) may be more complex than this with variable stoichiometry. It is possible to use more complex models to try and fit the data generated and these may well give a better fit for the data however without more information to refine these modelling strategies they can't really be applied. In the case of the IKK proteins interacting with Aurora A, although there is evidence, as seen in previous chapters, that there are multiple binding sites on IKK α/β for Aurora A, including the KD and NBDs there simply wasn't enough data to accurately use this to develop a more complex binding model. It is also possible that in solution the IKK enzymes will be a heterogenous population with monomers and dimers or even higher order complexes present. This too could be factored into a complex binding model but without information as to the ratio of these different complexes this cannot be accurately incorporated when modelling the data. Due to these limitations using more complex models was not possible and therefore all the data was fitted according to the 1:1 binding models.

The K_D values calculated for both IKKα (5.25nM) and IKKβ (2.25nM) fall in the low nanomolar when binding studies were developed using lower IKKα/β analyte concentration ranges, suggesting that the interaction between both IKKα/β and Aurora A have similar affinities. This indicated very tight binding occurs between Aurora A and either IKKα/β. These values however are only approximate as it was not possible to accurately fit both the k_a and the k_d values for each subunit. The parameters required to be fitted well to generate an accurate K_D. However the calculated values are certainly within the correct order of magnitude for these interactions.

The interesting elements of the data came from the differences that have been observed in the k_a and k_d values between IKKα and IKKβ. The calculated on-rate for IKKα in Figure 4.8 was 1.64 $x10^{10}$ Ms^{-1} which is very fast, in fact close to the limits of detection of the BiaCore instrument. The on-rate also never reached equilibrium instead began to disassociate even before the analyte injection finished. This suggested that the binding of IKKα to Aurora A occurs very quickly however in a transient manner suggesting that the function of this interaction could be to mediate a post-translational modification such as phosphorylation which supports the findings of *Prajapati et al.* (2006) Although the fit used to calculate this on-rate was of a less desirable quality, the on-rate that was calculated was in fact slower than the sensorgram reported which implies that in actuality this interaction has an even faster on-rate than as reported. IKKβ on the other hand has a much slower calculated k_a value of 3.32 $x10^5$ Ms^{-1} which is well fitted by the 1:1 binding model as seen in Figure 4.10.

The calculated k_d values for IKKα and IKKβ also differ, with the k_d value for the IKKα and Aurora A binding measured to be 85.99s^{-1} which fitted well by this model. IKKβ on the other hand displayed a k_d value of 9.14 $x10^{-4}$ s^{-1}, which was fitted poorly in the model and in fact maybe slower. This off-rate was poorly fitted as from the sensorgram it was apparent that the disassociation occurred in an almost bi-phasic manner with a fast off-rate observed immediately after the analyte injection ended with the rate then settling as very slow for the remainder of the disassociation phase. This made the data hard to fit with a simple 1:1 binding model. However, it can still be seen that the off-rates for IKKα and IKKβ were very different with the k_d of IKKβ shown to be five orders of magnitude slower than that of IKKα. The on-rate was also five orders of magnitude slower for IKKβ than for IKKα and this observation when viewed in conjunction with the differences in the k_d rates between IKKα and IKKβ illustrated and identified that the kinetics of IKKα and IKKα interaction with Aurora A are very different. The quick on- and off-rates of IKKα suggest a transient interaction, however the slower on- and off-rates for IKKβ indicate a stronger more scaffolding role that this interaction may play. Collectively, this may imply that these interactions have a different role functionally though these elements of differential IKK-Aurora A complex formation remain to be examined fully in a cellular setting.

In these studies attempts were made to utilise peptides derived from the IKKs that encompass the NEMO Binding Domain of these proteins, one of the identified binding sites in Chapter 3, however these investigations were unsuccessful. The peptides used

proved to be insoluble at the concentrations of DMSO required to give accurate results using SPR as DMSO gives a very large refractive index change when used in this system therefore in order to yield good results the concentration must be as low as possible. At low concentrations of DMSO the peptides were not soluble and accumulated in the microfluidic systems on the chip and therefore no data could be obtained on Aurora A-NBD binding. The use of a TAT sequences on the peptides, which not only confers the ability to penetrate cell membrane but also improves solubility, was also tried but again at the optimal DMSO concentrations for SPR it was not possible to keep them in solution and therefore the use of SPR to investigated the binding of the NBD peptides to Aurora A was not pursued further.

Previous studies have been carried out using SPR and related biophysical techniques to provide insight into the interaction of IKKβ and NEMO (Lo et al, 2008). These studies utilised truncated forms of both IKKβ (680-756) and NEMO (38-196) and show a concentration dependent high affinity interaction of IKKβ and NEMO mediated at the NEMO binding domain with K_D values for this interaction calculated at 3.4nM which is close to that observed with Aurora A in this chapter. However, when using shorter NBD peptides the association/disassociation of IKKβ NBD peptide (735-745) and NEMO was too quick to determine any reliable kinetic parameters for this interaction suggesting that the affinity of the IKKβ NBD peptide is weak, which would explain why the concentrations required to get a cellular response are high (*Lo et al, 2008*). This study highlighted the role of the surrounding residues of the NEMO binding domain in mediating this interaction and due to low levels of homology may be explain any divergence in IKKβ and IKKβ/NEMO interactions which can further be extrapolated to apply to Aurora A which has been identified as interacting both IKKα and IKKβ at the NEMO binding domain (Chapter 3) however has very different kinetics between IKKα/β (Chapter 4).

The kinetic information obtained through these experiments has given a novel insight into the nature of the interactions between IKKα, IKKβ and Aurora A and has built on the results of Chapter 3. What remains to be examined is whether there may be some divergence in the relative importance of individual or groups of amino acid present within the C-terminii, both within and outwith the NBD, of the IKKs that dictates the relative affinities of these kinases for binding to Aurora A. Understanding these potential differences between interactions may potentially be exploitable when

considering the design of drugs targeting the interaction(s) of the IKKs with Aurora A in a subunit specific manner.

There is considerable scope for the further investigation of the IKK and Aurora A interactions through bio-physical means, it was however not plausible in the confines of this study to fully pursue this avenue. There is a range of different ways in which this could be further investigated.

These experiments were designed to minimise any artefactual features of the binding such as mass transport limitations or the re-binding of analytes to the surface. However it was still not possible to derive totally accurate kinetic values and further optimisation was out-with the time-frame of this study. To help inform further on these results and the kinetics of these interactions it would be useful to fully understand the nature of the homodimer formation of each of the IKK subunits, this could be studied through further SPR analysis using the IKK proteins as both analyte and ligand. This information could be used in conjunction with the data already obtained to determine if some of the features of the kinetic profiles for the IKK binding to Aurora A were in fact due to analyte dimerisation at the ligand surface rather than a true interaction between analyte and ligand.

Another approach which could be utilised to give a more accurate understanding of the kinetics of these interactions is through the use of alternative coupling methods to immobilise Aurora A on the chip surface. Using an immobilisation method utilising the recombinant protein tag it would be possible to create a more homogenous surface, which may improve the activity of the ligand on the surface and give more accurate values for the rate constants. By using an NTA chip, proteins can be immobilised by a His-Tag through the addition of Ni ions to the surface and using this immobilisation method between runs the protein surface can be stripped and regenerated using fresh ligand which will remove any analyte build up on the surface (Nieba et al, 1998).

To further understand the stoichiometry of this interaction Multi-angle Light scattering (MALS) can also be used, this would therefore provide greater insight into the IKK/Aurora A binding and allow for a more complex model to be applied to give a more accurate kinetic information about these interactions.

The calculated K_D values should also be confirmed through the use of complimentary biophysical techniques such as isothermal calorimetry to validate these findings.

4.6 Conclusions

In summary, through the use of SPR it has been possible firstly to confirm the interaction of full-length purified recombinant IKKα and IKKβ with Aurora A further validating the findings presented in Chapter 3 utilising peptide array strategies. Additionally, the use of SPR has enabled the generation of initial kinetic data highlighting that IKKα and IKKβ each display different binding affinities and kinetics in their individual interactions with Aurora A. These approaches have also shown that these interactions have a low nanomolar K_D value indicating a high affinity. It has also been possible to establish conditions for the use full-length IKK proteins to investigate protein-protein interactions initially with Aurora A using surface plasmon resonance. This could subsequently be further exploited in the pursuit of identifying novel IKK substrates and regulators. The data obtained from the studies investigation IKK interactions with Aurora A indicates the requirement to investigate the functional significance of these interactions and any outcomes apparent upon disruption of these interactions in a cellular setting.

CHAPTER 5: CHARACTERISING THE FUNCTIONAL OUTCOMES OF DISRUPTING IKK/AURORA SIGNALLING

5.1 Introduction

The IKK complex is a well-characterised component of the NF-κB inflammatory signalling pathway first identified by *Chen et al* (1996) as a large multi-sub-unit complex. The IKK complex is comprised of two catalytic sub-units IKKα and IKKβ that can assemble in various homo- and hetero-dimers with the interaction of scaffolding/regulatory member IKKγ/NEMO (*Rothwarf et al, 1998*). The interaction of IKKα and IKKβ with IKKγ is required to promote catalytic function of this complex (*Solt et al, 2009*), this interaction is mediated through the C-terminal domains of IKKα and IKKβ which contain a homologous hexapeptide sequence which has been termed the NEMO binding domain (NBD) (*May et al, 2000*).

The NEMO binding domain was initially identified through the use of hydropathy plots *by May et al* (2000) and identified the conserved central sequence, L-D-W-S-W-L as the essential binding site for interaction of IKKα and IKKβ with IKKγ which have been further detailed by *Rushe et al* (2008) through the use of co-crystallisation studies of the IKKα/β C-terminii and IKKγ. These studies highlighted the critical residues to the interactions as the central tryptophan residues, however the surrounding residues although not critical were important for this interaction (*May et al, 2002, Rushe et al, 2008*). Studies have also suggested that the NEMO binding domain can act as a substrate for PLK1, which can phosphorylate the central serine of the NBD hexapeptide, which down-regulates IKK activity (*Higashimoto et al, 2008*). This highlights the potential for the NEMO binding domain to function as a multi-functional protein binding site.

In Chapter 3, through the use of peptide array mapping of the interaction of IKKα and IKKβ with Aurora A the NBD was identified as a region of strong binding between these proteins. When these regions were further investigated it was identified that the conserved NBD sequence was essential for the interaction of Aurora A and IKK proteins at this site. When further investigated in a cellular system however it was not possible to elucidate the function of the NBD in Aurora A interactions due to experimental challenges. The data presented in Chapter 4 shed further light on the interaction of both IKKα and IKKβ with Aurora A through the biophysical characterisation of the interaction through the use of Surface Plasmon Resonance. These experiments however were carried out using full-length WT IKK proteins and as such were unable

to inform further on the role of the NBD in this interaction and due to solubility issues it was not possible to measure NBD peptide binding to Aurora A by this method.

Therefore, in order to further investigate the role of the NBD in Aurora A interactions in this chapter a short peptide derived from the surrounding primary sequence and including the NBD of IKKβ in a cell-permeable was taken forward as a competitive inhibitor of NBD binding events. This is a well-defined pharmacological tool, which targets interactions of the IKKs initially described by *May et al* (2000) as a competitive disruptor of IKKβ and NEMO binding and inhibiting cytokine-induced NF-κB activity that had no effect on basal activity of IKKs. Futhermore, the NBD peptides have been investigated in several disease models both *in vitro* and *in vivo* and shown to be effective tools for the inhibition of IKK mediated cellular disease without effecting basal activity (*Jimi et al, 2004, Tas et al, 2005*). This peptide can therefore also be utilised to investigate the potential effects of disrupting the IKKα/β-Aurora A interactions mediated, at least in part, by the NBD.

The aims of this chapter were to:

1. Further investigate the interactions of Aurora A and the IKK NBD through the use of the NBD peptides
2. To investigate functional outcomes of treating PC3 with cell permeable forms of the NBD peptides
3. Further elucidation of the relationship between IKK and Aurora A signalling.

5.2 Modelling of IKKα/β interactions with Aurora A

The binding of Aurora A to peptide sequences derived from both IKKα/β was shown previously to map to the C-terminal region NBD (Section 3.1; Figure 3.1) When the binding of the IKK proteins with Aurora A was investigated IKKβ was observed to bind to the same region as that bound by TPX2, a key Aurora A activating protein (*Bayliss et al, 2003*). This observation was further pursued through the use of a rigid body protein docking simulation as a method to model potential confirmations of the interactions of the NBD related peptide derived from of IKKα and IKKβ with Aurora A.

This methodology uses individually determined crystal structures of two proteins and through the use of complex algorithms to assess a range of parameters including shape complementarity and electrostatic attraction (*Chen et al, 2003*) model potential docking of the crystal structures. The aims of which are to identify potential confirmations for the interaction of two candidate binding proteins/partners. This method relies simply on two rigid structures and doesn't account for the conformational changes proteins can undergo when forming complexes and as such is known as 'soft docking'. The highly complex nature of these potential conformational changes in protein-protein interactions although possible to model with algorithms, can take hundreds of hours to run the simulations for each protein-protein interaction. Therefore, 'soft-docking' is a useful tool to in the initial investigation of potential interactions between proteins and can provide insight into potential interacting sites. Algorithms developed by *Chen et al* (2002) known as ZDOCK were applied to the crystal structures of the truncated IKKα and IKKβ NBD binding with Aurora A to simulate potential poses of the NBD sequences with the TPX2 binding site on Aurora A.

5.2.1 Rigid bound docking of the IKKα/β NBD with Aurora A

Although no binding was observed with IKKα and the Aurora A peptide array (Section 3.3.1; Figure 3.4), IKKβ showed binding across amino acids 176-230 and 261-285 of Aurora A (Figure 3.2). The region between residues 176-285 was therefore used to refine the potential site of docking of the NBDs of IKKα and IKKβ with Aurora A. As identified previously by the alanine-scanning and truncation arrays it was also possible

to refine the amino acids of the NBD that were critical to the binding of IKKα/β with Aurora A which were identified as the central tryptophan residues of the NEMO binding domain hexapeptide (Section 3.3.1-3.3.4.3.2). These arrays also suggested the methionine and phenylalanine residues of IKKα and IKKβ respectively, preceding the NBD, were also important for this interaction. These residues have all been identified as essential components of NEMO binding (*May et al 2002*, *Rushe et al 2008*) and therefore have been used as the residues of the NBD that were examined to potentially interact with Aurora A in this model.

The IKKβ binding to Aurora A at 176-230 and 261-285 interestingly contained many of the essential residues for TPX2 binding, as identified by *Bayliss et al* (2003) (Figure 5.1).

```
        10         20         30         40         50         60
MDRSKENCIS GPVKATAPVG GPKRVLVTQQ FPCQNPLPVN SGQAQRVLCP SNSSQRVPLQ

        70         80         90        100        110        120
AQKLVSSHKP VQNQKQKQLQ ATSVPHPVSR PLNNTQKSKQ PLPSAPENNP EEELASKQKN

       130        140        150        160        170        180
EESKKRQWAL EDFEIGRPLG KGKFGNVYLA REKQSKFILA LKVLFKAQLE KAGVEHQLRR

       190        200        210        220        230        240
EVEIQSHLRH PNILRLYGYF HDATRVYLIL EYAPLGTVYR ELQKLSKFDE QRTATYITEL

       250        260        270        280        290        300
ANALSYCHSK RVIHRDIKPE NLLLGSAGEL KIADFGWSVH APSSRRTTLC GTLDYLPPEM

       310        320        330        340        350        360
IEGRMHDEKV DLWSLGVLCY EFLVGKPPFE ANTYQETYKR ISRVEFTFPD FVTEGARDLI

       370        380        390        400
SRLLKHNPSQ RPMLREVLEH PWITANSSKP SNCQNKESAS KQS
```

Figure 5.1 Identification of IKKβ and TPX2 binding sites within the primary amino acid sequence of Aurora A.

Primary amino acid sequence of Aurora A (NCBI. Number NP_940839.1), Essential residue for TPX2 binding are annotated in red, IKKβ binding site identified from peptide arrays annotated in green, residues which are common to TPX-2 and IKKβ binding are annotated in blue

Figure 5.2 i) shows the crystal structure of Aurora A without a surface prepared and in ii) the sites which are blocked i.e. not modelled for interactions, are indicated in yellow on the structure. The structures have been orientated with the TPX2 binding site at the front of the image and the ATP binding cleft behind this. The IKK NBD structures are shown in Figure 5.2 iii) and the residues which have been used for the docking simulation are shown as ball and stick models these are M736/W740/W742 for IKKα and F734/W739/W741 for IKKβ. All other residues for this sequence were blocked for

the docking simulation. Figure 5.3 shows Aurora A with predicted solid surface modelled and on the surface the residues essential for TPX2 binding and were also within the IKKβ/Aurora A binding sites are highlighted in yellow. TPX2 is also shown bound to the Aurora A as a ball and stick representation. The binding of TPX2 with Aurora A was shown by the co-crystallisation of Aurora and two fragments of TPX2 (amino acids 6-21 and 26-42) from which the structure of Aurora A used for this simulation was derived (*Zhao et al, 2008*) (pdb: 3HA6). The crystal structures of the IKK NBDs used were sourced from the IKK/NEMO binding domain architecture study carried out by *Rushe et al* (2008) (α pdb: 3BRT, β pdb: 3BRV).

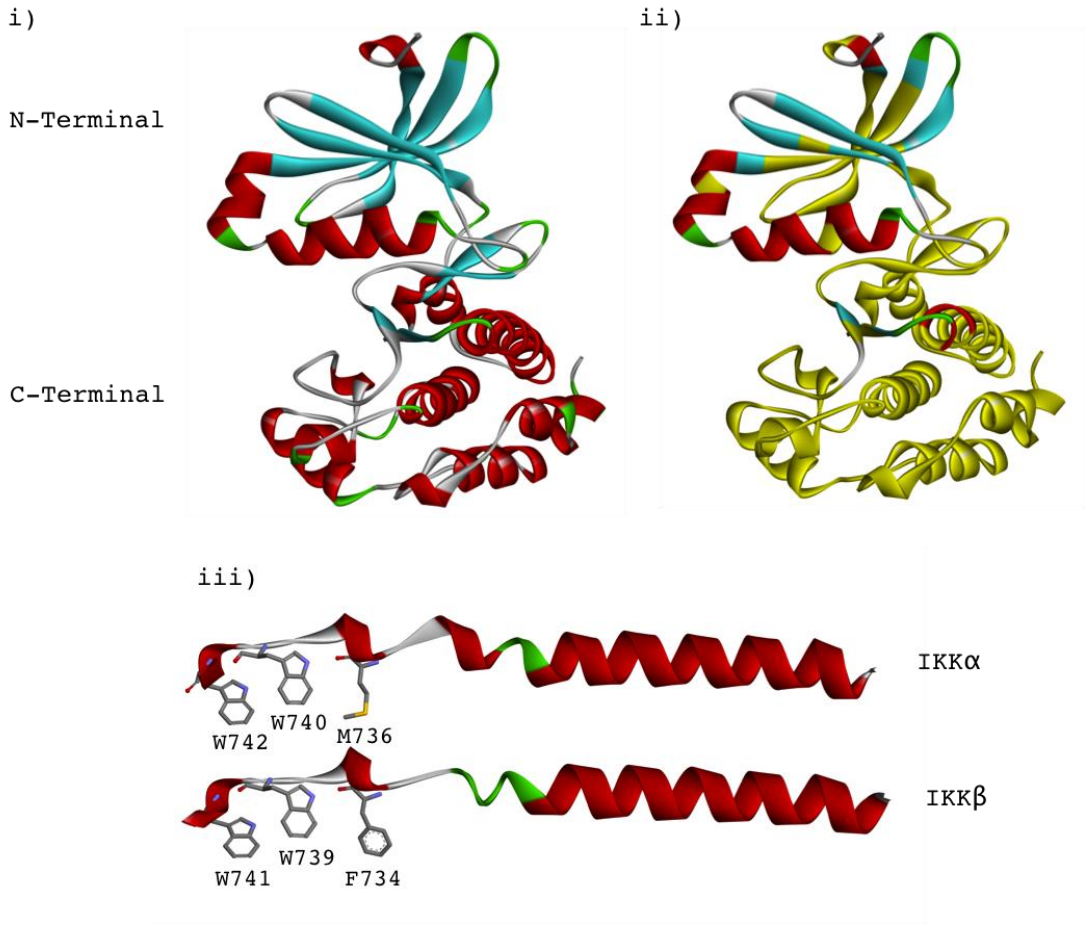

Figure 5.2 Models of Aurora A and the NBDs of IKKα and IKKβ.

The crystal structures of Aurora A and the NBDs of IKKα and IKKβ represented as a backbone and ribbon diagrams. i) Crystal structure of Aurora from pdb code 3HA6 ii) Crystal structure of Aurora from pdb code 3HA6 with ligand blocked sites highlighted in yellow iii) IKK1 NBD taken from chain A of pdb code 3BRT; IKK2 NBD taken from chain A of pdb code 3BRV residues indicated as ball and stick residues are those used for ligand docking. Images prepared by Accelrys Discovery studio 3.1. In the figures Red indicates an α-helix structure, Blue indicates a β-sheet and Green are hinge regions.

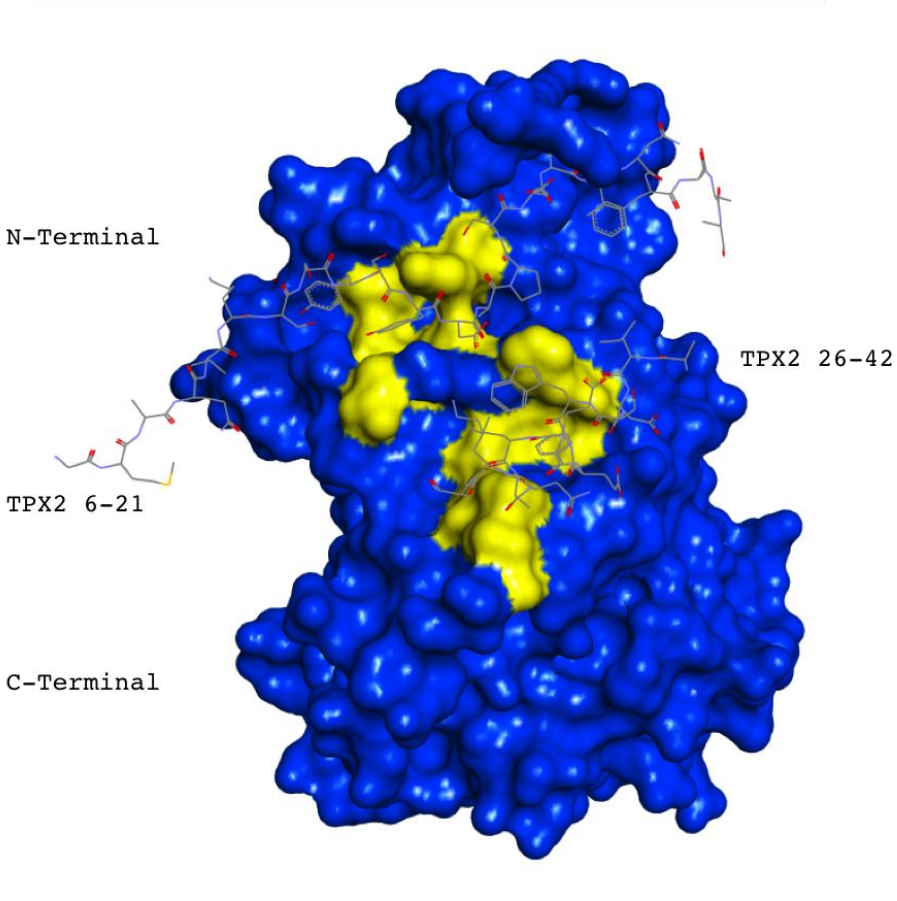

Figure 5.3 Aurora A surface filled with TPX2 structure.

Aurora A structure surface filled and bound to TPX2 fragments from pdb code 3HA6. Full structure of Aurora A-TPX2 binidng; TPX2 shown as ball and stick diagram in grey. Aurora A predicted surface in blue and regions highlighted in yellow correspond to residues essential for TPX2 binding that overlap with identified IKKβ/Aurora A binding sites. TPX2 fragment sequence are shown below structures. Images prepared by Accelrys Discovery studio 3.1.

The protein-protein docking simulation was run with the refinements as previously described and generated >2000 poses for both IKKα/β binding to Aurora A. The poses were separated into clusters and then the highest scoring pose of each cluster was then visually assessed for best modelling of the potential interaction. For both IKKα/β 2 poses were considered to be the best fits, these are shown in Figure 5.4 and Figure 5.5.

5.2.1.2 IKKα NBD docking with Aurora A

The two poses of IKKα are shown in Figure 5.4. Panels i) and iv) show the poses as compared to TPX2 across the whole protein, panels ii) and v) are magnified and focused images of the binding sites and iii) and vi) are the focused images of the binding site with the TPX2-derived fragments overlaid. The poses of the IKKα NBD docked with Aurora A both show similar binding patterns as observed with TPX2. αNBD POSE 1 fits well into the Aurora A groove which also contains several of the essential Aurora A residues for TPX2 binding, as indicated by the yellow surface on Aurora A (Figure 5.4 ii). When The TPX2 binding is also shown alongside αNBD POSE 1 (Figure 5.4 iii) the residues mediating the interaction of IKKα closely follows the TPX2 binding pattern. The αNBD POSE 2 identified (Figure 5.4 iv), shows a very different confirmation with the binding site in a cleft further towards the N-terminal. The site of binding falls within region identified by the peptide arrays for IKKβ binding on Aurora A and does not correlate with the residues identified for TPX2 binding and IKKβ binding. This this pose was overlaid with TPX2 binding (Figure 5.4 vi) the tryptophans 740/742 of the IKKα NBD match closely with the hydrophobic phenylalanine residues 16/19 within the C-terminal of the 2-21 TPX2 fragment which have been identified as components of the Aurora A/TPX2 interaction.

The two poses identified for the IKKα NBD both follow the TPX2 binding site with similar arrangement of amino acids and good positioning in the binding grooves of Aurora A. Interestingly αNBD POSE 2 shows an interaction with Aurora A at the N-terminal binding site that doesn't correlate with the TPX2 critical residues that fall in the identified IKKβ/Aurora A interaction sites identified from the peptide arrays and may be an alternative site of binding of IKKα and Aurora A.

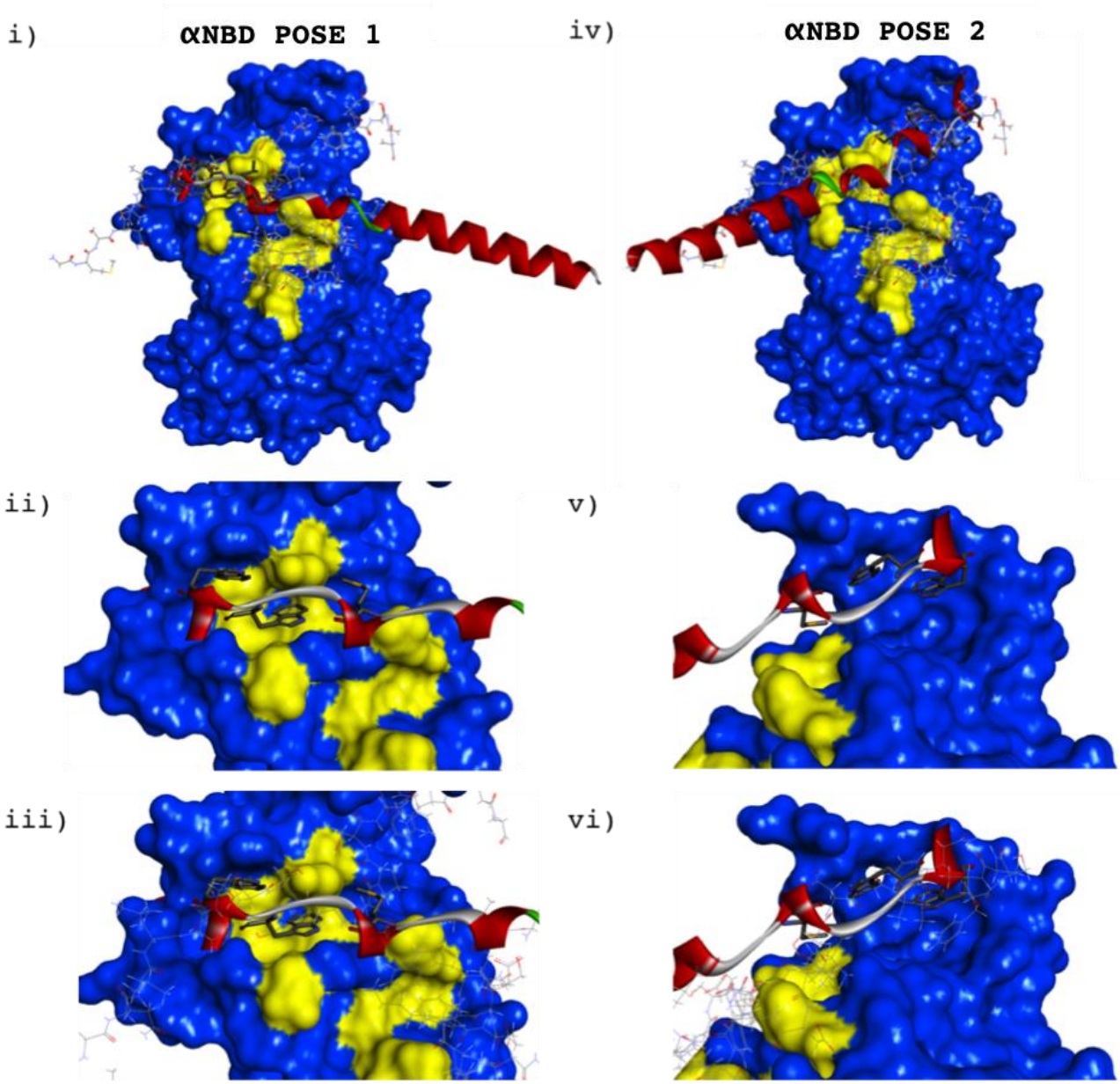

Figure 5.4 Poses identified for IKKα NBD binding to Aurora A

Poses as identified by ZDOCK software. i) αNBD POSE 1 with whole Aurora A structure ii) αNBD POSE with binding region magnified iii) αNBD POSE 1 magnified and overlaid with TPX2 binding from original crystal structure iv) αNBD POSE 2 with whole Aurora A structure v) αNBD POSE 2 binding region magnified vi) αNBD POSE 1 binding region magnified and overlaid with TPX2 binding from original crystal structure. Aurora A structure surface filled and bound to TPX2 fragments from pdb code 3HA6. TPX2 is shown as ball and stick diagram in grey. Aurora A predicted surface is displayed in blue and regions highlighted in yellow correspond to residues essential for TPX2 binding that overlaps with identified IKKβ/Aurora A binding sites. ZDOCK analysis and images prepared by Accelrys Discovery studio 3.1.

5.2.1.2 IKKβ NBD docking with Aurora A

The interaction of Aurora A and IKKβ was previously mapped to this region of the Aurora A peptide arrays the kinase domain of Aurora A. The NBD of IKKβ was also shown to mediate a strong interaction with Aurora A when the IKK full-length arrays were investigated with the overlay of recombinant Aurora A. As with IKKα two poses for IKKβ NBD interaction with Aurora A were identified as the best models for this interaction based on the software-derived scores alongside visual assessment. The two poses of IKKβ NBD-Aurora A interaction are shown in Figure 5.5. Panels i) and iv) show the poses as compared to TPX2 across the whole protein, ii) and v) are magnified and focused images of the binding sites and iii) and vi) are the focused images of the binding site with the TPX2 overlaid. These poses both show IKKβ NBD binding to Aurora A in very similar confirmations to that observed with IKKα NBD. βNBD POSE 1 docks well with the TPX2 binding groove of Aurora A suggesting binding in the same region as the overlapping TPX2/IKKβ binding residues (Figure 5.5 ii). When this pose is shown overlaid with the TPX2 binding from the co-crystal it can be seen that the tryptophans 739/741 of βNBD align well with the C-terminal tyrosines 8/10 of TPX2, both critical residues for Aurora A binding (Figure 5.5 iii). βNBD POSE 2 (Figure 5.5 iv) is orientated at a slightly different angle to that seen in αNBD POSE 2 (Figure 5.4 iv) however the binding site fits within the same cleft. The docking at this site fits well and when overlaid with the TPX2 sequence shows βNBD tryptophan 741 aligning with the TPX2 phenylalanine 19, unlike αNBD POSE 2 the binding of the βNBD phenyalanine is orientated further towards the TPX2 binding groove which contains the overlapping TPX2/IKKβ binding residues and aligns with the TPX2 proline 13 binding to Aurora A at residues identified by *Bayliss et al* (2008) as a point of interaction.

As with the αNBD both poses identified align well with the TPX2 binding sites on Aurora A, with both pose of βNBD following the TPX2/IKKβ binding residues more closely which is to be expected as these were identified by the IKKβ overlay on an Aurora A full length peptide array.

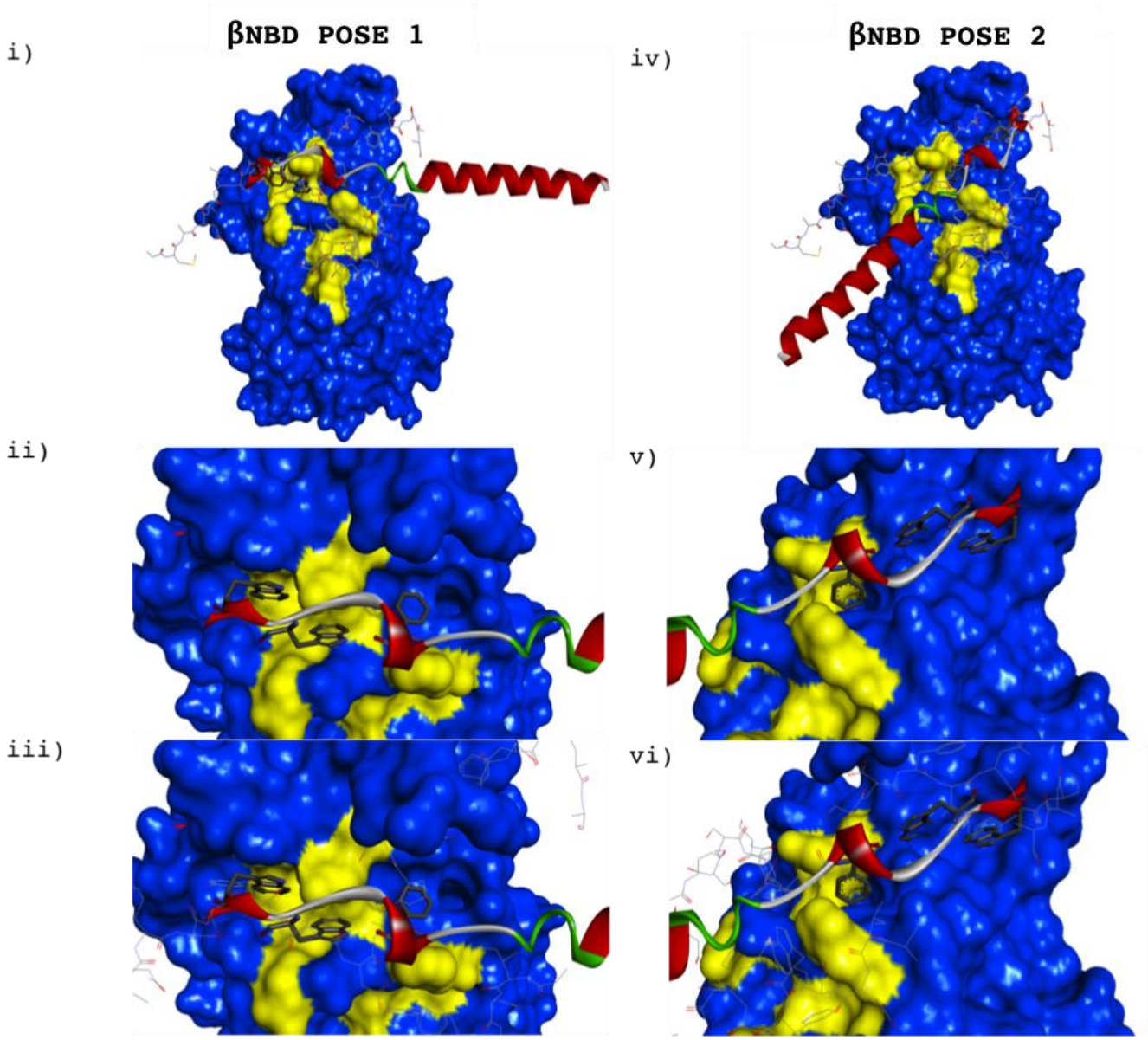

Figure 5.5 Poses identified for IKKβ NBD binding to Aurora A.

Poses as identified by ZDOCK software. i) βNBD POSE 1 with whole Aurora A structure ii) βNBD POSE 1 binding region magnified iii) βNBD POSE 1 binding region magnified and overlaid with TPX2 binding from original crystal structure iv) βNBD POSE 2 with whole Aurora A structure v) βNBD POSE 2 binding region magnified vi) βNBD POSE 1 magnified binding region. Aurora A structure surface filled and bound to TPX2 fragments from pdb code 3HA6. TPX2 is shown as ball and stick diagram in grey. Aurora A predicted surface in blue and regions highlighted in yellow correspond to residues essential for TPX2 binding that overlaps with identified IKKβ/Aurora A binding sites. ZDOCK analysis and images prepared by Accelrys Discovery studio 3.1.

5.3 Investigating the Aurora A/NEMO binding domain interaction with Nanohole Arrays.

The use of the rigid body docking algorithms highlights that there are several confirmations by which the NBD of both IKKα and IKKβ can bind to Aurora A. In order to further investigate the interactions of the NBD with Aurora A peptides mimicking the NBD domain were utilised. The use of the peptides mimicking the NEMO binding domain was an essential tool used for the identification of the key residues that regulate the IKK/NEMO interactions (*May et al, 2000*). An 11 amino acid peptide was synthesised which included the NEMO binding domain hexapeptide L-D-W-S-W-L, a TAT sequence was added to the N-Terminal of this peptide also to aid solubility and allow for translocation across cell membrane for use in cells. When using these peptides a control mutant form was also used in which the essential NBD tryptophans were mutated to alanine that was shown to reverse inhibition of the NF-κB pathway mediated by the use of a NBD targeting peptide (*Dai et al, 2004*). Peptides synthesised are shown in Figure 5.6 with the key residues of Aurora A binding, as identified in Chapter 3, and the IKK/NEMO (*May et al, 2002*) interaction highlighted.

Y-G-R-K-K-R-R-Q-R-R-R-F-T-A-L-D-W-S-W-L-Q-T NBD WT CPP
Y-G-R-K-K-R-R-Q-R-R-R-F-T-A-L-D-A-S-A-L-Q-T NBD MT CPP

Figure 5.6 NEMO binding domain peptides

The sequences of the cell permeable NEMO binding domain peptides (NBD CPP) used in all assays in this chapter. Highlighted in blue is the TAT sequence derived from HIV that allow for the peptides to cross the cell membrane, the amino acids in red are the critical residues for both IKK-Aurora A and IKK-NEMO interactions. The mutant peptide (NBD MT CPP) has the essential tryptophans mutated to alanine (also highlighted in red).

The use of the peptides in SPR was attempted to assess binding (as detailed in Chapter 4) however it was not possible to develop the assay as there were significant problems with solubility of the NBD peptides without the TAT sequence. The TAT sequence is lysine/arginine rich which makes these peptides highly charged which will give significant non-specific interactions with the dextran matrices of the SPR chips and

therefore make binding events difficult to measure. Therefore, alternative binding assays were sought. The work described in this section was carried out in collaboration with a colleague from the Department of Pure and Applied Chemistry at the University of Strathclyde.

To further probe the interaction between the NBD WT CPP and Aurora A, surface-enhanced Raman scattering (SERS) was used. SERS is a sensitive vibrational spectroscopic technique complementary to SPR, which can give chemically specific information about the analyte and can detect and quantify analyte binding at very low concentrations.

To investigate the potential NBD peptide-Aurora A interactions a bimetallic nanohole array was used as the SERS-active surface. This surface has been characterised previously and shown to generate good SERS enhancement profiles. The nanohole arrays were functionalised with a self-assembled monolayer (SAM) of 16-mercaptohexaundecanoic acid resulting in a monolayer of carboxylic acid-terminated molecules. NBD WTand NBD MT peptides (to act as a knock-out control) were bound to the functionalised nanohole array surface via EDC/NHS chemistry as used in the SPR studies described in Section 2. The surface was then blocked with ethanolamine to terminate and remove any unreacted carboxylic acids.

For this investigation, Aurora A was selected to be labelled with a SERS-active dye so as to allow easy detection by SERS and also so that multiple ligands could be assessed simultaneously. Aurora A was functionalised with Malachite green (MG), a well characterised SERS-active dye that gives a strong and easily identifiable Raman spectrum, using EDC/NHS chemistry to link malachite green to both the N-terminus and any lysine side chains of Aurora A. This gave a heterogenous population of dye coupled His-Aurora A.

The assay method was based on the approach used in the SPR investigation discussed in Chapter 4 as SPR and SERS are related and complementary techniques to one another.

12μM His-Aurora A-MG was incubated with the peptide-functionalised surfaces for a time period of 30 minutes. Three separate interactions were carried out on one functionalised surface for both the wild-type and mutant peptides, with each separate interaction being carried out in a separate well. After 30 minutes, the surfaces were

thoroughly washed with PBS. The surfaces were then analysed using an excitation wavelength of 633 nm. These conditions have been shown in previous reports to give good Raman spectra. Eight replicate scans were taken across each interaction well. In order to evaluate the data, the peak height of a well-defined peak, as shown in Figure 5.7, was calculated for each spectrum collected allowing calculation of both the mean signal and the standard deviation from the wild-type and the mutant interactions with MG-labelled His-Aurora A.

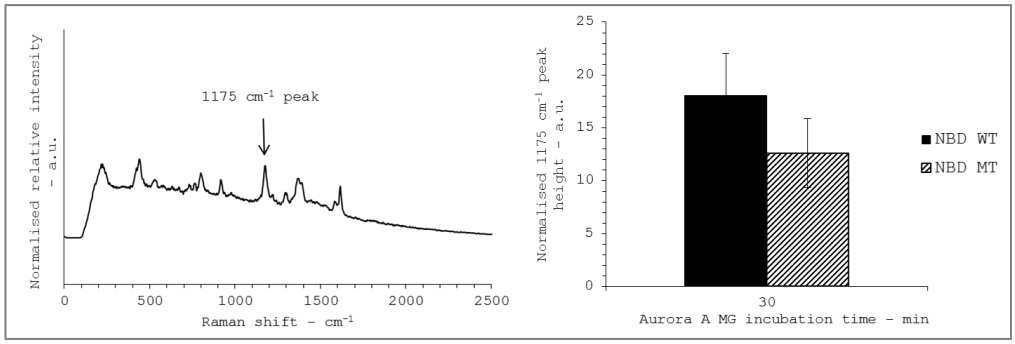

Figure 5.7 MG-Aurora A peak at 633nm and interaction of Aurora A with immobilised NBD WT and NBD MT peptides.

The peak height measured for the His-Aurora A-MG at 1175cm-1 is shown alongside the results of the His-Aurora A-MG binding to WT NBD and MT NBD peptides. Data shown is representative of 3 independent experiments, analysed with one tailed un-paired t-test at $P<0.05$.

It can be concluded from Figure 5.7 that although the average signal collected from the interaction of Aurora A with the WT NBD peptide was greater than that from the interaction of His-Aurora-MG with the NBD MT peptide, the standard deviation values were not significantly different indicating His-Aurora A-MG did not discriminate between the wild type and mutant peptides. The lack of discrimination between the wild type and mutant peptide interactions may be a result of non-specific binding between the peptide functionalised surface and the MG-labelled Aurora A.

A one-tailed t-test at 95% confidence level was then performed with the results generated to determine whether the difference between the mean signal from the NBD WT CPP and the NBD MT CPP binding was statistically significant. The t-test results showed t_{calc} was greater than t_{crit} ($t_{calc}>t_{crit}$) and so the null hypothesis was rejected; the

difference between wild type and mutant mean Raman signal was significant and not due to random error. The results of the statistical analysis indicate that there is a significant difference in the interaction of MG-labelled Aurora A with the NBD WT CPP compared with that of the NBD MT CPP. This investigation was designed to be a proof-of-concept study to determine if there was any measurable difference in binding of the NBD WT CPP to Aurora A compared to the binding of the NBD MT CPP to Aurora A. It was also designed to ascertain if this method could be used in a peptide-binding screening process. This methodology is advantageous as a single array surface could be functionalised with numerous possible peptide-binding targets allowing a high-throughput screening assay to be developed although further investigation is needed to fully develop this assay methodology

5.4 Effects of the NEMO binding domain cell permeable peptide on Aurora A status in a cellular system

The disruption of the NF-κB pathway has been the focus of considerable research due to its essential role in regulating the immune response to infection. The main focus of this research has been in the development of kinase inhibitors targeting the ATP-binding pocket of IKKα/β. This however has limitations such as potential off-target effects due to the high levels of homology observed in all kinase domains and drug resistance due to mutations in this region. This has led to the investigation of allosteric sites that may inhibit the activity of the catalytic IKK components. The effect of disrupting NEMO binding to IKKα/β with the use of a cell permeable peptide (CPP) was shown by *May et al* (2000) to inhibit cytokine-induced NF-κB activation. As previously described considerable research has been carried out to investigate the use of the CPPs targeting the NBD of IKKα/β as a potential target for drug intervention. As seen in (Section 3.2) the interaction of Aurora A and IKKα/β was mapped to the NBDs of IKKα and IKKβ suggesting the NBD to function as a multi-protein binding site. Preliminary experiments also investigated the interaction of recombinant Aurora A with the NBD CPP (NBD WT) versus a mutant form of the peptide (NBD MUT) and identified a significant difference between the interaction of recombinant Aurora A with the NBD WT over the NBD MT, which further supports the critical role of the central NBD tryptophans to regulate Aurora A and IKK interactions at this site.

Therefore, the NBD peptide was subsequently used as a tool to further investigate the role of IKKα/β in Aurora A signalling when the interaction with the IKKs were disrupted by targeting the NBD site in a cellular system. NBD peptides (11-mer), as used in the nanohole-binding assay,

were then coupled to a TAT-derived amino acid membrane transduction sequence (YGRKKRRQRRR) to generate a CPP form and taken forward for use in all cell-based experiments.

5.4.1 NBD CPP effects on Aurora A in an asynchronous cell population

5.4.1.1 Characterisation of the effects of NBD WT CPP treatment on TNF-α stimulated NF-κB signalling and Aurora A status in PC3 cells.

The effects of the NBD CPP peptides were investigated initially in relation to classical NF-κB signalling, notably the phosphorylation of transcription factor p65 (*Hayden et al, 2008*). The NBD peptide has been shown to inhibit NF-κB in relation to cytokine induced activation of the IKK proteins but does not affect basal IKK activity (*May et al, 2000*). Therefore, the effect of the NBD WT was investigated in relation to stimulation of cells over time with TNF-α, a well-described agonist of the NF-κB signalling cascade (*Wajant et al, 2003*). The mutant peptide, NBD MT, served as a negative control as the mutation of the central NBD trytophans to alanine residues ablates the peptides' ability to disrupt IKK-NEMO interaction,its inhibitory function and thus should show no effect on agonist-stimualted NF-κB signalling.

Figure 5.8 shows the effect of WT and MT NBD CPP on agonist-stimulated NF-κB signalling. After 24 hours serum starvation cells were pre-treated with 100μM NBD WT or MT CPPs for 2 hours prior to exposure to TNF-α (20ng/ml) for 15, 30 and 60 minutes. The peptides were dissolved in 100% DMSO to counteract the solubility issues as identified in Chapter 4 and therefore all experiments used DMSO as the control. It can be observed that pre-treatment with the WT NBD CPP inhibited TNFα-mediated phosphorylation of p65 at Ser^{536} at all time points compared to both the DMSO and MT NBD controls. The induction of p65 phosphorylation by TNF-α was maximal for this experiment at the 15 minute time point (2.76 fold ± 0.83; n=2) and decreased with time but did not return to basal levels, by comparison pre-treatment of cells with the WT NBD CPP inhibited TNFα-stimulated p65 phosphorylation significantly at this time point (0.85 fold ± 0.3; n=2) and remained at near basal levels across all time-points. Pretreatment of cells with the MT NBD CPP did not affect TNF□-stimulated p65

phosphorylation at any of the time points examined. This indicated that the NBD WT CPP was acting on NF-κB signalling as previously described by (*May et al, 2000*).

Interestingly, when Aurora A levels were investigated in this experiment the WT NBD CPP induced the degradation of Aurora A. In the TNF-α stimulated vehicle controls, there was no significant degradation of Aurora A observed, however in the NBD WT CPP pretreated, TNF-α-stimulated samples there was a significant reduction in Aurora A expression at 15 min (85 ± 7%; n=3), 30 min (86 ± 5%; n=3) and 60 min (79 ± 7%; n=3). The degradation of Aurora A across all TNF-α stimulated time points was consistent and was identified as significant statistically to $P < 0.05$. The degradation was not observed in the TNF-α stimulated DMSO vehicle nor the NBD MT CPP controls that suggest this was a NBD WT CPP induced effect. Degradation was also observed in the cells pretreated with the NDB WT CPP alone however this change was not shown to be statistically significant. This is likely due to the large variability within these samples and with a larger experimental group may become significant.

i)

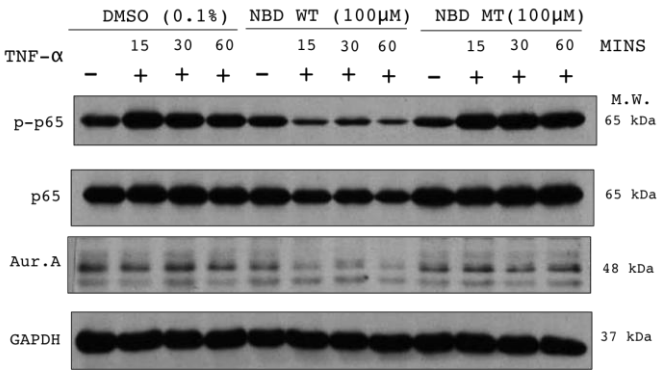

ii)

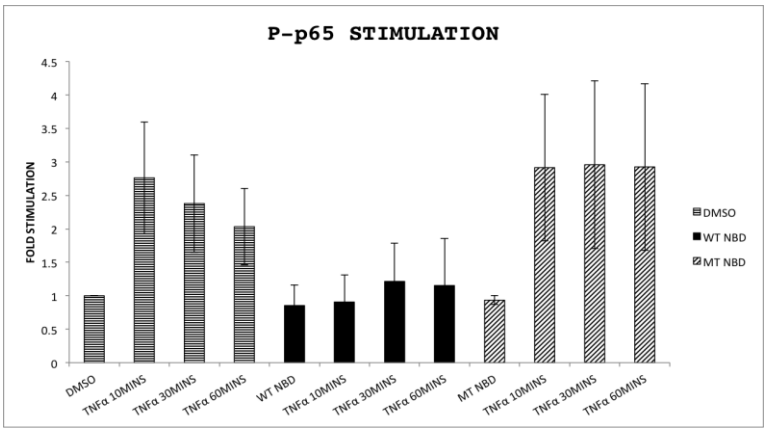

iii)

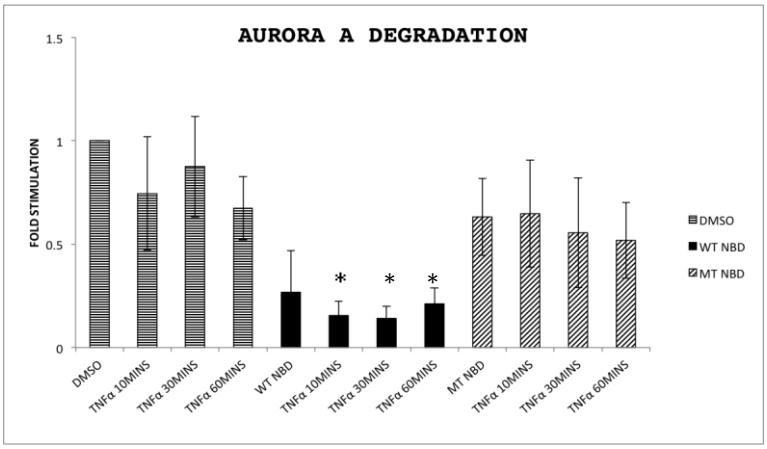

Figure 5.8 NBD WT CPP mediated inhibition of TNFα-stimulated p65 phosphorylation and induction of Aurora A degradation in PC3 cells.

PC3 cells were pre-treated with NBD CPPs (100μM) for 2hours prior to stimulation with TNF-α (20ng/ml) for 15, 30,60 min. Whole cell lysates were prepared in sample buffer and separated by SDS-PAGE and assessed for p-p65 (S536), p65,Aurora A and GAPDH expression by Western blotting. GAPDH was used as a loading control and protein levels were normalised to loading controls before analysis. i) Fold stimulation of p-p65 (n=2) iii) Fold stimulation of Aurora A (n=3) analysed by 1-way ANOVA with Dunnets test relative to DMSO unstimulated control. All values calculated by scanning densitometry and shown as mean ± SEM. (* indicates $P < 0.05$).

5.4.1.1 Characterisation of the concentrations dependent effects of NBD WT CPP on TNF-α stimulated NF-kB signalling and aurora A status in PC3 cells.

To further investigate the nature of the NBD WT CPP-induced Aurora A degradation experiments were constructed to pre-treat cells with variable concentrations of the peptides. In order to confirm the inhibitory activity of the peptide it was necessary to stimulate the cells with TNF-α and also determine the effect on phosphorylation of p65 at variable concentrations. It was observed in Figure 5.8 that the maximal TNFα-stimulated phosphorylation of p65 occurred at the 15-minute time point therefore this time point was used for examination of the effects of all concentrations of NBD CPPs. The cells were pre-treated with the variable peptide concentrations for 2 hours prior to stimulation.

Figure 5.9 shows the concentration dependent effect of the peptide on TNF-stimulated phosphorylation of p65. It was seen that upon exposure of cells, pre-treated with the varying concentrations of DMSO vehicle, to TNF-α the stimulation of p65 phosphorylation was consistent, 2.2 ± 0.4 (n=2) fold compared to the un-stimulated cells. This showed no effect of DMSO concentration on TNF-α-induced phosphorylation of p65. Pre-treatment of cells with increasing concentrations of the NBD WT CPP however showed a concentration dependent inhibition of TNFα-stimulated phosphorylation of p65. Cell pre-treated with the highest concentration of NBD WT CPP alone showed no effect of on p65 phosphorylation status however in cells pre-treated in a similar manner but exposed to TNF-α treatment displayed significant inhibition of TNFα-stimulated p65 phosphorylation, 0.73 ± 0.44 (n=2) fold. Pre-treatment with decreasing concentrations resulted in the reversal of the inhibition of TNFα-stimulated p65 phosphorylation. At the 30μM concentration TNFα-stimulated phosphorylation of p65 was observed to be 1.8 ± 2.2 (n=2) fold over untreated controls and at the 10μM concentration p65 phosphorylation was equivalent to the vehicle controls (2.2 fold ± 0.8; n=2). Pre-treatment with the NBD MT CPP showed no effects compared to the controls at the highest concentration, 2.3 ± 1.07 (n=2) fold stimulation. This indicated that the NBD WT CPP acted to inhibit TNF-stimulated phosphorylation of p65 in a concentration-dependent manner.

Figure 5.9 iii) shows the effect of the NBD WT CPP on Aurora A status when cells were treated with the CPP at variable concentrations. It was observed in this experiment that

at the 100μM concentration the NBD WT CPP induced a significant degradation of Aurora A in both the stimulated (81 ± 10% n=3) and unstimulated (50 ± 5% n=3) treated cells. At the lower concentrations, with TNF-α stimulation, however, the degradation of Aurora A was not significant, pre-treatment with 30μM showed a 25 ± 16 % (n=3) reduction and the 10μM displayed a total reversal of degradation and showed an increase of 16 ± 22% (n=3) in Aurora A levels. The NBD MT CPP showed no effect on Aurora A expression compared to the vehicle controls.

Therefore, Figure 5.8 and 5.9 identified that the effect of the NBD WT CPP on Aurora A degradation in an asynchronous population of cells was independent of TNF-α stimulation and also the NBD WT CPP acted in a concentration dependent manner. This suggested that the NBD WT CPP was inducing the degradation of Aurora A.

i)

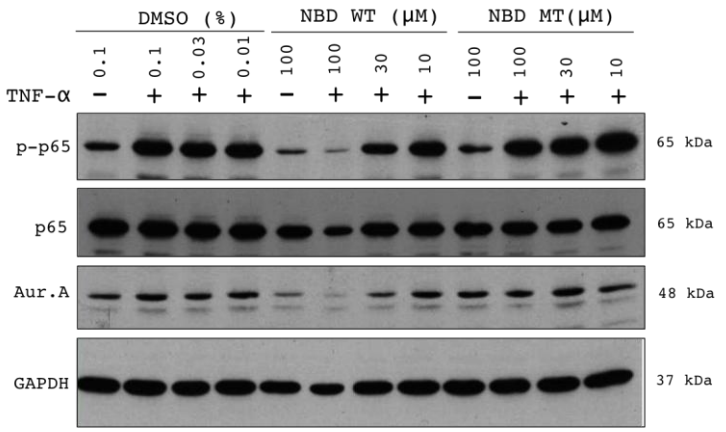

ii)

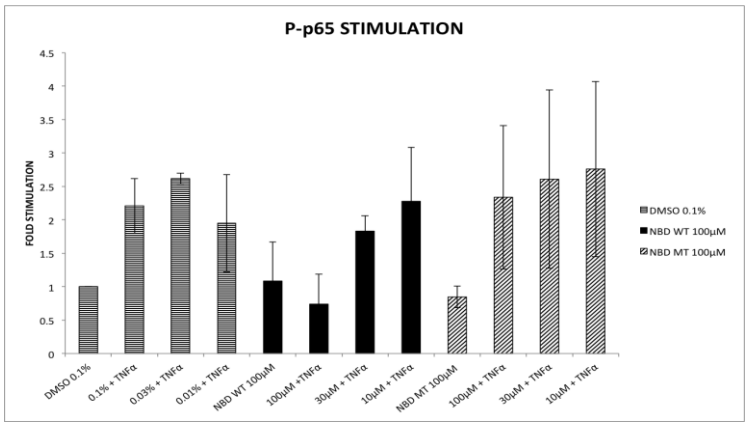

iii)

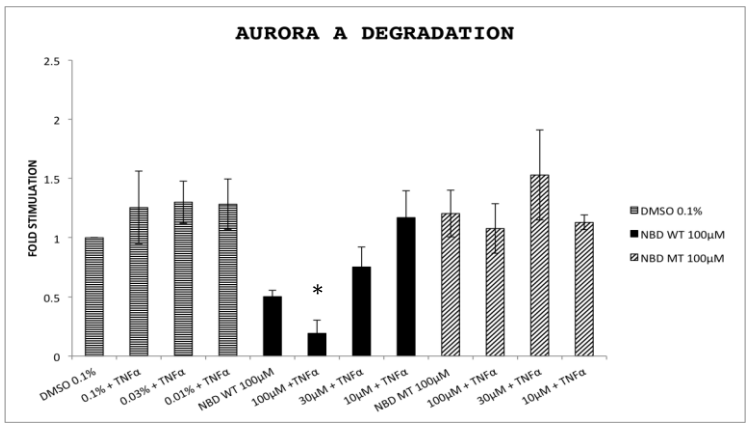

Figure 5.9 Concentration dependent effect of NBD CPP on TNFα-stimulated phosphorylation of p65 and induction of Aurora A degradation.

PC3 cells pre-treated with NBD CPPs (100μM, 30μM and 10μM) for 2 hours prior to stimulation with TNF-α (20ng/ml) for 15mins. Whole cell lysates were prepared in sample buffer, separated by SDS-PAGE and assessed for p-p65 (S536), p65, Aurora A and GAPDH expression. GAPDH was used as a loading control and protein levels were normalised to loading controls before analysis. i) Fold stimulation of p-p65 (n=2) iii) Fold stimulation of Aurora A (n=3) analysed by 1-way ANOVA with Dunnets test relative to DMSO unstimulated control . All values calculated by scanning densitometry and shown as mean ± SEM. (* indicates $P < 0.05$).

5.4.2 the effects of pretreatment with the NBD CPP on Aurora A status in a synchronous Cell population.

Aurora A kinase is an essential component to mitotic progression of mammalian cells and its expression is temporally regulated to be expressed maximally during mitosis (*Fu et al, 2007*). Expression of Aurora A then returns to a baseline level in the cell upon completion of cytokinesis through APC/C^{cdh1}-mediated ubiquitination and subsequent degradation (*Vader et al, 2008*). Therefore to inform further on the effect of the NBD WT CPP on Aurora A status/signalling it was necessary to investigate the effects of the NBD-related peptides on Aurora A during mitosis.

Initially a double thymidine trap and release treatment as described in (Section 2.2.1.6) was used to synchronise the cells at G_1/S-phase. Figure 5.10 shows the trap and release of the cells over a 24 hour period with samples prepared every two hours post release. Expression of cellular components were then assessed by SDS-PAGE for phospho-Aurora A (Thr 288) /Aurora A and IKKα/β expression alongside a range of cell cycle markers to indicate the progression of the cells through mitosis. It can be seen that both Aurora A and p-Aurora A levels increased at 14 hours alongside survivin and p-cdc2 (Tyr 15) which are both markers of G_2/M phase of the cycle. The Aurora A co-factor TPX2 also increased in expression at this time point. This suggested that the cells were transitioning into the G_2/M-phase at 14 hours post-release from the double thymidine trap. The IKKα/β expression however remained unchanged through the cycle, which was to be expected, as they are not cell cycle regulated proteins. This method of synchronisation however was not suitable for use for the treatment with the NBD WT CPPP as treating the cells for 14 hours with the peptide was likely to induce high levels of cell death or alternatively the NBD WT CPP may be degraded/broken down within the cell with a long incubation which would compromise interpretation of any potential NBD CPP mediated effects. Therefore another synchronisation methodology was utilised to synchronise the cells at the pro-metaphase. At this point of the cycle it was anticipated that the Aurora A expression and associated phosphorylation at Thr 288 would be at their maximum and would allow enable a more straightforward assessment of any effects of the peptide(s). To synchronise the cells at this phase of the cycle Nocodazole was used in a trap and release methodology as described in Section 2.2.1.6.

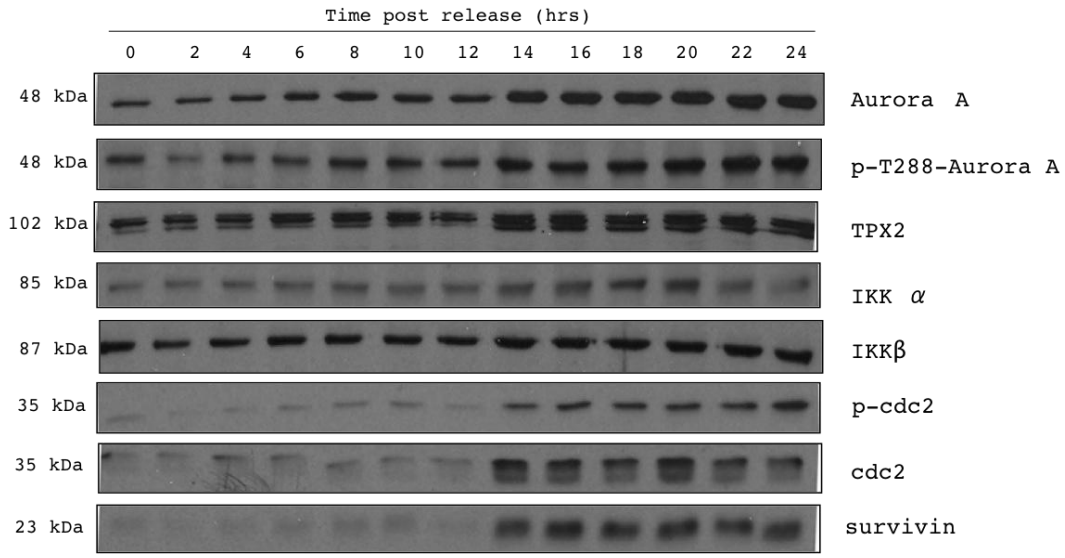

Figure 5.10 Characterisation of cell cycle components after Double thymididine trap and release

PC3 cells were treated with 2mM thymidine for 16hrs, media was changed and cells were released for 8hrs and then treated again with 2mM thymidine for 16hrs. Media was then changed and cells were released from trap and whole cell lysates prepared for separation by SDS-PAGE and analysis by immunoblotting with the specified antibodies. Data presented is representative of two independent experiments.

To establish optimal conditions for nocodazole arrest various concentrations and time points of treatment of cells were examined, established as a 16-hour treatment with a 50ng/ml concentration of Nocodazole (data not shown). Nocodazole acts to prevent microtubule polymerisation and as such prevents the cells from progressing into mitosis due to a spindle checkpoint failure and an arrest in pro-metaphase (*Jordan, 1992*). PC3 cells were therefore treated with said 50ng/ml Nocodazole for 16 hours and then released by washing the cells twice with fresh media. The release was subsequently followed for 8 hours post-release with whole cell lysates prepared every 2hours or in parallel cells were collected every 2 hours by trypsinisation and fixed with 70% ethanol overnight prior to analysis by flow cytometry. Figure 5.11 i) shows the trap and release of the cells assessed by DNA content using propidium iodide staining measured by Fluorescent Associated Cell Sorting (FACS) analysis. It can be seen that at the 0hr time point 75% of the cells were arrested in G_2/M phase of the cycle with 15% at G_1 and 7% in S phase. This shows that nocodazole treatment successfully trapped the cells in G_2/M phase of the cycle and upon release it can be seen that the cells return to a ratio of 60% G_1 to 30% G_2/M phase 4 hours after release and was observed to stay at this ratio at the subsequent time points. This indicated that the cells moved progressively through the cycle post-release from the nocodazole trap and the cells exited mitosis by the 4 hour time point (Figure 5.11 i)). At these time points the Aurora A expression and phosphorylation were also investigated by immunoblotting as shown in Figure 5.11 ii) which showed at the 0 hour time point Aurora A was maximally expressed and was at its highest level of phosphorylation. The expression and phosphorylation of Aurora A was subsequently reduced as the cells were released from the trap with a basal level achieved at the 4 hour time point which was observed consistently at 6 hours and 8 hours post-release also. The phosphorylation of Aurora A however was reduced much faster than the observed decrease in total protein expression; at 2 hours the level was almost at basal levels. This was due perhaps to the lesser functional role of Aurora A in the latter stages of mitosis. The phosphorylation of Aurora B (threonine 232) was also assessed in these samples and from this it can be observed that Aurora B phosphorylation was present at a higher level than that of Aurora A until the 6 hour time point and this again is consistent with the reported functions of Aurora B in the latter stages of mitosis (*Fu et al, 2007*). The expression levels of IKKα and IKKβ were also assessed and show no change in expression following release from the nocodazole trap. This was consistent with the observations

in Figure 5.11 that the catalytic IKK subunits expression remained constant through the cell cycle.

Collectively, these data identified and confirmed that the nocodazole trap and release methodology could be used for the arrest of PC3 cells at the G_2/M phase transition and upon release successfully move through the cell cycle. Furthermore, these experimental conditions could also be utilised in the further examination of any modulatory effects of the NBD WT CPP upon Aurora A status/expression and associated phosphorylation.

i)

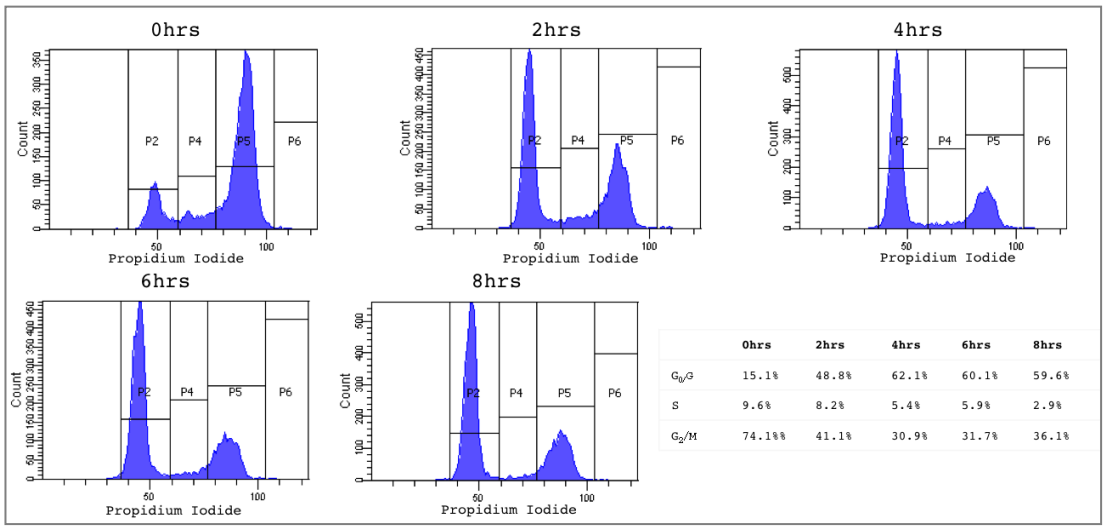

	0hrs	2hrs	4hrs	6hrs	8hrs
G_0/G	15.1%	48.8%	62.1%	60.1%	59.6%
S	9.6%	8.2%	5.4%	5.9%	2.9%
G_2/M	74.1%%	41.1%	30.9%	31.7%	36.1%

ii)

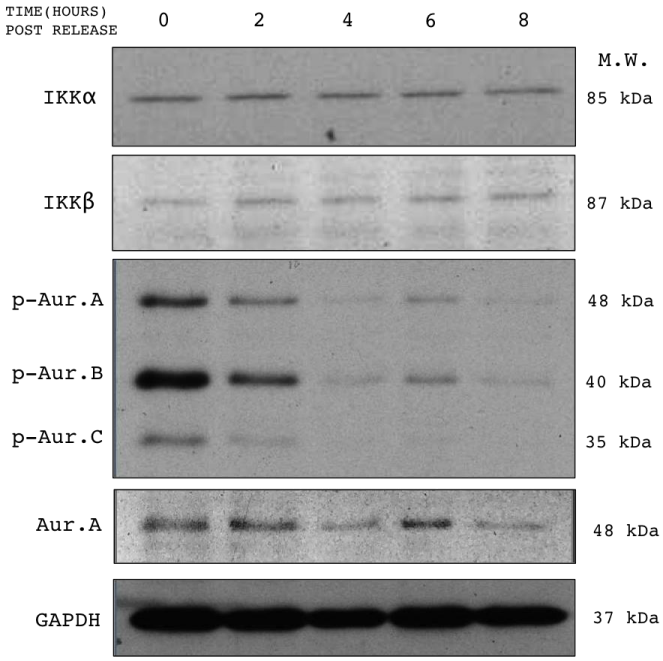

Figure 5.11 Characterisation of IKKα/β and Aurora A status through the cell cycle following release fromNocodazole trap of PC3 cells

PC3 cells were incubated with 50ng/ml overnight with nocodazole and released by washing twice with fresh media. Cells were either fixed for FACS analysis in 70% ethanol overnight or whole cell lysates prepared for SDS-PAGE. i) FACS analysis of the cells post-trap and release, times indicated as hours post-release. Propidium iodide staining is shown in the graphs and is relative to cellular DNA content measured using a PE filter at excitation wavelength 488nM with FACSCANTO Flow cytometer. Gates shown on graphs indicate measured cell cycle populations (P2=G_1, P4=S, P5=G_2/M) and shown as percentage of total measured population in the table. ii) Whole cell lysates were analysed by immunoblotting at specified time points for IKKα/β and pan-p-Aurora (AurA Thr288/AurB Thr 232/Aur C 198) and total Aurora A levels. Data presented is representative of two independent experiments.

5.4.2.1 Characterisation of the effects of the NBD WT CPP on PC3 cell cycle progression.

Figure 5.11 showed that nocodazole trap and release was a suitable method for the arrest of cells at the G_2/M phase transition (pro-metaphase) and these cells could subsequently be released to progress through the cell cycle. The observation that Aurora A degradation was induced by an acute treatment of the NBD WT CPP in an asynchronous population of PC3 cells (see Figures 5.8 and 5.9), prompted the re-examination of the effects of the NBD WT CPP on cells as they moved through the G_2/M phase transition, the phase of the cycle in which Aurora A is highly active, maximally expressed and critical to mitotic function. The NBD CPPs were used again at a concentration of 100μM which was shown previously to induce significant degradation of Aurora A. The cells were treated with the NBD CPPs at the point of release after nocodazole washout; a DMSO vehicle control was also used for each time point that showed the normal progression of the cells through mitosis. At each time point cells were collected by typsinisation and then fixed with ethanol overnight before RNase digestion and staining with propidium iodide.

The effect of the NBD WT CPP on the progression through the cell cycle was striking with an almost complete failure of the cells to progress through mitosis after 2 hours of treatment with the NBD WT CPP, the failure of the cells to pass through the cycle after 2 hours was not observed to reverse totally over time as seen in Figure 5.12. There were no comparable populations observed between all conditions in these samples in any of the experiments carried out after the release from nocodazole trap and therefore the % of each population has not been quantified for these samples. However, the gating indicates how the different populations could be measured (P4=G_1, P5=S, P6=G_2/M) and shows the relative levels of the cells at different phases and allow for visual comparison of differences in the cell cycle for each condition. The normal cell cycle progression without peptide can be seen in the vehicle control (DMSO) samples which showed the reversal of the arrest at the 2 hour time point with the cells returning to predominantly G_1 phase and this was maintained through the rest of the time points. The NBD MT CPP also showed the same progression with the cells progressing through mitosis. The cells were observed to be mainly in G_1 at the 2 hour time point and as seen

in the vehicle control this remained the case for the remaining time points. The NBD WT CPP treated cells however arrested at S phase and G_2/M phase of the cycle at 2 hours post-release and did not progress normally through the cycle, there was a reduction in the accumulation at the 6 hour time point post-release however this was still considerably higher than that observed in either the NBD MT CPP or the vehicle controls. This suggested that the NBD WT CPP was disrupting the normal progression of the cells through mitosis and this may be due to either perturbation of IKK-NEMO interactions and/or IKK NBD-Aurora A interactions. To further investigate the functional response to the NBD WT CPP, lower concentrations of peptide were also used to determine if this effect was concentration dependent. Figure 5.13 shows the effect of treatment of PC3 cells with the NBD WT CPP at 30μM and 10μM on cell cycle progression. The effects of the NBD WT CPP appeared to occur in a concentration-dependent manner; at 30μM there was an accumulation of the cells in G_2/M phase at 2 hours post-release and this accumulation in G_2/M phase remained at all time points examined. The 10μM concentrations of NBD WT CPP however showed virtually no accumulation relative to the vehicle control. The NBD MT CPP was also tested in parallel at matching concentrations and showed no differences to the DMSO vehicle control (data not shown). This showed that the NBD WT CPP was acting on the cell cycle in a concentration-dependent manner, these experiments however were only carried out once and therefore requires further confirmation by additional independent replicates.

The result of NBD WT CPP on the progression of the cells through mitosis was clearly apparent in these experiments, however it was also observed that there was an increased population of cells at sub-G_0 indicated by the increased cell count prior to gate P4. This accumulation of sub- G_0 cells can be seen in both Fig. 5.12 and Figure 5.13 at all time points, and is charactersitic of cells undergoing apoptosis suggesting that the NBD WT CPP was inducing an apoptic response in the PC3 cells after nocodazole trap and release. This observation requires further investigation however through the analysis of apoptotic markers such as annexin v alongside cell cycle analysis it will be possible to assess the extent of the apoptotic response to the NBD WT CPP in PC3 cells.

The effect of the NBD WT CPP is striking on the cell cycle when analysed by flow cytometry, this however only informs on gross changes to DNA content and not by which mechanism of action the peptide is functioning i.e. if these changes are mediated through the disruption of Aurora A signalling or through the inhibition of IKK signalling

by the NBD WT CPP. In order to investigate the effects of the peptide on Aurora A signalling it was essential to determine the effects on the phosphorylation status as well as on total Aurora A levels within the cell to further our understanding by what mechanism the peptide is acting on Aurora A. The effect of the NBD WT CPP occurs within 2hrs of treatment post release (Figure 5.11) and the characterisation of the p-Aurora A status in Figure 5.11 showed that the p-Aurora A levels was considerably lower 2hrs post release therefore a shorter time scale was used for analysis of Aurora A signalling with respect to treatment with the peptide.

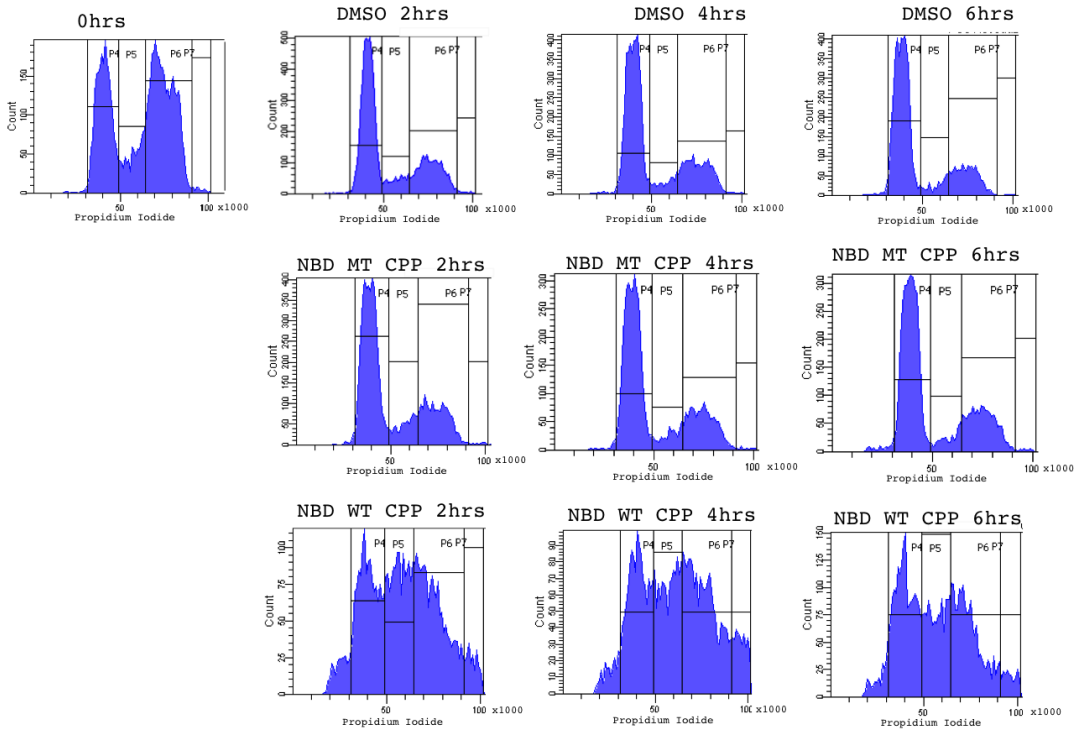

Figure 5.12 The effects of NBD WT CPP on PC3 cell cycle progression after nocodazole trap and release.

PC3 cells were treated with 50ng/ml Nocodazole for 16hrs to induce an arrest at pro-metaphase, cells were released from trap by washing with fresh media and treated with NBD CPPs at specified concentrations upon release. Samples were collected by trypsinisation and fixed in 70% ethanol overnight prior to RNase digestion and staining with propidium iodide to analyse DNA content. Flow cytometry analysis of DNA content was carried out using a FACSCANTO flow cytometer and data processed using FACSDiva software. Data is representative of 4 independent experiments.

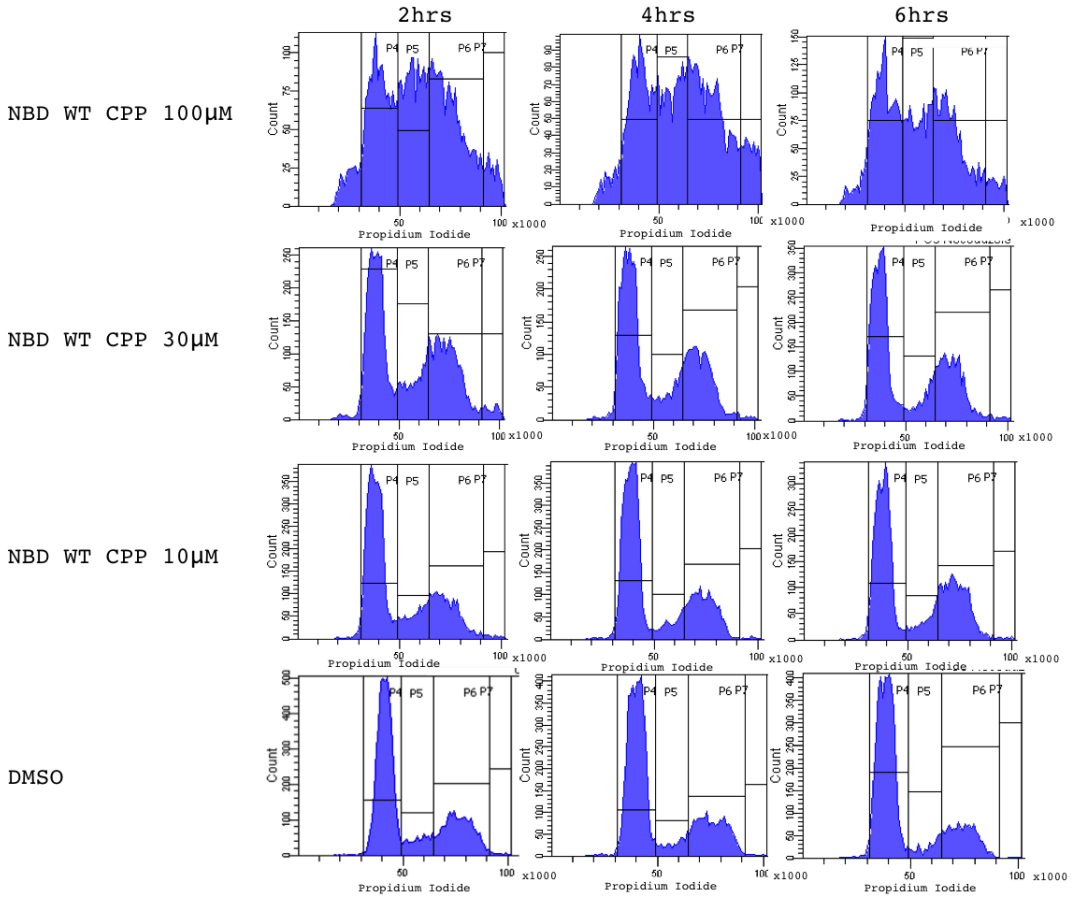

Figure 5.13 Concentration dependent effects of the NBD WT CPP on PC3 cell cycle progression after Nocodazole trap and release.

PC3 cells were treated with 50ng/ml Nocodazole for 16 hours to induce an arrest at pro-metaphase, cells were released from trap by washing with fresh media and treated with NBD CPPs at specified concentrations upon release. Control 0hours is the same control sample as presented in Figure 5.13. Samples were collected by trypsinisation and fixed in 70% ethanol overnight prior to RNase digestion and staining with propidium iodide to analyse DNA content. Flow cytometry analsysis of DNA content was carried out using a FACSCANTO flow cytometer and data processed using FACSDiva software. Data is representative of 1 independent experiment.

5.4.2.2 Characterisation of effects of the NBD WT CPP on cellular Aurora A status.

Cellular Aurora A was observed to be degraded over time post-release from nocodazole trap and its phosphorylation status also decreases with time although this occurred more rapidly than the decrease in total expression (Figure 5.11 ii). Therefore, to investigate the effect of the NBD WT CPP on Aurora A status after release from synchronisation at pro-metaphase Aurora A expression and phosphorylation were examined by Western blotting at 30, 60 and 120 minute time points. These experiments sought to determine if the NBD WT CPP at 100μM was disrupting normal Aurora A expression/function or if the cell cycle progression effects were mediated through an alternative mechanism.

Figure 5.14 i) and ii) show the treatment of cells with the NBD WT CPP inhibited significantly the phosphorylation of Aurora A relative to the levels observed in the vehicle control at 0 min. At 30 min the phosphorylation of Aurora was reduced following NBD CPP treatment by 71 ± 7% (n=3) and at 60 mins by 84 ± 3% (n=3). The observed decrease in Aurora A phosphorylation was statistically significant to $P < 0.01$. However at 120 minutes post-release from the Nocodazole trap the reduction of Aurora A phosphorylation was still statistically significant but the reduction in Aurora A phosphorylation was also significantly reduced ($P < 0.01$) in both the vehicle control and the NBD MT CPP treated cells, at this time point. In these three samples the reduction of Aurora A phosphorylation was 60 ± 4% (n=3) for the vehicle control, 71 ± 1% (n=3) for the NBD MT CPP and 88 ± 5% (n=3) in the NBD WT CPP treated cells. This shows that over this time course the levels of Aurora A phosphorylation were reduced naturally, however the NBD WT CPP induced a significant decrease in the phosphorylation of Aurora A independently of the inhibition seen over time. The total levels of Aurora A were also assessed to determine if the loss of phosphorylation was associated or linked to a comparative a loss of Aurora A or through dephosphorylation by the NBD WT CPP. Figure 15 14 iii) shows that there was a significant loss of total Aurora A induced by the peptide at 30min (38 ± 2 %; n=3), 60 min (35 ± 6%; n=3) and there was a significant reduction observed also at 120 min (40 ±8% n=3). However, there was also significant loss in both the vehicle controls (40 ± 0.1% n=3) and NBD MT

CPP treated cells (64 ± 8% n=3) at this time point which illustrated that Aurora A levels were being reduced over time, as observed in Figure 5.11 ii). This finding therefore suggested that the NBD WT CPP induced a degradation of Aurora A as observed in the asynchronous cells (Figure 5.8 and 5.9) and this was promoting an inhibition of Aurora A phosphorylation. The rate of degradation of Aurora A however was slower kinetically than the loss of phosphorylation and suggested therefore that Aurora A dephosphorylation may preceed any loss in total expression of Aurora A protein. Figure 5. 14 i) also showed the inhibition of the phosphorylation of Aurora B and Aurora C upon treatment with the NBD WT CPP; The total levels of Aurora B and C however were not assessed and therefore it remains to to be determined if the observed cellular effect of the NBD WT CPP was an inhibitory phenomenon common to all Aurora kinases and was linked in any way to degradation of these additional Aurora kinases .

The effect of the NBD WT CPP on the classical components of the NF-κB pathway were also assessed for one of these experiments and it was observed that there was little impact on IKKα/β, p65 and IκBα status with only a small reduction in p65 phosphorylation suggested with respect to either treatment with the NBD WT CPP or after the release of the cells for pro-metaphase arrest (Figure 5.15) and further independent replicates are required to confirm these preliminary findings.

i)

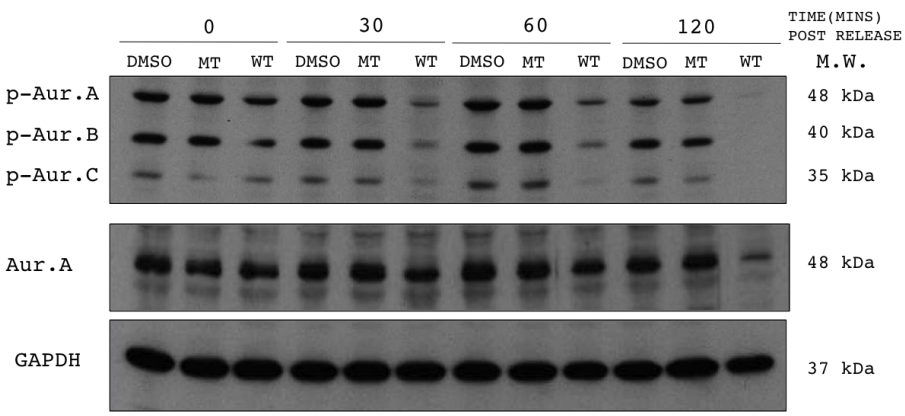

ii)

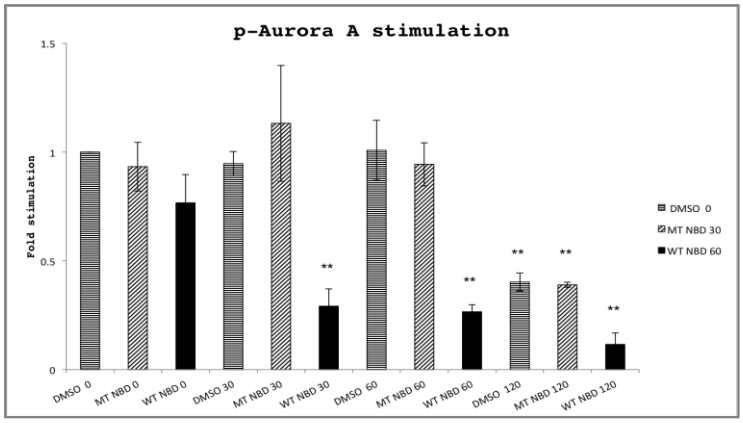

iii)

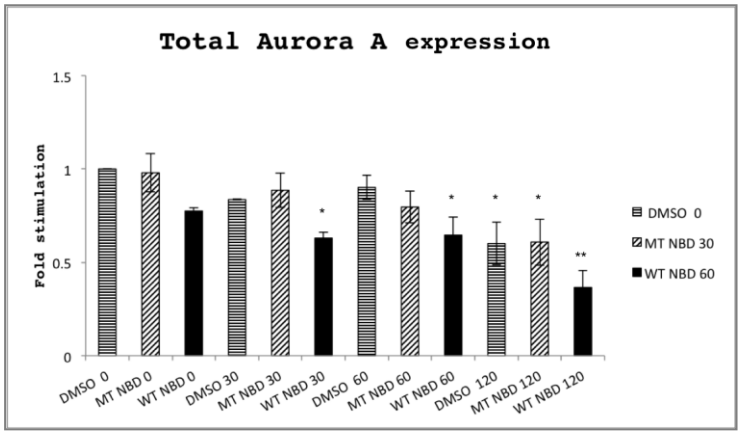

Figure 5.14 Effects of NBD WT CPP on cellular Aurora A status after Nocodazole trap and release.

PC3 cells were treated with Nocodazole (50ng/ml) for 16 hours and treated with specified NBD CPP (100μM) or DMSO as a vehicle control upon release. Whole cell lysates were prepared at indicated time points and analysed by SDS-PAGE and proteins levels assessed by immunoblotting with specific antibodies at concentrations previously described. Data presented is representative of three independent experiments. Two-tailed 1-way ANOVA with Dunnetts test was used to determine statistical significance of observed changes relative to vehicle control at 0 mins (* = $p<0.05$, ** = $p<0.01$).

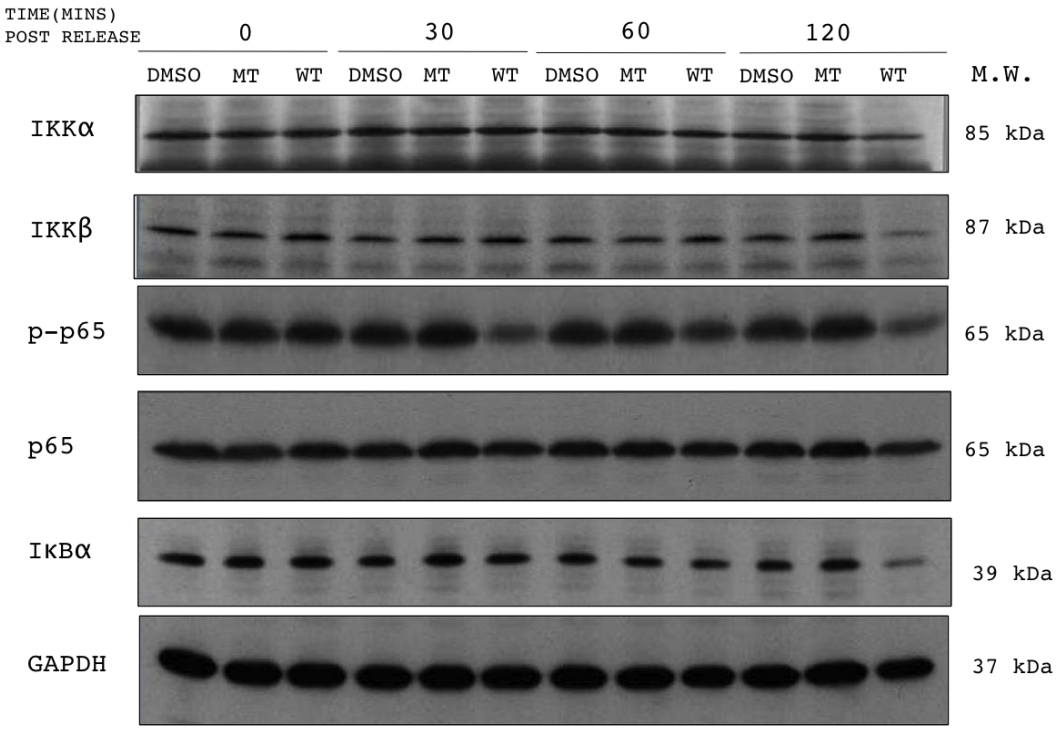

Figure 5.15 Effects of NBD WT CPP on IKK-NF-κB pathway components after Nocadazole trap and release.

PC3 cells were treated with Nocodazole (50ng/ml) for 16 hours and treated with specified NBD CPP (100μM) or DMSO as a vehicle control upon release. Whole cell lysates were prepared at indicated time points and analysed by SDS-PAGEand proteins levels assessed by immunoblotting with specific antibodies at concentrations previously described. Data presented is representative of one independent experiment.

5.4.3 Characterisation of the role of IKKα/β in the cell cycle

The NBD WT CPP mimics the NBD of IKKβ, that is homologous with the NBD of IKKα, and acts to disrupt the binding of IKKα/β with the scaffolding protein IKKγ/NEMO. The scaffolding of the IKK complex by NEMO mediated through the NBDs is essential in the regulation of classical agonist-stimualted NF-κB activation (*Solt et al, 2009*). The NBD WT CPP however has been shown to interact with Aurora A (Section 5.3) and can induce the degradation of Aurora A (Section 5.4.2). The use of the NBD WT CPP in this context however cannot inform on whether the effects observed occurred through the direct interaction of Aurora A with the NBD WT CPP or through the perturbation of the IKK complex. *Prajapati et al* (2006) suggested that Aurora A was a substrate for IKKα, regulating the activity of Aurora A and therefore driving mitotic entry. In addition, *Irelan et al* (2007) reported a role for IKKβ in the β-TRCP-induced degradation of Aurora A. Both studies used siRNA targeted knockdown of the IKK proteins to measure the effect of loss of IKKα/β on the cell cycle however these results of these studies studies were conflicting in the effects of IKKβ 'run-down' upon cell cycle progression. In order to investigate the potential role of the individual catalytic IKKs in cell cycle progression in PC3 cells, siRNA targeted run-down of either IKKα or IKKβ relative to a scrambled non-targeting sequence (N/T) was pursued and analysed by FACS.

5.4.3.1 Effect of siRNA run down of IKKα/β on PC3 Cell cycle progression.

IKKα and IKKβ were targeted with specific siRNAs utilising optimised transfection conditions with concentration of targeting sequences and transfection reagent established as 100nM siRNA and 5μl lipofectamine respectively. Each subunit was targeted individually and the expression of IKKα was knocked down successfully by 75 ± 9% (n=3) following 48 hours of transfection whilst IKKβ was also knocked down similarly with a total reduction in protein of 85 ± 2% (n=3), with no effect observed with the non-targeting sequence (Figure 5.16 i) and ii)). The siRNA sequences utilised were able to knockdown specifically the expression of the targeted subunit in the absence of any off-target effects (Figure 5.16). Parallel identically treated samples

were then assessed by FACS analysis to determine whether the total loss of expression of each IKK induced any cell cycle arrest in the treated PC3 cells. Figure 5.16 iii) shows the cell populations and their distribution through the cell cycle after 48 hours of IKKα/β knockdown. No large changes in the cell cycle distribution were observed in these samples, however a small increase in S-phase after targeted IKKβ run-down was observed (10%), otherwise the cells all conformed to the same distribution of the G_1 and G_2/M phases regardless of the knockdown of the IKK proteins. This change in S-phase however was not consistent between experiments and therefore was not considered to be due to the targeted knockdown of IKKβ. The cells were analysed in an asynchronous population, as the loss of the IKK proteins should induce an arrest over time and shift the distribution of cells if the IKK proteins are contributing to mitotic progression. The effect of IKKα and IKKβ knockdown on total Aurora A levels and phosphorylation status was also assessed by immunoblotting (Figure 5.16 i)) however no effect on Aurora A levels were observed under these conditions although the phosphorylation status was very difficult to assess as the levels were very low. This low level of Aurora A phosphorylation was again in fact characteristic of normal cell cycle progression and the observed lack of Aurora A phosphorylation suggests that there was no effect of the IKK proteins on Aurora A expression or activity as suggested previously in the literature.

i)

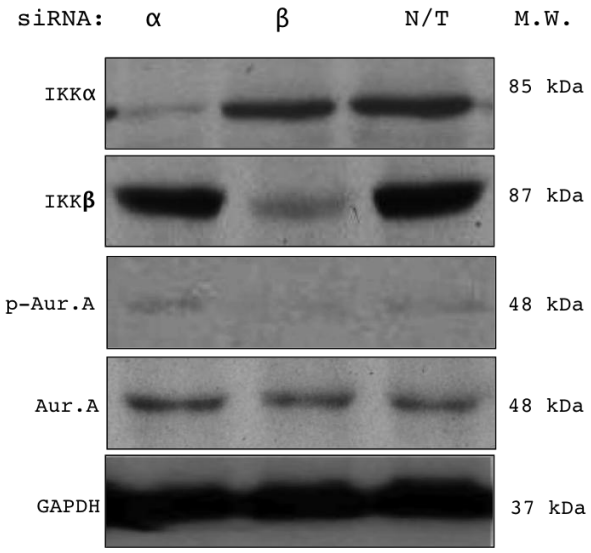
siRNA: α β N/T M.W.
IKKα
IKKβ
p-Aur.A
Aur.A
GAPDH
85 kDa
87 kDa
48 kDa
48 kDa
37 kDa

ii)

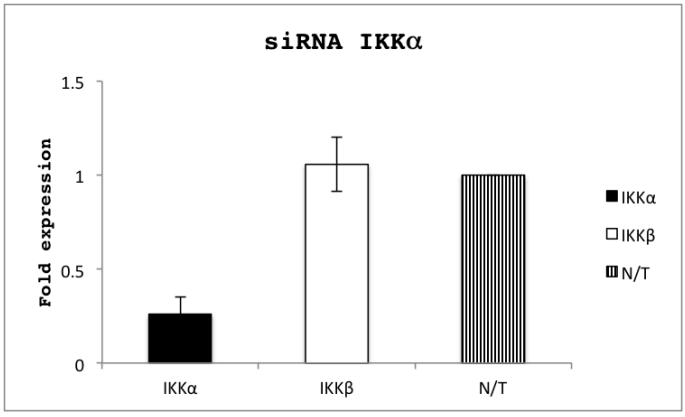
siRNA IKKα
Fold expression
1.5
1
0.5
0
IKKα
IKKβ
N/T
IKKα
IKKβ
N/T

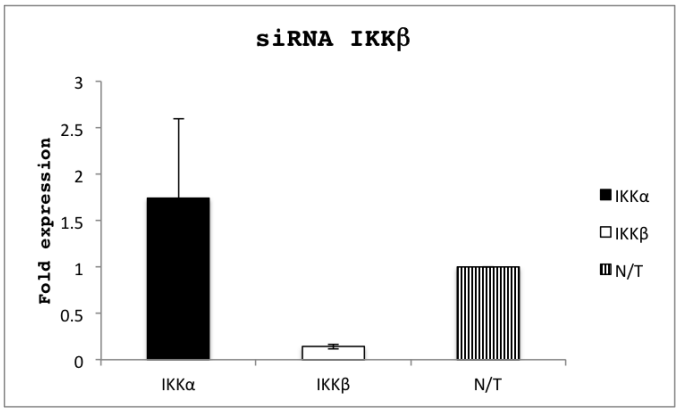
siRNA IKKβ
Fold expression
3
2.5
2
1.5
1
0.5
0
IKKα
IKKβ
N/T
IKKα
IKKβ
N/T

iii)

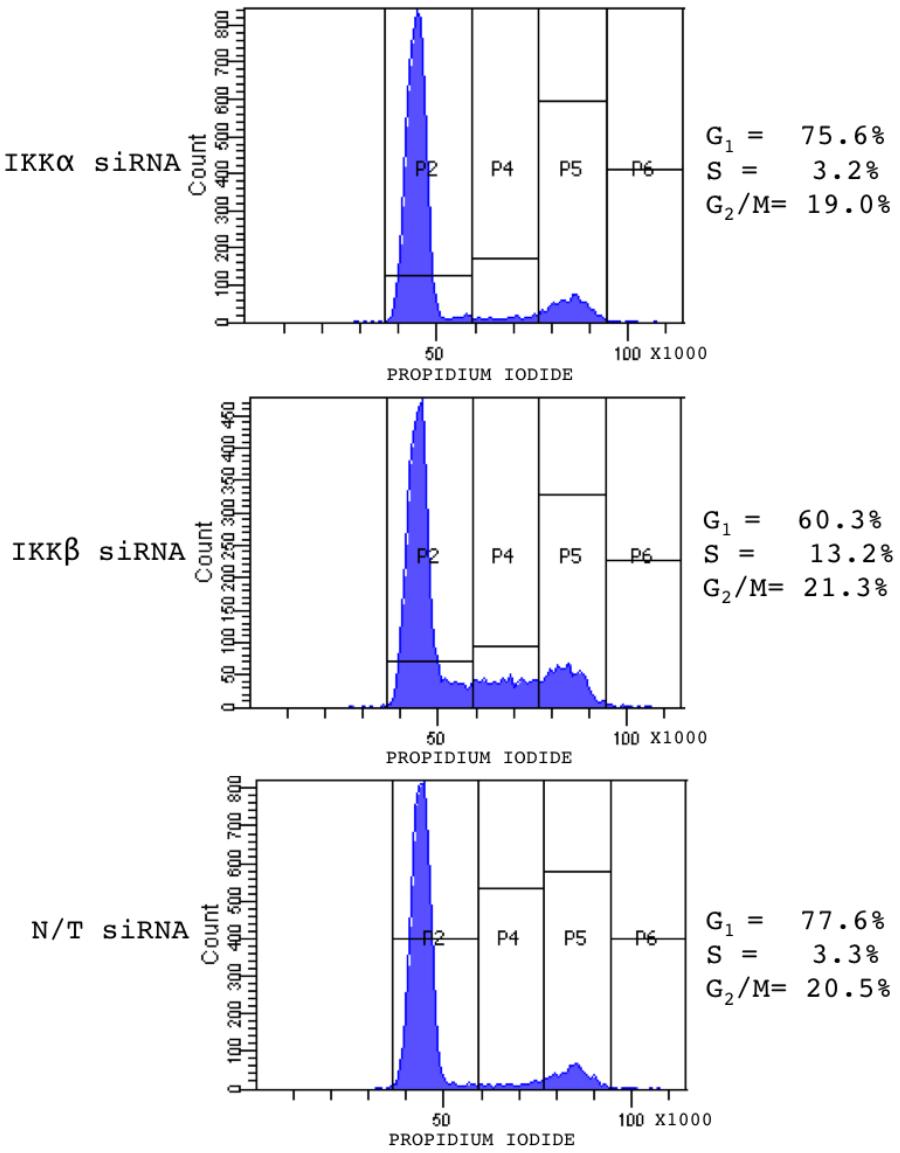

Figure 5.16 The effect of siRNA targeted of IKKα/β on cell cycle progression in PC3 cells..

PC3 cells were treated with 100nM siRNA targeting IKKα, IKKβ or Non-targetting (N/T) for 16 hours, cells were washed and grown in fresh full media for a further 32 hours. Samples were collected by trypsinisation at 48hrs post siRNA treatment and fixed in 70% ethanol overnight prior to RNase digestion and staining with propidium iodide to analyse DNA content. Flow cytometry analsysis of DNA content carried out using a FACSCANTO flow cytometer and data processed using FACSDiva software. Data presented is representative of 3 independent experiments.

5.4.4 Investigation of potential IKK-Aurora a cross-phosphorylation events by kinase assay in vitro

The findings that siRNA knockdown of the IKK proteins had no effect on the cell cycle nor on Aurora A phosphorylation and expression (Figure 5.16) and the observations that Aurora A was binding the kinase domains of both IKKα/β (Section 3.2) led to the investigation of any potential relationship between Aurora A and the IKK proteins in terms of kinase function. The ability of either the IKKs or Aurora A to modulate and/or catalyse auto- and/or cross—phosphorylation of each other was then assessed by means of recombinant protein–based kinase assays performed *in vitro*.

Individual recombinant kinases (His-IKKα, His-IKKβ, His-Aurora A) were incubated either alone or in IKK-Aurora A combinations with 50μM ATP/3μCi ^{32}P-ATP at 30^{o}C for 30 min following which reactions were terminated with SDS-PAGE sample buffer, boiled and run on SDS-PAGE gels. Any incorporation of radioactive phosphate into proteins was then visualised by autoradiography. Preceding co-incubation of the IKKs with Aurora A the relative activity of each of the IKK proteins was investigated with respect to potential phosphorylation of recombinant GST-IκBαN, a truncated fusion protein derived from full-length IκBα, a well-recognised substrate of the IKKs *in vitro*. A series of enzyme amounts (3, 10 and 30ng) were prepared in combination with 1μg GST-IκBαN. Aurora A was also prepared at matching amounts and incubated with 1μg GST-IκBαN. Each enzyme was incubated in the experiment individually with the IKK substrate and kinase mix and incorporation of radioactive phosphate determined. Figure 5.17 i) shows that the incorporation of ^{32}P-ATP into GST-IκBαN occurred in a enzyme-dependent manner for both IKKα and IKKβ, with considerably more incorporation catalysed by IKKα than IKKβ, which suggested a higher intrinsic catalytic activity of this enzyme. Interestingly, increasing amounts of Aurora A also showed increasing phosphorylation of GST-IκBαN suggesting that it can act as a substrate for Aurora A *in vitro*. The auto-phosphorylation of these proteins was also assessed by incubating the highest amount of enzyme alone with the kinase mix in the absence of substrate. For each enzyme no detectable levels of auto-phosphorylation were visible without substrate however with the addition of substrate levels of auto-phosphorylation increased for both IKKα and Aurora A but not IKKβ. Therefore, all three enzymes were confirmed to be catalytically activity, the IKKs validated as IκBα kinase and additionally IκBα was identified as a potential substrate for Aurora A.

To determine if IKKα/β acts as substrates for Aurora A, a constant amount of recombinant IKK enzymes (30ng) were incubated in combination with variable Aurora A amounts (3,10 and 30ng) and 50μM ATP/3μCi ^{32}P-ATP (Figure 5.16 ii)). Similar conditions were developed with a constant amount of Aurora A in combination with increasing amounts of IKKα/β (Figure 5.17 iii))In each set of incubations the potential auto-phosphorylation of each kinase was also assessed by incubation of enzymes alone at their highest amount with 50μM ATP/3μCi ^{32}P-ATP, in the absence of any recombinant substrate. Although auto-phosphorylation of IKKβ was clearly visible at the highest amount of enzyme or as IKKβ amount increased, Figure 5.17 ii) and iii) indicated there was no significant cross-phosphorylation of either the IKKs or Aurora A under any of the conditions developed suggesting that Aurora A-IKK interactions may not influence either their own kinase function of that of any interacting kinase partner.

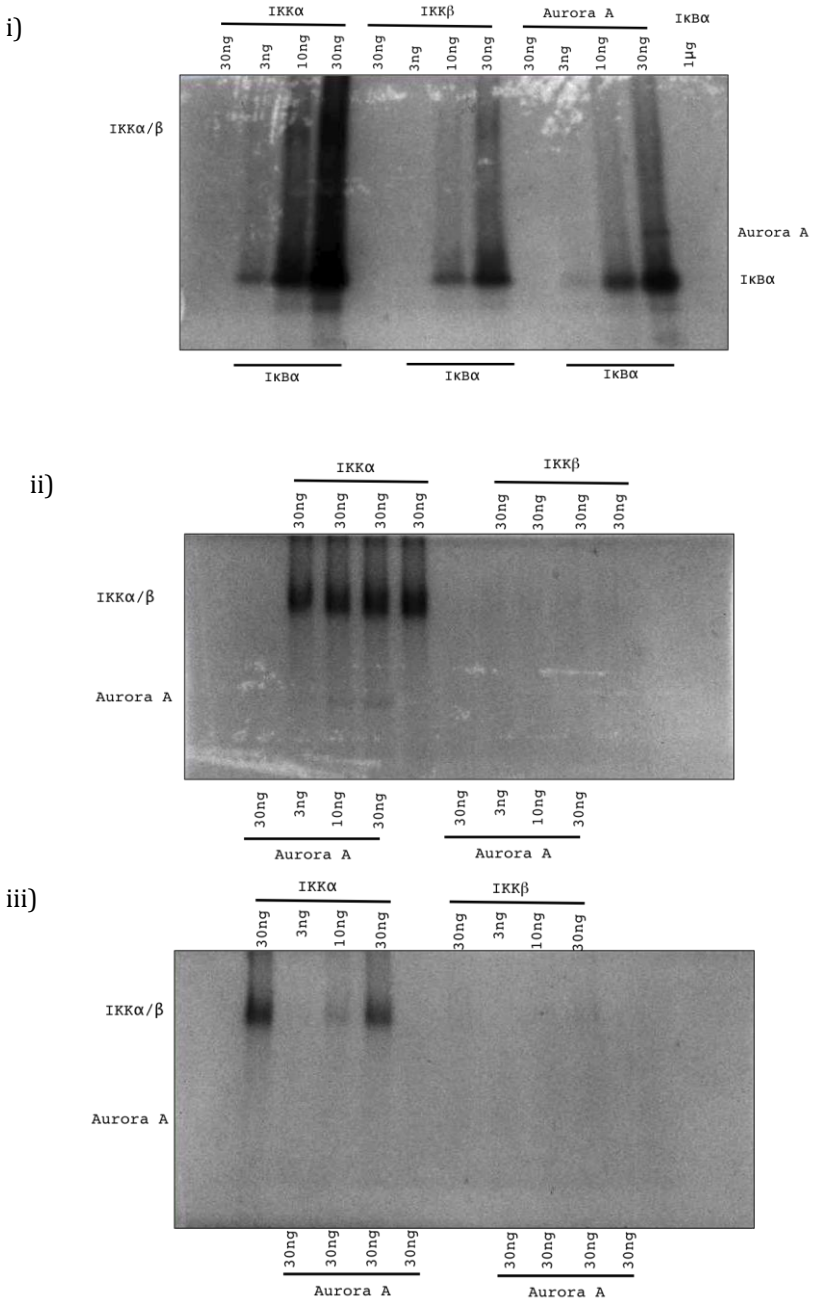

Figure 5.17 Characterisation of Aurora A as a substrate of IKKα/β

In vitro kinase assays were carried out using specified amounts of recombinant His-IKKs and His-Aurora A enzymes with 50μM ATP/3μCi ^{32}P-ATP and activity assessed by incorporation of ^{32}P-ATP into substrate visualised by autoradiography. i) IKKα, IKKβ and Aurora A activity assessed by incubation with 1μg recombinant GST-IκBαN ii) IKK phosphorylation of Aurora A assessed with static concentration of IKK enzymes (30ng) and Aurora A (3, 10, 30ng) iii) IKK phosphorylation of Aurora A assessed using variable concentrations of IKK proteins (3, 10, 30ng) and constant Aurora A protein (30ng). All experiments constructed with enzyme alone controls to assess auto-phosphorylation.

5.5 Discussion

The aims of this chapter were to further assess the interaction of Aurora A and IKKα/β, specifically to investigate the role of the IKK NBD as this was identified in Chapter 3, Figure 3.1 as one of two potential interacting regions, the other being the IKK kinase domains. The focus of this chapter in examining protein-protein interactions was on the NBD as this region is a well characterised protein-protein binding site for the scaffolding of the IKK complex (*May et al, 2000, May et al, 2002, Rushe et al. 2008*). It has also been identified as a potential multi-protein binding site (*Higashimoto et al 2008*). With the identified interaction and binding of Aurora A to this domain it developed the theme of the NBD functioning as a multi-protein site further and therefore was investigated by means of both theoretical (*in silico*) and experimental investigations.

5.5.1 Modelling of IKKα/β NBD with Aurora A

The use of rigid bound docking algorithms allowed the further investigation of the potential binding sites identified by experimental means *in silico* in association with the use of crystallographic information. Using the crystal structures identified in the literature for the NEMO binding domains of both IKKα/IKKβ (*Rushe et al, 2008*) and the full structure of Aurora A bound to TPX2 fragments (*Bayliss et al, 2003*) it was possible to identify several potential regions where IKKα/β-Aurora A interactions maybe occurring. In Chapter 3 (Figure 3.4) it was identified that IKKβ was interacting with amino acids within the kinase domain of Aurora A and the binding site was overlapping with those regions identified as TPX-2 binding sites as reported by *Bayliss et al* (*2003*). The docking was therefore targeted to the amino acid regions of Aurora A identified in Chapter 3; Figure 3.4) as the IKKβ binding sites on Aurora A. The docking simulation showed that the binding of both IKKα and IKKβ NBDs closely aligned with the binding sites of TPX2, particularly the N-terminal fragment comprising residues 6-21 of TPX2. No poses of the NBD peptide comparable to the C-terminal fragment of TPX2 were observed. This was an interesting observation as it is the C-terminal fragment of TPX2 that induces a conformational change in Aurora A which protects the phosphorylated

residue threonine 288 essential for activation of Aurora A (*Bayliss et al, 2003*). This suggests that the NBD of the IKKs are not acting by this mechanism. The poses identified for IKK NBD and Aurora A binding were however closely aligned to the N-terminal fragment of TPX2 which is the site that orientates correctly the TPX2 protein for binding, therefore the binding of the NBDs at this site may act to disrupt the binding of TPX2. This in turn could prevent the conformational change in Aurora A which protects the threonine 288 residue from de-phosphorylation PP1 and prevents Aurora A degradation.

The use of rigid body docking can give a limited understanding of potential sites of binding however it does not account for the flexibility of proteins which is a possible reason for the NBD/TPX2 sequences not aligning fully if they are in fact binding at the same sites. The use of more complex calculations to account for the protein flexibility are possible but outwith the time-frame of this project, however the outcomes of the molecular modelling to date provide promising indications that the sites depicted may identify potentially the biologically relevant sites of interaction. This technique was also limited in the assessment of IKK/Aurora A binding as there is no full-length IKK crystal structures available which include the NBD and therefore it is not possible to determine how the rest of the IKK protein structure may orientate or effect the docking of these two proteins. The residues identified in the structure for docking in this model were almost identical with the only difference being the presence of phenylalanine (734) of IKKβ versus the presence of a methionine (736) residue in a similar position in the IKKα. These residues both possess hydrophobic side chains and this may account for the similarities in poses identified for the docking, however small differences were still observed in the orientations. If the docking model was further refined and more residues for docking on both IKKα and IKKβ structures were included it may be possible to differentiate further how the two subunits may interact at this site. The structural analysis of Aurora A and IKK binding however will never be fully resolved without the co-crystallisation of these proteins and/or co-crystallisation of Aurora A with the NBD peptides. This however was beyond the scope of this project but would be an interesting avenue to pursue.

5.5.2 Functional outcomes of disrupting Aurora A/IKK interactions.

Using SERS and the immobilisation of the NBD CPPs on a functionalised nanohole array it was possible to show that the interaction of Aurora A with these peptides was occurring differentially with a greater level of binding observed with the NBD WT CPP compared to the NBD MT CPP. Although some binding was still observed between the NBD MT CPP and Aurora A this may be due to non-specific interactions of Aurora A and the functionalised surface due to high pI of Aurora A which would result in it being overall positively charged under the established assay conditions and this may lead to binding with the negatively charged functionalised surface. Alternatively, the total ablation of binding was not observed as the NBD MT peptide still contained the phenylalanine residue prior to the NBD which may play a role in the interaction of Aurora A as it does with the IKK proteins (*Rushe et al, 2008*) although it has not been identified as critical for the interaction this may be enough to mediate binding in this setting. The buffer conditions for Aurora A also were not ideal and may have led to a decrease in activity of the protein and may have led to the low levels of discrimination observed between the two peptides also. This was ultimately a proof of concept experiment used to determine if differences in Aurora A binding could be observed with the two NBD CPP peptides, however this assay could be with further optimisation developed into a screening assay to investigate further the characteristics of the NBD/Aurora A interactions.

The peptides were formulated with a cell membrane transduction sequence so that the effects of treatment with this peptide and the effect of disrupting Aurora A/IKK binding in this region could be assessed as seen in Section 5.4.1 . Upon treatment of cells, the NBD WT CPP was observed to have significant effects on Aurora A phosphorylation and to some extent expression whilst the NBD MT CPP had none. The NBD CPPs were tested against classical IKK function to prove their activity and they showed the same profile of inhibition, e.g. inhibiting TNFα-stimulated p65 Ser^{536} phosphorylation in a concentration-dependent manner, similar to that reported previously in the literature (*May et al, 2000, Dai et al, 2004, Gaurnier-Hausser et al 2011*). It was observed initially that NBD WT CPP induced the degradation of Aurora A in an asynchronous cell population in a concentration -dependent manner independently of agonist stimulation. To investigate the mechanism by which this degradation was occurring experiments using a proteasome inhibitor, MG132, were carried out however the

results were inconsistent and thus no conclusions could be drawn (data not shown) though the degradation of Aurora A by a ubiquitin-linked mechanism has been reported previously (*Crane et al, 2004; Irelan et al, 2007*). Irrespective, the effect of the NBD WT CPP on Aurora A expression and its degradation was quite profound however as Aurora A is not highly expressed nor active in the any of the cell cycle phases except G_2./M phase it was essential to investigate the effects of the peptide on a synchronised cell population where Aurora A would be highly active and expressed. Nocodazole was used in the synchronisation of the cells at pro-metaphase (Section 5.4.2) and experiments were carried out to show the effect of the CPP on the synchronised cells. The effect of treatment of cells released from the nocadazole 'trap' with the NBD WT CPP was even more striking. The NBD WT CPP was observed to induce to significant de-phosphorylation and degradation of Aurora A. It was also observed in parallel to reduce Aurora B and C phosphorylation. By means of FACS the effect of the peptide on cell cycle progression was assessed and observed to induce a catastrophic arrest of the cells with a clear accumulation of cells in S-phase and G_2/M phase. This effect occurred in a concentration-dependent manner. This is a novel observation as the NBD WT CPP has previously only been considered in the context of NF-κB signalling and this finding supports a novel role for the NBD and it's perturbation in the context of Aurora A signalling and highlights a potential novel interaction to exploit in the development of therapeutics. The observation that the NBD WT CPP also induced the de-phosphorylation of Aurora B and Aurora C (Section 5.4.2.2; Figure 5.14) corresponds to the findings of Chapter 3 in that IKKβ was observed to bind to the peptide arrays for all three members of the Aurora kinase family. The NBD WT CPP induced de-phosphorylation of all three of the Aurora kinases can be taken as further evidence that the interactions of IKKβ and the Aurora kinases are being mediated via the IKK NBDs and the Aurora kinase domains and could potentially also be exploited in all three kinases when considering novel drug targets. The cell cycle effects of the NBD WT CPP are also consistent with those observed with the inhibition of the Aurora A kinase (*Wysong et al, 2009*) through the use of MLN8054 a Aurora A specific inhibitor, however it remains to be determined as to whether the NBD WT CPP or related peptides function to modulate Aurora A catalytic activity in a manner similar to MLN8054. In fact, given the suggested site of binding of the NBD peptide with Aurora A this may proceed via an allosteric mechanism that requires further investigation. It does however further support the suggestion that the NBD WT CPP is acting to inhibit Aurora A in the cells in parallel to preventing IKK activation. Further characterisation

of the NBD WT CPP effects on the cell cycle is required with a larger range of concentrations as well as further investigation into the expression/phosphorylation status of other key cell cycle components. Therefore, such analyses are essential to furthering the understanding of how the NBD WT CPP is acting on Aurora A.

To determine if this was an effect of disrupting the IKK/Aurora A interaction or if this was in fact a NBD WT CPP mediated effect the use of alternative methods of perturbing IKK functions were explored. *Prajapati et al* (2006) and *Irelan et al* (2007) have linked Aurora A function to IKKα and IKKβ respectively, showing in the former study that IKKα plays a role in regulating Aurora A activity by direct phosphorylation of threonine 288 and in the latter study IKKβ regulates bipolar spindle assembly by acting as an antagonist for Aurora A during the cell cycle and increasing stability of Aurora A. Both these studies showed the effect of siRNA knock down of IKKβ but with contradictory effects. *Irelan et al* (2006) showed a delay in cell cycle expression whilst Prajapati *et al* (2007) showed no effect with this treatment. However, in the same study by *Prajapati et al* it was shown that IKKα induced a cell cycle arrest and mitotic delay. When this was investigated in the PC3 cells as shown in Section 5.4.3. no effect was observed with the knock-down of either IKKα/β on normal cell cycle progression. This may be due to this being a cell-type specific event that was not recapitulated in the PC3 cells. However, further studies using the siRNA knock-down conditions established with a synchronised population may show or highlight the effect of disrupting the IKK/Aurora A signalling more clearly. Due to time constraints this could not be pursued fully although preliminary experiments showed no effect (data not shown). Alternatively, IKK kinase inhibitors could be utilised for the further characterisation of any cell cycle effects due to the disruption of IKK signalling. It has been identified previously that the IKKβ selective compound BMS-34551 can induce a cell cycle arrest in G_2/M phase and down-regulate the phosphorylation of Aurora A (*Blazkova et al, 2007*). This therefore suggests that disruption of the catalytic activity of the IKKs can induce an arrest. These observations were recapitulated in the PC3 cells with a concentration-dependent delay in progression through mitosis observed (data not shown) however these experiments were incomplete and the effect of BMS-34551 on Aurora A phosphorylation was not investigated in this cell type and must be pursued with BMS-34551 in order to better understand the effect of the NBD WT CPP on Aurora A signalling.

The effect of the NBD WT CPP could also be further investigated with the use of fluorescent microscopy to determine if the NBD WT CPP was localising with Aurora A

during the cell cycle, and also to follow functional outcomes such as multipolar spindles and multi-nucleated cells after cytokinesis which are both characteristic outcomes of Aurora A inhibition.

5.5.3 Aurora A as an IKK substrate

There is limited literature which links Aurora A and the IKKs and therefore it was attempted to recapitulate the findings of *Prajapati et al (2006)* which identified Aurora A as a substrate for IKKα with an *in vitro* recombinant protein kinase assay. The experiments however did not show any direct phosphorylation of Aurora A by IKKα, these experiments were carried out using equivalent amounts of protein which should indicate any cross phosphorylation however none was observed with static concentrations of either IKK or Aurora A. The study which initially showed this cross phosphorylation however used Aurora A in gross excess with the stated amount of Aurora used as 10μg (*Parajapati et al, 2006*), this seems somewhat excessive and this observation may therefore not be wholly accurate. This study suggests that IKKβ has no role in the phosphorylation of Aurora A however a study by *Irelan et al* (*2007*) indicates that Aurora A acts as a substrate for IKKβ, these experiments IKKβ was not observed to have any ability to phosphorylate Aurora A. The findings in Section 5.4.4 suggest that rather than Aurora A acting as a substrate for the IKK complex it may in fact be playing a scaffolding role and consequently regulating function through alternative mechanisms. This could be examined in a cellular setting by the use of catalytically-inactive/dominant-negative forms of the IKKs.

Cross talk between the NF-κB pathway and Aurora A has also been identified with Aurora A able to induce NF-κB activation through the phosphorylation of IκBα in breast cancer (*Briassouli et al, 2007*). This was confirmed *in vitro* in Section 5.4.4; Figure 5.16 i) which has shown the direct phosphorylation of IκBα by Aurora A. The potential of Aurora A mediating cellular IκBα phosphorylation remains to be examined in PC3 cells and if apparent the implications for downstream NFκB activation merits additional investigation.

This observation suggests that Aurora A has alternative functions out-with the cell cycle and also makes Aurora A an even more attractive drug target. The effect of

inhibiting Aurora A function with Aurora kinase inhibitors and the NBD WT CPP on the IκBα phosphorylation and degradation in both the cell and *in vitro* kinase assays is an essential part of understanding the function of the IKK/Aurora A interactions within the cell.

5.6 Conclusions

The results gathered in this chapter suggest that the disruption of Aurora A signalling is induced by the direct interaction of the NBD WT CPP with Aurora A. The molecular modelling ouputs predicted several regions that are highly plausible poses for IKK NBD/Aurora A docking (Section 5.2). This interaction was then confirmed by the use of a novel protein/peptide binding assay which showed the differential binding of Aurora A with both NBD WT CPP and NBD MT CPP, with the levels of NBD WT CPP observed to be higher (Section 5.3). Furthermore, the use of this peptide in a cellular system showed functional outcomes consistent with the inhibition of Aurora A activity/function in the cell (Section 5.4.2). The previously reported roles of the IKKα/β in the cell cycle identified through the use of siRNA knock down were not however recapitulated in this study (Section 5.4.3). In addition Aurora A was not seen to be phosphorylated by IKKα or IKKβ using a recombinant kinase assay system (Section 5.4.4). These results when taken together make a compelling case for the role of the NBD WT CPP interacting with Aurora A and directly affecting Aurora A kinase function; this is a novel observation which may be exploitable in the context of further drug design. There is still a considerable amount of research to be carried out to fully understand the relationship between the IKKs and Aurora A however the findings presented in this chapter strongly suggest that the NBD WT CPP can directly act upon Aurora A and as such may be a very useful pharmacological tool in furthering the understanding of IKK/Aurora signalling.

CHAPTER 6:

GENERAL DISCUSSION

6.0 General Discussion

The relationship between the mitotic kinase Aurora A and the IKK complex remains poorly understood. At the start of this project Aurora A had been proposed as a substrate of IKKa (*Prajapati et al., 2006*) or a target of IKKb-stimulated bTRCP-mediated degradation (Irelan et al., 2007). These studies reported contradictory roles for the IKKs in regulation of Aurora A with respect to functional outcome, identifying contradictory influences of the IKKs on cell cycle/mitotic progression.. Therefore, the clear demonstration of the interaction of these proteins and the functional relationship between these kinases remained to be elucidated clearly. Through the work developed in this study the Aurora A-IKK interactions have been confirmed, the sites of binding and the key residues within them have been identified and the targeting of this interaction with a peptide based strategy has identified novel modulation of Aurora A status that correlated with perturbation of mitotic progression. Each of these outcomes is discussed below.

6.1 Mapping of the IKK-Aurora A interactions.

Although previous studies have proposed interactions between Aurora A and each individual member of the IKK complex, these suggested binding events have only been demonstrated through indirect methods, either through the use of cellular fractionation and immunoprecipitation (*Prajapati et al, 2006*) or through the use of endogenous immunoprecipitation of the IKKs incubated with recombinant Aurora A (*Irelan et al, 2007*). Through the use of peptide arrays, displaying 25-mer peptides derived from both the IKK and Aurora A primary amino acid sequences, it has been possible to confirm a direct interaction of Aurora A with IKKα/β/γ derived peptide sequences and map the interaction to two key regions of IKKα and IKKβ. The first identified region fell in the kinase domain of both IKKα and IKKβ and binding in this region may suggest that either Aurora A can act as a potential substrate or alternatively that the IKKs act in a regulatory/scaffolding manner with regards to Aurora A. The second observed region of interaction fell at the extreme C-termini of both IKKα and IKKβ, and the peptides identified for both IKKα and IKKβ both contained the

homologous NEMO binding domain hexapeptide sequence; L-D-W-S-W-L. This sequence was first characterised by *May et al* (*2002*) as a scaffolding motif for the complexation of IKKα/β with NEMO, then further investigated in crystallographic studies of the NBD and IKK binding by *Rushe et al* (2008). However, more recently, the identification of the central serine of this sequence as a potential PLK1 phosphorylation site has suggested this sequence to play a multifunctional role in IKK signalling (*Higashimoto et al, 2008*). Interestingly PLK1 is known to be activated through phosphorylation by Aurora A mediated by the co-factor Bora and in a negative feedback mechanism induces Bora degradation (*Seki et al, 2008a; Seki et al, 2008b*). This cross association could be mediated through the interactions of these proteins at the NEMO binding domain and potentially be part of a protein cycling mechanism at this site.

The identification of the C-termini regions of both IKKα/β as potential regions of interaction for Aurora A and the fact the identified peptides sequences all contained the NBD hexapeptide further supports the role of the NBD as a multi-protein docking site. The use of alanine scanning and truncation arrays identified that the NBD hexapeptide tryptophans were essential for the binding of Aurora A with both IKKα and IKKβ, with the more C-terminal tryptophan identified as the critical residue. Several other residues were also identified in both IKKα and IKKβ as contributing to the interactions of Aurora A however these were not essential for the interactions but may play a role in differentiating between IKKα and IKKβ or potentially for substrate specific targeting. This therefore highlights the key role the NBD plays in Aurora A binding and supports the idea that the NBD has a greater role that just regulating NEMO binding, acting as a multi-protein docking site with Aurora A. These arrays also highlighted the essential role that the C-terminal extension after the NBD of IKKβ can play in Aurora A binding, this is a region which has not been considered at all in relation of IKK/NEMO binding let alone in the context of alternative binding partners and therefore may constitute an Aurora A specific binding site allowing for the specific targeting of IKKβ/Aurora A interactions over IKKα/Aurora A or IKKβ/NEMO. The use of chimeric constructs of the IKK NBDs using the C-terminal extension of IKKβ in conjunction with the full length IKKα could be pursued to investigate the role of this region in NEMO binding and potentially could modulate the classical functions of the IKKs. These constructs may also give insight into the nature of this regions interactions with Aurora A and other potential substrates of the IKKs.

The binding of IKKβ and an Aurora A/B/C full-length peptide array was also carried out and successfully showed binding of full-length IKKβ protein with peptides derived from all three of the Aurora kinases, although there was no binding of IKKα seen with these arrays. This showed interestingly the interaction of IKKβ and the Aurora kinases to fall within the kinase domains and with significantly overlap with many of the key residues identified as critical for TPX2 binding with Aurora A (*Bayliss et al, 2006*). The confirmation of binding with full length IKKβ and Aurora A in an SPR setup further supported the observation that a direct interaction between these proteins was occurring and suggested that the interactions of IKKβ are not just limited to Aurora A but with Aurora B/C also which remains an entirely novel observation.

This peptide array technique is not without its limitations however; it can only assess binding in a discontinuous manner with the full-length primary amino acid sequences broken up into 25 amino acid peptides. This therefore cannot really confer any secondary structure or account for how the proteins may be folded which can lead to both false positive binding events and also account for potential binding sites unable to be formed. This may account for the lack of interaction between full-length IKKα and the Aurora A/B/C arrays, and could suggest that the interactions observed with Aurora A full-length proteins and the IKKα array were in fact due to homology with IKKβ as these two subunits share 52% sequence homology. Alternatively, the non-continuous nature of the peptide arrays may have led to the binding site of Aurora A being improperly folded and therefore not recognised by IKKα.

The identification of the NBD as a potential interaction site for Aurora A is a completely novel observation and supports the role of the NBD as a multi-protein docking site. However there are considerably more identified sites of binding on both the IKKα/β arrays when overlaid with Aurora A recombinant protein and with IKKβ recombinant proteins overlaid on the full length Aurora A/B/C arrays. These identified sites may all represent potential targets to disrupt IKK/Aurora binding and could therefore be further investigated with alanine scanning and truncation arrays.

The interaction of Aurora A and IKKα/β was confirmed using peptide arrays in a recombinant protein based system and therefore to further evaluate the interactions of Aurora A and IKKα/β a cellular based system was also pursued. Through these experiments in a prostate cancer cell line it was possible to prove the interaction of IKKα and IKKβ with Aurora A endogenously through co-immunoprecipitation, which

has not been observed previously. To further investigate the role of the NBD and its residues and the implication of truncating the IKK C-termini either before or after the NBD in the interaction of Aurora A and the IKK proteins a transient transfection system was set up using the exogenous expression of Aurora A and IKKβ NBD mutants. This facet of the study however showed significant problems, with non-specific interactions of the exogenously expressed proteins with the antibody support structure (Protein-G sepharose beads) in the immunoprecipitation and as such made the interpretation of any interactions and the relative importance of the mutated residues impossible. These are key experiments for the further understanding of the IKK/Aurora A interactions and as such it is imperative that alternative strategies for immunoprecipitation are investigated such as through the use of magnetic beads as the antibody support structure instead of agarose/sepharose beads. This may reduce the non-specific interactions as magnetic beads may have differential surface charge or alternatively may be a smoother surface compared to the rougher agarose/sepharose bead structures.

The lack of success in investigating the interactions through the use of immunoprecipitation therefore led to alternative methods being utilised to prove Aurora A/IKK full-length protein binding. Therefore biophysical methods were pursued to further the understanding of these interactions.

6.2 Analysis of IKK/Aurora A interactions by SPR.

The use of SPR to characterise cellular interactions has been well established and with this technique it was possible to prove a direct interaction of recombinant full-length IKKα and IKKβ with a full-length form of Aurora A. This was a novel observation as it illustrated direct binding interactions of the IKKs and Aurora A. Previous reports in the literature both utilised indirect binding methodologies such as co-immunoprecipitation from centrosomal fractions (*Prajapati et al, 2006*) or in association with recombinant protein (*Irelan et al, 2007*). The further investigation of Aurora A and IKKα/β binding kinetics also provided novel insight into the nature, and in part the relative affinities, of these interactions. It was observed that IKKα and IKKβ showed divergent kinetic profiles in regards to the interactions with Aurora A. Although it was not possible to

accurately calculate the K_D values for these interactions due to the poor fitting to a 1:1 binding model, approximate values for the affinity of binding were calculated for IKKα/β and these values were in the low nanomolar range indicating a very strong interaction of Aurora A and the IKKs. Furthermore, these values were comparable to the K_D values calculated for the IKKβ/NEMO interaction (*Lo et al, 2008*). The kinetic profiles of binding differed substantially between the two subunits with IKKα exhibiting a more transient interaction profile with a very fast on- rate and also off-rate, fitting with the observations by *Prajapati et al* (2006) that Aurora A acts as a substrate for IKKα as the interactions mediating post-translational modifications are likely to be transient. This fast on- and off-rate may also explain why it was not possible to observe interactions of IKKα and Aurora A with the peptide arrays as the interactions were transient and over time removed. One strategy to examine this further may be the pursuit of potential Aurora A phosphorylation experiments on the peptide arrays to investigate any IKKα/β-mediated phosphorylation of Aurora A, although evidence from *in vitro* phosphorylation experiments suggested that the IKKs did not phosphorylate Aurora A significantly in the test tube. The kinetic profile of IKKβ on the other hand was far slower with on-rate 5 orders of magnitude slower than IKKα with a considerably slower off-rate also. This profile suggests that this interaction may potentially be mediating a more regulatory role.

The studies carried out using SPR provide completely novel information on the interactions of IKKα/β with Aurora A and gave considerable insight into the potential kinetics of these interactions. However, there is yet more optimisation required prior to establishing definitive K_D values and 100% accurate k_a and k_d values. The use of tags to orientate Aurora A to give a homologous ligand surface and also a better understanding of IKK dimerisation would also help inform and allow more complex modelling of these interactions and so enable more accurate kinetic evaluation of these interactions. The use of complimentary biophysical techniques such as isothermal calorimetry and multi-angled light scattering could also be used in the pursuit of better understanding the relationships between the IKKs and Aurora A and provide more accurate assessment of the binding affinities.

The use of NBD CPPs in SPR was also attempted although due to poor solubility of these peptides when used as an analyte no analysis of the interactions with Aurora A was possible. Through the use of longer peptide sequences or tagged peptides to aid solubility the binding of the NBD and the critical residues required for Aurora A

binding could be used in this assay. The use of the NBD CPPs however as a pharmacological tool in prostate cancer cells (PC3) was utilised in the investigation of this region as a potential interaction site with Aurora A.

6.3 Characterisation of the functional outcomes associated with treatment of Prostate cancer cells with the NBD WT CPP.

The interactions of Aurora A and the IKK proteins was shown through the use of recombinant proteins in SPR (Chapter 4), this interaction was mapped by peptide arrays to be mediated by the NBD of the IKKs to a region of the kinase domain of Aurora A analogous to and encompassing the identified binding sites for TPX2. The potential for IKKα and IKKβ NBD interactions with Aurora A around the TPX2 binding region was therefore assessed through the use of rigid body docking methods. This illustrated that there was several possible alignments of both IKKα and IKKβ interactions with Aurora A binding closely to the TPX2 binding sites which suggested that the NBDs of the IKKs can hypothetically bind to Aurora A in the same region as TPX2. The direct interactions of the IKK NBDs with Aurora A were subsequently confirmed through the use of SERS based nanohole array assay which established a significantly higher level of binding of the NBD WT CPP when compared to the NBD MT CPP identifying the NBD tryptophans as fact critical for the IKK/Aurora A interaction.

Through several methods the IKK NBDs were identified as potential sites of binding and through the use of peptide based strategies was further investigated. Fortuitously the use of NBD CPPs has been well characterised as a pharmacological tool for the inhibition of NF-κB signalling (*May et al, 2000; Baima et al, 2010*) and therefore could be utilised to further inform on the effects of disrupting IKK/Aurora A interactions. The effect of treatment of the PC3 cells with the NBD WT CPP was striking, showing a significant effect on the phosphorylation status of Aurora A in mitosis and also induced a significant level of degradation of Aurora A in an asynchronous population as well as in synchronised cells. The effect of the NBD WT CPP was also shown to induce a severe arrest of the cells in the cell cycle, although it was not possible to determine through these assays if these effects were due to a direct interaction of the NBD WT CPP and Aurora A or through the disruption of IKK/NEMO binding. When these results were

taken in conjunction with previous findings from the peptide arrays and nano-hole arrays that both indicate that a direct interaction of the NBD WT CPP was occurring, the NBD WT CPP can be identified as potentially acting to directly inhibit Aurora A signalling. Further experiments to clarify whether these peptide-mediated effects upon Aurora A were direct or indirect rely on the pursuit of studies in murine embryonic fibroblasts (MEFs) with variable IKK backgrounds. Ideally CPP-based experiments would be pursued in double IKK knockout MEFs to determine the effect of the CPPs on Aurora A and other members of the Aurora kiase family are recapitulated in a null-IKKα/β background and this is being developed in the laboratory presently. Furthermore, IKKα or IKKβ-deficient MEFs reconstituted with IKKα ΔNBD or IKKβ ΔNBD have also been secured however a MEF line with both IKKα and β reconstituted with both IKKα/β in ΔNBD forms have not as yet been established, though this is being pursued in association with Dr. M. May presently. A MEF background with this phenotype will be invaluable in informing on the importance of the IKK NBD and the cellular effects of the CPPs on Aurora A signalling.

The interaction of IKKβ and Aurora A was shown to be occurring in the TPX2 binding region of Aurora A or regions very similar in Chapter 3 and the rigid docking model also identified the IKK NBD to potentially bind in the same regions as TPX2 (Chapter 5). The potential disruption of the TPX2-Aurora A interaction may be the mechanism by which the NBD WT CPP is acting to induce the de-phosphorylation and degradation of Aurora A. However to validate this mechanism of action of the peptide it is required to further investigate the nature of the effects of NBD WT CPP treatment through the use of co-immunoprecipitation studies to determined if the NBD WT CPP peptide disrupts Aurora A/TPX2 binding or the association/disassociation of PP2A, the protein phosphatase which regulates Aurora A degradation (*Horn et al, 2007*). The further investigation of IKK/Aurora A signalling can also be pursued though the use of IKK kinase inhibitors or through the use of siRNA knock-down of the IKK proteins which could further inform on whether these effects were mediated through inhibition of IKK signalling. Although the siRNA knock down of the IKKs in this study showed no effect on cell cycle progression further characterisation with synchronous populations of cells is required to fully assess the effects of loss of the IKKs on the cell cycle. *Prajapati et al* (2006) and *Irelan et al* (2007) both showed siRNA knock-down of the IKKs induced mitotic delay and inhibition of cell cycle progression in HeLa cells. However, again, these studies are contradictory of each other with regard to the relative importance of

each IKK subunit. Therefore, it is difficult to speculate on the effects that siRNA knockdown may have in the PC3 cells and subsequently the effects the global reduction of IKK levels may have on Aurora A signalling.

These two studies also showed that Aurora A can act as an IKK substrate *in vitro* but again the conclusions they presented are contradictory with *Prajapati et al* (*2006*) suggesting Aurora A can act as substrate for IKKα and not IKKβ however *Irelan et al* (*2007*) showed that a constitutively active form of IKKβ can stimulate phosphorylation of Aurora A. These observations were once again not recapitulated in this study.

6.4 Therapuetic potential in the targeting of Aurora A-IKK interactions.

Throughout this study it has been shown that the IKK NBD is a potential binding site for the Aurora A/IKK interactions and through the use of an IKK NBD CPP it has been possible to identify novel functionality of this pharmacological tool in Aurora A inhibition and potentially Aurora B/C also. The drug development strategies targeting the IKKs and Aurora A are currently focussed on the either kinase domain/ATP-competitive inhibitors and those focussed upon Aurora A are failing in the clinical environment. Therefore, the re-purposing of the IKK NBD CPP as an Aurora A inhibitor through either direct inhibition of TPX2 binding or through an indirect mechanism of IKK inhibition may serve as an attractive strategy for the development of peptide based disruptors. The development of these peptides as Aurora A specific inhibitors and divergence of their functions by iterative development away from NEMO binding and Aurora B/C effects will require the development of stringent binding assays to investigate the relative importance of each residue of the NBD in relation to Aurora A/B/C binding alongside NEMO. A recent study of NBD interactions with IKKβ uses extensive computational analysis alongside a fluorescent anisotropy assay to investigate 'hot spots' that mediate NEMO binding with IKKβ at the NBD (*Golden et al, 2013*), which could be similarly applied to Aurora A. Fluorescent polarisation or FRET-based assays will also be useful as screening methods to effectively investigate the relative importance of individual residues of the IKK C-terminii to discriminate binding between Aurora A and NEMO and potentially also between Aurora A/B/C.

To date, there is a dearth of treatments available for prostate cancers, particularly in the latter stages of the advanced disease. This study has potentially identified the NBD CPP as a 'hit' to take forward in the targeting of allosteric binding sites of Aurora A and the IKKs and this therefore may provide the basis for the development of peptidomimetics and small molecule disruptors to provide ultimately novel therapeutics for prostate cancer. This could potentially be applicable to other cancer/tumour settings beyond the prostate, which display over-expression or constitutively active Aurora A and B.

REFERENCES

Abdollah, F., J. Schmitges, M. Sun, C. Jeldres, Z. Tian, A. Briganti, S.F. Shariat, P. Perrotte, F. Montorsi, and P.I. Karakiewicz. 2012. Comparison of mortality outcomes after radical prostatectomy versus radiotherapy in patients with localized prostate cancer: a population-based analysis. *Int J Urol*. 19:836-844; author reply 844-835.

Abe, Y., M. Ohsugi, K. Haraguchi, J. Fujimoto, and T. Yamamoto. 2006. LATS2-Ajuba complex regulates γ-tubulin recruitment to centrosomes and spindle organization during mitosis. *FEBS Letters*. 580:782-788.

Aggarwal, S., Y. Takada, S. Singh, J.N. Myers, and B.B. Aggarwal. 2004. Inhibition of growth and survival of human head and neck squamous cell carcinoma cells by curcumin via modulation of nuclear factor-kappaB signaling. *Int J Cancer*. 111:679-692.

Agnese, V., V. Bazan, F. Fiorentino, D. Fanale, G. Badalamenti, G. Colucci, V. Adamo, D. Santini, and A. Russo. 2007. The role of Aurora-A inhibitors in cancer therapy. *Annals of Oncology*. 18:vi47-vi52.

Agou, F. 2004. Inhibition of NF- κB Activation by Peptides Targeting NF- κB Essential Modulator (NEMO) Oligomerization. *Journal of Biological Chemistry*. 279:54248-54257.

Agou, F., G. Courtois, J. Chiaravalli, F. Baleux, Y.M. Coic, F. Traincard, A. Israel, and M. Veron. 2004. Inhibition of NF-kappa B activation by peptides targeting NF-kappa B essential modulator (nemo) oligomerization. *J Biol Chem*. 279:54248-54257.

Albright, F., C. Teerlink, T. Werner, and L. Cannon-Albright. 2012. Significant evidence for a heritable contribution to cancer predisposition: a review of cancer familiality by site. *BMC Cancer*. 12:138.

Andrade, P., M.M. Brites, R. Vieira, A. Mariano, J.P. Reis, O. Tellechea, and A. Figueiredo. 2012. Epidemiology of basal cell carcinomas and squamous cell carcinomas in a Department of Dermatology: a 5 year review. *An Bras Dermatol*. 87:212-219.

Andrews, P.D., Y. Ovechkina, N. Morrice, M. Wagenbach, K. Duncan, L. Wordeman, and J.R. Swedlow. 2004. Aurora B Regulates MCAK at the Mitotic Centromere. *Developmental Cell*. 6:253-268.

Annunziata, C.M., R.E. Davis, Y. Demchenko, W. Bellamy, A. Gabrea, F. Zhan, G. Lenz, I. Hanamura, G. Wright, W. Xiao, S. Dave, E.M. Hurt, B. Tan, H. Zhao, O. Stephens, M. Santra, D.R. Williams, L. Dang, B. Barlogie, J.D. Shaughnessy Jr, W.M. Kuehl, and L.M. Staudt. 2007. Frequent Engagement of the Classical and Alternative NF-κB Pathways by Diverse Genetic Abnormalities in Multiple Myeloma. *Cancer Cell*. 12:115-130.

Avo Santos, M., C. van de Werken, M. de Vries, H. Jahr, M.J.M. Vromans, J.S.E. Laven, B.C. Fauser, G.J. Kops, S.M. Lens, and E.B. Baart. 2011. A role for Aurora C in the chromosomal passenger complex during human pre-implantation embryo development. *Human Reproduction*. 26:1868-1881.

Baima, E.T., J.A. Guzova, S. Mathialagan, E.E. Nagiec, M.M. Hardy, L.R. Song, S.L. Bonar, R.A. Weinberg, S.R. Selness, S.S. Woodard, J. Chrencik, W.F. Hood, J.F. Schindler, N. Kishore, and G. Mbalaviele. 2010. Novel Insights into the Cellular Mechanisms of the Anti-inflammatory Effects of NF-κB Essential Modulator Binding Domain Peptides. *Journal of Biological Chemistry*. 285:13498-13506.

Bakkar, N., J. Wang, K.J. Ladner, H. Wang, J.M. Dahlman, M. Carathers, S. Acharyya, M.A. Rudnicki, A.D. Hollenbach, and D.C. Guttridge. 2008. IKK/NF-κB regulates skeletal myogenesis via a signaling switch to inhibit differentiation and promote mitochondrial biogenesis. *The Journal of Cell Biology*. 180:787-802.

Bancroft, C.C., Z. Chen, J. Yeh, J.B. Sunwoo, N.T. Yeh, S. Jackson, C. Jackson, and C. Van Waes. 2002. Effects of pharmacologic antagonists of epidermal growth factor receptor, PI3K and MEK signal kinases on NF-κB and AP-1 activation and IL-8 and VEGF expression in human head and neck squamous cell carcinoma lines. *International Journal of Cancer*. 99:538-548.

Barr, A.R., and F. Gergely. 2007. Aurora-A: the maker and breaker of spindle poles. *J Cell Sci*. 120:2987-2996.

Bayliss, R., T. Sardon, I. Vernos, and E. Conti. 2003. Structural Basis of Aurora-A Activation by TPX2 at the Mitotic Spindle. *Molecular Cell*. 12:851-862.

Becker, C., M.C. Fantini, C. Schramm, H.A. Lehr, S. Wirtz, A. Nikolaev, J.r. Burg, S. Strand, R. Kiesslich, S. Huber, H. Ito, N. Nishimoto, K. Yoshizaki, T. Kishimoto, P.R. Galle, M. Blessing, S. Rose-John, and M.F. Neurath. 2004. TGF-β Suppresses Tumor Progression in Colon Cancer by Inhibition of IL-6 trans-Signaling. *Immunity*. 21:491-501.

Beinke, S., M.J. Robinson, M. Hugunin, and S.C. Ley. 2004. Lipopolysaccharide Activation of the TPL-2/MEK/Extracellular Signal-Regulated Kinase Mitogen-Activated Protein Kinase Cascade Is Regulated by IκB Kinase-Induced Proteolysis of NF-κB1 p105. *Molecular and Cellular Biology*. 24:9658-9667.

Berggård, T., S. Linse, and P. James. 2007. Methods for the detection and analysis of protein–protein interactions. *PROTEOMICS*. 7:2833-2842.

Beutling, U., K. Stading, T. Stradal, and R. Frank. 2008. Large-scale analysis of protein-protein interactions using cellulose-bound peptide arrays. *Adv Biochem Eng Biotechnol*. 110:115-152.

Bibby, R.A., C. Tang, A. Faisal, K. Drosopoulos, S. Lubbe, R. Houlston, R. Bayliss, and S. Linardopoulos. 2009. A Cancer-associated Aurora A Mutant Is Mislocalized and Misregulated Due to Loss of Interaction with TPX2. *Journal of Biological Chemistry*. 284:33177-33184.

Bird, A.W., and A.A. Hyman. 2008. Building a spindle of the correct length in human cells requires the interaction between TPX2 and Aurora A. *The Journal of Cell Biology*. 182:289-300.

Bischoff, J.R., L. Anderson, Y. Zhu, K. Mossie, L. Ng, B. Souza, B. Schryver, P. Flanagan, F. Clairvoyant, C. Ginther, C.S.M. Chan, M. Novotny, D.J. Slamon, and G.D. Plowman. 1998. A homologue of Drosophila aurora kinase is oncogenic and amplified in human colorectal cancers. *EMBO J*. 17:3052-3065.

Bishop, J.D., and J.M. Schumacher. 2002. Phosphorylation of the Carboxyl Terminus of Inner Centromere Protein (INCENP) by the Aurora B Kinase Stimulates Aurora B Kinase Activity. *Journal of Biological Chemistry*. 277:27577-27580.

Blackwell, N.M., P. Sembi, J.S. Newson, T. Lawrence, D.W. Gilroy, and P.S. Kabouridis. 2004. Reduced infiltration and increased apoptosis of leukocytes at sites of inflammation by systemic administration of a membrane-permeable IkappaBalpha repressor. *Arthritis Rheum*. 50:2675-2684.

Blazkova, H., C. von Schubert, K. Mikule, R. Schwab, N. Angliker, J. Schmuckli-Maurer, P.C. Fernandez, S. Doxsey, and D.A. Dobbelaere. 2007. The IKK Inhibitor BMS-345541 Affects Multiple Mitotic Cell Cycle Transitions. *Cell Cycle*. 6:2531-2540.

Bolanos-Garcia, V.M. 2005. Aurora kinases. *The International Journal of Biochemistry & Cell Biology*. 37:1572-1577.

Bonanno, L., A. Jirillo, and A. Favaretto. 2011. Mechanisms of acquired resistance to epidermal growth factor receptor tyrosine kinase inhibitors and new therapeutic perspectives in non small cell lung cancer. *Curr Drug Targets*. 12:922-933.

Bonifacino, J.S., E.C. Dell'Angelica, and T.A. Springer. 2001. Immunoprecipitation. *In* Current Protocols in Molecular Biology. John Wiley & Sons, Inc.

Bonizzi, G., and M. Karin. 2004. The two NF-κB activation pathways and their role in innate and adaptive immunity. *Trends in Immunology*. 25:280-288.

Booth, D.G., F.E. Hood, I.A. Prior, and S.J. Royle. 2011. A TACC3/ch-TOG/clathrin complex stabilises kinetochore fibres by inter-microtubule bridging. *EMBO J*. 30:906-919.

Boss, D.S., J.H. Beijnen, and J.H.M. Schellens. 2009. Clinical Experience with Aurora Kinase Inhibitors: A Review. *The Oncologist*. 14:780-793.

Bremner, P., and M. Heinrich. 2002. Natural products as targeted modulators of the nuclear factor-kappaB pathway. *J Pharm Pharmacol*. 54:453-472.

Briassouli, P., F. Chan, K. Savage, J.S. Reis-Filho, and S. Linardopoulos. 2007. Aurora-A Regulation of Nuclear Factor- κB Signaling by Phosphorylation of IκB *Cancer Research*. 67:1689-1695.

Brown, J.R., K.K. Koretke, M.L. Birkeland, P. Sanseau, and D.R. Patrick. Evolutionary relationships of Aurora kinases: implications for model organism studies and the development of anti-cancer drugs 2004. *BMC Evolutionary Biology*. 4:39.

Bubici, C., S. Papa, K. Dean, and G. Franzoso. 2006. Mutual cross-talk between reactive oxygen species and nuclear factor-kappa B: molecular basis and biological significance. *Oncogene*. 25:6731-6748.

Burke, J.R., M.A. Pattoli, K.R. Gregor, P.J. Brassil, J.F. MacMaster, K.W. McIntyre, X. Yang, V.S. Iotzova, W. Clarke, J. Strnad, Y. Qiu, and F.C. Zusi. 2003. BMS-345541 is a highly selective inhibitor of I kappa B kinase that binds at an allosteric site of the enzyme and blocks NF-kappa B-dependent transcription in mice. *J Biol Chem*. 278:1450-1456.

Cancilla, M.T., M.M. He, N. Viswanathan, R.L. Simmons, M. Taylor, A.D. Fung, K. Cao, and D.A. Erlanson. 2008. Discovery of an Aurora kinase inhibitor through site-specific dynamic combinatorial chemistry. *Bioorganic & Medicinal Chemistry Letters*. 18:3978-3981.

Cao, Y., G. Bonizzi, T.N. Seagroves, F.R. Greten, R. Johnson, E.V. Schmidt, and M. Karin. 2001. IKKα Provides an Essential Link between RANK Signaling and Cyclin D1 Expression during Mammary Gland Development. *Cell*. 107:763-775.

Cao, Y., J.-l. Luo, and M. Karin. 2007. IκB kinase α kinase activity is required for self-renewal of ErbB2/Her2-transformed mammary tumor-initiating cells. *Proceedings of the National Academy of Sciences*. 104:15852-15857.

de Paula Careta, F., S. Gobessi, R.A. Panepucci, E. Bojnik, F. Morato de Oliveira, D. Mazza Matos, R.P. Falcao, L. Laurenti, M.A. Zago, and D.G. Efremov. 2012. The Aurora A and B kinases are up-regulated in bone marrow-derived chronic lymphocytic leukemia cells and represent potential therapeutic targets. *Haematologica*. 97:1246-1254.

Carmena, M., and W.C. Earnshaw. 2003. The cellular geography of Aurora kinases. *Nat Rev Mol Cell Biol*. 4:842-854.

Carmena, M., S. Ruchaud, and W.C. Earnshaw. 2009. Making the Auroras glow: regulation of Aurora A and B kinase function by interacting proteins. *Current Opinion in Cell Biology*. 21:796-805.

Carter, B.S., T.H. Beaty, G.D. Steinberg, B. Childs, and P.C. Walsh. 1992. Mendelian inheritance of familial prostate cancer. *Proceedings of the National Academy of Sciences*. 89:3367-3371.

Carvajal, R.D., A. Tse, and G.K. Schwartz. 2006. Aurora Kinases: New Targets for Cancer Therapy. *Clinical Cancer Research*. 12:6869-6875.

Castro, A.C., L.C. Dang, F. Soucy, L. Grenier, H. Mazdiyasni, M. Hottelet, L. Parent, C. Pien, V. Palombella, and J. Adams. 2003. Novel IKK inhibitors: beta-carbolines. *Bioorg Med Chem Lett*. 13:2419-2422.

Catley, M.C., M.B. Sukkar, K.F. Chung, B. Jaffee, S.-M. Liao, A.J. Coyle, E.-B. Haddad, P.J. Barnes, and R. Newton. 2006. Validation of the Anti-Inflammatory Properties of Small-Molecule IŒ∫B Kinase (IKK)-2 Inhibitors by Comparison with Adenoviral-Mediated Delivery of Dominant-Negative IKK1 and IKK2 in Human Airways Smooth Muscle. *Molecular Pharmacology*. 70:697-705.

Chan, C., and D. Botstein. 1993. Isolation and Characterization of Chromosome-Gain and Increase-in-Ploidy Mutants in Yeast. *Genetics*. 135:677-691.

Chapoval, S.P., A. Al-Garawi, J.M. Lora, I. Strickland, B. Ma, P.J. Lee, R.J. Homer, S. Ghosh, A.J. Coyle, and J.A. Elias. 2007. Inhibition of NF-kappaB activation reduces the tissue effects of transgenic IL-13. *J Immunol*. 179:7030-7041.

Chariot, A. 2009. The NF-κB-independent functions of IKK subunits in immunity and cancer. *Trends in cell biology*. 19:404-413.

Cheeseman, I.M., J.S. Chappie, E.M. Wilson-Kubalek, and A. Desai. 2006. The Conserved KMN Network Constitutes the Core Microtubule-Binding Site of the Kinetochore. *Cell*. 127:983-997.

Cheetham, G.M., P.A. Charlton, J.M. Golec, and J.R. Pollard. 2007. Structural basis for potent inhibition of the Aurora kinases and a T315I multi-drug resistant mutant form of Abl kinase by VX-680. *Cancer Lett*. 251:323-329.

Chefetz, I., J.C. Holmberg, A.B. Alvero, I. Visintin, and G. Mor. 2011. Inhibition of Aurora-A kinase induces cell cycle arrest in epithelial ovarian cancer stem cells by affecting NF-κB pathway. *Cell Cycle*. 10:2206-2214.

Chen, R., L. Li, and Z. Weng. 2003. ZDOCK: An initial-stage protein-docking algorithm. *Proteins: Structure, Function, and Bioinformatics*. 52:80-87.

Chen, R., and Z. Weng. 2002. Docking unbound proteins using shape complementarity, desolvation, and electrostatics. *Proteins: Structure, Function, and Bioinformatics*. 47:281-294.

Chen, R., and Z. Weng. 2003. A novel shape complementarity scoring function for protein-protein docking. *Proteins: Structure, Function, and Bioinformatics*. 51:397-408.

Chen, W., Z. Li, L. Bai, and Y. Lin. 2011. NF-kappaB in lung cancer, a carcinogenesis mediator and a prevention and therapy target. *Front Biosci*. 16:1172-1185.

Chen, Z.J., L. Parent, and T. Maniatis. 1996. Site-specific phosphorylation of IkappaBalpha by a novel ubiquitination-dependent protein kinase activity. *Cell*. 84:853-862.

Chieffi, P., L. Cozzolino, A. Kisslinger, S. Libertini, S. Staibano, G. Mansueto, G. De Rosa, A. Villacci, M. Vitale, S. Linardopoulos, G. Portella, and D. Tramontano. 2006. Aurora B expression directly correlates with prostate cancer malignancy and influence prostate cell proliferation. *The Prostate*. 66:326-333.

Console, S., C. Marty, C. Garcia-Echeverria, R. Schwendener, and K. Ballmer-Hofer. 2003. Antennapedia and HIV transactivator of transcription (TAT) "protein transduction domains" promote endocytosis of high molecular weight cargo upon binding to cell surface glycosaminoglycans. *J Biol Chem*. 278:35109-35114.

Cooper, S., G. Iyer, M. Tarquini, and P. Bissett. 2006. Nocodazole does not synchronize cells: implications for cell-cycle control and whole-culture synchronization. *Cell and Tissue Research*. 324:237-242.

Crane, R., A. Kloepfer, and J.V. Ruderman. 2004. Requirements for the destruction of human Aurora-A. *Journal of Cell Science*. 117:5975-5983.

Crawford, E.D. 2009. Understanding the Epidemiology, Natural History, and Key Pathways Involved in Prostate Cancer. *Urology*. 73:S4-S10.

Crosio, C., G.M. Fimia, R. Loury, M. Kimura, Y. Okano, H. Zhou, S. Sen, C.D. Allis, and P. Sassone-Corsi. 2002. Mitotic Phosphorylation of Histone H3: Spatio-Temporal Regulation by Mammalian Aurora Kinases. *Molecular and Cellular Biology*. 22:874-885.

D'Amico, A.V., J.W. Denham, J. Crook, M.H. Chen, S.Z. Goldhaber, D.S. Lamb, D. Joseph, K.H. Tai, S. Malone, C. Ludgate, A. Steigler, and P.W. Kantoff. 2007. Influence of Androgen Suppression Therapy for Prostate Cancer on the Frequency and Timing of Fatal Myocardial Infarctions. *Journal of Clinical Oncology*. 25:2420-2425.

Dai, J., B.A. Sullivan, and J.M.G. Higgins. 2006. Regulation of Mitotic Chromosome Cohesion by Haspin and Aurora B. *Developmental Cell*. 11:741-750.

Dai, S., T. Hirayama, S. Abbas, and Y. Abu-Amer. 2004. The IkappaB kinase (IKK) inhibitor, NEMO-binding domain peptide, blocks osteoclastogenesis and bone erosion in inflammatory arthritis. *J Biol Chem*. 279:37219-37222.

Danaei, G., S. Vander Hoorn, A.D. Lopez, C.J.L. Murray, and M. Ezzati. 2005. Causes of cancer in the world: comparative risk assessment of nine behavioural and environmental risk factors. *The Lancet*. 366:1784-1793.

Dar, A.A., A. Belkhiri, and W. El-Rifai. 2009. The aurora kinase A regulates GSK-3beta in gastric cancer cells. *Oncogene*. 28:866-875.

Dasgupta, S., M. Jana, Y. Zhou, Y.K. Fung, S. Ghosh, and K. Pahan. 2004. Anti-neuroinflammatory effect of NF-kappaB essential modifier-binding domain peptides in the adoptive transfer model of experimental allergic encephalomyelitis. *J Immunol*. 173:1344-1354.

Dees, E.C., R.B. Cohen, M. von Mehren, T.E. Stinchcombe, H. Liu, K. Venkatakrishnan, M. Manfredi, H. Fingert, H.A. Burris, and J.R. Infante. 2012. Phase I Study of Aurora A Kinase Inhibitor MLN8237 in Advanced Solid Tumors: Safety, Pharmacokinetics, Pharmacodynamics, and Bioavailability of Two Oral Formulations. *Clinical Cancer Research*. 18:4775-4784.

Denmeade, S.R., and J.T. Isaacs. 2004. Development of prostate cancer treatment: The good news. *The Prostate*. 58:211-224.

Diamond, J.R., S.G. Eckhardt, A.C. Tan, T.P. Newton, H.M. Selby, K.L. Brunkow, M.I. Kachaeva, M. Varella-Garcia, T.M. Pitts, M.R. Bray, G.C. Fletcher, and J.J. Tentler. 2012. Predictive Biomarkers of Sensitivity to the Aurora and Angiogenic Kinase Inhibitor ENMD-2076 in Preclinical Breast Cancer Models. *Clin Cancer Res* 19; 291

Diaz, R., B. Golbourn, M. Shekarforoush, C. Smith, and J. Rutka. 2012. Aurora kinase B/C inhibition impairs malignant glioma growth in vivo. *Journal of Neuro-Oncology*. 108:349-360.

Diaz, R.J., B. Golbourn, M. Shekarforoush, C.A. Smith, and J.T. Rutka. 2012. Aurora kinase B/C inhibition impairs malignant glioma growth in vivo. *Journal of Neuro-Oncology*. 108:349-360.

DiDonato, J.A., F. Mercurio, and M. Karin. 2012. NF-κB and the link between inflammation and cancer. *Immunological Reviews*. 246:379-400.

Ditchfield, C., V.L. Johnson, A. Tighe, R. Ellston, C. Haworth, T. Johnson, A. Mortlock, N. Keen, and S.S. Taylor. 2003. Aurora B couples chromosome alignment with anaphase by targeting BubR1, Mad2, and Cenp-E to kinetochores. *J Cell Biol*. 161:267-280.

Downward, J. 2003. Targeting RAS signalling pathways in cancer therapy. *Nat Rev Cancer*. 3:11-22.

Ducat, D., and Y. Zheng. 2004. Aurora kinases in spindle assembly and chromosome segregation. *Experimental Cell Research*. 301:60-67.

Dutertre, S. 2004. Phosphorylation of CDC25B by Aurora-A at the centrosome contributes to the G2-M transition. *Journal of Cell Science*. 117:2523-2531.

Elkins, J.M., S. Santaguida, A. Musacchio, and S. Knapp. 2012. Crystal Structure of Human Aurora B in Complex with INCENP and VX-680. *Journal of Medicinal Chemistry*. 55:7841-7848.

Ethridge, R.T., K. Hashimoto, D.H. Chung, R.A. Ehlers, S. Rajaraman, and B.M. Evers. 2002. Selective inhibition of NF-kappaB attenuates the severity of cerulein-induced acute pancreatitis. *J Am Coll Surg*. 195:497-505.

Etzioni, R., R. Gulati, A. Tsodikov, E.M. Wever, D.F. Penson, E.A. Heijnsdijk, J. Katcher, G. Draisma, E.J. Feuer, H.J. de Koning, and A.B. Mariotto. 2012. The prostate cancer conundrum revisited: treatment changes and prostate cancer mortality declines. *Cancer*. 118:5955-5963.

Eyers, P.A., E. Erikson, L.G. Chen, and J.L. Maller. 2003. A Novel Mechanism for Activation of the Protein Kinase Aurora A. *Current biology : CB*. 13:691-697.

Feldman, B.J., and D. Feldman. 2001. The development of androgen-independent prostate cancer. *Nat Rev Cancer*. 1:34-45.

Ferchichi, I., S. Sassi Hannachi, A. Baccar, R. Marrakchi Triki, J.Y. Cremet, K. Ben Romdhane, C. Prigent, and A. Ben Ammar El Gaaied. 2013. Assessment of Aurora A kinase expression in breast cancer: a tool for early diagnosis? *Dis Markers*. 34:63-69.

Fernandez-Majada, V., C. Aguilera, A. Villanueva, F. Vilardell, A. Robert-Moreno, A. Aytes, F.X. Real, G. Capella, M.W. Mayo, L. Espinosa, and A. Bigas. 2007. Nuclear IKK activity leads to dysregulated Notch-dependent gene expression in colorectal cancer. *Proceedings of the National Academy of Sciences*. 104:276-281.

Fizazi, K., H.I. Scher, A. Molina, C.J. Logothetis, K.N. Chi, R.J. Jones, J.N. Staffurth, S. North, N.J. Vogelzang, F. Saad, P. Mainwaring, S. Harland, O.B. Goodman Jr, C.N. Sternberg, J.H. Li, T. Kheoh, C.M. Haqq, and J.S. de Bono. 2012. Abiraterone acetate for treatment of metastatic castration-resistant prostate cancer: final overall survival analysis of the COU-AA-301 randomised, double-blind, placebo-controlled phase 3 study. *The Lancet Oncology*. 13:983-992.

Francisco, L., W. Wang, and C.S. Chan. 1994. Type 1 protein phosphatase acts in opposition to IpL1 protein kinase in regulating yeast chromosome segregation. *Molecular and Cellular Biology*. 14:4731-4740.

Frank, R. 2002. The SPOT-synthesis technique. Synthetic peptide arrays on membrane supports--principles and applications. *J Immunol Methods*. 267:13-26.

Friedman, L.S., E.A. Ostermeyer, C.I. Szabo, P. Dowd, E.D. Lynch, S.E. Rowell, and M.-C. King. 1994. Confirmation of BRCA1 by analysis of germline mutations linked to breast and ovarian cancer in ten families. *Nat Genet*. 8:399-404.

Fu, D.H., W. Jiang, J.T. Zheng, G.Y. Zhao, Y. Li, H. Yi, Z.R. Li, J.D. Jiang, K.Q. Yang, Y. Wang, and S.Y. Si. 2008. Jadomycin B, an Aurora-B kinase inhibitor discovered through virtual screening. *Mol Cancer Ther*. 7:2386-2393.

Fu, J., M. Bian, Q. Jiang, and C. Zhang. 2007. Roles of Aurora Kinases in Mitosis and Tumorigenesis. *Molecular Cancer Research*. 5:1-10.

Fukuda, T., Y. Mishina, M.P. Walker, and R.P. DiAugustine. 2005. Conditional Transgenic System for Mouse Aurora A Kinase: Degradation by the Ubiquitin Proteasome Pathway Controls the Level of the Transgenic Protein. *Molecular and Cellular Biology*. 25:5270-5281.

Furukawa, J., H. Miyake, A. Takenaka, I. Hara, and M. Fujisawa. 2007. Persistent expression of Aurora-A after neoadjuvant hormonal therapy as a predictor of a poor clinical outcome in patients undergoing radical prostatectomy for prostate cancer. *BJU International*. 100:310-314.

Gable, A., M. Qiu, J. Titus, S. Balchand, N.P. Ferenz, N. Ma, E.S. Collins, C. Fagerstrom, J.L. Ross, G. Yang, and P. Wadsworth. 2012. Dynamic reorganization of Eg5 in the mammalian spindle throughout mitosis requires dynein and TPX2. *Molecular Biology of the Cell*. 23:1254-1266.

Gamble, C., K. McIntosh, R. Scott, K.H. Ho, R. Plevin, and A. Paul. 2012. Inhibitory kappa B kinases as targets for pharmacological regulation. *British Journal of Pharmacology*. 165:802-819.

Garber, K. 2006. The second wave in kinase cancer drugs. *Nat Biotechnol*. 24:127-130.

Garima Jain, C.V., Anna Tobias, Klaus-Dieter Spindler, Peter Möller, Marcus V Cronauer and Ralf B Marienfeld. 2012. IκB Kinases Modulate the Activity of the Androgen Receptor in Prostate Carcinoma Cell Lines. *Neoplasia*. 14:178–189. .

Gaurnier-Hausser, A., R. Patel, A.S. Baldwin, M.J. May, and N.J. Mason. 2011. NEMO-Binding Domain Peptide Inhibits Constitutive NF- B Activity and Reduces Tumor Burden in a Canine Model of Relapsed, Refractory Diffuse Large B-Cell Lymphoma. *Clinical Cancer Research*. 17:4661-4671.

Gautheron, J., and G. Courtois. 2010. "Without Ub I am nothing": NEMO as a multifunctional player in ubiquitin-mediated control of NF-κB activation. *Cellular and Molecular Life Sciences*. 67:3101-3113.

Gautschi, O., J. Heighway, P.C. Mack, P.R. Purnell, P.N. Lara, and D.R. Gandara. 2008. Aurora Kinases as Anticancer Drug Targets. *Clinical Cancer Research*. 14:1639-1648.

Giet, R., and C. Prigent. 1999. Aurora/Ipl1p-related kinases, a new oncogenic family of mitotic serine-threonine kinases. *Journal of Cell Science*. 112:3591-3601.

Giet, R.g., and D.M. Glover. 2001. Drosophila Aurora B Kinase Is Required for Histone H3 Phosphorylation and Condensin Recruitment during Chromosome Condensation and to Organize the Central Spindle during Cytokinesis. *The Journal of Cell Biology*. 152:669-682.

Gilmore, T.D. 2006. Introduction to NF-κB: players, pathways, perspectives. *Oncogene*. 25:6680-6684.

Girdler, F., F. Sessa, S. Patercoli, F. Villa, A. Musacchio, and S. Taylor. 2008. Molecular Basis of Drug Resistance in Aurora Kinases. *Chemistry & Biology*. 15:552-562.

Gittes, R.F. 1991. Carcinoma of the prostate. *N Engl J Med*. 324:236-245.

Giubettini, M., I.A. Asteriti, J. Scrofani, M. De Luca, C. Lindon, P. Lavia, and G. Guarguaglini. 2010. Control of Aurora-A stability through interaction with TPX2. *Journal of Cell Science*. 124:113-122.

Glover, D.M., M.H. Leibowitz, D.A. McLean, and H. Parry. 1995. Mutations in aurora prevent centrosome separation leading to the formation of monopolar spindles. *Cell*. 81:95-105.

Godinho, S.A., M. Kwon, and D. Pellman. 2009. Centrosomes and cancer: how cancer cells divide with too many centrosomes. *Cancer and Metastasis Reviews*. 28:85-98.

Goh, C.L., F.R. Schumacher, D. Easton, K. Muir, B. Henderson, Z. Kote-Jarai, and R.A. Eeles. 2012. Genetic variants associated with predisposition to prostate cancer and potential clinical implications. *Journal of Internal Medicine*. 271:353-365.

Gomella, L.G., J. Singh, C. Lallas, and E.J. Trabulsi. 2010. Hormone therapy in the management of prostate cancer: evidence-based approaches. *Therapeutic Advances in Urology*. 2:171-181.

Goto, H., Y. Yasui, A. Kawajiri, E.A. Nigg, Y. Terada, M. Tatsuka, K. Nagata, and M. Inagaki. 2003. Aurora-B regulates the cleavage furrow-specific vimentin phosphorylation in the cytokinetic process. *J Biol Chem*. 278:8526-8530.

Gringhuis, S.I., J.J. Garcia-Vallejo, B. van Het Hof, and W. van Dijk. 2005. Convergent actions of I kappa B kinase beta and protein kinase C delta modulate mRNA stability through phosphorylation of 14-3-3 beta complexed with tristetraprolin. *Mol Cell Biol*. 25:6454-6463.

Grivennikov, S.I., F.R. Greten, and M. Karin. 2010. Immunity, inflammation, and cancer. *Cell*. 140:883-899.

Gronberg, H. 2003. Prostate cancer epidemiology. *The Lancet*. 361:859-864.

Grover, A., A. Shandilya, A. Punetha, V.S. Bisaria, and D. Sundar. 2010. Inhibition of the NEMO/IKKβ association complex formation, a novel mechanism associated with the NF-κB activation suppression by Withania somnifera's key metabolite withaferin A. *BMC Genomics*. 11:S25.

Guo, J., M.G. Anderson, P. Tapang, J.P. Palma, L.E. Rodriguez, A. Niquette, J. Li, J.J. Bouska, G. Wang, D. Semizarov, D.H. Albert, C.K. Donawho, K.B. Glaser, and O.J. Shah. 2009. Identification of genes that confer tumor cell resistance to the aurora B kinase inhibitor, AZD1152. *Pharmacogenomics J*. 9:90-102.

Habelhah, H. 2010. Emerging Complexity of Protein Ubiquitination in the NF- κB Pathway. *Genes & Cancer*. 1:735-747.

Hanahan, D., and Robert A. Weinberg. 2011. Hallmarks of Cancer: The Next Generation. *Cell*. 144:646-674.

Hans, F., D.A. Skoufias, S. Dimitrov, and R.L. Margolis. 2009. Molecular Distinctions between Aurora A and B: A Single Residue Change Transforms Aurora A into Correctly Localized and Functional Aurora B. *Molecular Biology of the Cell*. 20:3491-3502.

Hao, N.B., M.H. Lu, Y.H. Fan, Y.L. Cao, Z.R. Zhang, and S.M. Yang. 2012. Macrophages in tumor microenvironments and the progression of tumors. *Clin Dev Immunol*. 2012:948098.

Harrington, E.A., D. Bebbington, J. Moore, R.K. Rasmussen, A.O. Ajose-Adeogun, T. Nakayama, J.A. Graham, C. Demur, T. Hercend, A. Diu-Hercend, M. Su, J.M. Golec, and K.M. Miller. 2004. VX-680, a potent and selective small-molecule inhibitor of the Aurora kinases, suppresses tumor growth in vivo. *Nat Med*. 10:262-267.

Harrington, E.A., D. Bebbington, J. Moore, R.K. Rasmussen, A.O. Ajose-Adeogun, T. Nakayama, J.A. Graham, C. Demur, T. Hercend, A. Diu-Hercend, M. Su, J.M.C. Golec, and K.M. Miller. 2004. VX-680, a potent and selective small-molecule inhibitor of the Aurora kinases, suppresses tumor growth in vivo. *Nat Med*. 10:262-267.

Hauf, S., R.W. Cole, S. LaTerra, C. Zimmer, G. Schnapp, R. Walter, A. Heckel, J. van Meel, C.L. Rieder, and J.M. Peters. 2003. The small molecule Hesperadin reveals a role for Aurora B in correcting kinetochore-microtubule attachment and in maintaining the spindle assembly checkpoint. *J Cell Biol*. 161:281-294.

Hayden, M.S., and S. Ghosh. 2008. Shared Principles in NF-κB Signaling. *Cell*. 132:344-362.

Hideshima, T., D. Chauhan, T. Kiziltepe, H. Ikeda, Y. Okawa, K. Podar, N. Raje, A. Protopopov, N.C. Munshi, P.G. Richardson, R.D. Carrasco, and K.C. Anderson. 2009. Biologic sequelae of IκB kinase (IKK) inhibition in multiple myeloma: therapeutic implications. *Blood*. 113:5228-5236.

Higashimoto, T., N. Chan, Y.-K. Lee, and E. Zandi. 2008. Regulation of IκB Kinase Complex by Phosphorylation of γ-Binding Domain of IκB Kinase β by Polo-like Kinase 1. *Journal of Biological Chemistry*. 283:35354-35367.

Hilper, K., D.F. Winkler, and R.E. Hancock. 2007. Cellulose-bound peptide arrays: preparation and applications. *Biotechnol Genet Eng Rev*. 24:31-106.

Hinz, M., P. Löser, S. Mathas, D. Krappmann, B. Dörken, and C. Scheidereit. 2001. Constitutive NF-κB maintains high expression of a characteristic gene network, including CD40, CD86, and a set of antiapoptotic genes in Hodgkin/Reed-Sternberg cells. *Blood*. 97:2798-2807.

Hirota, T., N. Kunitoku, T. Sasayama, T. Marumoto, D. Zhang, M. Nitta, K. Hatakeyama, and H. Saya. 2003. Aurora-A and an Interacting Activator, the LIM Protein Ajuba, Are Required for Mitotic Commitment in Human Cells. *Cell*. 114:585-598.

Hoberg, J.E., A.E. Popko, C.S. Ramsey, and M.W. Mayo. 2005. IκB Kinase -Mediated Derepression of SMRT Potentiates Acetylation of RelA/p65 by p300. *Molecular and Cellular Biology*. 26:457-471.

Hoffmann, A., G. Natoli, and G. Ghosh. 2006. Transcriptional regulation via the NF-kappaB signaling module. *Oncogene*. 25:6706-6716.

J. Homola, S.S. Yee, and G.n. Gauglitz. 1999. Surface plasmon resonance sensors: review. *Sensors and Actuators B: Chemical*. 54:3-15.

Honda, R., R. Körner, and E.A. Nigg. 2003. Exploring the Functional Interactions between Aurora B, INCENP, and Survivin in Mitosis. *Molecular Biology of the Cell*. 14:3325-3341.

Hoshino, K., T. Sugiyama, M. Matsumoto, T. Tanaka, M. Saito, H. Hemmi, O. Ohara, S. Akira, and T. Kaisho. 2006. IkappaB kinase-alpha is critical for interferon-alpha production induced by Toll-like receptors 7 and 9. *Nature*. 440:949-953.

Horn, V., J. Thelu, A. Garcia, C. Albiges-Rizo, M.R. Block, and J. Viallet. 2007. Functional interaction of Aurora-A and PP2A during mitosis. *Mol Biol Cell*. 18:1233-1241.

Hrabakova, R., M. Kollareddy, J. Tyleckova, P. Halada, M. Hajduch, S.J. Gadher, and H. Kovarova. 2012. Cancer cell resistance to Aurora kinase inhibitors: identification of novel targets for cancer therapy. *Journal of Proteome Research*:121114183623002.

Hsu, J.-Y., Z.-W. Sun, X. Li, M. Reuben, K. Tatchell, D.K. Bishop, J.M. Grushcow, C.J. Brame, J.A. Caldwell, D.F. Hunt, R. Lin, M.M. Smith, and C.D. Allis. 2000. Mitotic Phosphorylation of Histone H3 Is Governed by Ipl1/aurora Kinase and Glc7/PP1 Phosphatase in Budding Yeast and Nematodes. *Cell*. 102:279-291.

Hu, M.C., D.F. Lee, W. Xia, L.S. Golfman, F. Ou-Yang, J.Y. Yang, Y. Zou, S. Bao, N. Hanada, H. Saso, R. Kobayashi, and M.C. Hung. 2004. IkappaB kinase promotes tumorigenesis through inhibition of forkhead FOXO3a. *Cell*. 117:225-237.

Hu, Y., V. Baud, M. Delhase, P. Zhang, T. Deerinck, M. Ellisman, R. Johnson, and M. Karin. 1999. Abnormal morphogenesis but intact IKK activation in mice lacking the IKKalpha subunit of IkappaB kinase. *Science*. 284:316-320.

Huang, S., C.A. Pettaway, H. Uehara, C.D. Bucana, and I.J. Fidler. 2001. Blockade of NF-kappaB activity in human prostate cancer cells is associated with suppression of angiogenesis, invasion, and metastasis. *Oncogene*. 20:4188-4197.

Huben, R.P., and G.P. Murphy. 1986. Prostate Cancer: An Update. *CA: A Cancer Journal for Clinicians*. 36:274-292.

Huynh, Q.K., H. Boddupalli, S.A. Rouw, C.M. Koboldt, T. Hall, C. Sommers, S.D. Hauser, J.L. Pierce, R.G. Combs, B.A. Reitz, J.A. Diaz-Collier, R.A. Weinberg, B.L. Hood, B.F. Kilpatrick, and C.S. Tripp. 2000. Characterization of the recombinant IKK1/IKK2 heterodimer. Mechanisms regulating kinase activity. *J Biol Chem*. 275:25883-25891.

Imamoto, T., H. Suzuki, M. Yano, K. Kawamura, N. Kamiya, K. Araki, A. Komiya, N. Nihei, Y. Naya, and T. Ichikawa. 2008. The role of testosterone in the pathogenesis of prostate cancer. *International Journal of Urology*. 15:472-480.

Irelan, J.T., T.J. Murphy, P.D. DeJesus, H. Teo, D. Xu, M.A. Gomez-Ferreria, Y. Zhou, L.J. Miraglia, D.R. Rines, I.M. Verma, D.J. Sharp, V. Tergaonkar, and S.K. Chanda. 2007. A role for IκB kinase 2 in bipolar spindle assembly. *Proceedings of the National Academy of Sciences*. 104:16940-16945.

Iyer, J., and M.-Y. Tsai. 2012. A novel role for TPX2 as a scaffold and co-activator protein of the Chromosomal Passenger Complex. *Cellular Signalling*. 24:1677-1689.

Izmailova, E.S., N. Paz, H. Alencar, M. Chun, L. Schopf, M. Hepperle, J.H. Lane, G. Harriman, Y. Xu, T. Ocain, R. Weissleder, U. Mahmood, A.M. Healy, and B. Jaffee. 2007. Use of molecular imaging to quantify response to IKK-2 inhibitor treatment in murine arthritis. *Arthritis Rheum*. 56:117-128.

Jain, G., M.V. Cronauer, M. Schrader, P. Moller, and R.B. Marienfeld. 2012. NF-kappaB signaling in prostate cancer: a promising therapeutic target? *World J Urol*. 30:303-310.

Jimi, E., K. Aoki, H. Saito, F. D'Acquisto, M.J. May, I. Nakamura, T. Sudo, T. Kojima, F. Okamoto, H. Fukushima, K. Okabe, K. Ohya, and S. Ghosh. 2004. Selective inhibition of NF-kappa B blocks osteoclastogenesis and prevents inflammatory bone destruction in vivo. *Nat Med*. 10:617-624.

Johansson, E., G. Steineck, L. Holmberg, J.E. Johansson, T. Nyberg, M. Ruutu, and A. Bill-Axelson. 2011. Long-term quality-of-life outcomes after radical prostatectomy or watchful waiting: the Scandinavian Prostate Cancer Group-4 randomised trial. *Lancet Oncol*. 12:891-899.

Jones, D.H., T. Nakashima, O.H. Sanchez, I. Kozieradzki, S.V. Komarova, I. Sarosi, S. Morony, E. Rubin, R. Sarao, C.V. Hojilla, V. Komnenovic, Y.-Y. Kong, M. Schreiber, S.J. Dixon, S.M. Sims, R. Khokha, T. Wada, and J.M. Penninger. 2006. Regulation of cancer cell migration and bone metastasis by RANKL. *Nature*. 440:692-696.

Jordan, M.A., D. Thrower, and L. Wilson. 1992. Effects of vinblastine, podophyllotoxin and nocodazole on mitotic spindles. Implications for the role of microtubule dynamics in mitosis. *Journal of Cell Science*. 102:401-416.

Kabouridis, P.S., M. Hasan, J. Newson, D.W. Gilroy, and T. Lawrence. 2002. Inhibition of NF-kappa B activity by a membrane-transducing mutant of I kappa B alpha. *J Immunol*. 169:2587-2593.

Kanda, A., H. Kawai, S. Suto, S. Kitajima, S. Sato, T. Takata, and M. Tatsuka. 2005. Aurora-B//AIM-1 kinase activity is involved in Ras-mediated cell transformation. *Oncogene*. 24:7266-7272.

Karin, M. 2006. Nuclear factor-[kappa]B in cancer development and progression. *Nature*. 441:431-436.

Karthigeyan, D., S.B.B. Prasad, J. Shandilya, S. Agrawal, and T.K. Kundu. 2011. Biology of Aurora A kinase: Implications in cancer manifestation and therapy. *Medicinal Research Reviews*. 31:757-793.

Karvela, M., G.V. Helgason, and T.L. Holyoake. 2012. Mechanisms and novel approaches in overriding tyrosine kinase inhibitor resistance in chronic myeloid leukemia. *Expert Rev Anticancer Ther*. 12:381-392.

Katayama, H., W.R. Brinkley, and S. Sen. 2003. The Aurora kinases: Role in cell transformation and tumorigenesis. *Cancer and Metastasis Reviews*. 22:451-464.

Katayama, H., K. Sasai, H. Kawai, Z.-M. Yuan, J. Bondaruk, F. Suzuki, S. Fujii, R.B. Arlinghaus, B.A. Czerniak, and S. Sen. 2004. Phosphorylation by aurora kinase A induces Mdm2-mediated destabilization and inhibition of p53. *Nat Genet*. 36:55-62.

Katayama, H., and S. Sen. 2010. Aurora kinase inhibitors as anticancer molecules. *Biochimica et Biophysica Acta (BBA) - Gene Regulatory Mechanisms*. 1799:829-839.

Katz, C., L. Levy-Beladev, S. Rotem-Bamberger, T. Rito, S.G.D. Rudiger, and A. Friedler. 2011. Studying protein-protein interactions using peptide arrays. *Chemical Society Reviews*. 40:2131-2145.

Kawajiri, A., Y. Yasui, H. Goto, M. Tatsuka, M. Takahashi, K. Nagata, and M. Inagaki. 2003. Functional significance of the specific sites phosphorylated in desmin at cleavage furrow: Aurora-B may phosphorylate and regulate type III intermediate filaments during cytokinesis coordinatedly with Rho-kinase. *Mol Biol Cell*. 14:1489-1500.

Keen, N., and S. Taylor. 2009. Mitotic drivers—inhibitors of the Aurora B Kinase. *Cancer and Metastasis Reviews*. 28:185-195.

Kensche, T., F. Tokunaga, F. Ikeda, E. Goto, K. Iwai, and I. Dikic. 2012. Analysis of Nuclear Factor-κB (NF-κB) Essential Modulator (NEMO) Binding to Linear and Lysine-linked Ubiquitin Chains and Its Role in the Activation of NF-κB. *Journal of Biological Chemistry*. 287:23626-23634.

Kim, J., and G.A. Coetzee. 2004. Prostate specific antigen gene regulation by androgen receptor. *J Cell Biochem*. 93:233-241.

Kimmins, S., C. Crosio, N. Kotaja, J. Hirayama, L. Monaco, C. Höög, M. van Duin, J.A. Gossen, and P. Sassone-Corsi. 2007. Differential Functions of the Aurora-B and Aurora-C Kinases in Mammalian Spermatogenesis. *Molecular Endocrinology*. 21:726-739.

Kiriakidis, S., E. Andreakos, C. Monaco, B. Foxwell, M. Feldmann, and E. Paleolog. 2003. VEGF expression in human macrophages is NF-kappaB-dependent: studies using adenoviruses expressing the endogenous NF-kappaB inhibitor IkappaBalpha and a kinase-defective form of the IkappaB kinase 2. *J Cell Sci*. 116:665-674.

Kobori, M., Z. Yang, D. Gong, V. Heissmeyer, H. Zhu, Y.K. Jung, M.A. Gakidis, A. Rao, T. Sekine, F. Ikegami, C. Yuan, and J. Yuan. 2004. Wedelolactone suppresses LPS-induced caspase-11 expression by directly inhibiting the IKK complex. *Cell Death Differ*. 11:123-130.

Kollareddy, M., D. Zheleva, P. Dzubak, P.S. Brahmkshatriya, M. Lepsik, and M. Hajduch. 2012. Aurora kinase inhibitors: progress towards the clinic. *Invest New Drugs*. 30:2411-2432.

Koochekpour, S. 2010. Androgen receptor signaling and mutations in prostate cancer. *Asian Journal of Andrology*. 12:639-657.

Kosik, A., M.E. Bekier, J.D. Katusin, H. Kaur, X. Zhou, M. Diakonova, D.N. Chadee, and W.R. Taylor. 2009. Investigating the role of Aurora kinases in RAS signaling. *Journal of Cellular Biochemistry*. 106:33-41.

Kucharczak, J., M.J. Simmons, Y. Fan, and C. Gelinas. 2003. To be, or not to be: NF-kappaB is the answer--role of Rel/NF-kappaB in the regulation of apoptosis. *Oncogene*. 22:8961-8982.

Kumano, M., H. Miyake, T. Terakawa, J. Furukawa, and M. Fujisawa. 2009. Suppressed tumour growth and enhanced chemosensitivity by RNA interference targeting Aurora-A in the PC3 human prostate cancer model. *BJU International*. 106:121-127.

Kumano, M., H. Miyake, T. Terakawa, J. Furukawa, and M. Fujisawa. 2010. Suppressed tumour growth and enhanced chemosensitivity by RNA interference targeting Aurora-A in the PC3 human prostate cancer model. *BJU International*. 106:121-127.

Kuratnik, A., V.E. Senapati, R. Verma, B.G. Mellone, A.T. Vella, and C. Giardina. 2012. Acute sensitization of colon cancer cells to inflammatory cytokines by prophase arrest. *Biochemical Pharmacology*. 83:1217-1228.

Kwak, Y.T., R. Li, C.R. Becerra, D. Tripathy, E.P. Frenkel, and U.N. Verma. 2005. IkappaB kinase alpha regulates subcellular distribution and turnover of cyclin D1 by phosphorylation. *J Biol Chem*. 280:33945-33952.

Lamberti, C., K.M. Lin, Y. Yamamoto, U. Verma, I.M. Verma, S. Byers, and R.B. Gaynor. 2001. Regulation of beta-catenin function by the IkappaB kinases. *J Biol Chem*. 276:42276-42286.

Langmuir, I. 1916. THE CONSTITUTION AND FUNDAMENTAL PROPERTIES OF SOLIDS AND LIQUIDS. PART I. SOLIDS. *Journal of the American Chemical Society*. 38:2221-2295.

Lapenna, S., and A. Giordano. 2009. Cell cycle kinases as therapeutic targets for cancer. *Nat Rev Drug Discov*. 8:547-566.

Lee, E.C.Y. 2006. Targeting Aurora Kinases for the Treatment of Prostate Cancer. *Cancer Research*. 66:4996-5002.

Lee, S., C. Andrieu, F. Saltel, O. Destaing, J. Auclair, V. Pouchkine, J. Michelon, B. Salaun, R. Kobayashi, P. Jurdic, E.D. Kieff, and B.S. Sylla. 2004. IkappaB kinase beta phosphorylates Dok1 serines in response to TNF, IL-1, or gamma radiation. *Proc Natl Acad Sci U S A*. 101:17416-17421.

Lee, S., E. Kim, H. Lee, S. Kim, S. Oh, J. Ryu, D. Moon, J.-H. Ahn, and S.-W. Kim. 2013. A pilot study for the early assessment of the effects of BMS-754807 plus gefitinib in an H292 tumor model by [18F]fluorothymidine-positron emission tomography. *Investigational New Drugs*. 31:506-515.

Lengauer, C., K.W. Kinzler, and B. Vogelstein. 1998. Genetic instabilities in human cancers. *Nature*. 396:643-649.

Lens, S.M.A., E.E. Voest, and R.H. Medema. 2010. Shared and separate functions of polo-like kinases and aurora kinases in cancer. *Nature Reviews Cancer*. 10:825-841.

LeRoy, P.J., J.J. Hunter, K.M. Hoar, K.E. Burke, V. Shinde, J. Ruan, D. Bowman, K. Galvin, and J.A. Ecsedy. 2007. Localization of Human TACC3 to Mitotic Spindles Is Mediated by Phosphorylation on Ser558 by Aurora A: A Novel Pharmacodynamic Method for Measuring Aurora A Activity. *Cancer Research*. 67:5362-5370.

Li, J.J., and S.A. Li. 2006. Mitotic kinases: The key to duplication, segregation, and cytokinesis errors, chromosomal instability, and oncogenesis. *Pharmacology & Therapeutics*. 111:974-984.

Li, Z.-W., W. Chu, Y. Hu, M. Delhase, T. Deerinck, M. Ellisman, R. Johnson, and M. Karin. 1999. The IKKβ Subunit of IκB Kinase (IKK) is Essential for Nuclear Factor κB Activation and Prevention of Apoptosis. *The Journal of Experimental Medicine*. 189:1839-1845.

Licht-Murava, A., B. Plotkin, M. Eisenstein, and H. Eldar-Finkelman. 2011. Elucidating substrate and inhibitor binding sites on the surface of GSK-3beta and the refinement of a competitive inhibitor. *J Mol Biol*. 408:366-378.

Lichtenstein, P., N.V. Holm, P.K. Verkasalo, A. Iliadou, J. Kaprio, M. Koskenvuo, E. Pukkala, A. Skytthe, and K. Hemminki. 2000. Environmental and Heritable Factors in the Causation of Cancer - Analyses of Cohorts of Twins from Sweden, Denmark, and Finland. *New England Journal of Medicine*. 343:78-85.

Liedberg, B., C. Nylander, and I. Lunström. 1983. Surface plasmon resonance for gas detection and biosensing. *Sensors and Actuators*. 4:299-304.

Lin, Y.G., A. Immaneni, W.M. Merritt, L.S. Mangala, S.W. Kim, M.M. Shahzad, Y.T. Tsang, G.N. Armaiz-Pena, C. Lu, A.A. Kamat, L.Y. Han, W.A. Spannuth, A.M. Nick, C.N. Landen, Jr., K.K. Wong, M.J. Gray, R.L. Coleman, D.C. Bodurka, W.R. Brinkley, and A.K. Sood. 2008. Targeting aurora kinase with MK-0457 inhibits ovarian cancer growth. *Clin Cancer Res*. 14:5437-5446.

Littlepage, L.E. 2002. Identification of phosphorylated residues that affect the activity of the mitotic kinase Aurora-A. *Proceedings of the National Academy of Sciences*. 99:15440-15445.

Liu, D., and Michael A. Lampson. 2009. Regulation of kinetochore–microtubule attachments by Aurora B kinase. *Biochemical Society Transactions*. 37:976.

Liu, F., Y. Xia, A.S. Parker, and I.M. Verma. 2012. IKK biology. *Immunological Reviews*. 246:239-253.

Liu, Q., S. Kaneko, L. Yang, R.I. Feldman, S.V. Nicosia, J. Chen, and J.Q. Cheng. 2004. Aurora-A Abrogation of p53 DNA Binding and Transactivation Activity by Phosphorylation of Serine 215. *Journal of Biological Chemistry*. 279:52175-52182.

Liu, S., Z. Chen, F. Zhu, and Y. Hu. 2012. IκB Kinase Alpha and Cancer. *Journal of Interferon & Cytokine Research*. 32:152-158.

Lo, Y.-C., U. Maddineni, J.Y. Chung, R.L. Rich, D.G. Myszka, and H. Wu. 2008. High-Affinity Interaction between IKKβ and NEMO. *Biochemistry*. 47:3109-3116.

Long, Y.M., K. Chen, X.J. Liu, W.R. Xie, and H. Wang. 2009. Cell-permeable Tat-NBD peptide attenuates rat pancreatitis and acinus cell inflammation response. *World J Gastroenterol*. 15:561-569.

Lowenberg, B., P. Muus, G. Ossenkoppele, P. Rousselot, J.Y. Cahn, N. Ifrah, G. Martinelli, S. Amadori, E. Berman, P. Sonneveld, M. Jongen-Lavrencic, S. Rigaudeau, P. Stockman, A. Goudie, S. Faderl, E. Jabbour, and H. Kantarjian. 2011. Phase 1/2 study to assess the safety, efficacy, and pharmacokinetics of barasertib (AZD1152) in patients with advanced acute myeloid leukemia. *Blood*. 118:6030-6036.

Lukasiewicz, K.B., and W.L. Lingle. 2009. Aurora A, centrosome structure, and the centrosome cycle. *Environmental and Molecular Mutagenesis*. 50:602-619.

Luningschror, P., B. Kaltschmidt, and C. Kaltschmidt. 2012. Knockdown of IKK1/2 promotes differentiation of mouse embryonic stem cells into neuroectoderm at the expense of mesoderm. *Stem Cell Rev*. 8:1098-1108.

Luo, J.L., W. Tan, J.M. Ricono, O. Korchynskyi, M. Zhang, S.L. Gonias, D.A. Cheresh, and M. Karin. 2007. Nuclear cytokine-activated IKKalpha controls prostate cancer metastasis by repressing Maspin. *Nature*. 446:690-694.

Luqman, S., and J.M. Pezzuto. 2010. NFkappaB: a promising target for natural products in cancer chemoprevention. *Phytother Res*. 24:949-963.

MacMaster, J.F., D.M. Dambach, D.B. Lee, K.K. Berry, Y. Qiu, F.C. Zusi, and J.R. Burke. 2003. An inhibitor of IkappaB kinase, BMS-345541, blocks endothelial cell adhesion molecule expression and reduces the severity of dextran sulfate sodium-induced colitis in mice. *Inflamm Res*. 52:508-511.

Madge, L.A., and M.J. May. 2009. Inhibiting Proinflammatory NF-κB Signaling Using Cell-Penetrating NEMO Binding Domain Peptides. 512:209-232.

Madge, L.A., and M.J. May. 2011. The NF-κB paradox: RelB induces and inhibits gene expression. *Cell Cycle*. 10:6-7.

Maeda, S., H. Kamata, J.L. Luo, H. Leffert, and M. Karin. 2005. IKKbeta couples hepatocyte death to cytokine-driven compensatory proliferation that promotes chemical hepatocarcinogenesis. *Cell*. 121:977-990.

Manfredi, M.G., J.A. Ecsedy, K.A. Meetze, S.K. Balani, O. Burenkova, W. Chen, K.M. Galvin, K.M. Hoar, J.J. Huck, P.J. LeRoy, E.T. Ray, T.B. Sells, B. Stringer, S.G. Stroud, T.J. Vos, G.S. Weatherhead, D.R. Wysong, M. Zhang, J.B. Bolen, and C.F. Claiborne. 2007. Antitumor activity of MLN8054, an orally active small-molecule inhibitor of Aurora A kinase. *Proc Natl Acad Sci U S A*. 104:4106-4111.

Manning, G. 2002. The Protein Kinase Complement of the Human Genome. *Science*. 298:1912-1934.

Margalef, P., V. Fernández-Majada, A. Villanueva, R. Garcia-Carbonell, M. Iglesias, L. López, M. Martínez-Iniesta, J. Villà-Freixa, Mari C. Mulero, M. Andreu, F. Torres, Marty W. Mayo, A. Bigas, and L. Espinosa. 2012. A Truncated Form of IKKα Is Responsible for Specific Nuclear IKK Activity in Colorectal Cancer. *Cell Reports*. 2:840-854.

Marienfeld, R.B., L. Palkowitsch, and S. Ghosh. 2006. Dimerization of the I kappa B kinase-binding domain of NEMO is required for tumor necrosis factor alpha-induced NF-kappa B activity. *Mol Cell Biol*. 26:9209-9219.

Masson, S., R. Persad, and A. Bahl. 2012. HDR Brachytherapy in the Management of High-Risk Prostate Cancer. *Advances in Urology*. 2012:6.

May, M.J. 2000. Selective Inhibition of NF-kappa B Activation by a Peptide That Blocks the Interaction of NEMO with the Ikappa B Kinase Complex. *Science*. 289:1550-1554.

May, M.J. 2002. Characterization of the Ikappa B-kinase NEMO Binding Domain. *Journal of Biological Chemistry*. 277:45992-46000.

McKlveen Buschhorn, H., R.R. Klein, S.M. Chambers, M.C. Hardy, S. Green, D. Bearss, and R.B. Nagle. 2005. Aurora-A over-expression in high-grade PIN lesions and prostate cancer. *The Prostate*. 64:341-346.

Mellone, B.G., L. Ball, N. Suka, M.R. Grunstein, J.F. Partridge, and R.C. Allshire. 2003. Centromere Silencing and Function in Fission Yeast Is Governed by the Amino Terminus of Histone H3. *Current biology : CB*. 13:1748-1757.

Meraldi, P., R. Honda, and E. A.Nigg. 2002. Aurora-A overexpression reveals tetraploidization as a major route to centrosome amplification in p53-/- cells. *EMBO J*. 21:483-492.

Mercurio, F., H. Zhu, B.W. Murray, A. Shevchenko, B.L. Bennett, J.w. Li, D.B. Young, M. Barbosa, M. Mann, A. Manning, and A. Rao. 1997. IKK-1 and IKK-2: Cytokine-Activated IκB Kinases Essential for NF-κB Activation. *Science*. 278:860-866.

Miller, D.C., K.S. Hafez, A. Stewart, J.E. Montie, and J.T. Wei. 2003. Prostate carcinoma presentation, diagnosis, and staging. *Cancer*. 98:1169-1178.

Mirza, M., T.L. Griebling, and M.W. Kazer. 2011. Erectile dysfunction and urinary incontinence after prostate cancer treatment. *Semin Oncol Nurs*. 27:278-289.

Miyamoto, S. 2010. Nuclear initiated NF-κB signaling: NEMO and ATM take center stage. *Cell Research*. 21:116-130.

Molina, G., A. Vogt, A. Bakan, W. Dai, P.Q. de Oliveira, W. Znosko, T.E. Smithgall, I. Bahar, J.S. Lazo, B.W. Day, and M. Tsang. 2009. Zebrafish chemical screening reveals an inhibitor of Dusp6 that expands cardiac cell lineages. *Nature Chemical Biology*. 5:680-687.

Mori, D., Y. Yano, K. Toyo-oka, N. Yoshida, M. Yamada, M. Muramatsu, D. Zhang, H. Saya, Y.Y. Toyoshima, K. Kinoshita, A. Wynshaw-Boris, and S. Hirotsune. 2007. NDEL1 Phosphorylation by Aurora-A Kinase Is Essential for Centrosomal Maturation, Separation, and TACC3 Recruitment. *Molecular and Cellular Biology*. 27:352-367.

Mosquera, J.M., H. Beltran, K. Park, T.Y. Macdonald, B.D. Robinson, S.T. Tagawa, S. Perner, T.A. Bismar, A. Erbersdobler, R. Dhir, J.B. Nelson, D.M. Nanus, and M.A. Rubin. 2013. Concurrent AURKA and MYCN Gene Amplifications Are Harbingers of Lethal Treatment-Related Neuroendocrine Prostate Cancer. *Neoplasia*. 15:1-10.

Murata, T., M. Shimada, H. Kadono, S. Sakakibara, T. Yoshino, T. Masuda, M. Shimazaki, T. Shintani, K. Fuchikami, K.B. Bacon, K.B. Ziegelbauer, and T.B. Lowinger. 2004. Synthesis and structure-activity relationships of novel IKK-beta inhibitors. Part 2: Improvement of in vitro activity. *Bioorg Med Chem Lett*. 14:4013-4017

Murata, T., M. Shimada, S. Sakakibara, T. Yoshino, H. Kadono, T. Masuda, M. Shimazaki, T. Shintani, K. Fuchikami, K. Sakai, H. Inbe, K. Takeshita, T. Niki, M. Umeda, K.B. Bacon, K.B. Ziegelbauer, and T.B. Lowinger. 2003. Discovery of novel and selective IKK-beta serine-threonine protein kinase inhibitors. Part 1. *Bioorg Med Chem Lett*. 13:913-918.

Murata, T., M. Shimada, S. Sakakibara, T. Yoshino, T. Masuda, T. Shintani, H. Sato, Y. Koriyama, K. Fukushima, N. Nunami, M. Yamauchi, K. Fuchikami, H. Komura, A. Watanabe, K.B. Ziegelbauer, K.B. Bacon, and T.B. Lowinger. 2004. Synthesis and structure-activity relationships of novel IKK-beta inhibitors. Part 3: Orally active anti-inflammatory agents. *Bioorg Med Chem Lett*. 14:4019-4022.

Nachury, M.V., T.J. Maresca, W.C. Salmon, C.M. Waterman-Storer, R. Heald, and K. Weis. 2001. Importin β Is a Mitotic Target of the Small GTPase Ran in Spindle Assembly. *Cell*. 104:95-106.

Nair, J.S., A.L. Ho, and G.K. Schwartz. 2012. The induction of polyploidy or apoptosis by the Aurora A kinase inhibitor MK8745 is p53-dependent. *Cell Cycle*. 11:807-817.

Nakagawa, H., S. Akamatsu, R. Takata, A. Takahashi, M. Kubo, and Y. Nakamura. 2012. Prostate cancer genomics, biology, and risk assessment through genome-wide association studies. *Cancer Science*. 103:607-613.

Nakamori, Y., M. Emoto, N. Fukuda, A. Taguchi, S. Okuya, M. Tajiri, M. Miyagishi, K. Taira, Y. Wada, and Y. Tanizawa. 2006. Myosin motor Myo1c and its receptor NEMO/IKK-gamma promote TNF-alpha-induced serine307 phosphorylation of IRS-1. *J Cell Biol*. 173:665-671.

Naugler, W.E., and M. Karin. 2008. NF-κB and cancer—identifying targets and mechanisms. *Current Opinion in Genetics & Development*. 18:19-26.

Naugler, W.E., T. Sakurai, S. Kim, S. Maeda, K. Kim, A.M. Elsharkawy, and M. Karin. 2007. Gender Disparity in Liver Cancer Due to Sex Differences in MyD88-Dependent IL-6 Production. *Science*. 317:121-124.

Newton, R., N.S. Holden, M.C. Catley, W. Oyelusi, R. Leigh, D. Proud, and P.J. Barnes. 2007. Repression of inflammatory gene expression in human pulmonary epithelial cells by small-molecule IkappaB kinase inhibitors. *J Pharmacol Exp Ther*. 321:734-742.

Nezi, L., and A. Musacchio. 2009. Sister chromatid tension and the spindle assembly checkpoint. *Current Opinion in Cell Biology*. 21:785-795.

Nguyen, H.G., D. Chinnappan, T. Urano, and K. Ravid. 2005. Mechanism of Aurora-B Degradation and Its Dependency on Intact KEN and A-Boxes: Identification of an Aneuploidy-Promoting Property. *Molecular and Cellular Biology*. 25:4977-4992.

Nieba, L., S.E. Nieba-Axmann, A. Persson, M. Hämäläinen, F. Edebratt, A. Hansson, J. Lidholm, K. Magnusson, Ö.F. Karlsson, and A. Plückthun. 1997. BIACORE Analysis of Histidine-Tagged Proteins Using a Chelating NTA Sensor Chip. *Analytical Biochemistry*. 252:217-228.

Nikonova, A.S., I. Astsaturov, I.G. Serebriiskii, R.L. Dunbrack, Jr., and E.A. Golemis. 2013. Aurora A kinase (AURKA) in normal and pathological cell division. *Cell Mol Life Sci*. 70:661-687.

Nordin, H., M. Jungnelius, R. Karlsson, and O.P. Karlsson. 2005. Kinetic studies of small molecule interactions with protein kinases using biosensor technology. *Analytical Biochemistry*. 340:359-368.

Orange, J.S., and M.J. May. 2008. Cell penetrating peptide inhibitors of nuclear factor-kappa B. *Cell Mol Life Sci*. 65:3564-3591.

Osanto, S., and H. Van Poppel. 2012. Emerging novel therapies for advanced prostate cancer. *Ther Adv Urol*. 4:3-12.

Oslob, J.D., M.J. Romanowski, D.A. Allen, S. Baskaran, M. Bui, R.A. Elling, W.M. Flanagan, A.D. Fung, E.J. Hanan, S. Harris, S.A. Heumann, U. Hoch, J.W. Jacobs, J. Lam, C.E. Lawrence, R.S. McDowell, M.A. Nannini, W. Shen, J.A. Silverman, M.M. Sopko, B.T. Tangonan, J. Teague, J.C. Yoburn, C.H. Yu, M. Zhong, K.M. Zimmerman, T. O'Brien, and W. Lew. 2008. Discovery of a potent and selective Aurora kinase inhibitor. *Bioorganic & Medicinal Chemistry Letters*. 18:4880-4884.

Ouchi, M., N. Fujiuchi, K. Sasai, H. Katayama, Y.A. Minamishima, P.P. Ongusaha, C. Deng, S. Sen, S.W. Lee, and T. Ouchi. 2004. BRCA1 phosphorylation by Aurora-A in the regulation of G2 to M transition. *J Biol Chem*. 279:19643-19648.

Palkowitsch, L., J. Leidner, S. Ghosh, and R.B. Marienfeld. 2007. Phosphorylation of Serine 68 in the I B Kinase (IKK)-binding Domain of NEMO Interferes with the Structure of the IKK Complex and Tumor Necrosis Factor α -induced NF- κB Activity. *Journal of Biological Chemistry*. 283:76-86.

Palmberg, C., P. Koivisto, T. Visakorpi, and T.L. Tammela. 1999. PSA decline is an independent prognostic marker in hormonally treated prostate cancer. *Eur Urol*. 36:191-196.

Pan, C., M. Yan, J. Yao, J. Xu, Z. Long, H. Huang, and Q. Liu. 2008. Aurora kinase small molecule inhibitor destroys mitotic spindle, suppresses cell growth, and induces apoptosis in oral squamous cancer cells. *Oral Oncology*. 44:639-645.

Papatriantafyllou, M. 2012. Cell signalling: The NEMO guide to IkappaB. *Nat Rev Mol Cell Biol*. 13:408.

Park, K.J., V. Krishnan, B.W. O'Malley, Y. Yamamoto, and R.B. Gaynor. 2005. Formation of an IKKalpha-dependent transcription complex is required for estrogen receptor-mediated gene activation. *Mol Cell*. 18:71-82.

Pascreau, G., F. Eckerdt, A.L. Lewellyn, C. Prigent, and J.L. Maller. 2008. Phosphorylation of p53 Is Regulated by TPX2-Aurora A in Xenopus Oocytes. *Journal of Biological Chemistry*. 284:5497-5505.

Patel, V.R., M.F. Chammas, Jr., and S. Shah. 2007. Robotic assisted laparoscopic radical prostatectomy: a review of the current state of affairs. *Int J Clin Pract*. 61:309-314.

Perkins, N.D. 2006. Post-translational modifications regulating the activity and function of the nuclear factor kappa B pathway. *Oncogene*. 25:6717-6730.

Persico, A., R.I. Cervigni, M.L. Barretta, D. Corda, and A. Colanzi. 2010. Golgi Partitioning Controls Mitotic Entry through Aurora-A Kinase. *Molecular Biology of the Cell*. 21:3708-3721.

Peters, J.-M. 2006. The anaphase promoting complex/cyclosome: a machine designed to destroy. *Nat Rev Mol Cell Biol*. 7:644-656.

Pieters, B.R., D.Z. de Back, C.C.E. Koning, and A.H. Zwinderman. 2009. Comparison of three radiotherapy modalities on biochemical control and overall survival for the treatment of prostate cancer: A systematic review. *Radiotherapy and oncology : journal of the European Society for Therapeutic Radiology and Oncology*. 93:168-173.

Pinsky, B.A., and S. Biggins. 2005. The spindle checkpoint: tension versus attachment. *Trends in cell biology*. 15:486-493.

Plotnikova, O.V., A.S. Nikonova, Y.V. Loskutov, P.Y. Kozyulina, E.N. Pugacheva, and E.A. Golemis. 2012. Calmodulin activation of Aurora-A kinase (AURKA) is required during ciliary disassembly and in mitosis. *Mol Biol Cell*. 23:2658-2670.

Plotnikova, O.V., E.N. Pugacheva, R.L. Dunbrack, and E.A. Golemis. 2010. Rapid calcium-dependent activation of Aurora-A kinase. *Nature Communications*. 1:1-8.

Prajapati, S. 2002. Regulation of Ikappa B Kinase (IKK)gamma /NEMO Function by IKKbeta-mediated Phosphorylation. *Journal of Biological Chemistry*. 277:24331-24339.

Prajapati, S., Z. Tu, Y. Yamamoto, and R.B. Gaynor. 2006. IKKalpha regulates the mitotic phase of the cell cycle by modulating Aurora A phosphorylation. *Cell Cycle*. 5:2371-2380.

Qi, G., I. Ogawa, Y. Kudo, M. Miyauchi, B.S. Siriwardena, F. Shimamoto, M. Tatsuka, and T. Takata. 2007. Aurora-B expression and its correlation with cell proliferation and metastasis in oral cancer. *Virchows Arch*. 450:297-302.

Qi, W., L.S. Cooke, X. Liu, L. Rimsza, D.J. Roe, A.M.D.O. Persky, T.P. Miller, and D. Mahadevan. 2011. Aurora inhibitor MLN8237 in combination with docetaxel enhances apoptosis and anti-tumor activity in mantle cell lymphoma. *Biochemical Pharmacology*. 81:881-890.

Rahman, K.M., S. Ali, A. Aboukameel, S.H. Sarkar, Z. Wang, P.A. Philip, W.A. Sakr, and A. Raz. 2007. Inactivation of NF-kappaB by 3,3'-diindolylmethane contributes to increased apoptosis induced by chemotherapeutic agent in breast cancer cells. *Mol Cancer Ther*. 6:2757-2765.

Rajagopalan, H., and C. Lengauer. 2004. Aneuploidy and cancer. *Nature*. 432:338-341.

Regnier, C.H., H.Y. Song, X. Gao, D.V. Goeddel, Z. Cao, and M. Rothe. 1997. Identification and characterization of an IkappaB kinase. *Cell*. 90:373-383.

Rich, R.L., and D.G. Myszka. 2011. Survey of the 2009 commercial optical biosensor literature. *Journal of Molecular Recognition*. 24:892-914.

Rich, R.L., G.A. Papalia, P.J. Flynn, J. Furneisen, J. Quinn, J.S. Klein, P.S. Katsamba, M.B. Waddell, M. Scott, J. Thompson, J. Berlier, S. Corry, M. Baltzinger, G. Zeder-Lutz, A. Schoenemann, A. Clabbers, S. Wieckowski, M.M. Murphy, P. Page, T.E. Ryan, J. Duffner, T. Ganguly, J. Corbin, S. Gautam, G. Anderluh, A. Bavdek, D. Reichmann, S.P. Yadav, E. Hommema, E. Pol, A. Drake, S. Klakamp, T. Chapman, D. Kernaghan, K. Miller, J. Schuman, K. Lindquist, K. Herlihy, M.B. Murphy, R. Bohnsack, B. Andrien, P. Brandani, D. Terwey, R. Millican, R.J. Darling, L. Wang, Q. Carter, J. Dotzlaf, J. Lopez-Sagaseta, I. Campbell, P. Torreri, S. Hoos, P. England, Y. Liu, Y. Abdiche, D. Malashock, A. Pinkerton, M. Wong, E. Lafer, C. Hinck, K. Thompson, C.D. Primo, A. Joyce, J. Brooks, F. Torta, A.B. Bagge Hagel, J. Krarup, J. Pass, M. Ferreira, S. Shikov, M. Mikolajczyk, Y. Abe, G. Barbato, A.M. Giannetti, G. Krishnamoorthy, B. Beusink, D. Satpaev, T. Tsang, E. Fang, J. Partridge, S. Brohawn, J. Horn, O. Pritsch, G. Obal, S. Nilapwar, B. Busby, G. Gutierrez-Sanchez, R.D. Gupta, S. Canepa, K. Witte, Z. Nikolovska-Coleska, Y.H. Cho, R. D'Agata, K. Schlick, R. Calvert, E.M. Munoz, M.J. Hernaiz, T. Bravman, M. Dines, M.H. Yang, et al. 2009. A global benchmark study using affinity-based biosensors. *Anal Biochem*. 386:194-216.

Rickert, R.C., J. Jellusova, and A.V. Miletic. 2011. Signaling by the tumor necrosis factor receptor superfamily in B-cell biology and disease. *Immunol Rev*. 244:115-133.

Roitbak, T., L. Li, and L.A. Cunningham. 2008. Neural stem/progenitor cells promote endothelial cell morphogenesis and protect endothelial cells against ischemia via HIF-1α-regulated VEGF signaling. *Journal of Cerebral Blood Flow & Metabolism*. 28:1530-1542.

Rothwarf, D.M., E. Zandi, G. Natoli, and M. Karin. 1998. IKK-gamma is an essential regulatory subunit of the IkappaB kinase complex. *Nature*. 395:297-300.

Rushe, M., L. Silvian, S. Bixler, L.L. Chen, A. Cheung, S. Bowes, H. Cuervo, S. Berkowitz, T. Zheng, K. Guckian, M. Pellegrini, and A. Lugovskoy. 2008. Structure of a NEMO/IKK-Associating Domain Reveals Architecture of the Interaction Site. *Structure*. 16:798-808.

Sabino, D., N.H. Brown, and R. Basto. 2011. Drosophila Ajuba is not an Aurora-A activator but is required to maintain Aurora-A at the centrosome. *Journal of Cell Science*. 124:1156-1166.

Sakamoto, K., and S. Maeda. 2010. Targeting NF-kappaB for colorectal cancer. *Expert Opin Ther Targets*. 14:593-601.

Salmela, A.L., J. Pouwels, A. Varis, A.M. Kukkonen, P. Toivonen, P.K. Halonen, M. Perala, O. Kallioniemi, G.J. Gorbsky, and M.J. Kallio. 2009. Dietary flavonoid fisetin induces a forced exit from mitosis by targeting the mitotic spindle checkpoint. *Carcinogenesis*. 30:1032-1040.

Sanda, M.G., R.L. Dunn, J. Michalski, H.M. Sandler, L. Northouse, L. Hembroff, X. Lin, T.K. Greenfield, M.S. Litwin, C.S. Saigal, A. Mahadevan, E. Klein, A. Kibel, L.L. Pisters, D. Kuban, I. Kaplan, D. Wood, J. Ciezki, N. Shah, and J.T. Wei. 2008. Quality of Life and Satisfaction with Outcome among Prostate-Cancer Survivors. *New England Journal of Medicine*. 358:1250-1261.

Sanda, M.G., and I.D. Kaplan. 2009. A 64-Year-Old Man With Low-Risk Prostate Cancer: Review of Prostate Cancer Treatment. *JAMA: The Journal of the American Medical Association*. 301:2141-2151.

Sasco, A.J., M.B. Secretan, and K. Straif. 2004. Tobacco smoking and cancer: a brief review of recent epidemiological evidence. *Lung Cancer*. 45 Suppl 2:S3-9.

Schopf, L., A. Savinainen, K. Anderson, J. Kujawa, M. DuPont, M. Silva, E. Siebert, S. Chandra, J. Morgan, P. Gangurde, D. Wen, J. Lane, Y. Xu, M. Hepperle, G. Harriman, T. Ocain, and B. Jaffee. 2006. IKKbeta inhibition protects against bone and cartilage destruction in a rat model of rheumatoid arthritis. *Arthritis Rheum*. 54:3163-3173.

Schorl, C., and J.M. Sedivy. 2007. Analysis of cell cycle phases and progression in cultured mammalian cells. *Methods*. 41:143-150.

Schulz, T.F. 2000. Kaposi's sarcoma-associated herpesvirus (human herpesvirus 8): epidemiology and pathogenesis. *J Antimicrob Chemother*. 45 Suppl T3:15-27.

Scrittori, L. 2004. A Small C-Terminal Sequence of Aurora B Is Responsible for Localization and Function. *Molecular Biology of the Cell*. 16:292-305.

Sehdev, V., A. Katsha, J. Ecsedy, A. Zaika, A. Belkhiri, and W. El-Rifai. 2013. The combination of alisertib, an investigational Aurora kinase A inhibitor, and docetaxel promotes cell death and reduces tumor growth in preclinical cell models of upper gastrointestinal adenocarcinomas. *Cancer*. 119:904-914.

A: Seki, A., J.A. Coppinger, H. Du, C.-Y. Jang, J.R. Yates, and G. Fang. 2008. Plk1- and β-TrCP-dependent degradation of Bora controls mitotic progression. *The Journal of Cell Biology*. 181:65-78.

B: Seki, A., J.A. Coppinger, C.Y. Jang, J.R. Yates, and G. Fang. 2008. Bora and the Kinase Aurora A Cooperatively Activate the Kinase Plk1 and Control Mitotic Entry. *Science*. 320:1655-1658.

Sen S, Z.H.a.W.R. 1997. A putative serine/threonine kinase encoding gene BTAK on chromosome 20q13 is amplified and overexpressed in human breast cancer cell lines. *Oncogene*. 14:2195-2200.

Sessa, F., M. Mapelli, C. Ciferri, C. Tarricone, L.B. Areces, T.R. Schneider, P.T. Stukenberg, and A. Musacchio. 2005. Mechanism of Aurora B Activation by INCENP and Inhibition by Hesperadin. *Molecular Cell*. 18:379-391.

Shifera, A.S. 2010. Protein–protein interactions involving IKKγ (NEMO) that promote the activation of NF-κB. *Journal of Cellular Physiology*. 223:558-561.

Shostak, K., and A. Chariot. 2011. NF-kappaB, stem cells and breast cancer: the links get stronger. *Breast Cancer Res*. 13:214.

Shu, S.-K., Q. Liu, D. Coppola, and J.Q. Cheng. 2010. Phosphorylation and Activation of Androgen Receptor by Aurora-A. *Journal of Biological Chemistry*. 285:33045-33053.

Sil, A.K., S. Maeda, Y. Sano, D.R. Roop, and M. Karin. 2004. IkappaB kinase-alpha acts in the epidermis to control skeletal and craniofacial morphogenesis. *Nature*. 428:660-664.

Slattery, S.D., M.A. Mancini, B.R. Brinkley, and R.M. Hall. 2009. Aurora-C kinase supports mitotic progression in the absence of Aurora-B. *Cell Cycle*. 8:2986-2997.

Solc, P., V. Baran, A. Mayer, T. Bohmova, G. Panenkova-Havlova, A. Saskova, R.M. Schultz, and J. Motlik. 2012. Aurora Kinase A Drives MTOC Biogenesis but Does Not Trigger Resumption of Meiosis in Mouse Oocytes Matured In Vivo. *Biology of Reproduction*. 87:85-85.

Solt, L.A., L.A. Madge, and M.J. May. 2009. NEMO-binding Domains of Both IKKα and IKK Regulate IκB Kinase Complex Assembly and Classical NF- B Activation. *Journal of Biological Chemistry*. 284:27596-27608.

Solt, L.A., L.A. Madge, J.S. Orange, and M.J. May. 2007. Interleukin-1-induced NF-κB Activation Is NEMO-dependent but Does Not Require IKKβ. *Journal of Biological Chemistry*. 282:8724-8733.

Solt, L.A., and M.J. May. 2008. The IκB kinase complex: master regulator of NF-κB signaling. *Immunologic Research*. 42:3-18.

Song, L., W. Dong, M. Gao, J. Li, M. Hu, N. Guo, and C. Huang. 2010. A novel role of IKKα in the mediation of UVB-induced G0/G1 cell cycle arrest response by suppressing Cyclin D1 expression. *Biochimica et Biophysica Acta (BBA) - Molecular Cell Research*. 1803:323-332.

Staff, S., J. Isola, M. Jumppanen, and M. Tanner. 2010. Aurora-A gene is frequently amplified in basal-like breast cancer. *Oncol Rep*. 23:307-312.

Stenberg, E., B.r. Persson, H.k. Roos, and C. Urbaniczky. 1991. Quantitative determination of surface concentration of protein with surface plasmon resonance using radiolabeled proteins. *Journal of Colloid and Interface Science*. 143:513-526.

Stone, N.N., R.G. Stock, I. White, and P. Unger. 2007. Patterns of Local Failure Following Prostate Brachytherapy. *The Journal of urology*. 177:1759-1764.

Strnad, J., P.A. McDonnell, D.J. Riexinger, C. Mapelli, L. Cheng, H. Gray, R.P. Ryseck, and J.R. Burke. 2006. NEMO binding domain of IKK-2 encompasses amino acids 735–745. *Journal of Molecular Recognition*. 19:227-233.

Suh, J., F. Payvandi, L.C. Edelstein, P.S. Amenta, W.-X. Zong, C.l. G?linas, and A.B. Rabson. 2002. Mechanisms of constitutive NF-κB activation in human prostate cancer cells. *The Prostate*. 52:183-200.

Suh, J., and A.B. Rabson. 2004. NF-κB activation in human prostate cancer: Important mediator or epiphenomenon? *Journal of Cellular Biochemistry*. 91:100-117.

Sun, C., F. Chan, P. Briassouli, and S. Linardopoulos. 2007. Aurora kinase inhibition downregulates NF-κB and sensitises tumour cells to chemotherapeutic agents. *Biochemical and Biophysical Research Communications*. 352:220-225.

Suzuki, H., N. Kamiya, T. Imamoto, K. Kawamura, M. Yano, M. Takano, T. Utsumi, Y. Naya, and T. Ichikawa. 2008. Current topics and perspectives relating to hormone therapy for prostate cancer. *International Journal of Clinical Oncology*. 13:401-410.

Taioli, E., R.E. Flores-Obando, I. Agalliu, P. Blanchet, C.H. Bunker, R.E. Ferrell, M. Jackson, L.C.R. Kidd, S. Kolb, N.A. Lavender, N. McFarlane-Anderson, S.S. Morrison, L. Multigner, E.A. Ostrande, J.Y. Park, A.L. Patrick, T.R. Rebbeck, M. Romana, J.L. Stanford, F. Ukoli, T.T. VanCleave, C.M. Zeigler-Johnson, B. Mutetwa, and C. Ragin. 2011. Multi-institutional prostate cancer study of genetic susceptibility in populations of African descent. *Carcinogenesis*. 32:1361-1365.

Takada, Y., S. Singh, and B.B. Aggarwal. 2004. Identification of a p65 peptide that selectively inhibits NF-kappa B activation induced by various inflammatory stimuli and its role in down-regulation of NF-kappaB-mediated gene expression and up-regulation of apoptosis. *J Biol Chem*. 279:15096-15104.

Tanaka, M., M.E. Fuentes, K. Yamaguchi, M.H. Durnin, S.A. Dalrymple, K.L. Hardy, and D.V. Goeddel. 1999. Embryonic lethality, liver degeneration, and impaired NF-kappa B activation in IKK-beta-deficient mice. *Immunity*. 10:421-429.

Tanaka, M., A. Ueda, H. Kanamori, H. Ideguchi, J. Yang, S. Kitajima, and Y. Ishigatsubo. 2002. Cell-cycle-dependent Regulation of Human aurora A Transcription Is Mediated by Periodic Repression of E4TF1. *Journal of Biological Chemistry*. 277:10719-10726.

Tang, C.-J.C., C.-Y. Lin, and T.K. Tang. 2006. Dynamic localization and functional implications of Aurora-C kinase during male mouse meiosis. *Developmental Biology*. 290:398-410.

Tang, E.D., C.-Y. Wang, Y. Xiong, and K.-L. Guan. 2003. A Role for NF-κB Essential Modifier/IκB Kinase-γ (NEMO/IKKγ) Ubiquitination in the Activation of the IκB Kinase Complex by Tumor Necrosis Factor-α. *Journal of Biological Chemistry*. 278:37297-37305.

Tannock, I.F., R. de Wit, W.R. Berry, J. Horti, A. Pluzanska, K.N. Chi, S. Oudard, C. Theodore, N.D. James, I. Turesson, M.A. Rosenthal, and M.A. Eisenberger. 2004. Docetaxel plus prednisone or mitoxantrone plus prednisone for advanced prostate cancer. *N Engl J Med*. 351:1502-1512.

Tas, S.W., E.C. de Jong, N. Hajji, M.J. May, S. Ghosh, M.J. Vervoordeldonk, and P.P. Tak. 2005. Selective inhibition of NF-kappaB in dendritic cells by the NEMO-binding domain peptide blocks maturation and prevents T cell proliferation and polarization. *Eur J Immunol*. 35:1164-1174.

Tatsuka, M., S. Sato, S. Kitajima, S. Suto, H. Kawai, M. Miyauchi, I. Ogawa, M. Maeda, T. Ota, and T. Takata. 2004. Overexpression of Aurora-A potentiates HRAS-mediated oncogenic transformation and is implicated in oral carcinogenesis. *Oncogene*. 24:1122-1127.

Terada, Y. 2003. Interaction of Aurora-A and centrosomin at the microtubule-nucleating site in Drosophila and mammalian cells. *The Journal of Cell Biology*. 162:757-764.

Tewari, A., P. Sooriakumaran, D.A. Bloch, U. Seshadri-Kreaden, A.E. Hebert, and P. Wiklund. 2012. Positive surgical margin and perioperative complication rates of primary surgical treatments for prostate cancer: a systematic review and meta-analysis comparing retropubic, laparoscopic, and robotic prostatectomy. *Eur Urol*. 62:1-15.

Tinelli, A., D. Vergara, R. Martignago, G. Leo, A. Malvasi, and R. Tinelli. 2008. Hormonal carcinogenesis and socio-biological development factors in endometrial cancer: a clinical review. *Acta Obstet Gynecol Scand*. 87:1101-1113.

Toji, S., N. Yabuta, T. Hosomi, S. Nishihara, T. Kobayashi, S. Suzuki, K. Tamai, and H. Nojima. 2004. The centrosomal protein Lats2 is a phosphorylation target of Aurora-A kinase. *Genes to Cells*. 9:383-397.

Tomita, M., M. Toyota, C. Ishikawa, T. Nakazato, T. Okudaira, T. Matsuda, J.N. Uchihara, N. Taira, K. Ohshiro, M. Senba, Y. Tanaka, K. Ohshima, H. Saya, T. Tokino, and N. Mori. 2009. Overexpression of Aurora A by loss of CHFR gene expression increases the growth and survival of HTLV-1-infected T cells through enhanced NF-kappaB activity. *Int J Cancer*. 124:2607-2615.

Tornatore, L., A.K. Thotakura, J. Bennett, M. Moretti, and G. Franzoso. 2012. The nuclear factor kappa B signaling pathway: integrating metabolism with inflammation. *Trends Cell Biol*. 22:557-566.

Toughiri, R., X. Li, Q. Du, and C.J. Bieberich. 2013. Phosphorylation of NuMA by Aurora-A kinase in PC-3 prostate cancer cells affects proliferation, survival, and interphase NuMA localization. *J Cell Biochem*. 114:823-830.

Towbin, H., T. Staehelin, and J. Gordon. 1979. Electrophoretic transfer of proteins from polyacrylamide gels to nitrocellulose sheets: procedure and some applications. *Proc Natl Acad Sci U S A*. 76:4350-4354.

Tsai, M.-Y., C. Wiese, K. Cao, O. Martin, P. Donovan, J. Ruderman, C. Prigent, and Y. Zheng. 2003. A Ran signalling pathway mediated by the mitotic kinase Aurora A in spindle assembly. *Nat Cell Biol*. 5:242-248.

Vader, G., and S.M.A. Lens. 2008. The Aurora kinase family in cell division and cancer. *Biochimica et Biophysica Acta (BBA) - Reviews on Cancer*. 1786:60-72.

van Vugt, M.A.T.M., A. Br·s, and R.H. Medema. 2004. Polo-like Kinase-1 Controls Recovery from a G2 DNA Damage-Induced Arrest in Mammalian Cells. *Molecular Cell*. 15:799-811.

Venkataraman, S., I. Alimova, T. Tello, P.S. Harris, J.A. Knipstein, A.M. Donson, N.K. Foreman, A.K. Liu, and R. Vibhakar. 2012. Targeting Aurora Kinase A enhances radiation sensitivity of atypical teratoid rhabdoid tumor cells. *J Neurooncol*. 107:517-526.

Verma, U.N., Y. Yamamoto, S. Prajapati, and R.B. Gaynor. 2004. Nuclear Role of IκB Kinase-β/NF-κB Essential Modulator (IKKγ/NEMO) in NF-ŒʃB-dependent Gene Expression. *Journal of Biological Chemistry*. 279:3509-3515.

Vikis, H.G., and K.L. Guan. 2004. Glutathione-S-transferase-fusion based assays for studying protein-protein interactions. *Methods Mol Biol*. 261:175-186.

Villeneuve, P.J., and Y. Mao. 1994. Lifetime probability of developing lung cancer, by smoking status, Canada. *Can J Public Health*. 85:385-388.

Visintin, R., S. Prinz, and A. Amon. 1997. CDC20 and CDH1: A Family of Substrate-Specific Activators of APC-Dependent Proteolysis. *Science*. 278:460-463.

Volkmer, R., V. Tapia, and C. Landgraf. 2012. Synthetic peptide arrays for investigating protein interaction domains. *FEBS Lett*. 586:2780-2786.

Wajant, H., K. Pfizenmaier, and P. Scheurich. 2003. Tumor necrosis factor signaling. *Cell Death Differ*. 10:45-65.

Walter AO, S.W., Korver W, Sheung J, Lees E. 2000. The mitotic serine/threonine kinase Aurora2/AIK is regulated by phosphorylation and degradation. *oncogene*. 19:4906-4916.

Wang, Z., N. Cao, D. Nantajit, M. Fan, Y. Liu, and J.J. Li. 2008. Mitogen-activated Protein Kinase Phosphatase-1 Represses c-Jun NH2-terminal Kinase-mediated Apoptosis via NF- B Regulation. *Journal of Biological Chemistry*. 283:21011-21023.

Warner, S.L., S. Bashyam, H. Vankayalapati, D.J. Bearss, H. Han, D. Mahadevan, D.D. Von Hoff, and L.H. Hurley. 2006. Identification of a lead small-molecule inhibitor of the Aurora kinases using a structure-assisted, fragment-based approach. *Mol Cancer Ther*. 5:1764-1773.

Warner, S.L., B.J. Stephens, S. Nwokenkwo, G. Hostetter, A. Sugeng, M. Hidalgo, J.M. Trent, H. Han, and D.D. Von Hoff. 2009. Validation of TPX2 as a Potential Therapeutic Target in Pancreatic Cancer Cells. *Clinical Cancer Research*. 15:6519-6528.

Wear, M.A., A. Patterson, K. Malone, C. Dunsmore, N.J. Turner, and M.D. Walkinshaw. 2005. A surface plasmon resonance-based assay for small molecule inhibitors of human cyclophilin A. *Analytical Biochemistry*. 345:214-226.

Wei, Y., C.A. Mizzen, R.G. Cook, M.A. Gorovsky, and C.D. Allis. 1998. Phosphorylation of histone H3 at serine 10 is correlated with chromosome condensation during mitosis and meiosis in Tetrahymena. *Proceedings of the National Academy of Sciences*. 95:7480-7484.

Wen, D., Y. Nong, J.G. Morgan, P. Gangurde, A. Bielecki, J. DaSilva, M. Keaveney, H. Cheng, C. Fraser, L. Schopf, M. Hepperle, G. Harriman, B.D. Jaffee, T.D. Ocain, and Y. Xu. 2006. A Selective Small Molecule IκB Kinase β Inhibitor Blocks Nuclear Factor κB-Mediated Inflammatory Responses in Human Fibroblast-Like Synoviocytes, Chondrocytes, and Mast Cells. *Journal of Pharmacology and Experimental Therapeutics*. 317:989-1001.

Weng, H.-Y., M.-J. Hsu, C.-C. Wang, B.-C. Chen, C.-Y. Hong, M.-C. Chen, W.-T. Chiu, and C.-H. Lin. 2012. Zerumbone suppresses IKKα, Akt, and FOXO1 activation, resulting in apoptosis of GBM 8401 cells. *Journal of Biomedical Science*. 19:86.

Wilkinson, R.W., R. Odedra, S.P. Heaton, S.R. Wedge, N.J. Keen, C. Crafter, J.R. Foster, M.C. Brady, A. Bigley, E. Brown, K.F. Byth, N.C. Barrass, K.E. Mundt, K.M. Foote, N.M. Heron, F.H. Jung, A.A. Mortlock, F.T. Boyle, and S. Green. 2007. AZD1152, a Selective Inhibitor of Aurora B Kinase, Inhibits Human Tumor Xenograft Growth by Inducing Apoptosis. *Clinical Cancer Research*. 13:3682-3688.

Willard, F.S., and D.P. Siderovski. 2006. Covalent immobilization of histidine-tagged proteins for surface plasmon resonance. *Analytical Biochemistry*. 353:147-149.

Wilt, T.J., M.K. Brawer, K.M. Jones, M.J. Barry, W.J. Aronson, S. Fox, J.R. Gingrich, J.T. Wei, P. Gilhooly, B.M. Grob, I. Nsouli, P. Iyer, R. Cartagena, G. Snider, C. Roehrborn, R. Sharifi, W. Blank, P. Pandya, G.L. Andriole, D. Culkin, and T. Wheeler. 2012. Radical Prostatectomy versus Observation for Localized Prostate Cancer. *New England Journal of Medicine*. 367:203-213.

Woronicz, J.D., X. Gao, Z. Cao, M. Rothe, and D.V. Goeddel. 1997. IkappaB kinase-beta: NF-kappaB activation and complex formation with IkappaB kinase-alpha and NIK. *Science*. 278:866-869.

Wu, Z.-H., Y. Shi, R.S. Tibbetts, and S. Miyamoto. 2006. Molecular Linkage Between the Kinase ATM and NF-κB Signaling in Response to Genotoxic Stimuli. *Science*. 311:1141-1146.

Wysong, D.R., A. Chakravarty, K. Hoar, and J.A. Ecsedy. 2009. The inhibition of Aurora A abrogates the mitotic delay induced by microtubule perturbing agents. *Cell Cycle*. 8:876-888.

Xiao, G., E.W. Harhaj, and S.-C. Sun. 2001. NF-κB-Inducing Kinase Regulates the Processing of NF-κB2 p100. *Molecular Cell*. 7:401-409.

Xie, F., Q. Lang, M. Zhou, H. Zhang, Z. Zhang, Y. Zhang, B. Wan, Q. Huang, and L. Yu. 2012. The dietary flavonoid luteolin inhibits Aurora B kinase activity and blocks proliferation of cancer cells. *European Journal of Pharmaceutical Sciences*. 46:388-396.

Xu, G., Y.C. Lo, Q. Li, G. Napolitano, X. Wu, X. Jiang, M. Dreano, M. Karin, and H. Wu. 2011. Crystal structure of inhibitor of kappaB kinase beta. *Nature*. 472:325-330.

Yamamoto, Y. 2001. IKKgamma /NEMO Facilitates the Recruitment of the Ikappa B Proteins into the Ikappa B Kinase Complex. *Journal of Biological Chemistry*. 276:36327-36336.

Yamamoto, Y., and R.B. Gaynor. 2004. IκB kinases: key regulators of the NF-κB pathway. *Trends in Biochemical Sciences*. 29:72-79.

Yamamoto, Y., U.N. Verma, S. Prajapati, Y.-T. Kwak, and R.B. Gaynor. 2003. Histone H3 phosphorylation by IKK-[alpha] is critical for cytokine-induced gene expression. *Nature*. 423:655-659.

Yamamoto, Y., U.N. Verma, S. Prajapati, Y.T. Kwak, and R.B. Gaynor. 2003. Histone H3 phosphorylation by IKK-alpha is critical for cytokine-induced gene expression. *Nature*. 423:655-659.

Yan, A., L. Wang, S. Xu, and J. Xu. 2011. Aurora-A kinase inhibitor scaffolds and binding modes. *Drug Discovery Today*. 16:260-269.

Yang, J., T. Ikezoe, C. Nishioka, T. Tasaka, A. Taniguchi, Y. Kuwayama, N. Komatsu, K. Bandobashi, K. Togitani, H.P. Koeffler, H. Taguchi, and A. Yokoyama. 2007. AZD1152, a novel and selective aurora B kinase inhibitor, induces growth arrest, apoptosis, and sensitization for tubulin depolymerizing agent or topoisomerase II inhibitor in human acute leukemia cells in vitro and in vivo. *Blood*. 110:2034-2040.

Yang, J., R. Splittgerber, F.E. Yull, S. Kantrow, G.D. Ayers, M. Karin, and A. Richmond. 2010. Conditional ablation of Ikkb inhibits melanoma tumor development in mice. *Journal of Clinical Investigation*. 120:2563-2574.

Yang, K.S., G. Budin, T. Reiner, C. Vinegoni, and R. Weissleder. 2012. Bioorthogonal Imaging of Aurora Kinase A in Live Cells. *Angewandte Chemie International Edition*. 51:6598-6603.

Yao, J.-e., M. Yan, Z. Guan, C.-b. Pan, L.-p. Xia, C.-x. Li, L.-h. Wang, Z.-j. Long, Y. Zhao, M.-w. Li, F.-m. Zheng, J. Xu, D.-j. Lin, and Q. Liu. 2009. Aurora-A down-regulates IkappaBα via Akt activation and interacts with insulin-like growth factor-1 induced phosphatidylinositol 3-kinase pathway for cancer cell survival. *Molecular Cancer*. 8:95.

Yasui, Y., T. Urano, A. Kawajiri, K.-i. Nagata, M. Tatsuka, H. Saya, K. Furukawa, T. Takahashi, I. Izawa, and M. Inagaki. 2004. Autophosphorylation of a Newly Identified Site of Aurora-B Is Indispensable for Cytokinesis. *Journal of Biological Chemistry*. 279:12997-13003.

Yemelyanov, A., A. Gasparian, P. Lindholm, L. Dang, J.W. Pierce, F. Kisseljov, A. Karseladze, and I. Budunova. 2006. Effects of IKK inhibitor PS1145 on NF-kappaB function, proliferation, apoptosis and invasion activity in prostate carcinoma cells. *Oncogene*. 25:387-398.

Yu, X., K. Minter-Dykhouse, L. Malureanu, W.-M. Zhao, D. Zhang, C.J. Merkle, I.M. Ward, H. Saya, G. Fang, J. van Deursen, and J. Chen. 2005. Chfr is required for tumor suppression and Aurora A regulation. *Nat Genet*. 37:401-406.

Yuan, K., N. Li, Y. Huo, F. Yan, Y. Yang, T. Ward, C. Jin, and X. Yao. 2009. Recruitment of separase to mitotic chromosomes is regulated by Aurora B. *Cell Cycle*. 8:1433-1443.

Zandi, E., D.M. Rothwarf, M. Delhase, M. Hayakawa, and M. Karin. 1997. The IkappaB kinase complex (IKK) contains two kinase subunits, IKKalpha and IKKbeta, necessary for IkappaB phosphorylation and NF-kappaB activation. *Cell*. 91:243-252.

Zelefsky, M.J., V.E. Reuter, Z. Fuks, P. Scardino, and A. Shippy. 2008. Influence of Local Tumor Control on Distant Metastases and Cancer Related Mortality After External Beam Radiotherapy for Prostate Cancer. *The Journal of urology*. 179:1368-1373.

Zhang, D., T. Hirota, T. Marumoto, M. Shimizu, N. Kunitoku, T. Sasayama, Y. Arima, L. Feng, M. Suzuki, M. Takeya, and H. Saya. 2004. Cre-loxP-controlled periodic Aurora-A overexpression induces mitotic abnormalities and hyperplasia in mammary glands of mouse models. *Oncogene*. 23:8720-8730.

Zhang, D., T. Shimizu, N. Araki, T. Hirota, M. Yoshie, K. Ogawa, N. Nakagata, M. Takeya, and H. Saya. 2008. Aurora A overexpression induces cellular senescence in mammary gland hyperplastic tumors developed in p53-deficient mice. *Oncogene*. 27:4305-4314.

Zhang, L., J. Iyer, A. Chowdhury, M. Ji, L. Xiao, S. Yang, Y. Chen, M.Y. Tsai, and J. Dong. 2012. KIBRA Regulates Aurora Kinase Activity and Is Required for Precise Chromosome Alignment During Mitosis. *Journal of Biological Chemistry*. 287:34069-34077.

Zhao, B., A. Smallwood, J. Yang, K. Koretke, K. Nurse, A. Calamari, R.B. Kirkpatrick, and Z. Lai. 2008. Modulation of kinase-inhibitor interactions by auxiliary protein binding: Crystallography studies on Aurora A interactions with VX-680 and with TPX2. *Protein Science*. 17:1791-1797.

Zhao, Z.-s., J.P. Lim, Y.-W. Ng, L. Lim, and E. Manser. 2005. The GIT-Associated Kinase PAK Targets to the Centrosome and Regulates Aurora-A. *Molecular Cell*. 20:237-249.

Zhou, H., J. Kuang, L. Zhong, W.L. Kuo, J.W. Gray, A. Sahin, B.R. Brinkley, and S. Sen. 1998. Tumour amplified kinase STK15/BTAK induces centrosome amplification, aneuploidy and transformation. *Nat Genet*. 20:189-193.

Ziegelbauer, K., F. Gantner, N.W. Lukacs, A. Berlin, K. Fuchikami, T. Niki, K. Sakai, H. Inbe, K. Takeshita, M. Ishimori, H. Komura, T. Murata, T. Lowinger, and K.B. Bacon. 2005. A selective novel low-molecular-weight inhibitor of IkappaB kinase-beta (IKK-beta) prevents pulmonary inflammation and shows broad anti-inflammatory activity. *Br J Pharmacol*. 145:178-192.